

SUSTAINABLE DESIGN AND OPTIMIZATION OF SHALE GAS ENERGY  
SYSTEMES

A Dissertation

Presented to the Faculty of the Graduate School

of Cornell University

In Partial Fulfillment of the Requirements for the Degree of

Doctor of Philosophy

by

Jiyao Gao

August 2018

© 2018 Jiyao Gao

# SUSTAINABLE DESIGN AND OPTIMIZATION OF SHALE GAS ENERGY SYSTEMS

Jiyao Gao, Ph. D.

Cornell University 2018

This dissertation centers on the sustainable design and optimization of shale gas energy systems with mathematical programming models and tailored solution algorithms. Specifically, three research aims are proposed, including modeling sustainability in shale gas energy systems, leveraging data and statistical learning for hedging against uncertainty in shale gas energy systems, and modeling and optimization of decentralized shale gas energy systems.

There are three distinct research projects under the research topic of modeling sustainability in shale gas energy systems. In the first related project, we propose a novel mixed-integer nonlinear fractional programming model to investigate the economic and environmental implications of incorporating modular manufacturing into well-to-wire shale gas supply chains. To systematically evaluate the full spectrum of environmental impacts, an endpoint-oriented life cycle optimization framework is applied that accounts for up to 18 midpoint impact categories and three endpoint impact categories. Total environmental impact scores are obtained to evaluate the comprehensive life cycle environmental impacts of shale gas supply chains. In the second project, we analyze the life cycle environmental impacts of shale gas by using an integrated hybrid life cycle analysis (LCA) approach. Based on this integrated hybrid LCA framework, we further develop an integrated hybrid life cycle optimization (LCO) model, which enables automatic identification of sustainable alternatives in the design and operations of shale gas supply chains. In the third project, we propose a novel modeling framework

integrating the dynamic material flow analysis (MFA) approach with LCO methodology for sustainable design of energy systems. This dynamic MFA-based LCO framework provides high-fidelity modeling of complex material flow networks with recycling options, and it enables detailed accounting of time-dependent life cycle material flow profiles. The resulting optimization problem is formulated as a mixed-integer linear fractional program and solved by an efficient parametric algorithm.

The second aim centers on hedging against uncertainty in the shale gas energy system with special focus on stochastic optimization approach. In the corresponding project, we address the optimal design and operations of shale gas supply chains under uncertainty of estimated ultimate recovery (EUR). A two-stage stochastic mixed-integer linear fractional programming (SMILFP) model is developed to optimize the levelized cost of energy generated from shale gas. To reduce the model size and number of scenarios, we apply a sample average approximation method to generate scenarios based on the real-world EUR data. In addition, a novel solution algorithm integrating the parametric approach and the L-shaped method is proposed for solving the resulting SMILFP problem within a reasonable computational time.

The third aim addresses the modeling and optimization of decentralized shale gas energy systems. In the relevant project, we propose a novel game-theory-based stochastic model that integrates two-stage stochastic programming with a single-leader-multiple-follower Stackelberg game scheme for optimizing decentralized supply chains under uncertainty. Both the leader's and the followers' uncertainties are considered, which directly affect their design and operational decisions. The resulting model is formulated as a two-stage stochastic mixed-integer bilevel nonlinear program. An illustrative example of flight booking under uncertain flight delays and a large-scale application to shale gas supply chains is presented to demonstrate the applicability of the proposed framework.

## BIOGRAPHICAL SKETCH

Jiyao Gao grew up in Nanyang, China. He graduated from Tsinghua University, China in July 2013 with a Bachelor's degree in Chemical Engineering. He joined Professor Fengqi You's research group in late 2013 at Northwestern University to pursue a Ph.D. degree. In 2016 summer, he transferred to Cornell University with Professor You to continue his Ph.D. program. Jiyao's Ph.D. research focus on the sustainable design and optimization of shale gas energy systems.

## ACKNOWLEDGMENTS

First and foremost, I want to express my deep gratitude to my parents, who have been constantly supporting me even during my darkest time. I will never be able to go this far without their encouragement and love.

I would like to thank Professor Fengqi You for his support and guidance throughout the past five years. As my advisor in research and mentor in life, he was always there willing to talk and help. I have received extremely valuable educational experience and scientific training from the working experience with him. His meticulous attention to details and dedication to research will cast a life-long impact on my future work. Also, I would like to thank my committee members, Professor Jefferson Tester and Professor Linda Nozick, for their patience and guidance. They have offered very constructive comments and thoughtful feedbacks to make this dissertation possible.

Last but not the least, I need to thank all my colleagues, who has made the Ph.D. life so colorful and instructive. Dr. Dajun Yue was always the go-to person when I encountered any type of questions. I learned so much from him in my research. Dr. Jian Gong, as my senior colleague and close friend, was always willing to communicate and helped me get through so many challenges. Daniel Garcia and Karson Leperi helped me a lot by raising critical comments about my presentations and manuscripts. Most importantly, they were both amazing friends and I would never forget the happy hours we spent together. Dr. Chao Shang and Chao Ning helped me a lot in learning data-driven approaches and robust optimization . Xueyu Tian, Cen Guo, Shipu Zhao, and Aaron Mihorn, I wish I could have more time with you. Visiting scholars including Dr. Chang He, Minbo Yang, Dr. Hua Zhou, Dr. Na Luo, and Dr. Liang Zhao, thank you guys for the wonderful time with me.

## TABLE OF CONTENTS

BIOGRAPHICAL SKETCH.....	v
ACKNOWLEDGMENTS .....	vi
TABLE OF CONTENTS .....	vii
LIST OF FIGURES .....	x
LIST OF TABLES .....	xvi
INTRODUCTION.....	1
1.1 Shale gas and natural gas liquids.....	3
1.2 Overview of shale gas energy systems .....	6
1.3 Literature review.....	18
1.4 Outline of the dissertation.....	22
AN ENDPOINT-ORIENTED LIFE CYCLE OPTIMIZATION FRAMEWORK AND APPLICATION OF MODULAR MANUFACTURING .....	25
2.1 Introduction.....	25
2.2 Problem statement.....	28
2.3 Model formulation and solution method .....	39
2.4 Tailored global optimization algorithm .....	42
2.5 Results and discussion .....	45
2.6 Summary.....	66
2.7 Appendix A: Superstructure configuration description.....	67
2.8 Appendix B: Detailed model formulation for the overall-performance LCO model .....	89
2.9 Appendix C: Detailed computational performance of proposed tailored global optimization algorithm .....	90
2.10 Nomenclature .....	90

INTEGRATED HYBRID LIFE CYCLE ASSESSMENT AND OPTIMIZATION .	100
3.1 Introduction.....	100
3.2 Integrated hybrid LCA of shale gas .....	102
3.3 Integrated hybrid LCO model of shale gas supply chains .....	117
3.4 Summary .....	134
3.5 Appendix A: Detailed model formulation for the hybrid LCO model of shale gas supply chains .....	135
3.6 Appendix B: Hybrid LCO models minimizing life cycle water consumption and energy consumption.....	150
3.7 Appendix C: Optimization results of process-based LCO model.....	153
3.8 Appendix D: Computational performance of the proposed tailored global optimization algorithm .....	155
3.9 Nomenclature.....	156
DYNAMIC MATERIAL FLOW ANALYSIS-BASED LIFE CYCLE OPTIMIZATION .....	163
4.1 Introduction.....	163
4.2 Dynamic MFA-based LCO framework .....	166
4.3 Problem statement.....	168
4.4 Model formulation and solution algorithm .....	173
4.5 Results and discussion .....	192
4.6 Summary .....	205
4.7 Nomenclature.....	206
DECIPHERING AND HANDLING UNCERTAINTY WITH TWO-STAGE STOCHASTIC PROGRAMMING .....	212

5.1	Introduction.....	212
5.2	Problem statement.....	215
5.3	Model formulation .....	218
5.4	Solution approaches .....	226
5.5	Results and discussion .....	235
5.6	Summary .....	245
5.7	Appendix A.....	246
5.8	Appendix B .....	248
5.9	Appendix C.....	250
5.10	Appendix D .....	251
5.11	Nomenclature .....	253
A STOCHASTIC GAME THEORETIC FRAMEWORK FOR DECENTRALIZED OPTIMIZATION OF MULTI-STAKEHOLDER SUPPLY CHAINS UNDER UNCERTAINTY .....		257
6.1	Introduction.....	257
6.2	General problem statement and model formulation .....	259
6.3	Application to multi-stakeholder shale gas supply chain optimization .....	264
6.4	Summary .....	287
6.5	Nomenclature.....	288
CONCLUSIONS .....		293
REFERENCES .....		299

## LIST OF FIGURES

Figure 1. Overview of global shale gas resource (Source: EIA). .....	2
Figure 2. Illustrative figure of horizontal drilling and hydraulic fracturing. ....	4
Figure 3. Overview of a shale gas energy system. ....	7
Figure 4. Summary of shale water management strategies and corresponding technologies. ....	10
Figure 5. Generalized shale gas processing flowsheet. ....	14
Figure 6. Flowsheet of the basic turbo-expander process scheme. ....	16
Figure 7. Illustrative shale gas supply chain network. ....	29
Figure 8. Life cycle stages of shale gas in a well-to-wire system boundary (unit processes associated with modular manufacturing are in the red box). ....	32
Figure 9. Illustrative figure of midpoint and endpoint environmental impact categories considered in the endpoint-oriented LCO model. ....	35
Figure 10. Pseudo-code of the tailored global optimization algorithm for MINLFP problems. ....	43
Figure 11. Reference map of the well-to-wire shale gas supply chain based on Marcellus Shale in the case study. ....	46
Figure 12. Shale gas supply chain network considered in the case study. ....	48
Figure 13. Pareto-optimal curve illustrating the trade-offs between LCOE and ReCiPe endpoint environmental impact score per MWh electricity generation with breakdowns: pie charts for the LCOE breakdowns and donut charts for the breakdowns of environmental impact score per MWh electricity generation. ....	49

Figure 14. Design and planning decisions for modular LNG plants in different Pareto-optimal solutions. ....	53
Figure 15. Summary of CAPEX and OPEX regarding conventional processing plants and modular LNG plants in different Pareto-optimal solutions. ....	54
Figure 16. Drilling schedules and shale gas production profiles of different Pareto-optimal solutions. ....	56
Figure 17. Midpoint environmental impact score breakdowns of different Pareto-optimal solutions. ....	58
Figure 18. Absolute midpoint environmental impact scores of point A. ....	59
Figure 19. Endpoint environmental impact score breakdowns and comparison of different Pareto-optimal solutions (The environment-oriented solution A is selected as the reference solution and all the other solutions are presented with ratios of their results to that of point A). ....	61
Figure 20. Sensitivity analysis of average EUR of shale wells, average NGL composition in shale gas, average transportation distance, CAPEX for modular plant installation, and electricity demand. ....	63
Figure 21. Comparison of Pareto-optimal solutions of the proposed functional-unit-based LCO problem optimizing the functional-unit-based economic and environmental performances and the overall-performance LCO problem optimizing the overall economic and environmental performances. ....	65
Figure 22. Drilling schedules and production profiles in the Pareto-optimal solution point E of the functional-unit-based LCO problem and the Pareto-optimal solution point E' of the overall-performance LCO problem. ....	66

Figure 23. Illustration of integrated hybrid LCA approach.....	104
Figure 24. Illustrative figure of the $896 \times 896$ two-region IO table [135]. .....	109
Figure 25. Structure of the integrated hybrid LCA model for shale gas. ....	109
Figure 26. Breakdowns of (A) life cycle GHG emissions, (B) life cycle water consumption, and (C) life cycle energy consumption based on upstream of the process systems, downstream of the process systems, and the EIO systems (the best, balance, and worst cases corresponding to the lowest, the medium, and the highest environmental impacts, respectively). .....	111
Figure 27. Integrated hybrid LCA results regarding (A) life cycle GHG emissions, (B) life cycle water consumption, and (C) life cycle energy consumption with detailed contribution breakdowns (the best, balance, and worst cases corresponding to the lowest, the medium, and the highest environmental impacts, respectively). .....	114
Figure 28. Result comparison of the integrated hybrid LCA with existing shale gas LCA studies [17, 79, 84, 85, 95, 118, 132, 149]. .....	115
Figure 29. Comparison of life cycle GHG emissions of shale gas and other fossil fuels for electricity generation [137, 150]. .....	117
Figure 30. Pseudo-code of the tailored global optimization algorithm. ....	124
Figure 31. Reference map of the shale gas supply chain in the UK [154, 156]. .....	127
Figure 32. Pareto-optimal curve illustrating the trade-offs between LCOE and life cycle GHG emissions with breakdowns: pie charts for the LCOE breakdowns and donut charts for the breakdowns of life cycle GHG emissions. ....	129
Figure 33. Life cycle GHG emission breakdowns based on the 40 basic processes (indexed by $m$ ) of the process systems listed in Table 1. ....	130

Figure 34. Drilling schedules and production profiles of solution points A and B....	132
Figure 35. Summary of shale gas supply chain design and flow information for Pareto-optimal solution point A and point B. ....	133
Figure 36. Optimal water management strategies of solution points A and B.....	134
Figure 37. Illustration of the dynamic MFA-based LCO framework. ....	168
Figure 38. Illustrative MFA figure of the shale gas energy system. ....	169
Figure 39. Pseudo code of the parametric algorithm for MILFP problems. ....	192
Figure 40. 3D-Pareto optimal surface illustrating the trade-offs between economic, environmental, and resource performances. ....	194
Figure 41. Contour plot of the Pareto optimal surface on the X-Y surface.....	195
Figure 42. Breakdowns of (a) levelized cost of unit net energy output, (b) GHG emissions per unit net energy output, and (c) water consumption per unit net energy output.....	198
Figure 43. Life cycle profiles of (a) total GHG emissions and (b) total water consumption of Pareto optimal solution points A, B, C, and D. ....	200
Figure 44. Optimal drilling schedules (axis on the left) and shale gas production profiles (axis on the right) of Pareto optimal solution points A, B, C, and D throughout the planning horizon. ....	201
Figure 45. MFA of Pareto optimal solution point D. ....	203
Figure 46. Key material flow profiles associated with Pareto optimal solution point D. ....	205
Figure 47. Superstructure of shale gas supply chain network. ....	215
Figure 48. Flowchart on determining the sample size.....	227

Figure 49. Comparison of EUR distribution between exact data for Marcellus derived from literature and data from sample average approximation.....	229
Figure 50. Flowchart of the solution algorithm integrating parametric approach and L-shaped method. ....	231
Figure 51. Pseudo-code of the global optimization algorithm. ....	234
Figure 52. Converging process of the proposed algorithm. ....	237
Figure 53. Optimal design of shale gas supply chain network under EUR uncertainty. ....	238
Figure 54. Results of EVPI and VSS with 300 scenarios considered. ....	240
Figure 55. Possibility distribution of solutions from (a) deterministic model with nominal uncertainty value and (b) model with perfect information. ....	242
Figure 56. Sankey diagram of shale gas flow in the supply chain network. ....	244
Figure 57. Cost breakdown regarding capital investment and operating cost.....	245
Figure 58. Illustration of the modeling framework for optimization of decentralized multi-stakeholder supply chains under uncertainty. ....	261
Figure 59. Optimal NPVs of leader and followers in 200 scenarios based on the optimal strategy obtained in the two-stage stochastic MIBP model.....	280
Figure 60. Optimal expected NPVs of the leader and followers in the two-stage stochastic MIBP model and deterministic game theoretic models.....	282
Figure 61. Cumulative probability distribution of the leader’s NPV based on 200 scenarios in the two-stage stochastic MIBP model (solid line) and deterministic game theoretic models (dash lines). ....	283
Figure 62. Optimal drilling schedule and shale gas production profile of the leader.	285

Figure 63. Leader’s optimal strategy regarding selection of processing contracts from followers. ....	286
Figure 64. Optimal processing fees provided by the followers for different processing contracts.....	287

## LIST OF TABLES

Table 1. Summary of basic processes considered in the process systems.....	106
--	-----

## CHAPTER 1

### INTRODUCTION

Natural gas is recognized as a primal energy source that is widely used for heating, electricity generation, transportation, and chemical manufacturing. In recent decades, technological advancements, including the development of hydraulic fracturing and horizontal drilling, have led to a “shale revolution” that stimulated tremendous production of shale gas in the U.S. [1]. From 2005 to 2013, the dry natural gas production in the U.S. increased by 35%, and the natural gas share of total U.S. energy consumption rose from 23% to 28%. It is expected that the U.S. will become a net exporter of natural gas by 2017 [2]. Moreover, this unconventional energy source (i.e. shale gas) has drawn serious attention from countries all over the world (Figure 1). Based on the recent estimation from the U.S. EIA, there are 35,782 Trillion cubic feet (Tcf) risked shale gas in-place for 41 countries, of which 7,299 Tcf shale gas is considered technically recoverable. Countries that are known with the most recoverable shale gas reserves include the China, Argentina, Algeria, U.S., Canada, and Mexico. These countries in total possess more than two-thirds of the assessed, technically recoverable shale gas resources of the world [3]. Although currently only the U.S. and Canada have significant shale gas production, it is foreseeable that the global shale gas industry will undergo a rapid expansion in the near future.

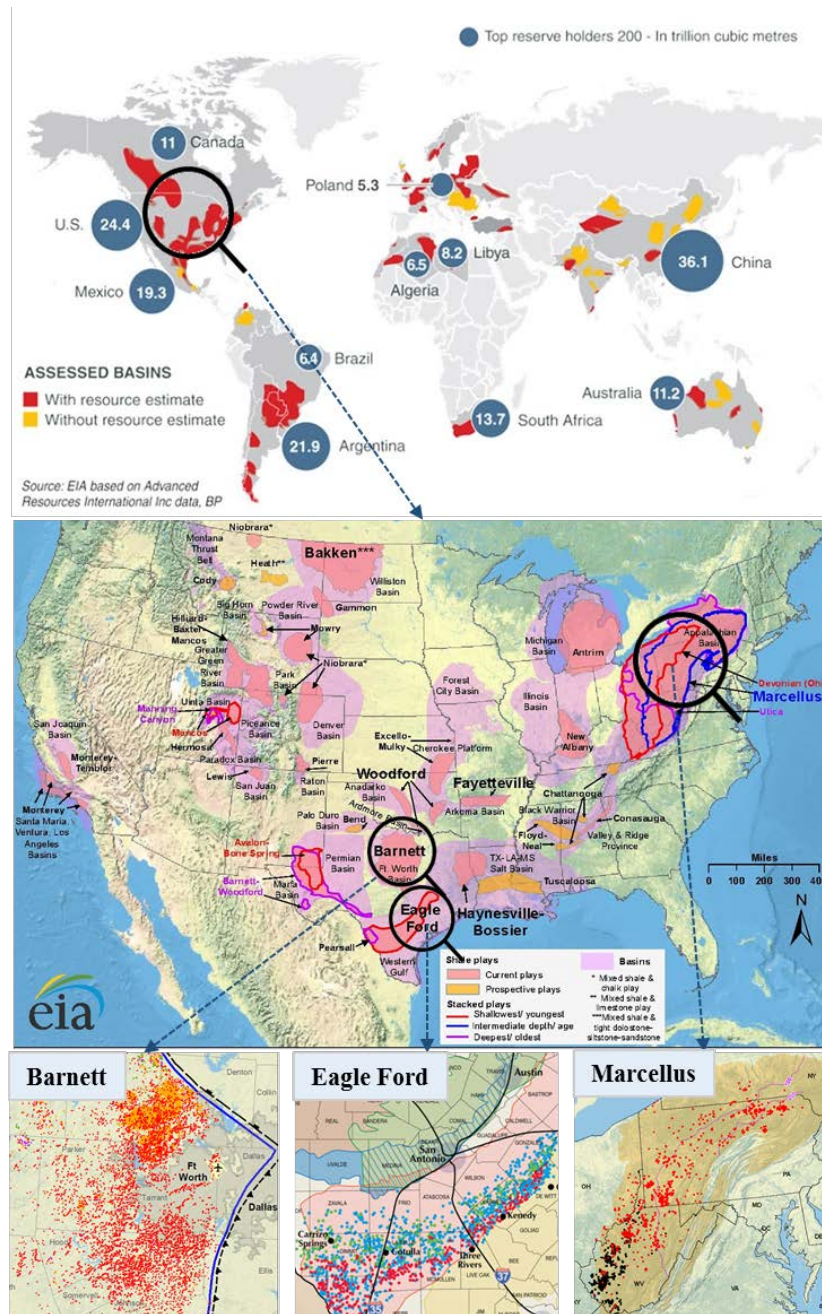


Figure 1. Overview of global shale gas resource (Source: EIA).

Under the current low price of natural gas as well as pressing environmental and social concerns on shale gas industry, it is imperative to design and optimize shale gas energy systems that are economically efficient [4, 5], environmentally sustainable [6, 7], and socially responsible [8, 9]. Towards this goal, the main research challenge is to develop

an integrated energy systems modeling framework that can systematically identify the optimal design and operational strategies and comprehensively account for multiple sustainability criteria. Additionally, there are other challenges impeding the design and optimization of shale gas energy systems, including optimization under multiple types of uncertainties, addressing conflict of interest among different stakeholders, and modeling multi-scale decisions with emerging technologies/operations in the shale gas energy systems. By properly tackling these challenges, the resulting shale gas energy system modeling framework is expected to be robust against uncertainty, reflect stakeholders' rational behaviors, and capture the multi-scale decisions as well as latest technological/operational advances. Therefore, it is the objective of this thesis to identify key research challenges and opportunities in the design and optimization of shale gas energy systems, and also chart a path to address these challenges.

## **1.1 Shale gas and natural gas liquids**

Shale gas is normally embedded in shale rocks that are a few thousand feet deep. Due to the low permeability of shales, special techniques are required to create artificial fractures for extra permeability, so the shale gas production in commercial quantities is possible. Hydraulic fracturing is a well-stimulation technique as shown in Figure 2. By pumping millions of gallons of fracturing fluid into the wellbore under high pressure, fractures are created and held open, forcing the shale gas flow back to the surface. Furthermore, the introduction of horizontal drilling technology boosts the production of shale gas by allowing multiple wells drilled at one shale pad. Horizontal drilling, as shown in Figure 2, allows the wellbore to be turned horizontally at depth. Compared

with vertical drilling sites, horizontal well sites generate more shale gas with less wellbores, so the corresponding capital cost is significantly reduced [10].

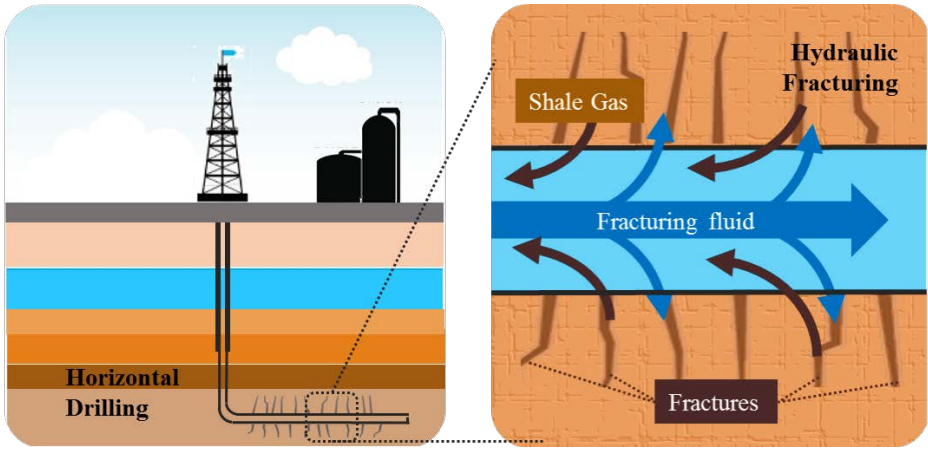


Figure 2. Illustrative figure of horizontal drilling and hydraulic fracturing.

Shale gas production profile for a single well generally features a high initial production rate, followed by a significant decline ranging from 60% to 90% after the first three years [11]. Such a characteristic is caused by the pressure depletion and inherently low permeability of the shale reservoir. As a consequence, shale gas operators need to regularly drill new wells or to refracture existing ones to maintain a stable production profile [12]. Depending on the geological location, shale gas produced from different wells will have variant compositions. In addition to the primal component, methane, shale gas typically includes heavier hydrocarbons, namely ethane, propane, butanes, etc., and other impurities, such as carbon dioxide, nitrogen, and hydrogen sulfide [13]. When the heavier hydrocarbons are processed and purified into final products, they are collectively referred to as “NGLs”. Based on the amount of NGLs, the raw shale gas can be classified as dry gas and wet gas. Dry gas is considered almost pure methane

with trace NGLs, while in wet gas, the amount of NGLs is significant enough to require further separation [14].

Natural gas is generally considered as a cleaner bridge energy between traditional fossil fuels and renewable energy sources. However, methane itself is a greenhouse gas (GHG) that is 25 times more potent than carbon dioxide based on the 100-year global warming potential [15]. Therefore, any leakage of shale gas during the production or transmission may result in non-negligible environmental impacts. According to the most recent life cycle analysis studies, the life cycle GHG emissions associated with shale gas are comparable to the conventional natural gas, but less than those of coal [16, 17]. In addition to the concerns on climate change, shale gas production based on hydraulic fracturing is known for its significant water footprint. The total direct water consumption for each shale well ranges from 2 to 20 million gallons of freshwater [18, 19]. Meanwhile, in the drilling and completion phases of shale gas production, large amount of flowback water and produced water is generated as highly contaminated water [20]. Improper handling of the wastewater could pollute to the local water resource and affect the public health [21, 22].

The NGLs are heavier hydrocarbons contained in the raw shale gas, including ethane, propane, butanes, pentanes, and even higher molecular weight hydrocarbons [13]. The raw shale gas produced in different shale regions has distinct amount of NGLs [23]. For shale plays that produce only dry gas, such as the Fayetteville and Haynesville shale plays, only dehydration and impurity removal processes are required to meet the pipeline specifications. Meanwhile for the wet wells in Marcellus and Barnett shale plays, the content of NGLs in shale gas is significant enough for further processing [24].

The presence of NGLs brings both challenges and opportunities to the shale gas industry. First, NGLs provide shale gas operators with extra income stream. This is evidenced by the fact that drilling activities in recent years have shown obvious movement towards wet shale plays [25]. However, the composition of NGLs normally varies from well to well, so properly addressing the shale gas composition uncertainty becomes crucial in shale gas development. Second, the processing, storage, and transportation of NGLs add more complexity to the design and operations of shale gas energy systems. The raw shale gas produced from shale wells requires extra processing service from midstream processing companies, so that pipeline-quality sales gas and NGLs are separated, and NGLs can be further fractionated. This leads to the problem of properly determining the location and capacity of processing plants, processing technologies, and processing contracts. Additionally, the increase of NGL production in recent years requires expansion of current midstream and downstream infrastructure, including shale gas processing, fractionation, ethylene cracking, and transportation facilities [26]. Last but not least, the production of NGLs connect the shale gas production with petrochemical industry. Primal components in the NGLs, namely ethane and propane, act as important feedstocks in the petrochemical plants and can be used to produce various high-value chemical products [27].

## **1.2 Overview of shale gas energy systems**

The shale gas energy system is a complex system consisting of multiple stages and various decisions. Depending on the physical locations and specific functionalities, a typical shale gas energy system can be divided into the upstream, midstream, and

downstream sectors (Figure 3). The goal of this section is to provide a comprehensive overview of a shale gas energy system and the major design and operations decisions.

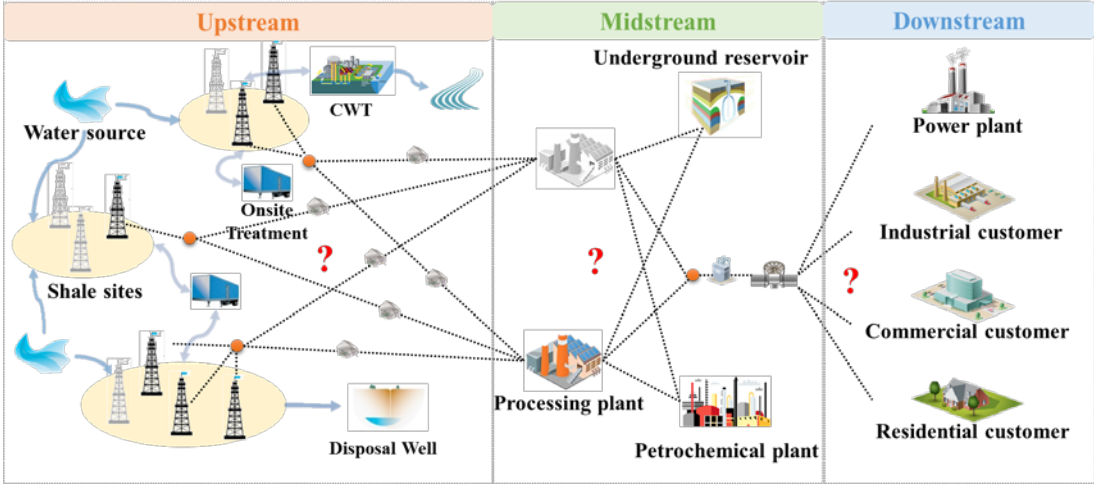


Figure 3. Overview of a shale gas energy system.

**1.2.1 Upstream**

The upstream activities include construction of shale sites for preparation, drilling and fracturing shale wells to bring shale gas to the surface, and the water acquisition, as well as produced water treatment. We go through these major activities one by one in the following subsections.

**1.2.1.1 Shale site construction**

To construct a shale site, a geological evaluation is first conducted to identify the potential shale site. Then, the shale gas operators/producers need to reach a lease agreement with the corresponding landowners and to obtain the drilling permits [28]. The operators bear the responsibility to guarantee that all the drilling and production activities taking place at the shale site will be carried out in accordance with relevant regulations. After the approval of the operator’s permit by local environmental

regulation agencies, the site construction can officially begin. Typical shale site constructions follow these steps: First one is the clearance of proposed area and accommodation of equipment; a road is then constructed to provide access to the shale site; next, impoundments are constructed to handle the fluids generated during drilling and fracturing processes; subsequently, transportation infrastructure (including gathering pipelines, injection lines, and water supply lines) are installed, and storage facilities such as storage tanks are built [29].

#### **1.2.1.2 Well drilling and completion**

Once a shale site is constructed, the drilling rig is moved on site and assembled. A conductor hole is predrilled, followed by injection of conductor pipes. Depending on the number, depth, and length of horizontal wells to be drilled, the drilling process can last for a few months [30]. During this period, a constant supply of drilling fluid is required, and proper handling of sediments and flowback water is needed. Besides, well casings made of steel are inserted into the corresponding drilling section of wellbore and cemented in place to prevent contamination of underground water resource. After the well drilling phase, the well completion phase starts, which refers to the process of finishing a well to make it ready for producing shale gas. The well completion phase includes three main stages [31, 32]. The first stage is perforation, where an electric current is sent by wire to a perforating gun, and the resulting charge shoots holes through the casing to a short distance into the shale. The second stage is hydraulic fracturing, where a mixture of water, sand, and chemical additives is injected underground at a high pressure to break up the shale-rock formations, so that fractures are created and the shale gas is extracted. The last stage is production. When all of the drilling and fracturing

activities are completed, a wellhead is constructed and the local gathering pipelines are prepared for the controlled extraction of natural gas.

### **1.2.1.3 Water management**

As mentioned above, shale gas development relies heavily on the usage of water resource. Both drilling and hydraulic fracturing operations require a significant amount of freshwater, resulting in a few million gallons of net water consumption for each well [18]. In water scarce regions such as the Eagle Ford shale play at south Texas, the significant withdrawal of water amplifies the water supply issue and affects the regular production plan [33]. In other regions where water scarcity is not so severe, such as Marcellus shale play, the spatial and seasonal variability of stream flow still raises the risk that water withdrawals may negatively impact local water resources [34].

In the drilling phase, drilling fluid with a water base is used. Meanwhile, drilling wastewater is generated and mostly reused in drilling processes. The remaining wastewater can either be injected underground or treated for discharge. Hydraulic fracturing takes place after well drilling. A certain percentage of water flows back to the surface as highly contaminated water, known as flowback water. Flowback water is normally defined as the water produced after hydraulic fracturing and is made up of hydraulic fracturing fluid and formation water, featuring relatively large flowrate and slightly lower total dissolved solids (TDS) concentration. Later, when the shale well begins producing shale gas, produced water is generated with small flowrate and high TDS concentration, and it is mainly composed of formation water [9]. Improper handling and disposal of the flowback/produced water is recognized as the main cause of water contamination [20]. Thus, in order to guarantee the water supply and minimize

the environmental impacts, shale gas operators have to develop sustainable strategies for water management.

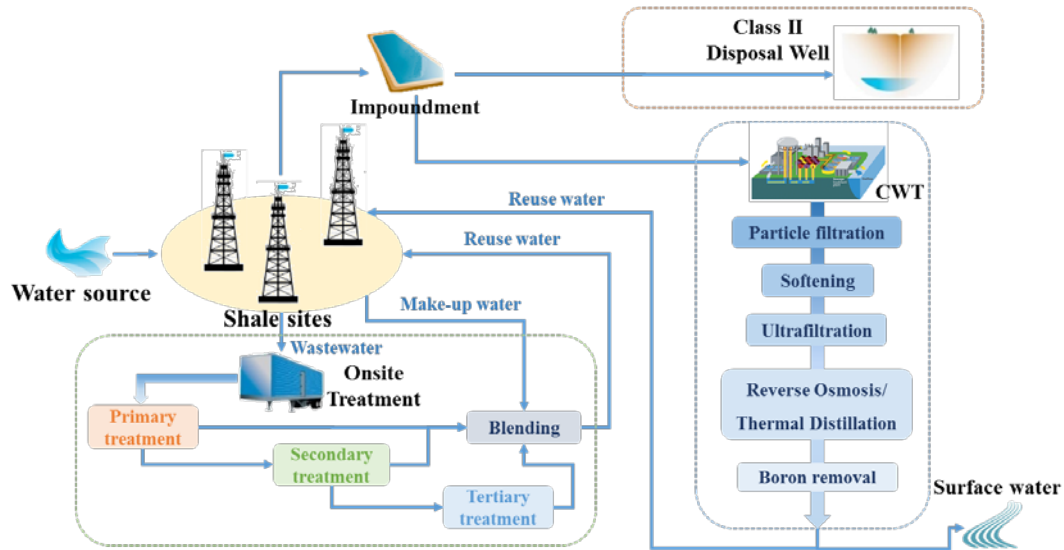


Figure 4. Summary of shale water management strategies and corresponding technologies.

In general, there are three major approaches to manage the wastewater generated in shale gas production, as shown in Figure 4 [22, 35]. The first option is injection into Class II disposal wells, which are defined as disposal wells for injection of brine associated with oil and gas operations in EPA’s Underground Injection Control program [21, 36]. The application of underground injection is normally constrained by the availability of disposal wells. For states where abundant disposal wells exist, such as Ohio and Texas, underground injection is a cost-effective option since no extra water treatment process is required. However, for states with very limited number of Class II disposal wells, such as Pennsylvania [37], the underground injection option suffers from the high transportation cost and becomes less attractive [38]. Additionally, there are concerns on the risks of underground water contamination and induced seismicity by

injecting wastewater into Class II disposal wells, so both the injection rate and total injection amount of wastewater need to be well regulated [39, 40].

The second option is the centralized wastewater treatment (CWT) facilities that are capable of treating flowback and produced water. The treated water can either be discharged to surface water bodies or be recycled to shale sites for reuse [37]. In general, a CWT facility consists of a sequence of treatment processes, including filtration to remove large objects, settling tank to allow settling of heavy solids and removal of free oil, softening with agitation, aeration and pH adjustment, ultrafiltration to remove particulates and macromolecules, desalination with membrane or thermal distillation techniques, and toxic elements removal [21]. The CWT treatment option brings water recycling to the shale water treatment, and features a relatively lower treatment cost as well as large operating capacities than onsite treatment. However, the economic viability of this option might be affected by the proximity of CWT facilities to shale sites. Besides, accidental discharges or spills during the transportation and treatment pose potential risks of water contamination, and the transportation activities add extra carbon footprint to the shale gas [9, 40].

The last option is onsite treatment for reuse, which is usually performed by mobile wastewater treatment units. The onsite treatment usually consists of three levels of treatment technologies, namely the primary, secondary, and tertiary treatment [21, 22]. The primary treatment only involves clarification to remove suspended matter, free oil and grease, iron, and microbiological contaminants. Technologies for the primary treatment include coagulation, flocculation, disinfection, microfiltration/ultrafiltration, adsorption, ozonation, and use of a hydrocyclone. The secondary treatment mainly

involves softening, where hardness ions such as  $\text{Ba}^{2+}$ ,  $\text{Sr}^{2+}$ ,  $\text{Ca}^{2+}$ , and  $\text{Mn}^{2+}$  are removed. The corresponding technologies include lime softening, ion exchange, and activated carbon. The tertiary treatment targets on desalination to remove the TDS. Major desalination technologies include membrane separation (e.g., reverse osmosis, forward osmosis, and membrane distillation) and thermal technologies (e.g., multi-effect distillation, multi-stage flash, and vapor compression) [41]. Notably, the wastewater treated by primary and secondary treatment normally needs to be blended with a certain percentage of make-up water to reduce the TDS concentration, so the reuse specification can be satisfied. For the tertiary treatment, wastewater will be blended with a certain amount of water to reduce the TDS concentration before the treatment, so it can be treated effectively by the following desalination technologies [41]. The wastewater treated onsite, after blended with some make-up water, can be reused for hydraulic fracturing. There is no transportation cost involved in onsite treatment. However, onsite treatment is limited by capacity and technical constraints, and its economic efficiency highly depends on the wastewater composition and the treatment technology applied. Apart from these three water management options, wastewater can be stored temporarily at the shale sites within tanks or impoundments [42], which function like inventory that can provide ‘buffer’ for transportation or treatment activities over time.

### **1.2.2 Midstream**

The midstream of shale gas supply chain is mainly managed by shale gas processing companies, who provide shale gas processing service to the upstream producers and link the upstream production with the downstream market through its distribution networks.

The midstream activities cover the gathering of raw shale gas from different shale sites, shale gas separation at processing plants, storage of natural gas as well as NGLs, and distribution of shale gas products.

#### **1.2.2.1 Shale gas gathering**

Shale gas is mainly transported through pipeline systems, which include all the necessary equipment such as pipelines, compressors, valves, and monitoring devices. Once the raw shale gas is produced, water and condensate are first removed at or near wellhead. Next, shale gas produced at different sites are gathered through the gathering pipeline network. Depending on the content of NGLs, the shale gas may be transported either to processing plants for separation or to the pipeline system for distribution [24].

#### **1.2.2.2 Gas processing**

As shown in Figure 5, the shale gas processing starts at the well head. When raw shale gas is produced, water and condensate need to be removed first before it enters the gathering pipeline. The shale gas processing commonly mentioned refers to the contract-based separation service provided by the midstream shale gas processors. There are three main types of processing contracts, known as the fee-based contracts, percentage of proceeds contracts, and keep-whole contracts [14, 43]. Under fee-based contracts, the processor charges the producer based on the amount of shale gas they process. In this case, the processor has no direct sensitivity to commodity prices since its revenue is solely linked to volume. Under percentage of proceeds contracts, the upstream producer retains title to both the gas and NGLs. Meanwhile, the processor is reimbursed by the producer with an agreed upon percentage of the actual proceeds of

the sales of gas and NGLs in addition to the basic operation cost. In this case, shale gas producer and processor share the risk of price fluctuations. Under keep-whole contracts, the processor retains the NGLs extracted and return the processed natural gas or equivalent value to the producer. In this case, processor gets a mix of commodity exposure. The duration of processing contracts ranges from a few months to several years. Intermediate terms of 1 to 10 years are also common [5, 14]. Based on the fluctuation of market prices, the processing company may choose different types of processing contract to maximize the margin [44].

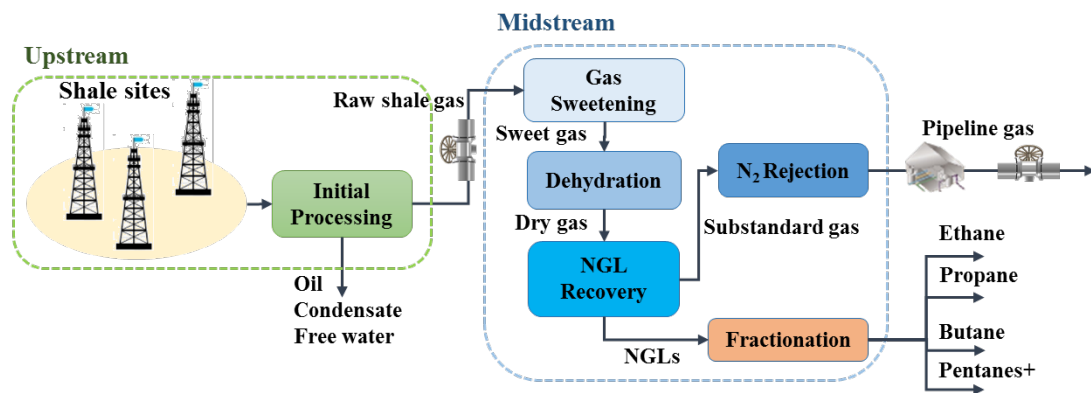


Figure 5. Generalized shale gas processing flowsheet.

From a process design perspective, a shale gas processing plant is a dedicated separation train consisting of four major processes, namely gas sweetening, dehydration, NGL recovery, and N<sub>2</sub> rejection. If economically feasible, the NGLs extracted from shale gas can be further fractionated into ethane, propane, butanes, and C<sub>5+</sub> streams in an additional fractionation train [14]. The gas sweetening process aims for removal of acid impurities, such as H<sub>2</sub>S and CO<sub>2</sub>, to prepare the shale gas for processing [45]. Depending on the gas composition, there are multiple process schemes that can be employed to

neutralize the shale gas, including the scavenger process, chemical absorption-based acid gas removal (AGR) process, and sulfur recovery process [46]. The shale gas that goes through the sweetening section is considered as sweet gas, which will pass a dehydration section to remove the water vapor, thus preventing condensation inside the pipelines during transportation. Regenerable adsorption in liquid triethylene glycol is a common technology applied in the dehydration section [47]. Once these impurities are removed from the feedstock, hydrocarbons are sent to the NGL recovery section to separate the gas and NGLs. Currently, most NGL recovery sections use cryogenic separation to separate heavy fractions [48]. A turbo-expansion configuration combined with an external refrigerant as shown in Figure 6 is able to recovery more than 80% of ethane from the dry gas [49]. Besides, there are a number of process scheme options evolved from the basic turbo-expander process scheme, including the gas sub-cooled (GSP), cold residue (CRR), recycle vapor-split (RSV) process schemes and enhanced NGL recovery process schemes (IPSI-1 and IPSI-2) [50]. The remaining gas, also called sales gas that mainly consists of methane, can be compressed as pipeline gas directly if its  $N_2$  content is low enough; Otherwise, it needs to go through a  $N_2$  rejection section since high  $N_2$  content would make the heating value of the pipeline gas lower than pipeline specification [14]. The marketable NGLs, including ethane, propane, butanes etc., are sequentially extracted by passing through a fractionation train consisting of a series of separation columns.

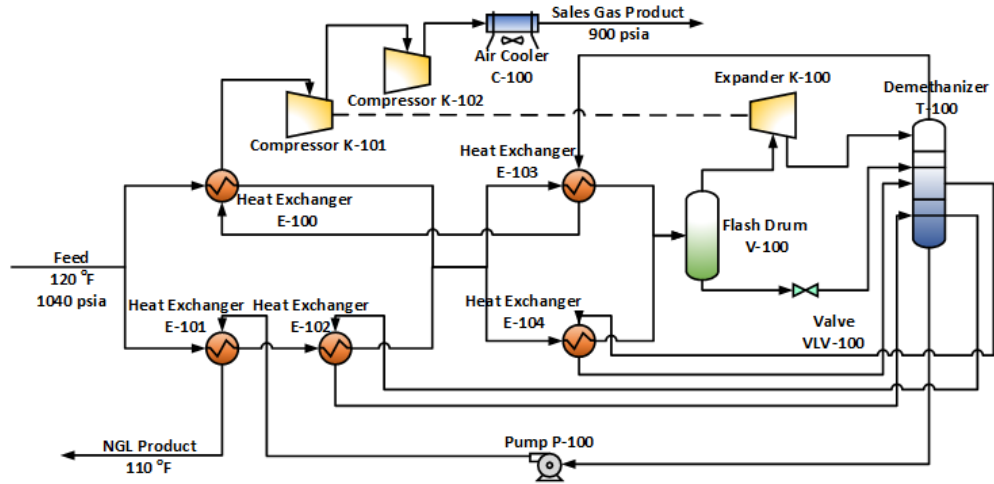


Figure 6. Flowsheet of the basic turbo-expander process scheme.

### 1.2.2.3 Storage and distribution

Like other commodities, produced pipeline-quality sales gas that is not directly transported to interstate/intrastate pipeline systems for distribution can be stored in underground reservoirs for an indefinite period of time. There are three principle types of underground storage sites in the U.S., including the depleted natural gas or oil fields, aquifers, and salt caverns [51]. Similarly, there are underground storage caverns and above ground storage tanks used to store mixed and pure NGLs. In the operation of shale gas supply chain, these storage facilities act as a “buffer” to accommodate fluctuations in demand and price for natural gas/NGLs. Despite the storage option, most shale gas enters the distribution system directly. While large customers such as power plants may receive gas directly from the interstate or intrastate pipelines, most individual customers buy gas from distribution companies.

### **1.2.3 Downstream**

The downstream of a shale gas supply chain involves the marketing and end use of shale gas. The sales gas (i.e. methane) is sent to the natural gas market for sale, and NGLs are normally traded as important feedstocks in petrochemical industry.

#### **1.2.3.1 Marketing**

Natural gas is priced and traded as a commodity at market hubs, which are normally located at the intersection of major pipeline systems. For instance, the largest market hub of natural gas in the U.S. is Henry Hub located in Louisiana, where the spot and future natural gas prices are generally considered as the primary price set for the North American natural gas market [52]. In addition to market hubs, natural gas can also be priced at citygates, which are defined as points or measuring stations where a distributing gas utility receives gas from a natural gas pipeline company or transmission system. There are two primary types of natural gas marketing and trading: physical trading and financial trading. Physical natural gas marketing is carried out through physical contracts negotiated between buyers and sellers. Main types of such contracts include swing contracts, base load contracts, and firm contracts. Financial trading involves derivatives and sophisticated financial instruments in which the buyer and seller never take physical delivery of the natural gas [38, 53].

#### **1.2.3.2 End use**

Most natural gas is sent to four major types of end-use customers, namely the electric power plants, residential customers, commercial customers, and industrial customers. Natural gas is recognized as the primal source of energy in residential and commercial

sectors. Moreover, the abundant supply of shale gas has expanded its usage in electric power generation and even the transportation sectors. In addition, shale gas boom significantly increases interest in C<sub>1</sub>, C<sub>2</sub>, and C<sub>3</sub> chemistry to convert methane, ethane, and propane to value-added products, respectively. For instance, the current industrial practice of steam reforming uses methane to produce syngas, which is an important intermediate to produce other chemical commodities. Besides, methane and ethane are recognized as two major chemicals that potentially lead to integration opportunities with other chemical manufacturing systems. These opportunities include, but are not limited to producing liquid fuels from methane [54], producing methanol from methane [55], and producing ethylene from ethane [49]. Different usage of shale gas resources will result in distinct life cycle energy, economic and environmental performance. The diversity of end uses has also created competitions with other energy sources among different sectors.

### **1.3 Literature review**

There is a rapidly growing number of publications on the design and optimization of shale gas energy system in recent years. These publications cover various topics, including the scheduling of drilling activity, planning of shale gas production, construction of infrastructure, shale water management, design of shale gas supply chain, exploration of processing schemes, selection of technologies and contracts, mitigation of environmental impacts, and modeling of new operations, etc. Besides, the scales of problems addressed in the literature range from a single process to the global shale gas industry.

By reviewing the existing literature, we can obtain the following remarks. First, although the global economic and environmental impacts of shale energy have been well acknowledged by both industry and academia, almost all the existing studies at national or global-scales are still limited to simple systems analysis. This is due to the limitation of computational power for exascale computing problems to account for many complex decisions in shale gas energy systems. Besides, a shale region normally includes thousands of shale wells, so it could easily result in a exascale mathematical problem that is computationally intractable. On the other hand, different shale plays feature distinctive production properties, environmental conditions, and regulation policies. Each shale well has its own ultimate recovery and shale gas composition that are usually different from others. Thus, integrated modeling of shale gas energy systems could involve huge amount of data and uncertainty. These challenges motivate the need of developing novel modeling frameworks and more efficient solution strategies for the shale gas energy systems. Second, most of the PSE publications mainly put their efforts on the supply chain scale problems. However, these articles either focus on the design and operations of shale gas supply chain [4, 5, 56] or center on the water management problem [57-59]. The water management issue is brought about by the shale gas development. Meanwhile, the shale gas production can be limited by multiple water-related constraints, such as fresh water availability and wastewater treatment. Therefore, it is necessary to develop an integrated modeling framework taking into consideration both shale gas development as well as water management. There are a few publications presenting such integrated modeling frameworks [6, 60]. Nevertheless, these models

either suffer from oversimplifications and restricted optimization criteria, or are computationally challenging to solve for large-scale applications.

Despite the importance of optimizing the shale gas processing system, there are only limited number of publications exploring the potential opportunities in process design and potential integration. To make use of the methane feedstock from shale gas industry, Martín and Grossmann [54] presented a superstructure optimization approach for the simultaneous production of liquid fuels and hydrogen from switchgrass and shale gas. Ehlinger, et al. [55] presented a shale gas processing design that aims to produce methanol with shale gas feedstock. In another work by Noureldin, et al. [61], an optimization model was proposed targeting on modeling and selection of reforming strategies for syngas generation from natural/shale gas. This work was further extended to account for economic and environmental performances for the production of methanol from shale gas [62]. In addition to methane, ethane is another important product from shale gas energy systems. He and You [49] proposed three novel process designs for integrating shale gas processing with ethylene production. Following this work, the authors extend the scope and further develop a novel process design for making chemicals from shale gas and bioethanol [63]. Recently, the same authors develop a mega-scale shale gas supply chain olefin production network model with explicit consideration of process designs, energy integration, and alternative processing technologies [64]. Additionally, an efficient cold energy integration scheme is proposed to integrate NGLs recovery from shale gas and liquefied natural gas (LNG) regasification at receiving terminals [65]. However, most works on shale processing design and synthesis are based on an isolated system, neglecting the impacts of shale

gas supply chains. Meanwhile, existing shale gas supply chain models typically approximate the shale gas processing plant as a simple input-output process without considering sufficient details. Now that shale gas processing is a crucial component in the shale gas supply chain, it is important to develop integrated multi-scale optimization frameworks for shale gas supply chain with explicit consideration of process design and operational decisions.

Moreover, although sustainable design of shale gas energy system is of great interest to both academy and public, current research on this topic heavily relies on the life cycle analysis (LCA) approach. The drawback of LCA approach is its incapability of discerning the optimal solution among multiple design alternatives. The environmental performance is normally calculated based on the average estimation of shale gas development. Thus, with different data and assumptions, the LCA approach may easily lead to disparate conclusions. To overcome this shortcoming, several studies aimed to incorporate sustainability perspectives into the design and optimization of shale gas energy systems. Attempts are made including choosing environment-oriented objective functions [57, 58], integrating LCA approach with multiobjective optimization [6, 7], introducing extra environmental constraints in the optimization model [59], and addressing safety concerns with quantitative risk analysis [66]. However, there are still a number of knowledge gaps: First, only certain types of environmental impact are considered, such as water consumption and GHG emissions, while a comprehensive evaluation of systems sustainability is absent in the literature. Besides, process-based LCA is the dominating method applied in the environmental impact analysis, which succeeds in modeling detail but suffers from systems boundary truncation. More

advance approaches such as hybrid LCA is expected to overcome this shortcoming [67, 68]. Besides, although multiple methodologies have been recognized as useful tools in sustainable design of energy systems [69], including material flow analysis (MFA), LCA, and mathematical optimization, they were typically applied in isolation. Since each tool has its advantages and drawback, it is of great value to explore the synergies among these tools and develop an integrated approach for the sustainable design of shale gas energy systems. Last but not least, important issues that are not fully addressed in the current literature includes hedging against multiple types of uncertainty, capturing interactions among multiple stakeholders, and modeling multi-scale decisions as well as emerging technologies and operations.

#### **1.4 Outline of the dissertation**

This dissertation addresses the sustainable design and optimization of shale gas energy systems. The roadmap of the dissertation is provided as follows.

In Chapter 2, we propose a novel mixed-integer nonlinear fractional programming model to investigate the economic and environmental implications of incorporating modular manufacturing into well-to-wire shale gas supply chains. An endpoint-oriented life cycle optimization framework is applied that accounts for up to 18 midpoint impact categories and three endpoint impact categories. Total environmental impact scores are obtained to evaluate the comprehensive life cycle environmental impacts of shale gas supply chains. A case study of a well-to-wire shale gas supply chain based on Marcellus Shale is presented to illustrate the application of the proposed modeling framework and solution algorithm.

In Chapter 3, we analyze the life cycle environmental impacts of shale gas by using an integrated hybrid LCA and optimization approach. Three environmental categories, namely the life cycle greenhouse gas emissions, water consumption, and energy consumption, are considered. We further developed an integrated hybrid life cycle optimization (LCO) model, which enables automatic identification of sustainable alternatives in the design and operations of shale gas supply chains. We applied the model to a well-to-wire shale gas supply chain in the UK to illustrate the applicability. In Chapter 4, we propose a novel modeling framework integrating the dynamic MFA approach with LCO methodology for sustainable design of energy systems. This dynamic MFA-based LCO framework provides high-fidelity modeling of complex material flow networks with recycling options, and it enables detailed accounting of time-dependent life cycle material flow profiles. The resulting optimization problem is formulated as a mixed-integer linear fractional program and solved by an efficient parametric algorithm. To illustrate the applicability of the proposed modeling framework and solution algorithm, a case study of Marcellus shale gas supply chain is presented.

In Chapter 5, we address the optimal design and operations of shale gas supply chains under uncertainty of estimated ultimate recovery (EUR). A two-stage stochastic mixed-integer linear fractional programming (SMILFP) model is developed in order to optimize the levelized cost of energy generated from shale gas. We apply a sample average approximation method to generate scenarios based on the real-world EUR data. In addition, a novel solution algorithm integrating the parametric approach and the L-shaped method is proposed for solving the resulting SMILFP problem within a

reasonable computational time. The proposed model and algorithm are illustrated through a case study based on the Marcellus shale play.

In Chapter 6, we propose a novel game-theory-based stochastic model that integrates two-stage stochastic programming with a single-leader-multiple-follower Stackelberg game scheme for optimizing decentralized supply chains under uncertainty. Both the leader's and the followers' uncertainties are considered. The resulting model is formulated as a two-stage stochastic mixed-integer bilevel nonlinear program. A large-scale application to shale gas supply chains are presented to demonstrate the applicability of the proposed framework.

The dissertation concludes in Chapter 7.

## CHAPTER 2

### AN ENDPOINT-ORIENTED LIFE CYCLE OPTIMIZATION FRAMEWORK AND APPLICATION OF MODULAR MANUFACTURING

#### **2.1 Introduction**

In recent years, the rapid expansion of shale gas industry leads to continuing growth in shale gas production. However, the lack of midstream infrastructure impedes the exploitation of shale gas resources [70]. On the one hand, conventional shale gas processing facilities involve tremendous capital investment and lengthy construction time, resulting in significant risks for shale gas developers. On the other hand, exploitation of remote shale gas reserves can be economically infeasible under the current low price of natural gas [71]. Modular manufacturing has been proposed as a viable approach to address the aforementioned issues [72, 73]. Modular manufacturing devices are small-scale, highly mobile process units that are produced as individual modules and shipped to the sites of interest for quick assembling. Thanks to the mass production of modular components, these modular manufacturing devices can potentially alter the disadvantaged economies of small scale and maintain relatively low capital expenditures. When a certain shale gas reserve is depleted, the associated modular manufacturing devices can be easily disassembled and transferred to the next hot spot [73]. With the application of modular manufacturing devices, shale gas from distant shale gas reserves can be directly converted to valuable liquid products at local modular manufacturing devices and further trucked to markets. Therefore, shale reserves that are originally inaccessible due to the lack of midstream infrastructure can be economically exploited. Besides, methane leakage during gas transportation through

pipelines can be mitigated. Thus, compared with the conventional shale gas processing plants, the modular manufacturing devices have the potential of reducing the capital expenditures, improving the accessibility of shale gas energy resource, and mitigating the life cycle environmental impacts. There are existing literature addressing various aspects on design and operations of shale gas energy systems, including the strategic design of shale gas supply chains [4, 60], water management [57, 58], process synthesis and integration [49, 74, 75], shale gas related uncertainties [56, 76], and noncooperative stakeholders [77, 78]. However, none of them account for the emerging modular manufacturing approach. To systematically investigate the economic and environmental implications of shale gas modular manufacturing, it is imperative to account for and optimize relevant modular manufacturing options in shale gas supply chain design and operations for better economic and environmental sustainability.

Optimization models were proposed to simultaneously address the economic and environmental concerns in the optimal design and operations of shale gas supply chains [7, 59, 63]. However, existing literature considering environmental impacts of shale gas restrict their perspectives to certain midpoint environmental impact indicators, namely the GHG emissions, energy use, and water consumption [19, 64, 79, 80]. Despite the importance of these environmental impact categories, other impact categories, such as land occupation, ecotoxicity, and resource depletion, are equally important and should be taken into account in the sustainable design and operations of shale gas supply chains [81]. Although focusing on a specific environmental impact category might reduce the modeling complexity, such a restricted perspective may lead to biased solutions, and fail to yield a full picture of the environmental impacts of shale gas. More importantly,

limited by the midpoint life cycle impact assessment (LCIA) approach, the endpoint environmental impacts of shale gas on the ecosystem, human health, and natural resources remain unclear. To tackle these research challenges, it is essential to develop an endpoint-oriented LCO framework for shale gas supply chains with consideration of comprehensive midpoint and endpoint environmental impact categories.

There are two main research objectives of this work. The primary objective is to investigate the economic and environmental implications of incorporating modular manufacturing devices in shale gas supply chains. A novel mixed-integer nonlinear fractional programming (MINLFP) model is proposed, where design and operational decisions regarding both the conventional processing plants and modular manufacturing devices are considered. The allocation, capacity selection, installment, moving, and salvage decisions of modular manufacturing devices are modeled with corresponding integer variables and logic constraints. The second objective of this work is to develop a general endpoint-oriented LCO framework that can quantify the full spectrum of environmental impacts in the optimal design and operations of shale gas supply chains. An endpoint-oriented LCIA method ReCiPe is adopted, which comprises of 18 midpoint impact categories and three endpoint impact categories [82]. This endpoint-oriented LCIA approach is further integrated into a functional-unit-based multiobjective LCO framework to connect the optimization decisions with their environmental impact scores characterized by ReCiPe. In this LCO framework, we consider the well-to-wire life cycle of shale gas from the well drilling at shale sites to electricity generation at natural gas combined cycle (NGCC) power plants. Correspondingly, the environmental objective is formulated as minimizing the total endpoint environmental impact score per

Megawatt-hour (MWh) of electricity generation. The economic objective is minimizing the levelized cost of electricity (LCOE) generated from shale gas. This multiobjective LCO model allows for the establishment of tradeoffs between the economic and comprehensive environmental performances of shale gas supply chains in a systematic way. We further present a tailored global optimization algorithm integrating the parametric algorithm with a branch-and-refine algorithm to solve the resulting MINLFP problem efficiently. To illustrate the applicability of proposed modeling framework and tailored global optimization algorithm, a case study of a well-to-wire shale gas supply chain based on Marcellus Shale is considered.

The major novelties of this work are summarized below:

- A novel MINLFP model is proposed to systematically investigate the economic and environmental implications of incorporating modular manufacturing in shale gas supply chains with explicit consideration of corresponding design and operational decisions;
- An endpoint-oriented LCO framework is proposed that considers the full spectrum of environmental impacts in the LCO of shale gas supply chains;
- A case study of a well-to-wire shale gas supply chain based on Marcellus Shale is considered.

## **2.2 Problem statement**

In this section, we formally state the endpoint-oriented LCO framework for shale gas supply chains with modular manufacturing devices. This endpoint-oriented LCO framework integrates the four phases of LCA, namely the goal and scope definition,

inventory analysis, impact assessment, and interpretation [83], with a multiobjective MINLFP model. It can systematically identify the optimal design and operational strategies for shale gas supply chains with modular manufacturing devices under both economic and environmental criteria. The details of this LCO framework are introduced in the following subsections.

### 2.2.1 Goal and scope definition

The primary goal of this LCO framework is to optimize the design and operations of shale gas supply chains with modular manufacturing devices considering both economic and comprehensive environmental performances. This LCO framework accounts for the well-to-wire life cycle of shale gas, which starts with the well drilling at shale sites and ends with the electricity generation at NGCC power plants, following existing LCA studies of shale gas systems [79, 84]. The shale gas supply chain network is illustrated in Figure 7.

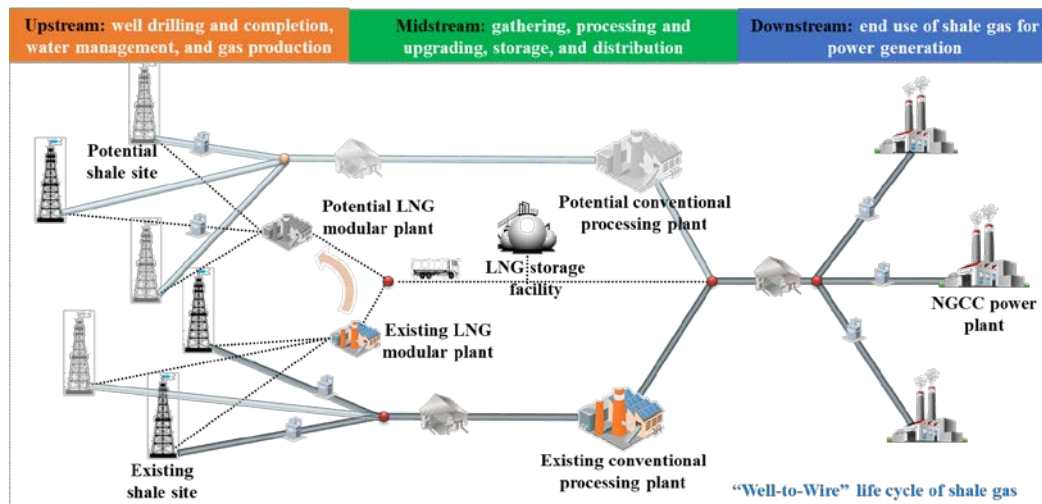


Figure 7. Illustrative shale gas supply chain network.

The system boundary of this well-to-wire life cycle of shale gas includes three major life cycle stages: shale gas production, shale gas processing and upgrading, and end use of shale gas. In addition to the conventional elements of a well-to-wire shale gas supply chain reported in the literature [64, 85, 86], we add new components regarding modular manufacturing, including modular liquefied natural gas (LNG) plants, LNG storage facilities, and corresponding transportation systems. The shale gas production stage involves all the development activities at a shale site, including the construction of shale sites, well drilling, hydraulic fracturing, water management, and shale gas production. The raw shale gas produced at shale sites then enters the shale gas processing and upgrading stage, where the shale gas can be either sent to the conventional processing plants or transported to the nearby modular manufacturing devices through pipelines. At both conventional processing plants and modular LNG plants, the raw shale gas goes through a series of processes, where impurities, such as water content, acid gas, and nitrogen, are removed, and two major products known as “pipeline-quality” natural gas and natural gas liquids (NGLs) are obtained [63]. In the modular LNG plants, the processed natural gas is further used to produce LNG. Since we focus on shale gas in this study, the separated NGLs are treated as by-products and sold at factory gate price in the well-to-wire shale gas supply chain directly [87]. Additionally, unlike the conventional processing plants, modular plants can be disassembled and moved to a new location throughout its life time [73]. We note that modular LNG plants are not the only application of modular manufacturing in monetizing shale gas. Another important application is to perform gas-to-liquids (GTL) conversion [72]. However, the GTL process leads to other types of products (e.g., diesel) that will not be used for electric

power generation. To better compare the economic and environmental performances of conventional and modular manufacturing devices in the well-to-wire shale gas supply chain, we focus on the modular LNG plants in this work. The natural gas from conventional processing plants can be directly distributed to local NGCC power plants through pipelines for electricity generation. Meanwhile, the LNG from modular plants can be either stored at storages facilities for a certain period or transported to the NGCC power plants when needed. Besides the power generation, there are other end uses of LNG. For instance, the report by the U.S. Department of Energy (DOE) summarized that the LNG chain provides natural gas consumed in homes and manufacturing and power generation facilities [88]. A recent report by GE claimed that rail, mining, remote stationary-power generation and trucking are the main markets for LNG produced at GE small-scale LNG plants [89]. However, to be consistent with the well-to-wire system boundary and compare the economic and environmental performances of modular LNG plants with conventional processing plants, we focus on the end use of power generation for both types of midstream equipment [90]. Unlike natural gas that is typically transported through pipelines, LNG can be easily transported by transport trailers [91]. In this study, corresponding to the well-to-wire life cycle of shale gas, we employ a functional unit of generating one MWh of electricity following the existing shale gas LCA studies [17, 79, 92]. Accordingly, both the economic and environmental performances are evaluated based this functional unit.

## 2.2.2 Inventory analysis

In the inventory analysis phase, the life cycle inventory (LCI) is established based on the predefined life cycle system boundary and functional unit to quantify the mass and energy input-output balance of each unit process across the shale gas life cycle. A detailed flow model is constructed based on the following flow chart in Figure 8, which consists of all the major unit process blocks and corresponding input and output flows within the well-to-wire system boundary. Specifically, the unit processes associated with modular manufacturing, including shale gas processing, LNG production, LNG storage, and distribution of LNG, are all considered and highlighted in the red box. The main data sources of this basic LCI are the most up-to-date LCA studies on shale gas and the Ecoinvent database v3.3 [19, 79, 81, 93]. Based on the basic LCI, an aggregated LCI is further developed to be compatible with the design and operational decisions in the LCO model. Accordingly, the mass and energy balance relationships of each unit process are formulated as mathematical constraints. In this way, the LCI of a set of design and operational alternatives can be simultaneously evaluated.

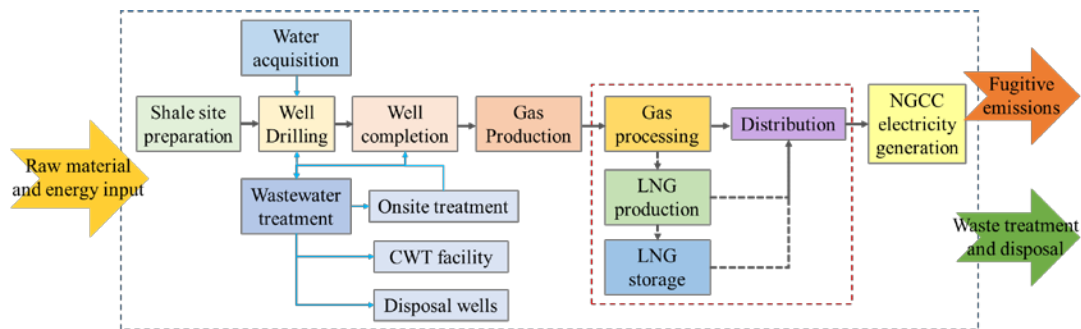


Figure 8. Life cycle stages of shale gas in a well-to-wire system boundary (unit processes associated with modular manufacturing are in the red box).

### 2.2.3 Impact assessment

In the phase of impact assessment, the LCI results are translated into corresponding environmental impacts under different impact categories based on the selected LCIA approaches. There are two types of impact categories, namely the midpoint impact categories reflecting the direct environmental impacts (e.g., climate change, ozone depletion, terrestrial acidification, etc.) of interventions, and the endpoint impact categories evaluating the ultimate environmental impacts from interventions or the midpoint impacts to the areas of protection (e.g., human health, ecosystem diversity, and resource availability). Based on these two types of environmental impact categories, there are midpoint-oriented LCIA methods, such as the one defined by the *Handbook on Life Cycle Assessment* [83] and endpoint-oriented methods, including the Eco-indicator 99 and the state-of-the-art ReCiPe methods [82, 94]. As mentioned before, most existing LCA studies of shale gas limit environmental impact assessments to certain midpoint indicators, namely the GHG emissions, energy use, and water consumption, instead of evaluating the comprehensive environmental impacts of shale gas [80, 92, 95-97]. In this study, we choose the endpoint-oriented LCIA approach ReCiPe to quantify the full spectrum of life cycle environmental impacts of shale gas supply chains with modular manufacturing devices. There are a total of 18 impact categories addressed at the midpoint level, including climate change, ozone depletion, terrestrial acidification, freshwater eutrophication, marine eutrophication, human toxicity, photochemical oxidant formation, particulate matter formation, terrestrial ecotoxicity, freshwater ecotoxicity, marine ecotoxicity, ionizing radiation, agricultural land occupation, urban land occupation, natural land transformation, water depletion,

mineral resource depletion, and fossil fuel depletion [82]. These midpoint impact categories are further converted and aggregated based on corresponding environmental mechanisms into three endpoint impact categories: damage to human health, damage to ecosystem diversity, and damage to resource availability [82]. A total endpoint environmental impact score can be obtained by following the ReCiPe methodology. A comprehensive environmental objective function can be further formulated. This environmental objective function in the LCO model enables automatic quantification of comprehensive environmental impacts of various design and operational alternatives. Figure 9 presents these environmental impact categories considered in this endpoint-oriented LCO framework. Here we emphasize the midpoint impact categories in blue boxes and the three endpoint impact categories, which are not addressed in most existing shale gas LCA studies.

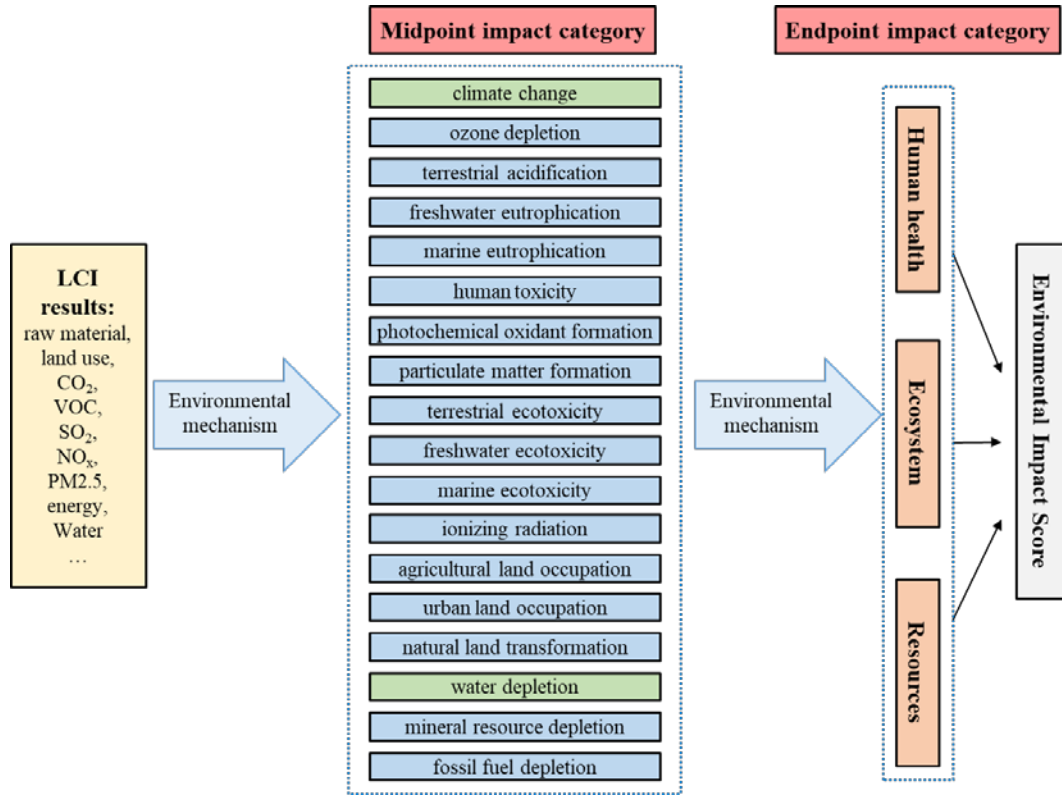


Figure 9. Illustrative figure of midpoint and endpoint environmental impact categories considered in the endpoint-oriented LCO model.

## 2.2.4 Interpretation

The interpretation phase is combined with solving the endpoint-oriented LCO problem. Through a comprehensive analysis of the economic and environmental performances associated with the optimal solutions, we can identify the key design and operational decisions that lead to the most economically and environmentally sustainable results. The trade-offs between economic and environmental performances are illustrated by a Pareto-optimal curve consisting of a series of solution points. The advantages and disadvantages of both the conventional processing plants and modular LNG plants can also be demonstrated under different preferences towards both criteria.

### **2.2.5 Detailed problem statement for endpoint-oriented LCO of shale gas supply chains with modular manufacturing devices**

In this section, we present the general endpoint-oriented LCO problem of the well-to-wire shale gas supply chain with modular manufacturing devices. The objective is to identify the optimal design and operational strategies in the shale gas supply chain, especially those regarding the modular manufacturing devices, considering both economic and comprehensive environmental performances.

We consider a planning horizon consisting of a set of time periods with identical intervals. Thus, the resulting LCO problem is a multi-period optimization problem. There are a set of shale sites, including existing ones with drilled wells ready to produce shale gas and potential ones to be developed. Each shale site allows multiple wells to be drilled, and the maximum number of wells that can be drilled at each shale site is given. The productivity profile, estimated ultimate recovery (EUR), and shale gas composition of each shale well are given as well. Three water management options are considered for handling wastewater, including centralized wastewater treatment (CWT), onsite treatment for reuse, and deep injection disposal wells [22, 36, 98]. For onsite treatment, we consider three wastewater treatment technologies, namely multi-stage flash (MSF), multi-effect distillation (MED), and reverse osmosis (RO) [99, 100]. Technology specific data regarding each of the water management options, such as capacities and water recovery factors, are all given.

The raw shale gas produced at shale sites is either sent to conventional processing plants or transported to modular LNG plants. We are given a set of existing processing plants and a set of potential ones to be constructed. Similarly, a set of existing and potential

modular LNG plants are given for gas processing and LNG production. For each modular LNG plant, there are a set of capacity levels to choose from. Once a modular LNG plant is constructed, it can be disassembled and moved to another location at any time. The processing efficiency of conventional processing plants and the production efficiency of modular LNG plants are all given. Besides, the salvage value of a modular LNG plant at the end of the planning horizon is given as a function of the modular device's life time.

The sales gas from the conventional processing plants is sent to a set of NGCC power plants with known electricity generation efficiency. LNG produced at modular plants, on the other hand, can be sent to a set of storage facilities for temporary storage or transported to a NGCC power plant directly for electricity generation. The capacities of storage facilities and electricity demand at each NGCC power plant are given.

There are two types of transportation links in this shale gas supply chain. Raw shale gas and sales gas are transported by pipelines, and LNG is transported by transport trailers. We are given a set of capacity levels for the pipeline network, and the transportation distance between each pair of locations is also given.

In this problem, the economic data, including the capital expenditure (CAPEX) associated with all the design decisions, as well as operating expenditure (OPEX) associated with all the operational decisions, are given. Additionally, the environmental impact scores associated with all the operational decisions are known. Based on the endpoint LCIA approach ReCiPe, these environmental impact scores are categorized into 18 midpoint impact categories and three endpoint impact categories.

Based on the given information, the objective of this LCO problem is to simultaneously optimize the economic and comprehensive environmental performances of the shale gas supply chain with modular manufacturing devices by optimizing the following decisions:

- Drilling schedule, production profile, and water management strategy at each shale site;
- Construction and capacity choices of conventional processing plants, locations and specs of modular manufacturing devices, moving schedule of modular manufacturing devices, and production planning of these two types of midstream processing infrastructure throughout the planning horizon;
- Installment and capacity selection of gathering pipeline networks, planning of transportation activities, and storage inventory management;
- Electric power generation profile at each NGCC power plant.

In accordance with the predefined well-to-wire system boundary and the functional unit of one MWh of electricity generation, we consider the following objective functions:

- Minimizing the LCOE generated from shale gas, which is formulated as the total net present cost (i.e., the summation of all the discounted future costs) throughout the shale gas supply chain divided by the total amount of electricity generated from shale gas.
- Minimizing the endpoint environmental impact score associated with producing one MWh of electricity, which is formulated as the total endpoint environmental impact score divided by the total amount of electricity generated from shale gas.

### 2.3 Model formulation and solution method

According to the problem statement in the previous section, a multiobjective MINLFP model is proposed to address the endpoint-oriented LCO of shale gas supply chains with modular manufacturing devices. For the compactness purpose, a general model formulation is presented here, and the detailed formulation is provided in Appendix A. All the parameters are denoted with lower-case symbols, and all the decision variables are denoted with upper-case symbols. The economic objective is to minimize the LCOE generated from shale gas, denoted as  $LCOE$  and formulated as the total net present cost ( $TC$ ) divided by the total amount of electricity generation ( $TGE$ ). The total net present cost ( $TC$ ) equals the summation of all the discounted future costs, including the CAPEX associated with the shale gas processing devices ( $C_{proc}^{CAPEX}$ ) and gathering pipelines ( $C_{trans}^{CAPEX}$ ), and the OPEX related to water management ( $C_{water,t}^{OPEX}$ ), drilling activities ( $C_{drill,t}^{OPEX}$ ), shale gas production operations ( $C_{prod,t}^{OPEX}$ ), shale gas processing and upgrading ( $C_{proc,t}^{OPEX}$ ), transportation activities ( $C_{trans,t}^{OPEX}$ ), LNG storage ( $C_{stor,t}^{OPEX}$ ), and electric power generation ( $C_{power,t}^{OPEX}$ ).  $C_{proc}^{CAPEX}$  involves concave terms that are formulated as exponential functions to calculate the CAPEX of conventional processing plants, as given by constraint (A3). The discount rate ( $dr$ ) is considered to account for the time value of money.  $TGE$  equals the summation of electricity generated by each NGCC power plant (indexed by  $g$ ) at each time period (indexed by  $t$ ), denoted as  $GE_{g,t}$ . The environmental objective is to minimize the endpoint environmental impact score per MWh electricity generation, denoted as  $UE$  and formulated as the total environmental impact score ( $TE$ ) divided by the total amount of electricity generation ( $TGE$ ). The total environmental

impact score accounts for the full spectrum of environmental impacts associated with water management ( $E_{water}$ ), shale well drilling, stimulation, and completion ( $E_{drill}$ ), shale gas production ( $E_{prod}$ ), shale gas processing ( $E_{proc}$ ), transportation ( $E_{trans}$ ), LNG storage ( $E_{stor}$ ), and electric power generation ( $E_{power}$ ). We note that both the numerator (i.e.,  $TC$  and  $TE$ ) and the denominator ( $TGE$ ) of the economic and environmental objective functions are major decisions variables to be optimized, thus resulting in two fractional objective functions. These fractional objective functions enable simultaneous optimization of economic and comprehensive environmental performances of the shale gas supply chain from a functional-unit-based perspective.

*Economic Objective:*

$$\min LCOE = \frac{TC}{TGE} = \frac{C_{proc}^{CAPEX} + C_{trans}^{CAPEX} + \sum_{t \in T} \left[ \frac{C_{water,t}^{OPEX} + C_{drill,t}^{OPEX} + C_{prod,t}^{OPEX} + C_{proc,t}^{OPEX} + C_{trans,t}^{OPEX} + C_{stor,t}^{OPEX} + C_{power,t}^{OPEX}}{(1+dr)^t} \right]}{\sum_{g \in G} \sum_{t \in T} GE_{g,t}} \quad (A1)$$

*Environmental Objective:*

$$\min UE = \frac{TE}{TGE} = \frac{E_{water} + E_{drill} + E_{prod} + E_{proc} + E_{trans} + E_{stor} + E_{power}}{\sum_{g \in G} \sum_{t \in T} GE_{g,t}} \quad (A24)$$

s.t. Economic Constraints (A2)-(A23)

Environmental Constraints (A25)-(A41)

Mass Balance Constraints (A42)-(A56)

Capacity Constraints (A57)-(A68)

Bounding Constraints (A69)-(A72)

Logic Constraints (A73)-(A85)

The constraints can be classified into six types, namely the economic constraints, environmental constraints, mass balance constraints, capacity constraints, bounding constraints, and logic constraints:

- Economic and environmental constraints are used to quantify the overall economic and environmental performances. Specifically, constraints (A2)-(A23) calculate the net present cost associated with different unit processes. Constraints (A25)-(A41) are used to evaluate the full spectrum of environmental impacts caused by different unit processes.
- Mass balance constraints describe the input-output mass balance relationships of different flows in all the unit processes across the shale gas supply chain. Specifically, the mass balance relationships associated with shale sites, conventional processing plants, modular manufacturing devices, LNG storage facilities, and NGCC power plants are presented by constraints (A42)-(A48), constraints (A49)-(A50) and (A53), constraints (A51)-(A52) and (A54), constraint (A55), and constraint (A56), respectively.
- Capacity constraints describe the capacity restrictions of different unit processes, including different water management options (constraints (A57)-(A60)), conventional shale gas processing (constraints (A61)), LNG production at modular manufacturing devices (constraints (A62)), LNG storage (constraints (A63)-(A65)), transportation (constraints (A66)-(A67)), and electricity generation (constraint (A68)).
- Bounding constraints link the midstream infrastructure design decisions with their corresponding operational decisions, including those regarding gathering

pipelines (constraints (A69)-(A70)), modular manufacturing devices (constraints (A71)), and conventional processing plants (constraints (A72)).

- Logic constraints describe the logic relationships among different strategic decisions, including those involved in well drilling (constraints (A73)-(A76)), water management (constraints (A77)), installment of gathering pipelines (constraints (A78)-(A79)), and construction and relocation activities of modular manufacturing devices (constraints (A80)-(A85)).

The economic and environmental objective functions of the proposed model are both fractional. As mentioned above, the economic objective function includes concave terms for calculating the CAPEX of conventional processing plants. All the constraints are linear with both integer and continuous variables. Therefore, the resulting problem is a nonconvex mixed-integer nonlinear programming (MINLP) problem that is computationally challenging for global optimization.

## **2.4 Tailored global optimization algorithm**

The resulting multiobjective MINLFP problem is computationally challenging to be optimized globally. Due to the combinatorial nature and pseudo-convexity of fractional objectives, large-scale mixed-integer fractional programming problems can be computationally intractable for general-purpose MINLP solvers [101, 102]. The concave terms in the fractional objective function introduce further computational complexity for global optimization [103, 104]. Based on the problem structure, we apply a tailored global optimization algorithm integrating the parametric algorithm [105] with a branch-and-refine algorithm [103, 106] to tackle this computational challenge.

Specifically, the parametric algorithm is implemented to tackle the fractional objectives, where an auxiliary parameter  $q$  is introduced to reformulate the original fractional objective function into a parametric one. Thus, the original optimal solution is identical to the optimal solution of the reformulated parametric problem with the parameter  $q^*$  such that  $F(q^*)=0$  [107]. The exact Newton's method is applied to iteratively converge to the optimal  $q^*$ . In each iteration of the parametric algorithm, we are facing a nonconvex MINLP due to the exponential function of CAPEX in the objective function. To tackle the separable concave functions, we adopt the branch-and-refine algorithm based on successive piecewise linear approximation. A pseudo-code of this algorithm is presented in Figure 10 to provide a comprehensive idea.

---

*Tailored Global Optimization Algorithm for MINLFP Problem*

---

```

1: Set  $q_0=0$ ,  $Iter^{out}=1$ ,  $obj=+\infty$ 
2: while  $obj \geq Tol^{out}$ 
3:   Set  $LB=-\infty$ ,  $UB=+\infty$ ,  $Iter^{in}=1$ ,  $gap=+\infty$ 
4:   Initialize the insertion points for piecewise approximation
5:   while  $gap \geq Tol^{in}$ 
6:     Solve piecewise approximated problem, and obtain optimal solution
        $x^*$  and optimal objective function value  $obj^{lo}$ 
7:     Evaluate the original objective function with  $x^*$ , and obtain  $obj^{up}$ 
8:     Reconstruct relaxed problem by adding a new partition point
9:     Set  $LB = \max\{LB, obj^{lo}\}$ ,  $UB = \min\{UB, obj^{up}\}$ ,  $gap = |1 - LB / UB|$ ,
        $Iter^{in} = Iter^{in} + 1$ 
10:   end while
11:   Update  $q^* = \frac{TC^*}{TGE^*}$ ,  $Iter^{out} = Iter^{out} + 1$ 
12: end while
13: output  $q^*$  and  $x^*$ 

```

---

Figure 10. Pseudo-code of the tailored global optimization algorithm for MINLFP

problems.

In this pseudo-code,  $q_0$  indicates the initial value of auxiliary parameter  $q$ .  $Iter^{out}$  and  $Iter^{in}$  are the iteration counting numbers for the outer loop and inner loop, respectively.  $Tol^{out}$  and  $Tol^{in}$  are the optimality tolerance for the parametric algorithm in the outer loop and the optimality tolerance for the branch-and-refine algorithm in the inner loop, respectively.  $UB$  and  $LB$  are the upper bound and lower bound for the inner loop, respectively.  $gap$  is an auxiliary parameter to record the relative gap between  $UB$  and  $LB$ .  $obj^{lo}$  and  $obj^{up}$  are auxiliary parameters to record the optimal objective values  $F(q)$  by solving the piecewise approximated problem and evaluating the original nonlinear objective function, respectively. As can be seen, the exact parametric algorithm is implemented in the outer loop to handle the fractional objective functions with  $q_0$  set to 0. Notably, the reformulated parametric problem is still a nonconvex MINLP with concave terms in the objective function  $F(q)$ . Thus, we replace the concave terms with successive piecewise linear approximation functions, and solve the resulting MILP problems iteratively following the branch-and-refine algorithm. The optimal objective value of this MILP provides a lower bound ( $LB$ ) of the objective value, and an upper bound ( $UB$ ) can be obtained by evaluating the original nonlinear objective function based on the optimal solution  $x^*$  of MILP. When the optimality criterion in the inner loop is satisfied, the next outer loop iteration starts with updated parameter  $q^*$ . This tailored global optimization algorithm is guaranteed to converge within finite iterations [108].

## **2.5 Results and discussion**

To illustrate the applicability of the proposed endpoint-oriented LCO model of shale gas supply chains with modular manufacturing devices, we consider a case study of a well-to-wire shale gas supply chain based on Marcellus Shale with both conventional shale gas processing plants and modular LNG plants. The detailed problem description is given below, and a reference map is provided in Figure 11. The shale site locations are based on the data reported by MarcellusGas.org [109]. Information on the existing conventional processing plants is reported by MarkWest Energy Partners, L.P [110]. The locations of power plants are based on the data provided by U.S. Energy Information Administration [111]. Notably, the proposed endpoint-oriented LCO framework and global optimization algorithm are general enough, so their applications are not limited to shale gas supply chains at any specific region.

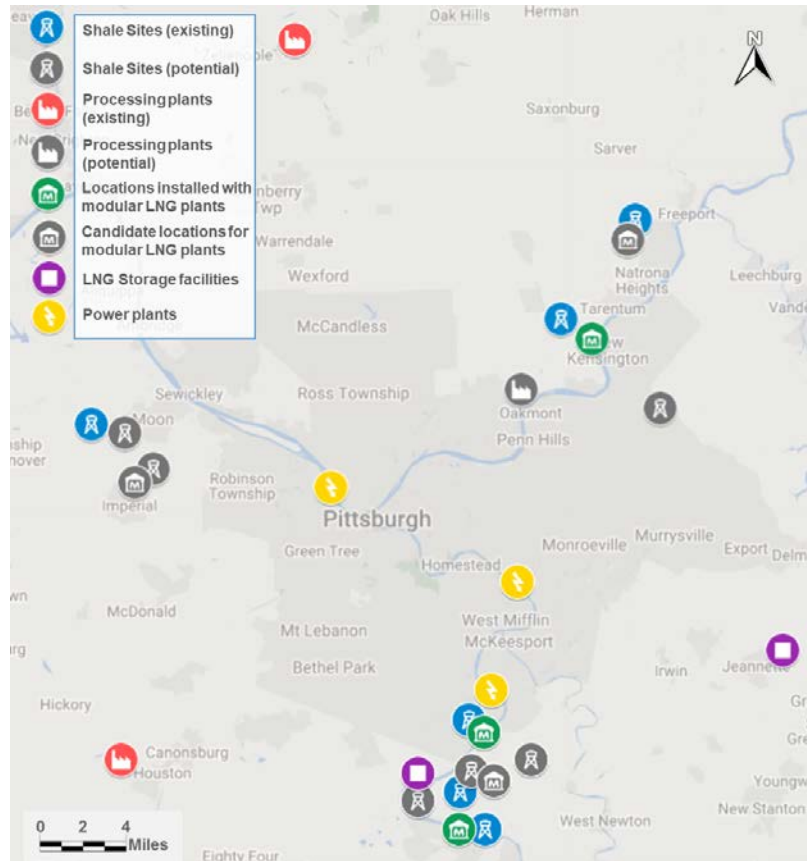


Figure 11. Reference map of the well-to-wire shale gas supply chain based on Marcellus Shale in the case study.

As can be seen in Figure 11, a total of 12 shale sites are considered, among which six shale sites are existing ones with active wells and six shale sites are potential ones to be developed. Each shale site allows for drilling of up to four to eight shale wells [112]. The EUR of each shale well is estimated based on the data reported in Marcellus Shale [2, 113]. There are two existing and one potential conventional shale gas processing plants [49]. Up to six locations are considered for the modular LNG plants, among which locations 2, 4, and 6 are installed with modular plants, and locations 1, 3, and 5 are candidate ones for the installation of modular plants. Based on the report by GE Oil & Gas [114], there are three capacity levels for the modular LNG plants, corresponding

to 25 kgal, 50 kgal, and 100 kgal maximum LNG production per day, respectively. For the gathering pipelines, we consider three capacity levels, which correspond to 4-inch, 8-inch, and 12-inch specs, respectively [70]. There are two LNG storage facilities where LNG products can be temporarily stored before being sent to the market. In this well-to-wire shale gas supply chain, there are three NGCC power plants with combined cycle gas turbines, and the average efficiency is 50% on a lower heating value (LHV) basis [96, 115]. A 10-year planning horizon is considered, which is close to the real productive life of Marcellus shale wells [116, 117]. The planning horizon is divided into 20 time periods, and each time period represents half a year. The corresponding shale gas supply chain network is presented in Figure 12, where existing facilities are presented in color and potential ones are given in grayscale. All detailed input data are based on existing literature and the Ecoinvent database v3.3 [4, 19, 64, 79, 81, 93, 96, 118-120]. Specifically, the CAPEX of conventional processing plants is calculated based on a typical concave function, which is widely applied in designs of general chemical processes and shale gas processing plants [4, 121]. Meanwhile, we adopt a capital cost curve from the literature to estimate the CAPEX associated with modular LNG plants [72]. The detailed model formulation is provided in Appendix A. Notably, the modular manufacturing technologies are still relatively immature in the market, so variations in the costs associated with modular plants are inevitable. To evaluate the influences of uncertainties, we conduct sensitivity analysis of multiple key parameters, including the average EUR of shale wells, average NGL composition in shale gas, average transportation distance, CAPEX for modular plant installation, and electricity demand. Moreover, to demonstrate the advantage of proposed functional-unit-based

LCO model over the conventional LCO model optimizing the overall economic and environmental performances (named as overall-performance LCO model), we add one section in the case study to present the difference in terms of their overall performances and specific optimal strategies.

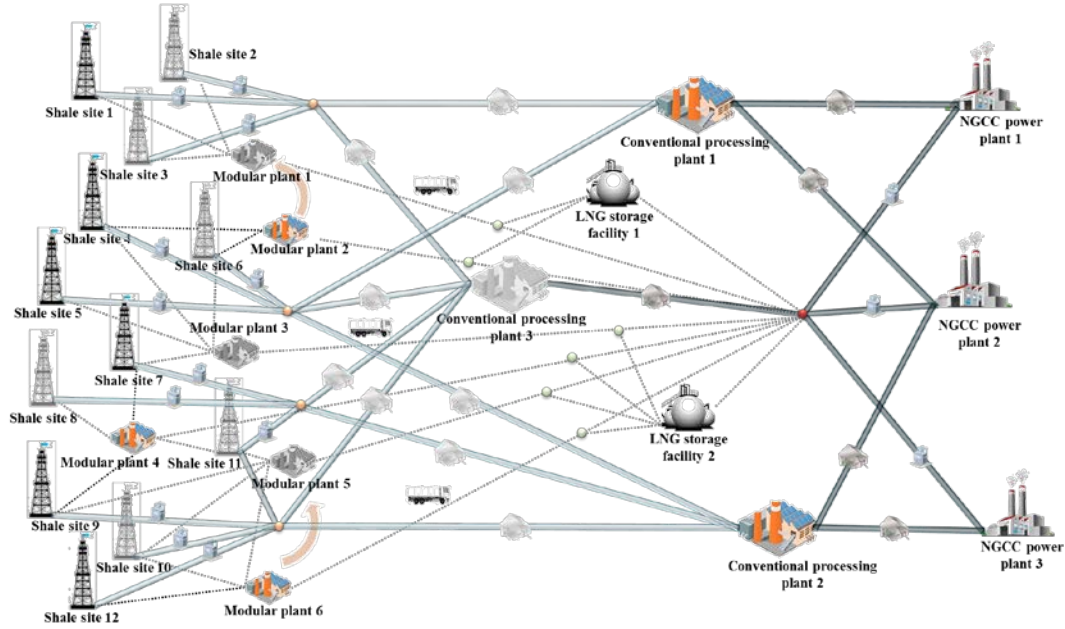


Figure 12. Shale gas supply chain network considered in the case study.

Based on the proposed LCO model, the resulting MINLFP problem has 4,012 integer variables, 13,767 continuous variables, and 9,556 constraints. All the models and solution procedures are coded in GAMS 24.7.3 [122] on a PC with an Intel® Core™ i7-6700 CPU and 32GB RAM, running the Window 10 Enterprise, 64-bit operating system. Furthermore, the MILP subproblems are solved using CPLEX 12.6.3. The absolute optimality tolerance of CPLEX is set to  $10^{-6}$ . The absolute optimality gap for the outer loop parametric algorithm ( $Tol^{out}$ ) is set to  $10^{-6}$ . The relative optimality gap ( $Tol^{in}$ ) for the inner loop branch-and-refine algorithm is set to  $10^{-2}$ . The detailed computational performance is presented in Appendix C.

### 2.5.1 Economic and environmental implications of modular manufacturing devices

The resulting MIBLFP problem is solved using the presented tailored global optimization algorithm and a Pareto-optimal curve consisting of 13 Pareto-optimal solutions is shown in Figure 13. The  $x$ -axis represents the ReCiPe endpoint environmental impact score per MWh electricity generation from shale gas. The  $y$ -axis represents the LCOE in the shale gas supply chain.

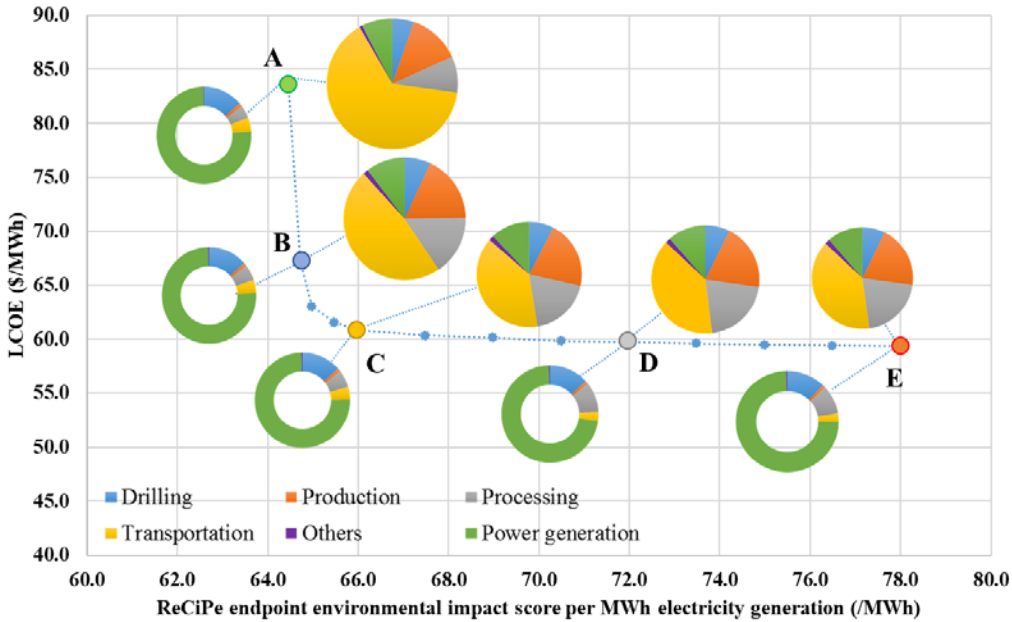


Figure 13. Pareto-optimal curve illustrating the trade-offs between LCOE and ReCiPe endpoint environmental impact score per MWh electricity generation with breakdowns: pie charts for the LCOE breakdowns and donut charts for the breakdowns of environmental impact score per MWh electricity generation. Along this Pareto-optimal curve, we choose 5 solution points from point A to point E for comparison. Point A indicates the optimal solution with the smallest ReCiPe

endpoint environmental impact score per MWh electricity generation as 64.5 points/MWh. Point E is the other extreme point with the lowest LCOE of \$59.4/MWh. Points B, C, and D are the in-between solutions. Their corresponding LCOE breakdowns are presented with pie charts above the curve, and the breakdowns of environmental impact score per MWh electricity generation are demonstrated with the donut charts below the curve. The sizes of these charts are proportional to the absolute values of total net present cost and total environmental impact score. For the cost breakdowns, the costs associated with transportation, gas processing, and gas production activities contribute most to the LCOE. From point A to point E, since more modular LNG plants are installed, the corresponding CAPEX under the category of processing increases as well. Meanwhile, less gathering pipelines are required with these modular LNG plants, resulting in less transportation cost. As to the breakdowns of environmental impact score per MWh electricity generation, the power generation sector accounts for around three-fourths of the environmental impact score. The remaining environmental impact score is mainly contributed by drilling, processing, and transportation activities. From point A to point E, the portion of environmental impact score associated with processing activities increases, and the portion associated with transportation activities decreases accordingly for the similar reason as discussed above on the LCOE breakdowns.

To investigate the strategic decisions regarding modular manufacturing devices that lead to distinct economic and environmental performances, in Figure 14 we present the detailed design and planning decisions for modular LNG plants in different Pareto-optimal solutions. As can be seen, in the optimal solution of point A minimizing the

environmental impact score per MWh electricity generation, there are four modular LNG plants. In addition to the existing modular plants installed at locations 2, 4, and 6, another modular plant with a capacity of 25 kgal LNG/day is installed at location 1 in the beginning. Since the construction time of modular plants considered in this case study is one year, the newly installed modular plant at location 1 becomes available after the first year [123]. Both point B and point C share the same design and planning decisions on modular LNG plants. Specifically, in addition to the existing ones, two modular plants with capacities of 25 kgal LNG/day are installed at location 1 and location 5 in the beginning, respectively. No moving activities are observed in the solutions of point A, point B, and point C. Points D and E have the same modular LNG plants as point B and point C installed in the beginning. However, relocation of modular LNG plants is observed in the optimal solutions of point D and point E. Specifically, for point D, the modular plant at location 5 with a capacity of 25 kgal LNG/day is moved to location 6 after three and a half years; meanwhile, the modular LNG plant at location 6 with a capacity of 50 kgal LNG/day is moved to location 5. For point E, the modular plant at location 5 with a capacity of 25 kgal LNG/day is moved to location 6 three years later, and the modular plant at location 6 with a capacity of 50 kgal LNG/day is moved to location 5 half a year later. Such an exchange of modular LNG plants matches the varying demand of processing capacity at different regions. Since no new shale wells are drilled near location 6, and the production of existing wells are decreasing with time, the original modular LNG plant (50 kgal LNG/day) provides more processing capacity than needed after a few years. Meanwhile, the modular plant at location 5 (25 kgal LNG/day) cannot handle the extra shale gas feedstock from the newly-drilled shale

wells. Therefore, it is considered more cost-effective to exchange the modular LNG plants at locations 5 and 6 than installing extra ones. The moving process takes around six months to complete, so the relocated modular LNG plant will be ready half a year later. The moving option of modular LNG plants offers more flexibility in the operations of a shale gas supply chain, and the overall economic performance can be improved. Nevertheless, the moving activities of modular plants incur extra environmental impacts, such as land use change, energy consumption, and emissions. Thus, the relocation of modular plants may not be preferred when minimizing the comprehensive environmental impacts is the main objective. These environmental impact results will be discussed in detail in the following “comprehensive environmental impacts assessment” subsection. Additionally, it is worth noting that these optimal strategies regarding the modular LNG plants are only obtained based on the specific model and input data considered in this study, and the actual strategy in practice may vary from case to case.

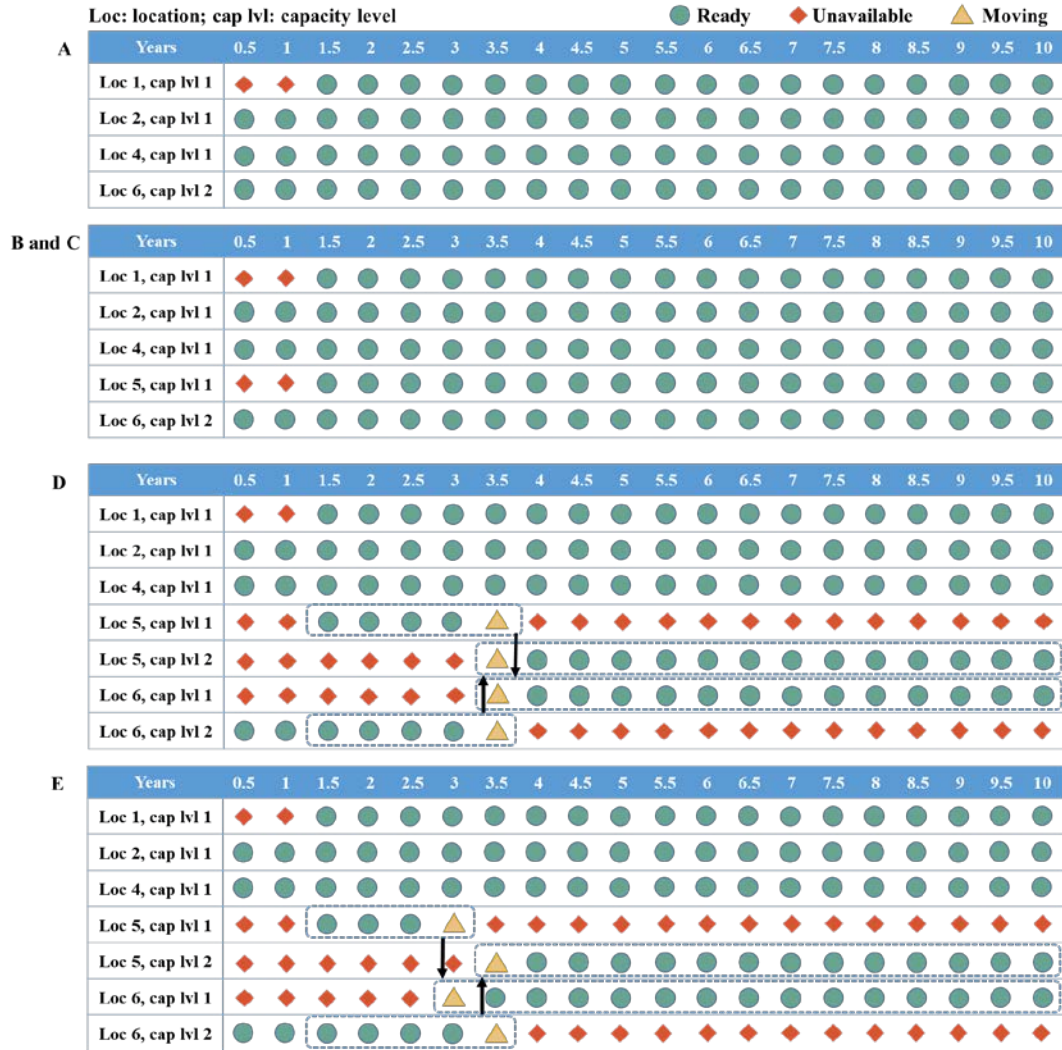


Figure 14. Design and planning decisions for modular LNG plants in different Pareto-optimal solutions.

In Figure 15, we summarize the CAPEX and OPEX regarding conventional processing plants and modular LNG plants of the five Pareto-optimal solutions. For all the five solution points, a conventional processing plant is constructed with 10 Tscf/year processing capacity in addition to two existing ones. Thus, all the five points have the same CAPEX for conventional processing plants. However, the OPEX of conventional processing plants in each solution is quite different. We identify that when the OPEX

associated with conventional processing plant decreases, the OPEX resulted from modular LNG plants increases accordingly, as can be induced by going from point A to point E. This is because the raw shale gas in each Pareto-optimal solution will be either processed by the conventional processing plants or sent to the modular LNG plants for LNG production. Therefore, we conclude that the application of modular LNG plants helps improve the economic performance of a shale gas supply chain. However, in terms of mitigating the overall environmental impacts, the modular LNG plants show no advantage over the conventional processing plants.

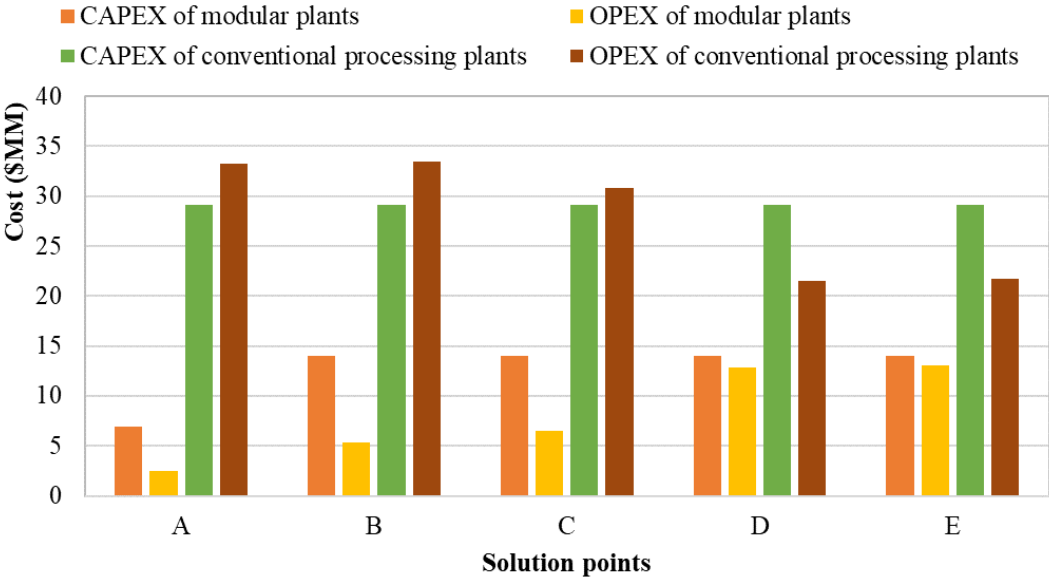


Figure 15. Summary of CAPEX and OPEX regarding conventional processing plants and modular LNG plants in different Pareto-optimal solutions.

Next, we present the detailed drilling schedules (on the left) and shale gas production profiles (on the right) corresponding to points A to E in Figure 16. From this comparison, we expect to gain some insight into the connection between upstream production and midstream infrastructure designs. For all the solution points, more shale

wells need to be drilled after the initial drilling activities to compensate for the decreasing production of shale wells. From the drilling schedules, we can find that more shale wells are drilled in the beginning in point A and point B, resulting in a higher peak in terms of shale gas production in the first few years. As to point D and point E, they have similar drilling schedules, which result in almost identical shale gas production profiles. Moreover, the drilling schedules of point D and point E show that three new wells are drilled at shale site 10 in the fourth year, resulting in a larger shale gas output near location 5 to be processed. This explains why the modular plant at location 6 with a capacity of 50 kgal LNG/day is moved to location 5 in the same year, as presented in Figure 14. The drilling schedule and corresponding shale gas production profile of point C are balanced between the environment-oriented solutions (point A and point B) and the economics-oriented solutions (point D and point E).

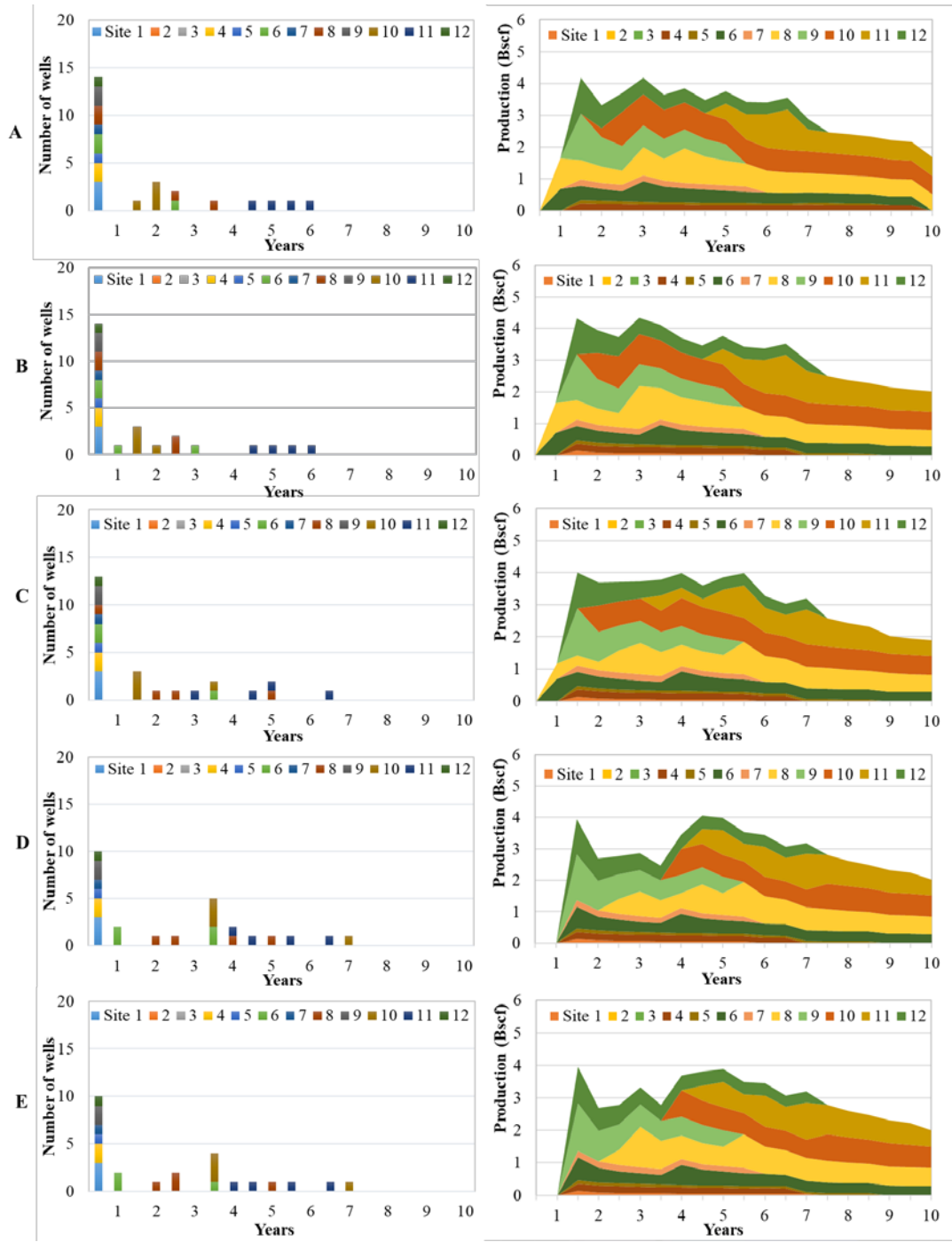


Figure 16. Drilling schedules and shale gas production profiles of different Pareto-optimal solutions.

In this section, we present and analyze the comprehensive environmental impact profiles of different Pareto-optimal solutions. As mentioned in the introduction section,

the ReCiPe approach for LCIA comprises of 18 midpoint impact categories and three endpoint impact categories [82]. The detailed midpoint environmental impact score breakdowns associated with Pareto-optimal solutions A to E are presented in Figure 17. As can be seen, all the five points share similar environmental impact score breakdowns except point A and point B, which differ in the category of water management. The impacts of climate change to human health (in green) and climate change to ecosystems (in orange) stand out as two major contributors especially in the life cycle stages of shale gas production, LNG storage, and power generation. Fossil depletion is one of the major midpoint impact categories in water management, drilling, shale gas processing, and transportation, which are all energy-intensive processes. The human toxicity is another key midpoint impact category especially in water management and drilling phases, when large amounts of chemicals and additives are used in drilling and fracturing fluids. The different wastewater treatment strategies also result in disparate environmental performance. Thus, when the objective focuses on mitigating the environmental impacts as shown in point A and point B, we observe a different environmental impact breakdown. By investigating the corresponding water management strategies, we identify RO technology for onsite treatment as the optimal wastewater treatment technology in point A and point B. Nevertheless, in points C to E, all the wastewater is treated by remote CWT facilities for a better economic performance.



Figure 17. Midpoint environmental impact score breakdowns of different Pareto-optimal solutions.

To identify the key midpoint impact categories that contribute most to the environmental impact score in the life cycle of shale gas, we further investigate the absolute midpoint environmental impact scores associated with different Pareto-optimal solutions. Since all the five Pareto-optimal solutions have similar midpoint environmental impact score

breakdowns, we present the absolute midpoint environmental impact scores of point A in Figure 18 for illustration. From this result, we identify the climate change impact on human health, climate change on ecosystems, and human toxicity as the most significant midpoint environmental impact categories. These impact categories contribute to around 91% of the total environmental impact score. Other important midpoint environmental impact categories include metal depletion, fossil depletion, particulate matter formation, and natural land transformation.

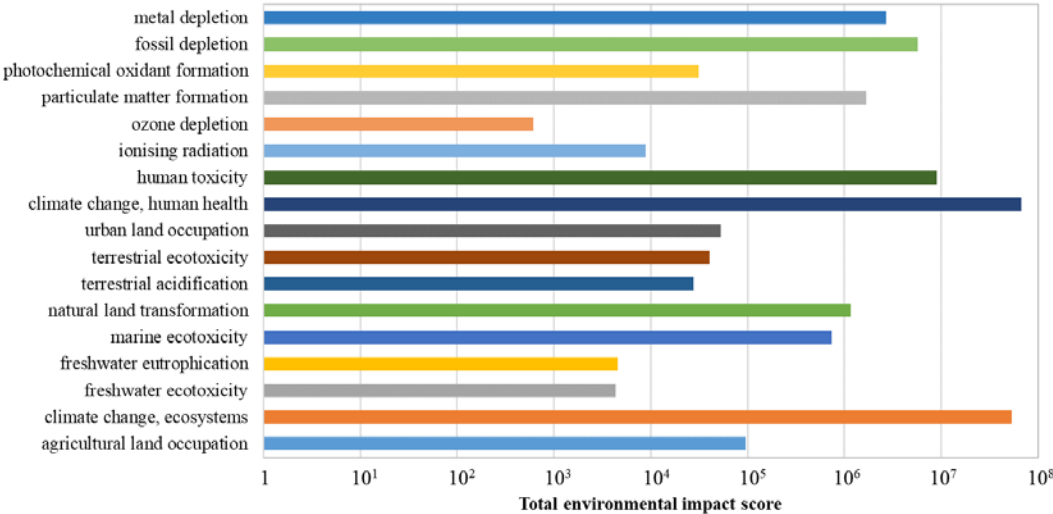


Figure 18. Absolute midpoint environmental impact scores of point A.

In Figure 19, we further present the endpoint environmental impact breakdowns corresponding to different Pareto-optimal solutions. Here we select the environment-oriented solution point A as the reference solution, and all the other solutions are presented with their ratios based on the result of point A. As can be seen, for all the three endpoint impact categories, namely ecosystem quality, human health, and resources, all the three points from C to E have higher environmental impact scores than

point A in certain life cycle stages, including water management, shale gas processing, and storage. The endpoint environmental impact score distribution of point B is similar to that of point A except a slightly higher impact score in storage. The endpoint environmental impact score distributions of points D and E are almost identical. Since the total endpoint environmental impact score is the summation of scores from the three endpoint impact categories, from the shapes of these four distributions we conclude that the environmental impacts on ecosystem quality and human health contribute most to the environmental impact score. Specifically, the environmental impacts on ecosystem quality account for 37%-39% of the total environmental impact score; the environmental impacts on human health contribute 54%-55% of the total environmental impact score; and the environmental impacts on resources result in 6%-7% of the total environmental impact score. The water management strategies and design and planning of midstream infrastructure are the key decisions that lead to distinct environmental performances.

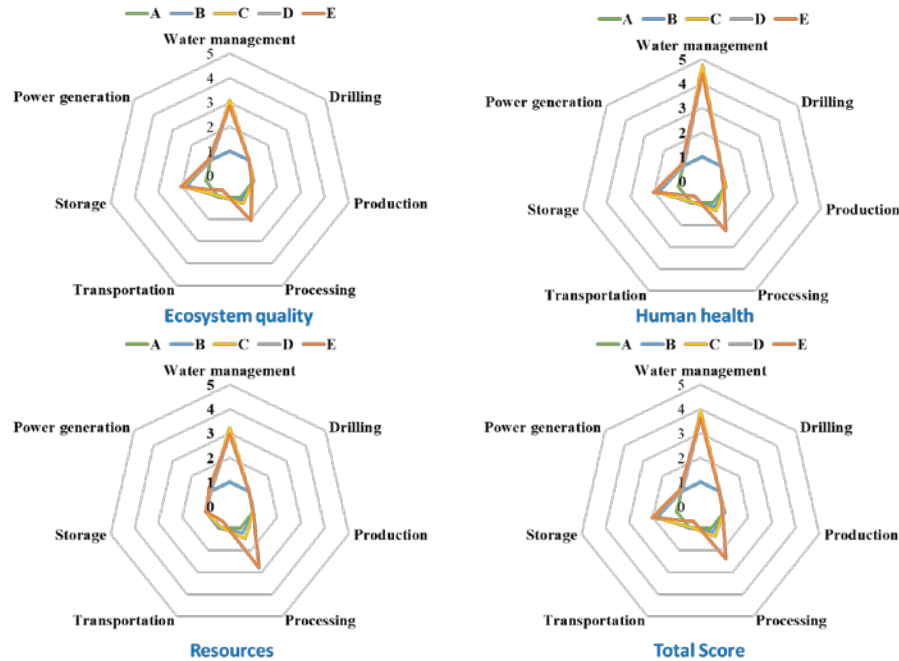


Figure 19. Endpoint environmental impact score breakdowns and comparison of different Pareto-optimal solutions (The environment-oriented solution A is selected as the reference solution and all the other solutions are presented with ratios of their results to that of point A).

### 2.5.2 Sensitivity analysis

In this section, we present a sensitivity analysis regarding several key parameters, including the average EUR of shale wells, average NGL composition in shale gas, average transportation distance, CAPEX for modular plant installation, and electricity demand. Their impacts on the two optimization objectives, namely the LCOE and the endpoint environmental impact score per MWh of electricity generation are summarized in Figure 20. A variance range of 80% to 120% is considered for the five types of uncertainties. As can be seen, the LCOE is most sensitive to the average transportation distance. Longer transportation distance results in extra transportation cost, and thus

leads to a higher LCOE. Another important factor is the average EUR of shale wells. With greater average EUR of shale wells, the cost efficiency of a certain shale well improves, resulting in a lower LCOE. The impact of CAPEX for modular plant installation is straightforward. More CAPEX leads to a higher value of LCOE. As the average NGL composition in the raw shale gas increases, the LCOE decreases due to the extra income from the sales of NGLs. The LCOE is least sensitive to the electricity demand. The endpoint environmental impact score per MWh of electricity generation does not follow the same trend as LCOE. The sensitivity analysis of average transportation distance leads to some interesting results. First, from the range of 80% to 100%, there is no significant change in the endpoint environmental impact score per MWh of electricity generation. This is mainly because transportation only contributes a small portion (3%) of the total environmental impact score. However, when the transportation distance increases to 120%, a different midstream design strategy will be adopted. More modular plants are installed to produce LNG instead of relying on the conventional processing plants. The change of midstream design strategy further leads to a higher endpoint environmental impact score per MWh of electricity generation. Both the electricity demand and the average EUR of shale wells have significant impacts on the endpoint environmental impact score per MWh of electricity generation. As the average EUR of shale wells increases, more shale gas can be produced with the same environmental impact score. The impacts of average NGL composition in shale gas and CAPEX for modular plant installation on the endpoint environmental impact score per MWh of electricity generation are almost negligible.

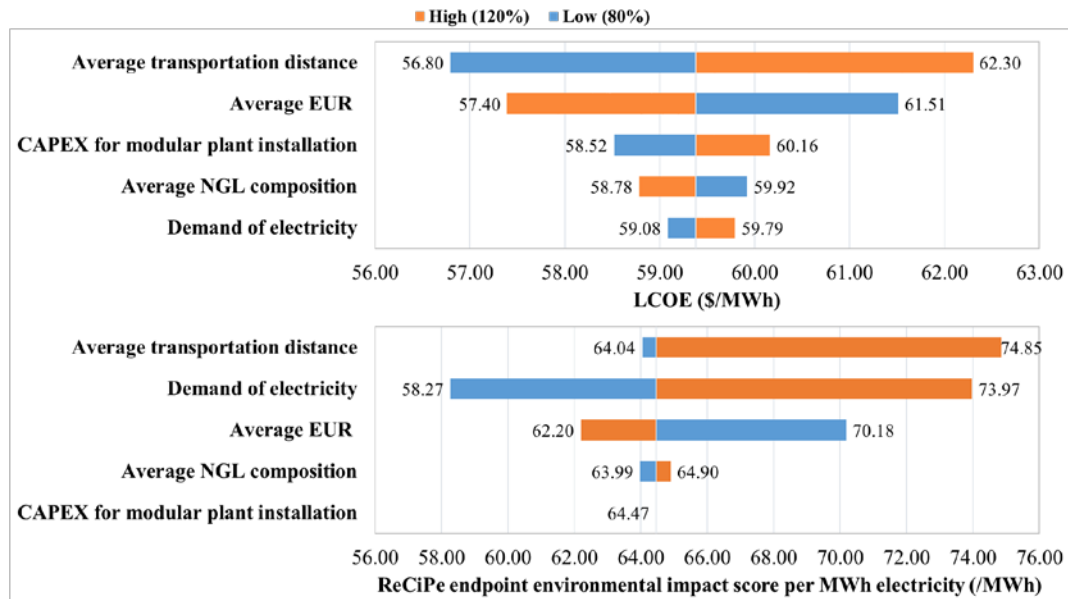


Figure 20. Sensitivity analysis of average EUR of shale wells, average NGL composition in shale gas, average transportation distance, CAPEX for modular plant installation, and electricity demand.

### 2.5.3 Comparison with the overall-performance LCO model

Functional-unit-based LCO model is known for its superiority in leading to more sustainable designs than traditional LCO models optimizing the overall economic and environmental performances of a product system. To demonstrate the advantage of proposed functional-unit-based LCO model, we consider another case study based on an overall-performance LCO model. In this overall-performance LCO model, the economic objective is to minimize the total net present cost ( $TC$ ), which is identical to the numerator of the economic objective function in the functional-unit-based LCO model. The economic objective function  $TC$  is nonlinear with separable concave terms calculating the CAPEX of conventional processing plants. The environmental objective is to minimize the total ReCiPe endpoint environmental impact score ( $TE$ ), which is the

numerator of the environmental objective function in the functional-unit-based LCO model. All the constraints in the overall-performance LCO model are identical to those in the functional-unit-based LCO model. The detailed formulation of this overall-performance LCO model is summarized in Appendix B.

By solving the overall-performance LCO problem, another Pareto-optimal curve can be obtained demonstrating the trade-offs between the total net present cost ( $TC$ ) and the total ReCiPe endpoint environmental impact score ( $TE$ ). To give a clear comparison, we present the Pareto-optimal solutions obtained by solving the overall-performance LCO problem (orange points) and the functional-unit-based LCO problem (blue points) in Figure 21. From this comparison, we can see the advantage of the proposed functional-unit-based LCO model on providing more sustainable solutions from both economic and environmental perspectives. The whole Pareto-optimal frontier of the overall-performance LCO problem lies within the suboptimal region of the functional-unit-based LCO problem, indicating that these Pareto-optimal solutions of the overall-performance LCO problem would incur higher cost or environmental impact score than those of the functional-unit-based LCO problem by producing one MWh of electricity. Specifically, we select two sets of extreme points, namely the environment-oriented solutions A and A', and the economics-oriented solutions E and E', for further comparison. As can be seen, the LCOE of point A' is slightly higher than that of point A, and the ReCiPe endpoint environmental impact score per MWh electricity generation of point A' is about 9% higher than that of point A. Although the ReCiPe endpoint environmental impact score per MWh electricity generation of point E' is slightly lower

than that of point E, its LCOE is 5% higher than that of point E, which can result in a significant difference in terms of economic performance.

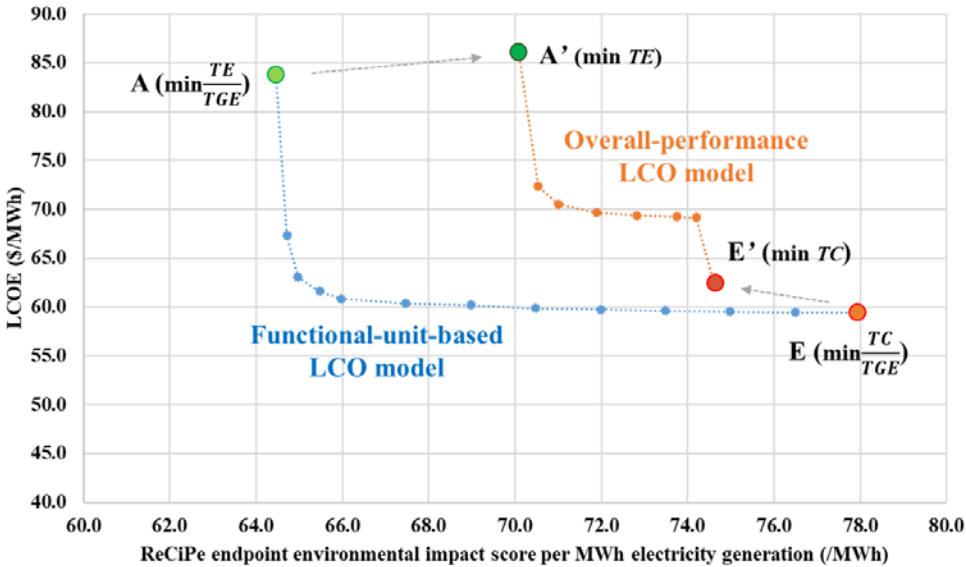


Figure 21. Comparison of Pareto-optimal solutions of the proposed functional-unit-based LCO problem optimizing the functional-unit-based economic and environmental performances and the overall-performance LCO problem optimizing the overall economic and environmental performances.

Additionally, in Figure 22, we present the optimal drilling schedules and shale gas production profiles obtained by solving the functional-unit-based LCO problem and the overall-performance LCO problem to further demonstrate the difference. Point E and point E' in Figure 21 are selected here for comparison. As can be observed, although both point E and point E' are optimizing the economic performance, the different objective functions adopted in the functional-unit-based LCO model and the overall-performance LCO model can lead to distinct design and operational decisions. Specifically, more wells are drilled in the optimal solution of the functional-unit-based LCO problem (point E) than in the optimal solution of the overall-performance LCO

problem (point E'). Consequently, the optimal shale gas production profile in point E deviates from that of point E'.

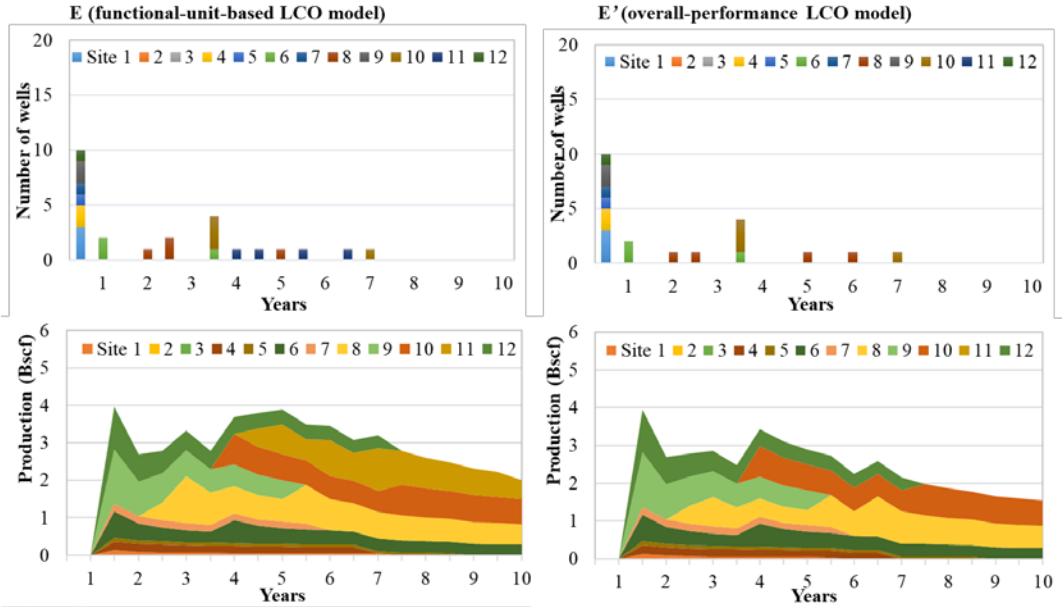


Figure 22. Drilling schedules and production profiles in the Pareto-optimal solution point E of the functional-unit-based LCO problem and the Pareto-optimal solution point E' of the overall-performance LCO problem.

### 2.6 Summary

In this work, a novel endpoint-oriented LCO model was proposed to investigate the economic and environmental implications of incorporating modular manufacturing devices in the optimal design and operations of shale gas supply chains. The resulting problem was formulated as an MINLFP problem, and a tailored global optimization algorithm was introduced to tackle this computational challenge. The applicability of proposed endpoint-oriented LCO framework and tailored global optimization algorithm was illustrated by a well-to-wire shale gas supply chain based on Marcellus Shale. Major

design and operational decisions, especially those regarding the modular manufacturing devices, such as allocation, capacity selection, installment, moving, and salvage decisions, were all captured. Through a detailed analysis and discussion, we came to a few important conclusions: (1) application of modular manufacturing devices could improve the economic performance of a shale gas supply chain. However, there was no obvious advantage of modular manufacturing devices over the conventional processing plants in terms of mitigating the overall environmental impacts; (2) the proposed endpoint-oriented LCO framework enabled quantification of the full spectrum of life cycle environmental impacts of shale gas supply chains, and thus leading to more sustainable solutions; (3) major design decisions regarding drilling schedule, water management, and midstream infrastructure design and planning were identified as the key factors that led to distinct economic and environmental performances in a shale gas supply chain.

## **2.7 Appendix A: Superstructure configuration description**

### **2.7.1 Economic objective**

The economic objective is to minimize the LCOE generated from shale gas, formulated as the total net present cost divided by the total electric power generation. The total net present cost comprises of the CAPEX associated with the shale gas processing devices ( $C_{proc}^{CAPEX}$ ) and gathering pipelines ( $C_{trans}^{CAPEX}$ ), and the OPEX related to water management ( $C_{water,t}^{OPEX}$ ), drilling activities ( $C_{drill,t}^{OPEX}$ ), shale gas production operations ( $C_{prod,t}^{OPEX}$ ), shale gas

processing and upgrading ( $C_{proc,t}^{OPEX}$ ), transportation activities ( $C_{trans,t}^{OPEX}$ ), LNG storage ( $C_{stor,t}^{OPEX}$ ), and electric power generation ( $C_{power,t}^{OPEX}$ ).

$$\min LCOE = \frac{C_{proc}^{CAPEX} + C_{trans}^{CAPEX} + \sum_{t \in T} \left[ \frac{C_{water,t}^{OPEX} + C_{drill,t}^{OPEX} + C_{prod,t}^{OPEX} + C_{proc,t}^{OPEX} + C_{trans,t}^{OPEX} + C_{stor,t}^{OPEX} + C_{power,t}^{OPEX}}{(1+dr)^t} \right]}{\sum_{g \in G} \sum_{t \in T} GE_{g,t}} \quad (A1)$$

The CAPEX of shale gas processing devices comprises of the CAPEX associated with conventional processing plants ( $C_{proc\_conv}^{CAPEX}$ ) and the CAPEX corresponding to modular manufacturing devices ( $C_{proc\_mod}^{CAPEX}$ ).

$$C_{proc}^{CAPEX} = C_{proc\_conv}^{CAPEX} + C_{proc\_mod}^{CAPEX} \quad (A2)$$

$C_{proc\_conv}^{CAPEX}$  is the total CAPEX associated with construction of conventional processing plants. In this study, we adopt a typical nonlinear function to calculate the CAPEX following the existing literature [4, 121].

$$C_{proc\_conv}^{CAPEX} = \sum_{p \in P_n} pri \cdot \left( \frac{PC_p}{prc} \right)^{sfp} \cdot \left( \frac{pci}{rpci} \right) \quad (A3)$$

where  $pri$  denotes the reference CAPEX of conventional processing plants.  $PC_p$  denotes the capacity of conventional processing plant  $p$ .  $prc$  denotes the reference capacity of conventional processing plants.  $sfp$  denotes the size factor of conventional processing plants.  $pci$  denotes the chemical engineering plant cost index for conventional processing plants.  $rpci$  denotes the chemical engineering plant cost index for conventional processing plant of the reference year.

$C_{proc\_mod}^{CAPEX}$  is the net CAPEX associated with modular LNG plants, given as the total installment cost subtracted by the total salvage value of modular LNG plants. The

CAPEX of modular LNG plant is estimated based on a capital cost curve from the literature, which is obtained by fitting the data on capital costs from existing and hypothetical LNG plants from the literature [72].

$$C_{proc\_mod}^{CAPEX} = \sum_{m \in M} \sum_{k \in K} \sum_{t \in T} \frac{cam_{m,k} \cdot ZI_{m,k,t}}{(1+dr)^t} - \sum_{m \in M} \sum_{k \in K} \sum_{t \in T} csm_{k,t} \cdot ZI_{m,k,t} \quad (A4)$$

where  $cam_{m,k}$  denotes the CAPEX for installing a modular LNG plant with capacity level  $k$  at location  $m$ .  $ZI_{m,k,t}$  is a binary variable that equals 1 if a modular LNG plant with capacity level  $k$  is installed at location  $m$  in time period  $t$ .  $dr$  is the discount rate per time period.  $csm_{k,t}$  denotes the discounted salvage value of a modular LNG plant with capacity level  $k$  installed at time period  $t$ .

$C_{trans}^{CAPEX}$  indicates the total CAPEX of gathering pipelines, calculated by,

$$C_{trans}^{CAPEX} = \sum_{i \in I} \sum_{p \in P} \sum_{r \in R} tpri_r \cdot XP_{i,p,r} \cdot lsp_{i,p} + \sum_{i \in I} \sum_{p \in P} \sum_{r \in R} tpri_r \cdot XM_{i,m,r} \cdot lsm_{i,m} \quad (A5)$$

where  $tpri_r$  denotes the reference CAPEX of gathering pipelines with capacity level  $r$ .  $XP_{i,p,r}$  is a binary variable that equals 1 if the gathering pipeline with capacity level  $r$  is installed to transport shale gas from shale site  $i$  to conventional processing plant  $p$ .  $lsp_{i,p}$  is the distance between shale site  $i$  and conventional processing plant  $p$ . Similarly,  $XM_{i,m,r}$  is a binary variable that equals 1 if the gathering pipeline with capacity level  $r$  is installed to transport shale gas from shale site  $i$  to modular LNG plant at location  $m$ .  $lsm_{i,m}$  is the distance between shale site  $i$  and modular LNG plant at location  $m$ .

The water management cost consists of water acquisition cost ( $C_{acq,t}$ ) and wastewater treatment costs corresponding to different technologies, namely Class-II disposal wells ( $C_{disp,t}$ ), CWT facilities ( $C_{cwt,t}$ ), and onsite treatment ( $C_{onsite,t}$ ).

$$C_{water,t}^{OPEX} = C_{acq,t} + C_{disp,t} + C_{cwt,t} + C_{onsite,t} \quad (A6)$$

$C_{acq,t}$  indicates the acquisition cost of freshwater in time period  $t$ , which is proportional to the amount of freshwater,

$$C_{acq,t} = \sum_{i \in I} fac \cdot FW_{i,t} \quad (A7)$$

where  $fac$  denotes the unit acquisition cost of freshwater.  $FW_{i,t}$  stands for the amount of freshwater acquired from water source to shale site  $i$  in time period  $t$ .

$C_{disp,t}$  denotes the cost associated with underground injection of disposal wells in time period  $t$ , given by,

$$C_{disp,t} = \sum_{i \in I} vd \cdot WTD_{i,t} \quad (A8)$$

where  $vd$  denotes the unit cost for underground injection of wastewater.  $WTD_{i,t}$  denotes the amount of wastewater transported from shale site  $i$  to disposal wells at time period  $t$ .

$C_{cwt,t}$  indicates the cost associated with CWT treatment facilities in time period  $t$ , calculated by,

$$C_{cwt,t} = \sum_{i \in I} vc \cdot WTC_{i,t} \quad (A9)$$

where  $vc$  denotes the unit treatment cost of wastewater at CWT facilities.  $WTC_{i,t}$  denotes the amount of wastewater transported from shale site  $i$  to CWT facilities at time period  $t$ .

$C_{onsite,t}$  is the total onsite treatment cost in time period  $t$ , given by,

$$C_{onsite,t} = \sum_{i \in I} \sum_{o \in O} vo_o \cdot WTO_{i,o,t} \quad (A10)$$

where  $vo_o$  denotes the unit treatment cost of wastewater by onsite treatment technology  $o$ .  $WTO_{i,o,t}$  denotes the amount of wastewater treated by onsite treatment technology  $o$  at shale site  $i$  in time period  $t$ .

$C_{drill,t}^{OPEX}$  indicates the total OPEX associated with drilling activities in time period  $t$ ,

$$C_{drill,t}^{OPEX} = \sum_{i \in I} sdc_{i,t} \cdot NN_{i,t} \quad (A11)$$

where  $sdc_{i,t}$  denotes the unit cost for shale well drilling and completion at shale site  $i$  in time period  $t$ .  $NN_{i,t}$  denotes the number of wells drilled at shale site  $i$  in time period  $t$ .

$C_{prod,t}^{OPEX}$  stands for the total cost associated with shale gas production activities in time period  $t$ , calculated as the difference between the gross cost proportional to the amount of shale gas production and the salvage value of shale wells at the end of planning horizon.

$$C_{prod,t}^{OPEX} = \sum_{i \in I} spc_{i,t} \cdot SP_{i,t} - \sum_{i \in I} psg \cdot (NN_{i,t} \cdot eur_i - SP_{i,t}) \quad (A12)$$

where  $spc_{i,t}$  denotes the unit cost for shale gas production at shale site  $i$  in time period  $t$ .  $SP_{i,t}$  denotes the shale gas production rate at shale site  $i$  in time period  $t$ .  $psg$  denotes the estimated average unit profit of shale gas remains to be produced in shale wells.  $eur_i$  denotes the estimated ultimate recovery of shale gas for a shale well at shale site  $i$ .

$C_{proc,t}^{OPEX}$  indicates the total OPEX for both modular LNG plant and conventional processing plant in time period  $t$ , calculated by,

$$C_{proc,t}^{OPEX} = C_{mod\_oper,t} + C_{mod\_move,t} + C_{conv\_oper,t} - I_{NGL,t} \quad (A13)$$

$C_{mod\_oper,t}$  is the total OPEX of modular LNG plants, calculated by,

$$C_{mod\_oper,t} = \sum_{i \in I} \sum_{m \in M} \sum_{k \in K} vmo_{m,k} \cdot SMP_{i,m,k,t} \quad (A14)$$

where  $vmo_{m,k}$  denotes the unit OPEX for modular LNG plant at location  $m$  with capacity level  $k$ .  $SMP_{i,m,k,t}$  denotes the amount of shale gas sent from shale site  $i$  to modular LNG plant at location  $m$  with capacity level  $k$  in time period  $t$ .

$C_{mod\_move,t}$  stands for the moving cost of modular LNG plants in time period  $t$ , which can be calculated by the following equation,

$$C_{mod\_move,t} = \sum_{m \in M} \sum_{m' \in M} \sum_{k \in K} (cdm_k + cmm_k \cdot ldm_{m,m'} + crm_k) \cdot ZR_{m,m',k,t} \quad (A15)$$

where  $cdm_k$  denotes the cost of disassembling a modular LNG plant with capacity level  $k$ .  $cmm_k$  denotes the cost of moving a modular LNG plant with capacity level  $k$  for unit distance.  $ldm_{m,m'}$  denotes the distance between potential modular LNG plant locations  $m$  and  $m'$ .  $crm_k$  denotes the cost of reassembling a modular LNG plant with capacity level  $k$ .  $ZR_{m,m',k,t}$  is a binary variable that equals 1 if a modular LNG plant with capacity level  $k$  is moved from location  $m$  to  $m'$  in time period  $t$ .

$C_{conv\_oper,t}$  is the total OPEX of conventional processing plants in time period  $t$ , given by,

$$C_{conv\_oper,t} = \sum_{i \in I} \sum_{p \in P} vro_p \cdot SRP_{i,p,t} \quad (A16)$$

where  $vro_p$  denotes the unit OPEX for conventional processing plant  $p$ .  $SRP_{i,p,t}$  denotes the amount of shale gas transported from shale site  $i$  to conventional processing plant  $p$  in time period  $t$ .

$I_{NGL,t}$  denotes the income from sales of NGLs in time period  $t$ , given as the summation of incomes from both conventional processing plants and modular LNG plants.

$$I_{NGL,t} = \sum_{p \in P} pl_t \cdot SRPL_{p,t} + \sum_{m \in M} pl_t \cdot SMPL_{m,t} \quad (A17)$$

where  $pl_t$  denotes the average unit price of NGLs in time period  $t$ .  $SRPL_{p,t}$  denotes the amount of NGLs produced at conventional processing plant  $p$  in time period  $t$ .  $SMPL_{m,t}$  denotes the amount of NGLs produced at modular LNG plant at location  $m$  in time period  $t$ .

$C_{trans,t}^{OPEX}$  stands for the total OPEX associated with all the transportation activities in time period  $t$ , given by,

$$C_{trans,t}^{OPEX} = C_{trans\_conv,t} + C_{trans\_mod,t} + C_{trans\_power,t} \quad (A18)$$

$C_{trans\_conv,t}$  indicates the variable transportation cost of shale gas from shale sites to conventional processing plants in time period  $t$ , given by,

$$C_{trans\_conv,t} = \sum_{i \in I} \sum_{p \in P} vrt \cdot lsp_{i,p} \cdot SRP_{i,p,t} \quad (A19)$$

where  $vrt$  denotes the unit transportation cost of shale gas.

$C_{trans\_mod,t}$  is the variable transportation cost associated with modular LNG plants, including the variable transportation cost of shale gas from shale sites to modular LNG plants and variable transportation cost of LNG from modular LNG plants to LNG storage facilities.

$$C_{trans\_mod,t} = \sum_{i \in I} \sum_{m \in M} \sum_{k \in K} vmt \cdot lsm_{i,m} \cdot SMP_{i,m,k,t} + \sum_{m \in M} \sum_{s \in S} vts \cdot lms_{m,s} \cdot SMPS_{m,s,t} \quad (A20)$$

where  $vmt$  denotes the unit transportation cost of shale gas from shale sites to modular LNG plants.  $vts$  denotes the unit transportation cost of LNG.  $lms_{m,s}$  denotes the distance between modular LNG plants and LNG storage facility  $s$ .  $SMPS_{m,s,t}$  denotes the amount

of LNG transported from modular LNG plant at location  $m$  to storage facility  $s$  in time period  $t$ .

$C_{trans\_power,t}$  indicates the variable transportation cost associated with power plants in time period  $t$ , given as,

$$C_{trans\_power,t} = \sum_{s \in S} \sum_{g \in G} vts \cdot lsg_{s,g} \cdot SSG_{s,g,t} + \sum_{m \in M} \sum_{g \in G} vts \cdot lmg_{m,g} \cdot SMPG_{m,g,t} + \sum_{p \in P} \sum_{g \in G} vtp \cdot lpg_{p,g} \cdot SPG_{p,g,t} \quad (A21)$$

where  $lsg_{s,g}$  denotes the distance from storage facility  $s$  to power plant  $g$ .  $SSG_{s,g,t}$  denotes the amount of LNG transported from storage facility  $s$  to power plant  $g$  in time period  $t$ .  $lmg_{m,g}$  denotes the distance from modular LNG plant at location  $m$  to power plant  $g$ .  $SMPG_{m,g,t}$  denotes the amount of LNG transported from modular LNG plant at location  $m$  to power plant  $g$  in time period  $t$ .  $vtp$  denotes the unit transportation cost of natural gas,  $lpg_{p,g}$  denotes the distance from conventional processing plant  $p$  to power plant  $g$ .  $SPG_{p,g,t}$  denotes the amount of natural gas transported from conventional processing plant  $p$  to power plant  $g$  in time period  $t$ .

$C_{stor,t}^{OPEX}$  is the total LNG storage cost in time period  $t$ , calculated by,

$$C_{stor,t}^{OPEX} = \sum_{s \in S} \left( \sum_{m \in M} v_{si} \cdot SMPS_{m,s,t} + \sum_{g \in G} v_{so} \cdot SSG_{s,g,t} \right) + \sum_{s \in S} v_s \cdot INL_{s,t} \quad (A22)$$

where  $v_{si}$  denotes the operating cost for unit input of LNG at storage facilities,  $v_{so}$  denotes the operating cost for unit output of LNG at storage facilities.  $v_s$  denotes the unit storage cost for LNG.  $INL_{s,t}$  denotes the amount of LNG stored at LNG storage facility  $s$  in time period  $t$ .

$C_{power,t}^{OPEX}$  indicates the total variable cost associated with electric power generation in time period  $t$ , calculated by,

$$C_{power,t}^{OPEX} = \sum_{g \in G} ve_g \cdot \left( \sum_{p \in P} SPG_{p,g,t} + \sum_{m \in M} SMPG_{m,g,t} + \sum_{s \in S} SSG_{s,g,t} \right) \quad (A23)$$

where  $ve_g$  denotes the unit cost for electricity generation from natural gas at power plant  $g$ .

## 2.7.2 Environmental objective

The environmental objective is to minimize the ReCiPe endpoint environmental score per MWh electricity generation from shale gas. The total environmental impact score accounts for the environmental impacts associated with water management ( $E_{water}$ ), shale well drilling, stimulation, and completion ( $E_{drill}$ ), shale gas production ( $E_{prod}$ ), shale gas processing ( $E_{proc}$ ), transportation ( $E_{trans}$ ), LNG storage ( $E_{stor}$ ), and electric power generation ( $E_{power}$ ).

$$\min UE = \frac{TE}{TGE} = \frac{E_{water} + E_{drill} + E_{prod} + E_{proc} + E_{trans} + E_{stor} + E_{power}}{\sum_{g \in G} \sum_{t \in T} GE_{g,t}} \quad (A24)$$

The environmental impacts of water management account for activities including water acquisition ( $E_{acq}$ ) and wastewater treatment corresponding to different technologies, namely Class-II disposal wells ( $E_{disp}$ ), CWT facilities ( $E_{cwt}$ ), and onsite treatment ( $E_{onsite}$ ).

$$E_{water} = E_{acq} + E_{disp} + E_{cwt} + E_{onsite} \quad (A25)$$

$E_{acq}$  indicates the environmental impact score resulting from freshwater acquisition activities, which is proportional to the amount of freshwater acquired from water sources.

$$E_{acq} = \sum_{i \in I} \sum_{t \in T} \sum_{ic \in IC} eac_{ic} \cdot FW_{i,t} \quad (A26)$$

where  $eac_{ic}$  denotes the environmental impact score under impact category  $ic$  associated with acquisition of unit amount of freshwater.

$E_{disp}$  represents the environmental impact score associated with underground wastewater injection, given by,

$$E_{disp} = \sum_{i \in I} \sum_{t \in T} \sum_{ic \in IC} ewd_{ic} \cdot WTD_{i,t} \quad (A27)$$

where  $ewd_{ic}$  denotes the environmental impact score under impact category  $ic$  associated with underground injection of unit amount of wastewater at disposal wells.

$E_{cwt}$  indicates the environmental impact score regarding water treatment activities at CWT facilities, calculated by,

$$E_{cwt} = \sum_{i \in I} \sum_{t \in T} \sum_{ic \in IC} ewc_{ic} \cdot WTC_{i,t} \quad (A28)$$

where  $ewc_{ic}$  denotes the environmental impact score under impact category  $ic$  associated with treatment of unit amount of wastewater at CWT facilities.

$E_{onsite}$  stands for the environmental impact score associated with onsite wastewater treatment, which is proportional to the amount of wastewater and dependent on the specific onsite treatment technology, calculated by,

$$E_{onsite} = \sum_{i \in I} \sum_{o \in O} \sum_{t \in T} \sum_{ic \in IC} ewo_{o,ic} \cdot WTO_{i,o,t} \quad (A29)$$

where  $ewo_{o,ic}$  denotes the environmental impact score under impact category  $ic$  associated with treating unit amount of wastewater by onsite treatment technology  $o$ .

$E_{drill}$  indicates the environmental impact score induced by shale wells drilling activities, where a series of processes including well pad construction, drilling, stimulation, and completion are considered.

$$E_{drill} = \sum_{i \in I} \sum_{t \in T} \sum_{ic \in IC} esd_{i,ic} \cdot NN_{i,t} \quad (A30)$$

where  $esd_{i,ic}$  denotes the environmental impact score under impact category  $ic$  associated with the drilling process of a shale well at shale site  $i$ .

$E_{prod}$  represents the environmental impact score resulting from shale gas production activities, including fracturing fluid additive manufacture, sand mining, energy usage of pump and compressors, hydraulic fracturing, workover flowback, venting, field separation, and corresponding transportation, etc.

$$E_{prod} = \sum_{i \in I} \sum_{t \in T} \sum_{ic \in IC} esp_{i,ic} \cdot SP_{i,t} \quad (A31)$$

where  $esp_{i,ic}$  denotes the environmental impact score under impact category  $ic$  associated with producing unit amount of shale gas at shale site  $i$ .

$E_{proc}$  is the environmental impact score associated with operations and movement of modular LNG plants as well as operations of conventional processing plants.

$$E_{proc} = E_{mod\_oper} + E_{mod\_move} + E_{conv\_oper} \quad (A32)$$

$E_{mod\_oper}$  indicates the environmental impact score associated with shale gas processing and LNG production at modular LNG plants, given by,

$$E_{mod\_oper} = \sum_{i \in I} \sum_{m \in M} \sum_{k \in K} \sum_{t \in T} \sum_{ic \in IC} emp_{k,ic} \cdot SMP_{i,m,k,t} \quad (A33)$$

where  $emp_{k,ic}$  denotes the environmental impact score under impact category  $ic$  associated processing unit amount of shale gas at modular LNG plant with capacity level  $k$ .

$E_{mod\_move}$  stands for the environmental impact score induced by the movement of modular LNG plants, calculated by,

$$E_{mod\_move} = \sum_{m \in M} \sum_{m' \in M} \sum_{k \in K} \sum_{t \in T} \sum_{ic \in IC} emm_{k,ic} \cdot ldm_{m,m'} \cdot ZR_{m,m',k,t} \quad (A34)$$

where  $emm_{k,ic}$  denotes the environmental impact score under impact category  $ic$  associated with moving modular LNG plant with capacity level  $k$  for unit distance.

$E_{conv\_oper}$  is the environmental impact score corresponding to shale gas processing at conventional processing plants, given by,

$$E_{conv\_oper} = \sum_{i \in I} \sum_{p \in P} \sum_{t \in T} \sum_{ic \in IC} erp_{p,ic} \cdot SRP_{i,p,t} \quad (A35)$$

Where  $erp_{p,ic}$  denotes the environmental impact score under impact category  $ic$  associated with processing unit amount of shale gas at conventional processing plant  $p$ .

$E_{trans}$  indicates the environmental impact score associated with all the transportation activities, including those associated with the conventional processing plants ( $E_{trans\_conv}$ ), modular LNG plants ( $E_{trans\_mod}$ ), and power plants ( $E_{trans\_power}$ ), calculated by,

$$E_{trans} = E_{trans\_conv} + E_{trans\_mod} + E_{trans\_power} \quad (A36)$$

$E_{trans\_conv}$  represents the environmental impact score induced by transporting shale gas from shale sites to conventional processing plants, given by,

$$E_{trans\_conv} = \sum_{i \in I} \sum_{p \in P} \sum_{t \in T} \sum_{ic \in IC} est_{ic} \cdot lsp_{i,p} \cdot SRP_{i,p,t} \quad (A37)$$

where  $est_{ic}$  denotes the environmental impact score under impact category  $ic$  associated with transportation of unit amount of shale gas for unit distance.

$E_{trans\_mod}$  indicates the environmental impact score associated with transporting shale gas from shale sites to modular LNG plants and from modular LNG plants to LNG storage facilities, given by,

$$E_{trans\_mod} = \sum_{i \in I} \sum_{m \in M} \sum_{k \in K} \sum_{t \in T} \sum_{ic \in IC} est_{ic} \cdot lsm_{i,m} \cdot SMP_{i,m,k,t} + \sum_{m \in M} \sum_{s \in S} \sum_{t \in T} \sum_{ic \in IC} elt_{ic} \cdot lms_{m,s} \cdot SMPS_{m,s,t} \quad (A38)$$

where  $elt_{ic}$  denotes the environmental impact score under impact category  $ic$  associated with transporting unit amount of LNG for unit distance.

$E_{trans\_power}$  represents the total environmental impact score associated with transporting natural gas or LNG from LNG storage facilities, modular LNG plants, and conventional processing plants to NGCC power plants, calculated by,

$$E_{trans\_power} = \sum_{s \in S} \sum_{g \in G} \sum_{t \in T} \sum_{ic \in IC} elt_{ic} \cdot lsg_{s,g} \cdot SSG_{s,g,t} + \sum_{m \in M} \sum_{g \in G} \sum_{t \in T} \sum_{ic \in IC} elt_{ic} \cdot lmg_{m,g} \cdot SMPG_{m,g,t} + \sum_{p \in P} \sum_{g \in G} \sum_{t \in T} \sum_{ic \in IC} est_{ic} \cdot lpg_{p,g} \cdot SPG_{p,g,t} \quad (A39)$$

$E_{stor}$  stands for the environmental impact score induced by LNG storage activities, calculated by,

$$E_{stor} = \sum_{s \in S} \sum_{t \in T} \sum_{ic \in IC} ess_{ic} \cdot INL_{s,t} \quad (A40)$$

where  $ess_{ic}$  denotes the environmental impact score under impact category  $ic$  associated with storage of unit amount of LNG.

$E_{power}$  indicates the environmental impact score associated with electric power generation, given by,

$$E_{power} = \sum_{g \in G} \sum_{t \in T} \sum_{ic \in IC} epg_{g,ic} \cdot \left( \sum_{p \in P} SPG_{p,g,t} + \sum_{m \in M} SMPG_{m,g,t} + \sum_{s \in S} SSG_{s,g,t} \right) \quad (A41)$$

where  $epg_{g,ic}$  denotes the environmental impact score under impact category  $ic$  associated with electricity generation from unit amount of natural gas at power plant  $g$ .

### 2.7.3 Mass balance constraints

The total water supply at each shale site comprises of freshwater from water sources and reused water from onsite treatment.

$$FW_{i,t} + \sum_{o \in O} lo_o \cdot WTO_{i,o,t} = FDW_{i,t}, \quad \forall i, t \quad (A42)$$

where  $lo_o$  denotes the recovery factor for treating wastewater of onsite treatment technology  $o$ .  $FDW_{i,t}$  denotes the freshwater demand of shale site  $i$  in time period  $t$ .

$$FDW_{i,t} = \frac{WP_{i,t}}{wrf_i} + wd_i \cdot NN_{i,t}, \quad \forall i, t \quad (A43)$$

The wastewater production rate during the fracking process is proportional to the total shale gas production rate at a shale site [124],

$$WP_{i,t} = cc_i \cdot SP_{i,t}, \quad \forall i, t \quad (A44)$$

where  $cc_i$  is the correlation coefficient for shale gas production and wastewater production of a shale well at shale site  $i$ .

At each shale site, the total amount of wastewater, including the wastewater from drilling, hydraulic fracturing, and completion, should equal to the total amount of water treated by different water management options, including CWT, disposal, and onsite treatment.

$$WP_{i,t} + wd_i \cdot wrd_i \cdot NN_{i,t} = WTC_{i,t} + WTD_{i,t} + \sum_{o \in O} WTO_{i,o,t}, \forall i, t \quad (\text{A45})$$

where  $wd_i$  denotes the average drilling water usage for each well at shale site  $i$ .  $wrd_i$  denotes the recovery ratio for drilling process at shale site  $i$ .

The total amount of shale gas produced at existing shale sites can be calculated by,

$$SP_{i,t} = ne_i \cdot spp_{i,t}, \forall i \in I_e, t \quad (\text{A46})$$

where  $ne_i$  denotes the number of existing shale wells drilled at shale site  $i$ .  $spp_{i,t}$  denotes the shale gas production of a shale well of age  $t$  at shale site  $i$ .

The total shale gas production rate at a shale site equals the summation of that of different wells.

$$SP_{i,t} = \sum_{t'=1}^{t-1} NN_{i,t'} \cdot spp_{i,t-t'}, \forall i \in I_n, t \geq 2 \quad (\text{A47})$$

where  $spp_{i,t-t'}$  denotes the shale gas production profile of a shale well drilled at time period  $t'$  at shale site  $i$  in time period  $t$ . Thus, the age of this well would be  $t - t'$ . We use this time-dependent parameter to describe the decreasing feature of the shale gas production profile of a certain well.

The shale gas production at each shale site is either transported to the conventional processing plants or modular LNG plants.

$$SP_{i,t} = \sum_{p \in P} SRP_{i,p,t} + \sum_{m \in M} \sum_{k \in K} SMP_{i,m,k,t}, \forall i, t \quad (\text{A48})$$

The methane and NGLs are separated at conventional processing plants, and their corresponding amounts are dependent on the processing efficiency and the composition of raw shale gas.

$$\sum_{i \in I} SRP_{i,p,t} \cdot pef \cdot mec_i = SRPM_{p,t}, \quad \forall p, t \quad (\text{A49})$$

$$\sum_{i \in I} SRP_{i,p,t} \cdot pef \cdot lc_i = SRPL_{p,t}, \quad \forall p, t \quad (\text{A50})$$

where  $pef$  denotes the NGL recovery efficiency at conventional processing plants.  $mec_i$  denotes the methane composition in shale gas at shale site  $i$ .  $lc_i$  denotes the NGL composition in shale gas at shale site  $i$ .

Similarly, the shale gas sent to modular LNG plants are processed first to separate natural gas and NGLs.

$$\sum_{i \in I} \sum_{k \in K} SMP_{i,m,k,t} \cdot mef \cdot mec_i = SMPM_{m,t}, \quad \forall m, t \quad (\text{A51})$$

$$\sum_{i \in I} \sum_{k \in K} SMP_{i,m,k,t} \cdot mef \cdot lc_i = SMPL_{m,t}, \quad \forall m, t \quad (\text{A52})$$

where  $mef$  denotes the NGL recovery efficiency at modular LNG plants.

The total amount of natural gas separated at a conventional processing plant equals the summation of natural gas transported from the processing plant to different power plants.

$$SRPM_{p,t} = \sum_{g \in G} SPG_{p,g,t}, \quad \forall p, t \quad (\text{A53})$$

The LNG produced at a modular LNG plant can either be transported to power plants for electric power generation directly or be transported to LNG storage facilities for temporary storage.

$$SMPM_{m,t} = \sum_{g \in G} SMPG_{m,g,t} + \sum_{s \in S} SMPS_{m,s,t}, \quad \forall m, t \quad (\text{A54})$$

For LNG at each LNG storage facility, the following input-output mass balance relationship should be satisfied.

$$\sum_{m \in M} SMPS_{m,s,t} + INL_{s,t-1} = \sum_{g \in G} SSG_{s,g,t} + INL_{s,t}, \quad \forall s, t \geq 2 \quad (\text{A55})$$

The total amount of electricity generation at a power plant in each time period is proportional to the amount of natural gas transported to the power plant from different sources, including the conventional processing plants, modular LNG plants, and LNG storage facilities.

$$GE_{g,t} = ue \cdot \left( \sum_{p \in P} SPG_{p,g,t} + \sum_{m \in M} SMPG_{m,g,t} + \sum_{s \in S} SSG_{s,g,t} \right), \quad \forall g, t \quad (\text{A56})$$

where  $ue$  denotes the amount of electricity generated per unit natural gas input.

#### 2.7.4 Capacity constraints

The total amount of wastewater from different shale sites treated by each CWT facility cannot exceed its capacity, given by,

$$\sum_{i \in I} WTC_{i,t} \leq cca_t, \quad \forall t \quad (\text{A57})$$

where  $cca_t$  denotes the capacity for wastewater treatment at CWT facility in time period  $t$ .

Similarly, the total amount of wastewater from all the shale sites handled by disposal wells should not exceed their disposal capacities,

$$\sum_{i \in I} WTD_{i,t} \leq dca_t, \quad \forall t \quad (\text{A58})$$

where  $dca_t$  denotes the capacity for underground injection at disposal wells in time period  $t$ .

If a certain onsite treatment technology is applied at a shale site, the amount of wastewater treated onsite should be bounded by its capacity; otherwise, the amount of

wastewater treated onsite should be zero. This relationship can be modeled by the following inequality,

$$ocl_o \cdot YO_{i,o} \leq WTO_{i,o,t} \leq ocu_o \cdot YO_{i,o}, \forall i, o, t \quad (\text{A59})$$

where  $ocl_o$  and  $ocu_o$  denote the minimum and maximum treatment capacities for onsite treatment technology  $o$ , respectively.  $YO_{i,o}$  is a binary variable that equals 1 if onsite treatment technology  $o$  is applied at shale site  $i$ .

To satisfy the reuse specification for hydraulic fracturing, the blending ratio of freshwater to treated water from onsite treatment must be greater than a certain value, given by,

$$\sum_{o \in O} rf_o \cdot lo_o \cdot WTO_{i,o,t} \leq FW_{i,t}, \forall i, t \quad (\text{A60})$$

where  $rf_o$  denotes the ratio of freshwater to wastewater required for blending after treatment by onsite treatment technology  $o$ .

The total amount of shale gas processed at a conventional processing plant cannot exceed its capacity,

$$\sum_{i \in I} SRP_{i,p,t} \leq PC_p, \forall p, t \quad (\text{A61})$$

Similarly, the amount of shale gas sent to a modular LNG plant is constrained by its working capacity,

$$\sum_{i \in I} SMP_{i,m,k,t} \leq MC_{m,k,t}, \forall m, k, t \quad (\text{A62})$$

where  $MC_{m,k,t}$  denotes the capacity of modular LNG plant at location  $m$  with capacity  $k$  in time period  $t$ .

For the LNG storage facilities, there are capacity constraints for the LNG in stock, LNG input, and LNG output streams, as given below.

$$INL_{s,t} \leq sca_s, \forall s, t \quad (A63)$$

$$\sum_{m \in M} SMPS_{m,s,t} \leq sic_s, \forall s, t \quad (A64)$$

$$\sum_{g \in G} SSG_{s,g,t} \leq soc_s, \forall s, t \quad (A65)$$

where  $sca_s$  denotes the capacity of LNG storage facility  $s$ .  $sic_s$  denotes the input capacity of LNG storage facility  $s$ .  $soc_s$  denotes the output capacity of LNG storage facility  $s$ .

The total amount of shale gas transported from a shale site to a conventional processing plant or a modular LNG plant is constrained by the transportation capacity of corresponding gathering pipeline.

$$SRP_{i,p,t} \leq \sum_{r \in R} TCP_{i,p,r}, \forall i, p, t \quad (A66)$$

$$\sum_{k \in K} SMP_{i,m,k,t} \leq \sum_{r \in R} TCM_{i,m,r}, \forall i, m, t \quad (A67)$$

The total electric power generation is constrained by the lower bound and upper bound of local demand.

$$dml_{g,t} \leq GE_{g,t} \leq dmup_{g,t}, \forall g, t \quad (A68)$$

where  $dml_{g,t}$  and  $dmup_{g,t}$  denote the minimum demand and maximum demand of electricity at power plant  $g$  in time period  $t$ , respectively.

### 2.7.5 Bounding constraints

If a gathering pipeline is installed, its capacity equals the reference capacity corresponding to its capacity level; otherwise, its capacity should be zero.

$$TCP_{i,p,r} = tprc_r \cdot XP_{i,p,r}, \forall i, p, r \quad (\text{A69})$$

$$TCM_{i,m,r} = tprc_r \cdot XM_{i,m,r}, \forall i, p, r \quad (\text{A70})$$

where  $tprc_r$  denotes the reference capacity of gathering pipelines with capacity level  $r$ . Similarly, if a modular LNG plant is constructed, its capacity equals the reference capacity of the design capacity level; otherwise, its capacity should be zero.

$$MC_{m,k,t} = rmc_k \cdot ZE_{m,k,t}, \forall m, k, t \quad (\text{A71})$$

where  $rmc_k$  denotes the reference capacity of modular LNG plants with capacity level  $k$ .  $ZE_{m,k,t}$  is a binary variable that equals 1 if a modular LNG plant with capacity level  $k$  exists at location  $m$  in time period  $t$ .

If a processing plant is established, its processing capacity should be bounded by the corresponding capacity range; otherwise, its capacity should be zero. This relationship can be modeled by the following inequality:

$$pcl_p \cdot YP_p \leq PC_p \leq pcup_p \cdot YP_p, \forall p \quad (\text{A72})$$

where  $pcl_p$  and  $pcup_p$  denote the minimum and maximum capacities of conventional processing plant  $p$ , respectively.  $YP_p$  is a binary variable that equals 1 if a conventional processing plant  $p$  is constructed.

### 2.7.6 Logic constraints

There can be a certain number of wells drilled at each shale site in each time period, given by,

$$\sum_{n=0}^{mn_i} YD_{i,n,t} = 1, \forall i, t \quad (\text{A73})$$

where  $YD_{i,n,t}$  is a binary variable that equals 1 if  $n$  shale wells at shale site  $i$  are drilled in time period  $t$ .  $mn_i$  denotes the maximum number of wells that can be drilled at shale site  $i$  per time period.

The total number of wells drilled at shale site  $i$  in time period  $t$  can be calculated by,

$$NN_{i,t} = \sum_{n=0}^{mn_i} n \cdot YD_{i,n,t}, \quad \forall i, t \quad (\text{A74})$$

The total number of wells that can be drilled at shale site  $i$  over the planning horizon is bounded, given by,

$$\sum_{t \in T} NN_{i,t} \leq tmn_i, \quad \forall i \quad (\text{A75})$$

where  $tmn_i$  denotes the maximum number of wells that can be drilled at shale site  $i$  over the planning horizon.

The existing shale sites are fully developed, so there will be no further drilling activities at these shale sites,

$$NN_{i,t} = 0, \quad \forall i \in I_e, t \quad (\text{A76})$$

For the selection of onsite treatment technologies, we note that at most one technology can be chosen at a shale site. This constraint is given by,

$$\sum_{o \in O} YO_{i,o} \leq 1, \quad \forall i \quad (\text{A77})$$

Only a certain capacity level can be chosen for each gathering pipeline among shale sites, conventional processing plants, and modular LNG plants, given by,

$$\sum_{r \in R} XP_{i,p,r} \leq 1, \quad \forall i, p \quad (\text{A78})$$

$$\sum_{r \in R} XM_{i,m,r} \leq 1, \quad \forall i, m \quad (\text{A79})$$

The existence of a modular LNG plant with a certain capacity level at a certain location in any time period depends on the previous condition, the installment decisions, and moving decisions of modular LNG plants. The complex logic relationship among these decision variables is depicted by the following equation,

$$ZE_{m,k,t} = ZE_{m,k,t-1} + ZI_{m,k,t-1} - \sum_{m' \in M \setminus \{m\}} ZR_{m,m',k,t} + \sum_{m' \in M \setminus \{m\}} ZR_{m',m,k,t-1}, \forall m, k, t \geq 2 \quad (\text{A80})$$

For each potential location, there is no more than one modular LNG plant installed, given by,

$$\sum_{k \in K} \sum_{t \in T} ZI_{m,k,t} \leq 1, \forall m \quad (\text{A81})$$

The moving of modular LNG plants only exists between two distinct locations,

$$ZR_{m,m,k,t} = 0, \forall m, k, t \quad (\text{A82})$$

The moving of a modular LNG plant can only happen once between any two locations,

$$\sum_{t \in T} ZR_{m,m',k,t} \leq 1, \forall m, m', k \quad (\text{A83})$$

There exists no more than one modular LNG plant at one location in any time period,

$$\sum_{k \in K} ZE_{m,k,t} \leq 1, \forall m, t \quad (\text{A84})$$

Only existing modular LNG plants can be moved from one location to another,

$$ZE_{m,k,t} \geq \sum_{m' \in M} ZR_{m,m',k,t}, \forall m, k, t \quad (\text{A85})$$

## 2.8 Appendix B: Detailed model formulation for the overall-performance LCO model

In this section, we present the specific model formulation of the overall-performance LCO model. The economic objective is to minimize the total net present cost ( $TC$ ). Notably,  $C_{proc\_conv}^{CAPEX}$  involves concave terms calculating the CAPEX of conventional processing plants, so the overall economic objective function  $TC$  is nonlinear. The environmental objective is to minimize the total ReCiPe endpoint environmental impact score ( $TE$ ). All the constraints are identical to those in the functional-unit-based LCO model. Therefore, we use the same equation numbers to indicate the specific formulation.

*Economic Objective:*

$$\min TC = C_{proc}^{CAPEX} + C_{trans}^{CAPEX} + \sum_{t \in T} \left[ \frac{C_{water,t}^{OPEX} + C_{drill,t}^{OPEX} + C_{prod,t}^{OPEX} + C_{proc,t}^{OPEX} + C_{trans,t}^{OPEX} + C_{stor,t}^{OPEX} + C_{power,t}^{OPEX}}{(1+dr)^t} \right]$$

*Environmental Objective:*

$$\min TE = E_{water} + E_{drill} + E_{production} + E_{processing} + E_{transportation} + E_{storage} + E_{power}$$

s.t. Economic Constraints	(A2)-(A23)
Environmental Constraints	(A25)-(A41)
Mass Balance Constraints	(A42)-(A56)
Capacity Constraints	(A57)-(A68)
Bounding Constraints	(A69)-(A72)
Logic Constraints	(A73)-(A85)

## 2.9 Appendix C: Detailed computational performance of proposed tailored global optimization algorithm

In this section, we present the detailed converging process for the solution of point E using the proposed tailored global optimization algorithm. As shown in Table C1, the tailored global optimization algorithm takes three outer loop iterations to find the optimal objective value of problem (P2). For each outer loop iteration, it takes one to two inner loop iterations to converge. During the inner loop, the upper bound decreases while the lower bound increases until they are close enough to satisfy the inner loop stopping criterion. In the last iteration of the outer loop, the reformulated linear objective function  $F(q) = TC - q^* \cdot TGE$  equals 0, indicating the convergence of this tailored global optimization algorithm. The total computational time is 5,910 CPU seconds. Notably, the absolute computational time varies when solving for different Pareto-optimal solutions. However, all the optimization problems can be solved to global optimum within a few hours.

Table C1. Converging process for the solution of point E.

$Iter^{out}$	$q$	$Iter^{in}$	$LB$	$UB$	$F(q)$	CPU seconds
1	0	1	306,109,900	307,325,000	306,109,900	1,509
2	0.062	1	-18,971,300	-17,948,700	-18,971,300	672
	0.062	2	-17,948,700	-17,948,700	17,948,700	1,531
3	0.059	1	-1,022,630	0	-1,022,630	304
	0.059	2	0	0	0	1,894

## 2.10 Nomenclature

### Sets

$G$	Set of power plants indexed by $g$
$I$	Set of shale sites indexed by $i$
$K$	Set of capacity levels for the modular LNG plant indexed by $k$
$M$	Set of potential modular LNG plant locations indexed by $m$
$N$	Set of number of wells indexed by $n$
$O$	Set of onsite treatment technologies indexed by $o$ ( $o_1$ : MSF; $o_2$ : MED; $o_3$ : RO)
$P$	Set of conventional processing plants indexed by $p$
$R$	Set of capacity levels for the gathering pipelines indexed by $r$
$S$	Set of storage facilities indexed by $s$
$T$	Set of time periods indexed by $t$

### Subsets

$I_e(i)$	Subset of existing shale site indexed by $i_e$
$I_n(i)$	Subset of newly constructed shale site indexed by $i_n$
$M'(m)$	Subset of potential modular LNG plant locations indexed by $m'$
$M_n(m)$	Subset of modular LNG plants that are potentially to be built indexed by $m_n$
$P_n(p)$	Subset of conventional processing plants that are potentially to be built indexed by $p_n$
$T'(t)$	Subset of time periods when wells are drilled indexed by $t'$

### Parameters

$cam_{m,k}$	Capital investment for installing a modular LNG plant with capacity level $k$ at location $m$
-------------	---

$cc_i$	Correlation coefficient for shale gas production and wastewater production of a shale well at shale site $i$
$cca_t$	Capacity for wastewater treatment at CWT facility in time period $t$
$cdm_k$	Cost of disassembling a modular plant with capacity level $k$
$cmm_k$	Cost of moving a modular plant with capacity level $k$ for unit distance
$crm_k$	Cost of reassembling a modular plant with capacity level $k$
$csm_{k,t}$	The discounted salvage value of a modular LNG plant with capacity level $k$ installed at time period $t$
$dca_t$	Capacity for underground injection at disposal wells in time period $t$
$dml_{g,t}$	Minimum demand of electricity at power plant $g$ in time period $t$
$dmup_{g,t}$	Maximum demand of electricity at power plant $g$ in time period $t$
$dr$	Discount rate per time period
$eac_{ic}$	Environmental score under impact category $ic$ associated with acquisition of unit amount of freshwater
$elt_{ic}$	Environmental score under impact category $ic$ associated with transporting unit amount of LNG for unit distance
$emm_{k,ic}$	Environmental score under impact category $ic$ associated with moving modular LNG plant with capacity level $k$ for unit distance
$emp_{k,ic}$	Environmental score under impact category $ic$ associated processing unit amount of shale gas at modular LNG plant with capacity level $k$
$epg_{g,ic}$	Environmental score under impact category $ic$ associated with electricity generation of unit amount of natural gas at power plant $g$
$erp_{p,ic}$	Environmental score under impact category $ic$ associated with processing unit amount of shale gas at conventional processing plant $p$
$esd_{i,ic}$	Environmental score under impact category $ic$ associated with the drilling process of a shale well at shale site $i$

$esp_{i,ic}$	Environmental score under impact category $ic$ associated with producing unit amount of shale gas at shale site $i$
$ess_{ic}$	Environmental score under impact category $ic$ associated with storage of unit amount of LNG
$est_{ic}$	Environmental score under impact category $ic$ associated with transportation of unit amount of shale gas for unit distance
$eur_i$	Estimated ultimate recovery of shale gas for a shale well at shale site $i$
$ewc_{ic}$	Environmental score under impact category $ic$ associated with treatment of unit amount of wastewater at CWT facilities
$ewd_{ic}$	Environmental score under impact category $ic$ associated with underground injection of unit amount of wastewater at disposal wells
$ewo_{o,ic}$	Environmental score under impact category $ic$ associated with treating unit amount of wastewater by onsite treatment technology $o$
$fac$	Unit acquisition cost of freshwater
$lc_i$	NGL composition in shale gas at shale site $i$
$ldm_{m,m'}$	Distance from potential modular LNG plant location $m$ to $m'$
$lo_o$	Recovery factor for treating wastewater of onsite treatment technology $o$
$lmg_{m,g}$	Distance from modular LNG plant $m$ to power plant $g$
$lms_{m,s}$	Distance from modular LNG plant $m$ to storage facility $s$
$lpg_{p,g}$	Distance from conventional processing plant $p$ to power plant $g$
$lsg_{s,g}$	Distance from storage facility $s$ to power plant $g$
$lsm_{i,m}$	Distance from shale site $i$ to modular LNG plant $m$
$lsp_{i,p}$	Distance from shale site $i$ to conventional processing plant $p$

$mec_i$	Methane composition in shale gas at shale site $i$
$mef$	NGL recovery efficiency at modular LNG plant
$mn_i$	Maximum number of wells that can be drilled at shale site $i$ per time period
$ne_i$	Number of existing shale wells drilled at shale site $i$
$ocl_o$	Minimum treatment capacity for onsite treatment technology $o$
$ocu_o$	Maximum treatment capacity for onsite treatment technology $o$
$pci$	Chemical engineering plant cost index for conventional processing plant
$pcl_p$	Minimum capacity of conventional processing plant $p$
$pcup_p$	Maximum capacity of conventional processing plant $p$
$pef$	NGL recovery efficiency at conventional processing plant
$pl_t$	Average unit price of NGLs in time period $t$
$prc$	Reference capacity of conventional processing plant
$pri$	Reference capital investment of conventional processing plant
$psg$	Estimated average unit profit of shale gas remains to be produced in shale wells
$rf_o$	Ratio of freshwater to wastewater required for blending after treatment of onsite treatment technology $o$
$rmc_k$	Reference capacity of modular LNG plant with capacity level $k$
$rpci$	Chemical engineering plant cost index for conventional processing plant of the reference year
$sca_s$	Capacity of LNG storage facility $s$

$sd_{i,t}$	Unit cost for shale well drilling and completion at shale site $i$ in time period $t$
$sfp$	Size factor of conventional processing plants
$sic_s$	Input capacity of LNG storage facility $s$
$soc_s$	Output capacity of LNG storage facility $s$
$spc_{i,t}$	Unit cost for shale gas production at shale site $i$ in time period $t$
$spp_{i,\tau}$	Shale gas production of a shale well of age $\tau$ at shale site $i$
$tmn_i$	Maximum number of wells that can be drilled at shale site $i$ over the planning horizon
$tprc_r$	Reference capacity of gathering pipeline with capacity level $r$
$tpri_r$	Reference capital investment of gathering pipeline with capacity level $r$
$ue$	Amount of electricity generated per unit natural gas input
$vc$	Unit cost for wastewater treatment at CWT facility
$vd$	Unit cost for underground injection of wastewater at disposal well
$ve_g$	Unit cost for electricity generation from natural gas at power plant $g$
$vmo_{m,k}$	Unit OPEX for a modular LNG plant at location $m$ with capacity level $k$
$vmt$	Unit transportation cost of shale gas from shale sites to modular LNG plants
$vo_o$	Levelized unit cost for wastewater treatment of onsite treatment technology $o$
$vro_p$	Unit OPEX for conventional processing plant $p$
$vrt$	Unit transportation cost of shale gas from shale sites to conventional processing plants

$vs$	Unit storage cost for LNG
$vs_i$	OPEX for unit input of LNG at storage facilities
$vs_o$	OPEX for unit output of LNG at storage facilities
$vtp$	Unit transportation cost of natural gas
$vt_s$	Unit transportation cost of LNG
$wd_i$	Average drilling water usage for each well at shale site $i$
$wrd_i$	Recovery ratio of water for drilling process at shale site $i$
$wrf_i$	Recovery ratio of water for hydraulic fracturing process at shale site $i$

### **Nonnegative Continuous variables**

$FDW_{i,t}$	Freshwater demand of shale site $i$ in time period $t$
$FW_{i,t}$	Amount of freshwater acquired from water source to shale site $i$ in time period $t$
$GE_{g,t}$	Amount of electricity generated at power plant $g$ in time period $t$
$INL_{s,t}$	Amount of LNG stored at storage facility $s$ in time period $t$
$MC_{m,k,t}$	Capacity of modular LNG plant at location $m$ with capacity $k$ in time period $t$
$NN_{i,t}$	Number of wells drilled at shale site $i$ in time period $t$
$PC_p$	Capacity of conventional processing plant $p$
$SMP_{i,m,k,t}$	Amount of shale gas sent from shale site $i$ to modular LNG plant at location $m$ with capacity level $k$ in time period $t$

$SMPG_{m,g,t}$	Amount of LNG transported from modular LNG plant at location $m$ to power plant $g$ in time period $t$
$SMPL_{m,t}$	Amount of NGLs produced at modular LNG plant at location $m$ in time period $t$
$SMPM_{m,t}$	Amount of methane produced at modular LNG plant at location $m$ in time period $t$
$SMPS_{m,s,t}$	Amount of LNG transported from modular LNG plant at location $m$ to storage facility $s$ in time period $t$
$SP_{i,t}$	Shale gas production rate at shale site $i$ in time period $t$
$SPG_{p,g,t}$	Amount of natural gas transported from conventional processing plant $p$ to power plant $g$ in time period $t$
$SRP_{i,p,t}$	Amount of shale gas transported from shale site $i$ to conventional processing plant $p$ in time period $t$
$SRPL_{p,t}$	Amount of NGLs produced at conventional processing plant $p$ in time period $t$
$SRPM_{p,t}$	Amount of methane produced at conventional processing plant $p$ in time period $t$
$SSG_{s,g,t}$	Amount of LNG transported from storage facility $s$ to power plant $g$ in time period $t$
$TCM_{i,m,r}$	Capacity of gathering pipeline with capacity level $r$ between shale site $i$ and modular LNG plant $m$

$TCP_{i,p,r}$	Capacity of gathering pipeline with capacity level $r$ between shale site $i$ and conventional processing plant $p$
$WP_{i,t}$	Wastewater production rate at shale site $i$ in time period $t$
$WTC_{i,t}$	Amount of wastewater transported from shale site $i$ to CWT facility in time period $t$
$WTD_{i,t}$	Amount of wastewater transported from shale site $i$ to disposal well in time period $t$
$WTO_{i,o,t}$	Amount of wastewater treated by onsite treatment technology $o$ at shale site $i$ in time period $t$

#### **Binary variables**

$XM_{i,m,r}$	0-1 variable. Equal to 1 if gathering pipeline with capacity level $r$ is installed to transport shale gas from shale site $i$ to modular LNG plant $m$
$XP_{i,p,r}$	0-1 variable. Equal to 1 if gathering pipeline with capacity level $r$ is installed to transport shale gas from shale site $i$ to conventional processing plant $p$
$YD_{i,n,t}$	0-1 variable. Equal to 1 if $n$ shale wells at shale site $i$ are drilled in time period $t$
$YO_{i,o}$	0-1 variable. Equal to 1 if onsite treatment technology $o$ is applied at shale site $i$
$YP_p$	0-1 variable. Equal to 1 if conventional processing plant $p$ is constructed

- $ZE_{m,k,t}$  0-1 variable. Equal to 1 if a modular LNG plant with capacity level  $k$  exists at location  $m$  in time period  $t$
- $ZI_{m,k,t}$  0-1 variable. Equal to 1 if a modular LNG plant with capacity level  $k$  is newly installed at location  $m$  in time period  $t$
- $ZR_{m,m',k,t}$  0-1 variable. Equal to 1 if a modular LNG plant with capacity level  $k$  is moved from location  $m$  to  $m'$  in time period  $t$

## CHAPTER 3

### INTEGRATED HYBRID LIFE CYCLE ASSESSMENT AND OPTIMIZATION

#### **3.1 Introduction**

Shale gas is considered as a “transition fuel” towards a low carbon economy [2]. However, producing shale gas requires significant amounts of water and energy resources with horizontal drilling and hydraulic fracturing technologies [3, 60, 80, 125]. Moreover, there are concerns that even small leakages of methane during shale gas extraction may offset the effects of lower carbon dioxide emissions [126-128]. LCA is a systematic way to investigate the environmental impacts of shale gas [64, 96, 97, 129]. Furthermore, LCO models integrating LCA with multiobjective optimization techniques are proposed to automatically identify the optimal design and operational alternatives in shale gas supply chains and process systems [6, 63, 130, 131]. Most existing shale gas LCA studies and all the LCO applications in the literature adopt a process-based LCA approach [1, 17, 79, 80, 84, 95, 118, 132]. Although process-based LCA provides more accurate and detailed process information, it suffers from system truncation, and thus underestimates the true environmental impacts [133]. Alternatively, the economic input-output (EIO)-based LCA utilizes national EIO data coupled with sectoral environmental impact factors to evaluate the environmental impacts of a product system [118]. Since all transaction activities within a country are recorded in national table, the system boundary of EIO-based LCA is generally considered more complete than that of process-based LCA. However, with aggregation of industries and commodities, the process-scale details are missing, which eventually affects the precision of EIO-based LCA results. Consequently, we are unable to guarantee the

accuracy and precision of LCA results simultaneously by solely relying on either the process-based LCA or the EIO-based LCA.

To address the aforementioned research challenge, we adopt an integrated hybrid LCA method to analyze the life cycle environmental impacts of shale gas. The integrated hybrid LCA approach has been applied to evaluate the environmental impacts of multiple systems, such as construction process, wind power generation, solar PV, and electricity generation [134-137]. To the best of our knowledge, this was the first integrated hybrid LCA study of shale gas. The integrated hybrid LCA combines the strengths of both process-based LCA and EIO-based LCA [68]. On the one hand, the process details associated with major processes within the system boundary are guaranteed by explicit process analysis. On the other hand, the truncated system is supplemented by the EIO systems. Moreover, the interactions between the process systems and the macroeconomic systems are explicitly modeled by upstream and downstream cutoff matrices. Thus, this integrated hybrid LCA approach overcomes the drawbacks of traditional process-based and EIO-based LCAs, and quantifies the life cycle environmental impacts of shale gas in a more precise and comprehensive manner. In this study, we consider life cycle GHG emissions, water consumption, and energy consumption. Based on this multi-criterion integrated hybrid LCA, a functional unit-based multi-objective hybrid LCO model is further developed, which enables automatic identification of the optimal design and operational alternatives in a “well-to-wire” shale gas supply chain. Major decisions associated with shale well drilling, fracturing and completion, shale gas production, water management, shale gas processing, transportation, and end use for electricity generation are all modeled and linked with

their corresponding economic and environmental impacts. The resulting hybrid LCO problem is a mixed-integer nonlinear programming (MINLP) problem that is computationally intractable for general-purpose global optimizers. Thus, a tailored global optimization algorithm integrating the parametric algorithm and a branch-and-refine algorithm is applied to tackle this computational challenge. The applicability of the proposed hybrid LCO model and global optimization algorithm is illustrated through a case study on shale gas supply chain design in UK.

## **3.2 Integrated hybrid LCA of shale gas**

### **3.2.1 Integrated hybrid LCA approach**

LCA approaches that integrate process-based and EIO-based analyses and combine the strengths of both are generally considered as hybrid LCA approaches [68]. Depending on how the life cycle inventory (LCI) is compiled, hybrid LCA approaches are classified into tiered hybrid LCA, EIO-based hybrid LCA, and integrated hybrid LCA [133, 138]. The tiered hybrid LCA is a combination of process-based LCA and EIO-based LCA by treating them separately. Process-based LCA is utilized to compile the LCIs of use and disposal phases as well as other important upstream processes, and the remaining LCIs are constructed using EIO-based LCA. The overall LCI is a summation of LCIs obtained by the process-based LCA and EIO-based LCA. Moriguchi et al. pioneered the advantage of the tiered hybrid approach [139], and its application is soon acknowledged by other LCA practitioners [140, 141]. Jiang et al. evaluated the life cycle GHG emissions and water consumption of shale gas using the tiered hybrid approach [19, 118]. The input-output (IO)-based hybrid LCA is carried out by disaggregating industry

sectors in the EIO table to improve the accuracy of the augmented EIO table. Meanwhile, the tiered hybrid LCA approach is applied to calculate the life cycle inventories of post-consumer phases, namely use and disposal [142].

In this study, we adopt the integrated hybrid LCA approach, which inherits the advantages and overcomes the drawbacks of these hybrid LCA methods [68, 143]. Specifically, the integrated hybrid LCA method uses explicit process analysis to estimate the environmental impacts associated with key life cycle processes in the “foreground process systems” [144]. Since process-specific data are generally considered more reliable than EIO-based data, this step improves the precision of analysis as compared with EIO-based LCA. Meanwhile, the truncated system boundary is complemented by including the “background macroeconomic systems” that the process systems interact with following the EIO-based LCA approach [140, 141]. Therefore, the resulting hybrid LCI not only retains the level of detail and specificity from process-based LCA but also has the completeness of macroeconomic systems from EIO-based LCA [145]. An illustrative figure is presented in Figure 23 to demonstrate the idea of integrated hybrid LCA approach.

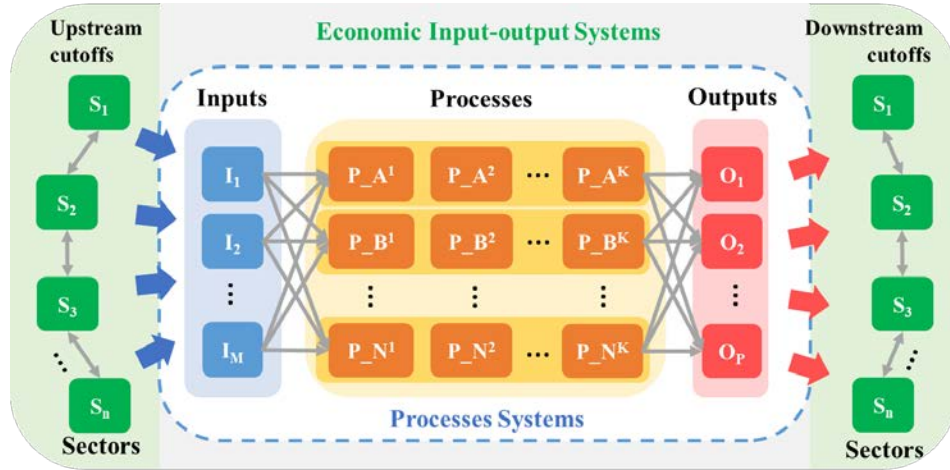


Figure 23. Illustration of integrated hybrid LCA approach.

Notably, unlike tiered hybrid LCA where the process systems and the macroeconomic systems are treated separately, the interactions between the process systems and the EIO systems are systematically captured in the integrated hybrid LCA by upstream and downstream cutoffs matrices. As can be seen in Figure 23, upstream cutoff flows are the inputs from industrial sectors in the EIO systems to the process systems. Downstream cutoff flows are the outputs from the process systems that are consumed by industrial sectors in the EIO systems. Therefore, the mathematical formulation for the integrated hybrid LCA model is given as follows:[133]

$$\text{Total environmental impact} = \begin{bmatrix} E_p & E_{io} \end{bmatrix} \begin{bmatrix} A_p & -C_d \\ -C_u & I - A_{io} \end{bmatrix}^{-1} \begin{bmatrix} y \\ 0 \end{bmatrix} \quad (1)$$

where  $A_p$  is the process matrix that represents the exchanges of goods among processes within the process system boundary.  $A_{io}$  is the direct requirements matrix describing the interdependencies among industrial sectors within the EIO systems.  $C_u$  and  $C_d$  are the upstream cutoff matrix and downstream cutoff matrix, respectively. The process matrix  $A_p$  and downstream cutoff matrix  $C_d$  are typically given in physical units. By contrast,

the direct requirements matrix  $A_{io}$  and upstream cutoff matrix  $C_u$  are typically specified in monetary units. The conversions between physical units and monetary units are done by using market price data.  $E_p$  and  $E_{io}$  are the environmental extension vectors corresponding to the process systems and the EIO systems, respectively.  $[y \ 0]^T$  is the functional unit column indicating the amount of final product that is produced per functional unit. With this integrated hybrid LCA methodology, we can quantify the total life cycle environmental impacts of shale gas, which consist of the environmental impacts originating from the foreground process systems of a shale gas supply chain (process environmental impacts) and the environmental impacts associated with background industrial sectors in the EIO systems (IO environmental impacts). We consider the specific application of this integrated hybrid LCA approach to shale gas in the following section. Furthermore, the hybrid LCA results are compared with those based on process-based LCA in the literature to demonstrate the need of taking the integrated hybrid LCA approach.

### **3.2.2 Hybrid LCA results**

In this section, we formally state the hybrid LCA study of shale gas. Specifically, we consider UK shale gas to illustrate the integrated hybrid LCA approach, and the reasons are summarized as follows. First, there have been extensive LCA studies on US shale gas [96, 129]. Meanwhile, shale gas extraction in the UK is in its early stage, and corresponding LCA studies are relatively rare. More importantly, the integrated hybrid LCA approach requires EIO data to be both up-to-date and comprehensive. However, the newest EIO data for the US are based on 2015 with 71 industries considered.

Although the 2007 version considers 389 industries, the data may not accurately reflect the current structure of the economy [16, 146]. To improve the accuracy of results, this study adopts a two-region (the UK and rest of the world) IO model recently reported for the UK that is considered state-of-the-art with sufficient completeness [135]. Accordingly, UK shale gas is selected for illustration to be consistent with this IO model. The four phases of this integrated hybrid LCA, namely the goal and scope definition, inventory analysis, impact assessment, and interpretation, are introduced sequentially as follows.

The goal of this hybrid LCA study is to evaluate the life cycle environmental impacts of shale gas for electricity generation considering both process and IO environmental impacts. For the process systems, a “well-to-wire” system boundary is considered that starts with the well drilling at shale sites and ends with electricity generation at combined cycle gas turbine (CCGT) power plants, following existing process-based LCA studies of shale gas [17, 79, 95]. The life cycle stages considered in the process systems include shale pad construction, shale well drilling, hydraulic fracturing and completion, water acquisition, wastewater treatment, shale gas production, processing, transportation, and end use of shale gas for electricity generation at CCGT power plants. Consistent with the “well-to-wire” process system boundary, we employ a functional unit of generating one Megawatt-hour (MWh) electricity from shale gas. Accordingly, the life cycle environmental impacts are evaluated based on this functional unit.

Table 1. Summary of basic processes considered in the process systems.

<b>Process ID</b>	<b>Description</b>	<b>Process ID</b>	<b>Description</b>

m <sub>1</sub>	Steel production, converter, chromium steel 18/8	m <sub>21</sub>	Soda ash, dense, to generic market for neutralizing agent
m <sub>2</sub>	Concrete production, for civil engineering, with cement CEM I	m <sub>22</sub>	Sodium persulfate production
m <sub>3</sub>	Tap water production, direct filtration treatment	m <sub>23</sub>	Sodium borates production
m <sub>4</sub>	Diesel production, low-sulfur	m <sub>24</sub>	Citric acid production
m <sub>5</sub>	Diesel, burned in building machine	m <sub>25</sub>	Pesticide production, unspecified
m <sub>6</sub>	Diesel, burned in diesel-electric generating set, 18.5kW	m <sub>26</sub>	N, N-dimethylformamide production
m <sub>7</sub>	Barite production	m <sub>27</sub>	UK electricity generation, with mixed energy inputs
m <sub>8</sub>	Bentonite quarry operation	m <sub>28</sub>	Transport, freight, lorry, all sizes, EURO3 to generic market for transport, freight, lorry, unspecified
m <sub>9</sub>	Chemical production, inorganic	m <sub>29</sub>	Injection in disposal well
m <sub>10</sub>	Chemical production, organic	m <sub>30</sub>	Wastewater treatment by CWT
m <sub>11</sub>	Lignite mine operation	m <sub>31</sub>	Onsite treatment with MSF
m <sub>12</sub>	Treatment of inert waste, inert material landfill	m <sub>32</sub>	Onsite treatment with MED
m <sub>13</sub>	Treatment of drilling waste, landfarming	m <sub>33</sub>	Onsite treatment- with RO
m <sub>14</sub>	Silica sand production	m <sub>34</sub>	Steam production, in chemical industry
m <sub>15</sub>	Petroleum refinery operation	m <sub>35</sub>	Tap water production, direct filtration treatment
m <sub>16</sub>	Isopropanol production	m <sub>36</sub>	Transporting gas through pipelines
m <sub>17</sub>	Hydrochloric acid production, from the reaction of hydrogen with chlorine	m <sub>37</sub>	Ethanolamine production
m <sub>18</sub>	Ethylene glycol production	m <sub>38</sub>	Ethylene glycol production
m <sub>19</sub>	Potassium chloride production	m <sub>39</sub>	Fugitive emissions of CO <sub>2</sub>
m <sub>20</sub>	Carboxymethyl cellulose production, powder	m <sub>40</sub>	Fugitive emissions of CH <sub>4</sub>

The LCI is established based on the predefined process system boundary and functional unit to quantify the mass and energy balances of all the processes across the life cycle

of shale gas. In this study, we adopt the data reported in the most recent LCA study for UK shale gas, as well as the Ecoinvent database v3.3 to construct the process-based LCI [81, 93]. Specifically, the process data of shale site preparation, shale well drilling, and well completion are provided by Cuadrilla, the largest shale gas company in the UK [147]. Meanwhile, the remaining data gaps are filled with the Ecoinvent database v3.3. with preference to the UK-specific data. A total of 40 basic processes are considered in the process systems, including steel, concrete, water, chemicals, transportation service, etc., as given in Table 1. The processes for raw material inputs cover the corresponding transportation activities. The drilling waste is handled by either landfill or landfarming options. Notably, the fugitive emissions of CO<sub>2</sub> and CH<sub>4</sub> are modeled explicitly as individual processes [23]. For the EIO systems, we adopt a two-region IO model as reported in the literature [135]. The resulting direct requirements matrix consists of four parts, including supply and use tables for the UK, and supply and use tables for the rest of the world (ROW). In each table, there are 224 sectors/commodities considered under the following broad categories: agriculture, mining, construction, manufacturing, wholesale trade, retail trade, transportation and warehousing, finance, professional and business services, education and health care, arts and entertainment, government, and others. Thus, the resulting direct requirement matrix has a dimension of 896 × 896. An illustrative IO table is presented in Figure 24, where the value of each cell is presented with color scales ranging from red to blue as the value increases [135]. Following the idea of sensitivity analysis, three cases with distinct LCIs are adopted from the LCA literature of UK shale gas, namely the best, balance, and worst cases corresponding to

the lowest, the medium, and the highest environmental impacts, respectively [81]. The overall structure of this integrated hybrid LCA model is illustrated with Figure 25.

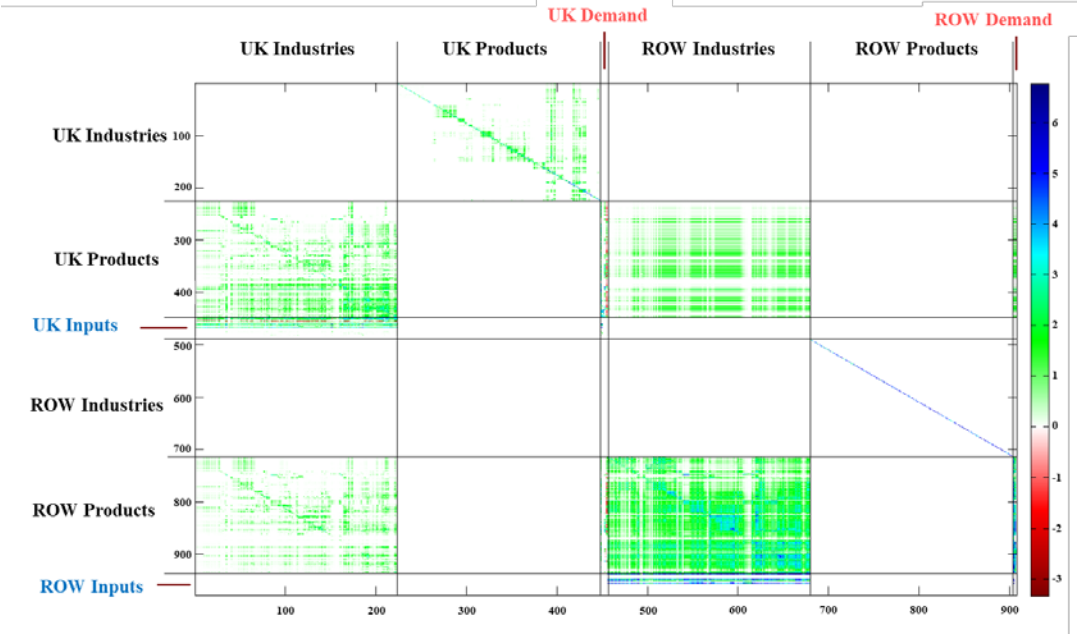


Figure 24. Illustrative figure of the  $896 \times 896$  two-region IO table [135].

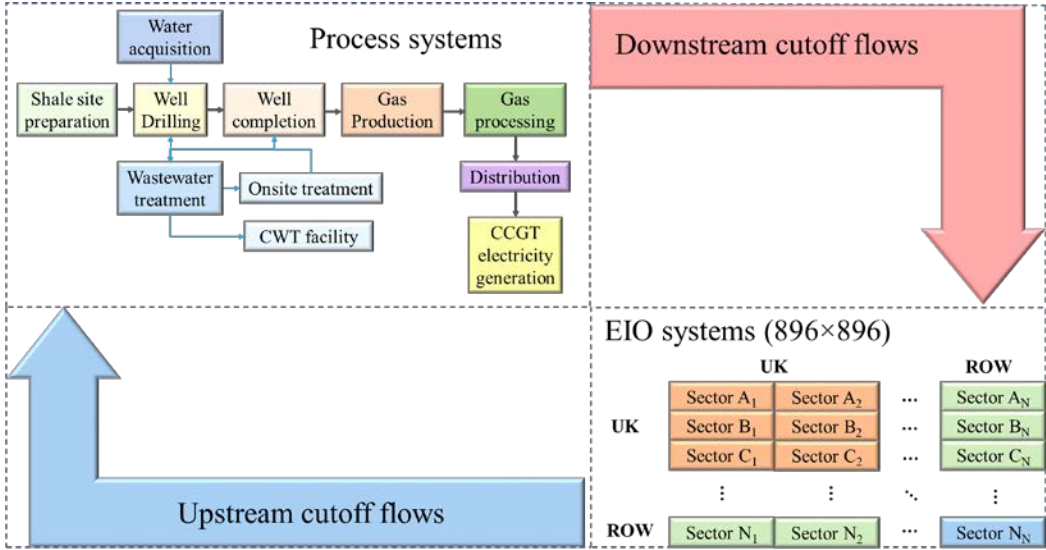


Figure 25. Structure of the integrated hybrid LCA model for shale gas.

Unlike most existing shale gas LCA studies that only consider GHG emissions, we consider three key environmental categories for shale gas, namely the life cycle GHG

emissions, water consumption, and energy consumption in this work [80]. Due to the limited availability of data, especially those regarding the environmental extension vectors corresponding to the EIO systems, we focus on these three environmental impacts. The GHG emissions considered include CO<sub>2</sub>, CH<sub>4</sub>, N<sub>2</sub>O, HFCs, PFCs, and SF<sub>6</sub>. We use the 100-year global warming potential (GWP) factors reported in the fifth assessment report by IPCC to convert these GHG emissions to carbon dioxide equivalents [148]. As for the water consumption and energy consumption, we consider not only the direct resource consumption in the whole system, but also the indirect consumption incurred by all the material inputs and activities. In Figure 26, we summarize the breakdowns of life cycle GHG emissions, life cycle water consumption, and life cycle energy consumption based on upstream of the process systems, downstream of the process systems, and the EIO systems. Specifically, the upstream of the process systems indicates the life cycle stages from shale site preparation at shale sites to the distribution of sales gas to the CCGT power plants. The downstream of the process systems represents electricity generation activity at CCGT power plants. The environmental impacts associated with inputs from the EIO systems to the process systems are all counted under the category of EIO systems.

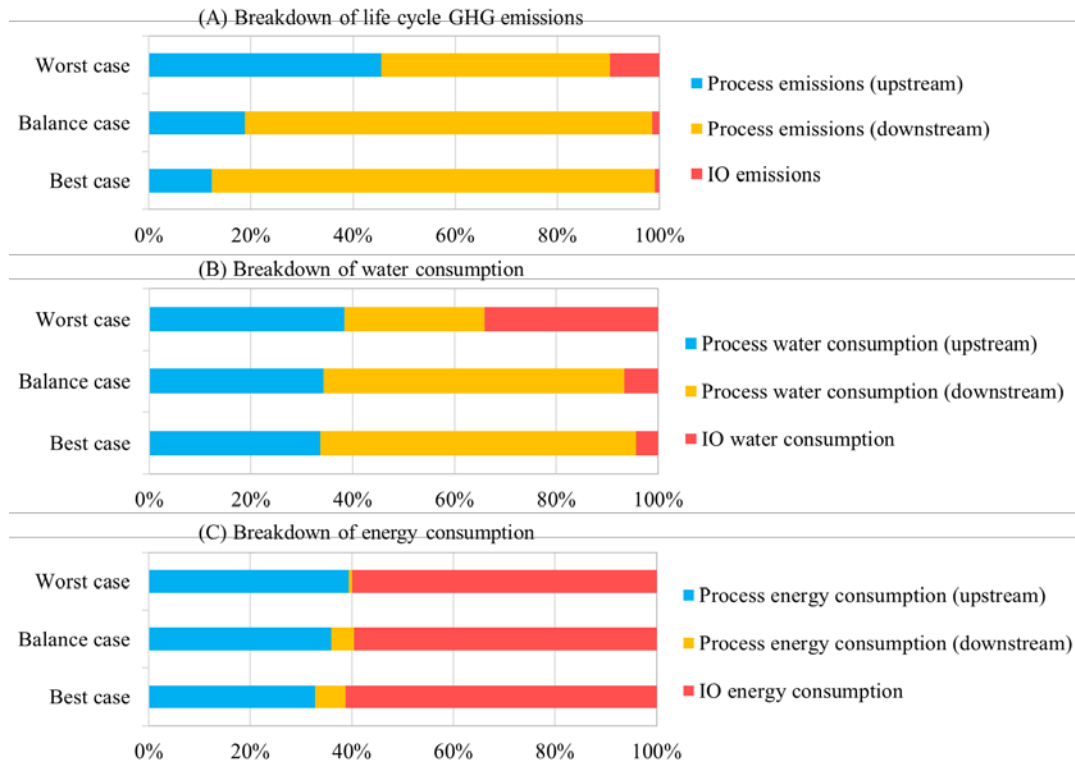


Figure 26. Breakdowns of (A) life cycle GHG emissions, (B) life cycle water consumption, and (C) life cycle energy consumption based on upstream of the process systems, downstream of the process systems, and the EIO systems (the best, balance, and worst cases corresponding to the lowest, the medium, and the highest environmental impacts, respectively).

As can be seen in Figure 26, the three environmental categories have different breakdown results. The downstream of the process systems, namely the electricity generation process where natural gas is burnt directly and turned into carbon dioxide, contributes the most GHG emissions ranging from 45% to 87% in the three cases. Correspondingly, the IO emissions resulting from the EIO systems contribute a relatively small portion of the total life cycle GHG emissions. However, the amount of IO emissions is comparable to that of the upstream process emissions. In the worst case,

the upstream process emissions are more than double of those in other cases due to the pessimistic estimation of LCI. Meanwhile, the IO emissions are also more significant in the worst case. In terms of water consumption, since a vast amount of cooling water is required in the electricity generation process, the downstream process systems contribute a large amount of water consumption. The upstream process water consumption does not change much in the best and the balance cases of LCI. Nevertheless, in the worst case, both the water consumption in the drilling process and the IO water consumption are substantial. In the last figure of energy consumption, we observe the significant role of the EIO systems, which contribute about 60% of the life cycle energy consumption throughout the three cases. The remaining energy consumption mainly comes from the upstream process activities, including drilling, processing, transportation, etc. The downstream electricity generation process consumes much less energy compared with other processes.

In Figure 27, we present the integrated hybrid LCA results regarding the three environmental categories. The stacked columns demonstrate the detailed contributions from different processes. In the best case, the life cycle GHG emissions, water consumption, and energy consumption are 320 kg CO<sub>2</sub>-eq/MWh, 1,717 kg/MWh, and 654 MJ/MWh, respectively. For the balance case, the life cycle GHG emissions, water consumption, and energy consumption are 435 kg CO<sub>2</sub>-eq/MWh, 2,254 kg/MWh, and 1,109 MJ/MWh, respectively. These environmental impact indicators are much higher in the worst case, given as 932 kg CO<sub>2</sub>-eq/MWh, 5,799 kg/MWh, and 10,805 MJ/MWh, respectively. The shale well drilling, gas transportation, and electricity generation processes are the main sources of GHG emissions. In the shale gas production process,

we consider the flaring and venting activities, of which the GHG emissions are much smaller than other life cycle processes. As for water consumption, shale gas processing results in more water consumption than transportation activities. For shale gas processing, we consider the energy consumption of electricity, material inputs of steam, cooling water, ethanolamine, ethylene glycol, and fugitive emissions involved in the shale gas processing process. The drilling process, including hydraulic fracturing and completion, is identified as the most energy-intensive process from a life cycle perspective. The EIO systems play a key role in evaluating the life cycle environmental impacts of shale gas, especially when a pessimistic LCI is considered or the energy consumption is of interest.

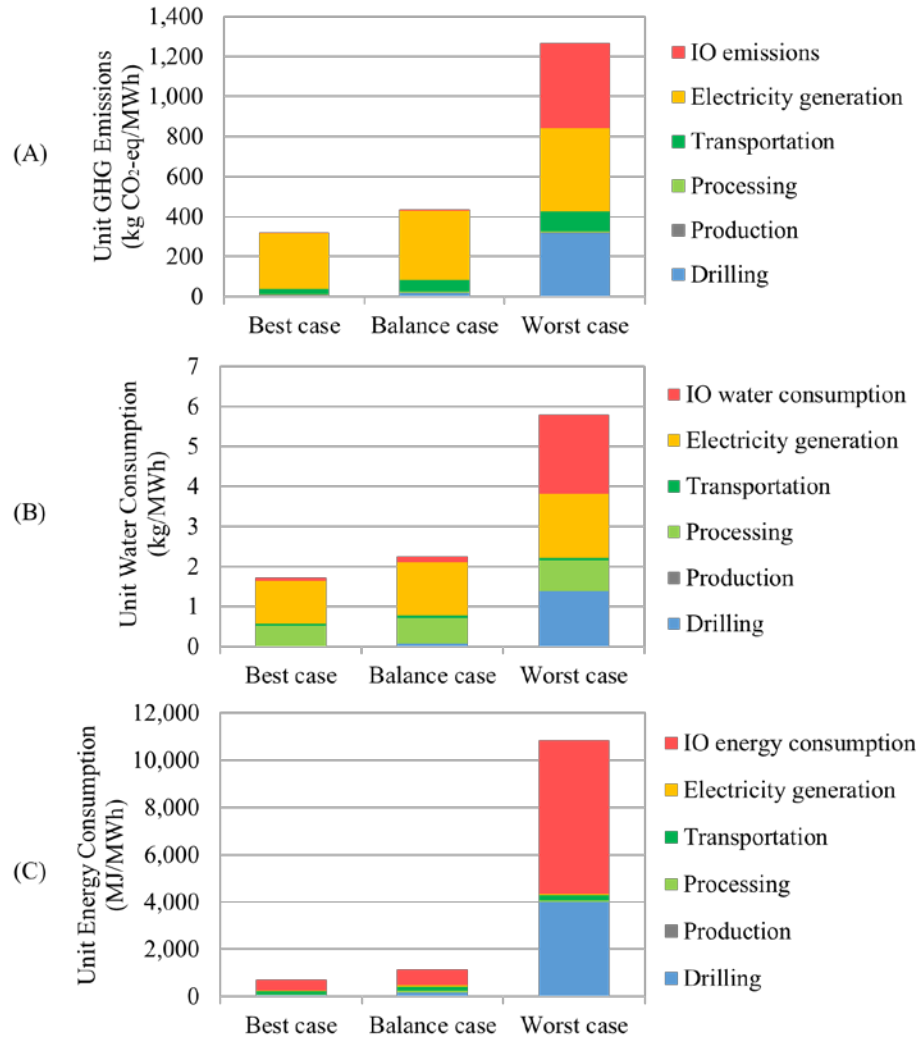


Figure 27. Integrated hybrid LCA results regarding (A) life cycle GHG emissions, (B) life cycle water consumption, and (C) life cycle energy consumption with detailed contribution breakdowns (the best, balance, and worst cases corresponding to the lowest, the medium, and the highest environmental impacts, respectively).

### 3.2.3 Comparison with existing LCA studies

To illustrate the different results obtained using process-based LCA approach and integrated hybrid LCA approach, we compare the shale gas life cycle GHG emissions obtained in the previous section with those of the representative shale gas LCA studies in Figure 28.

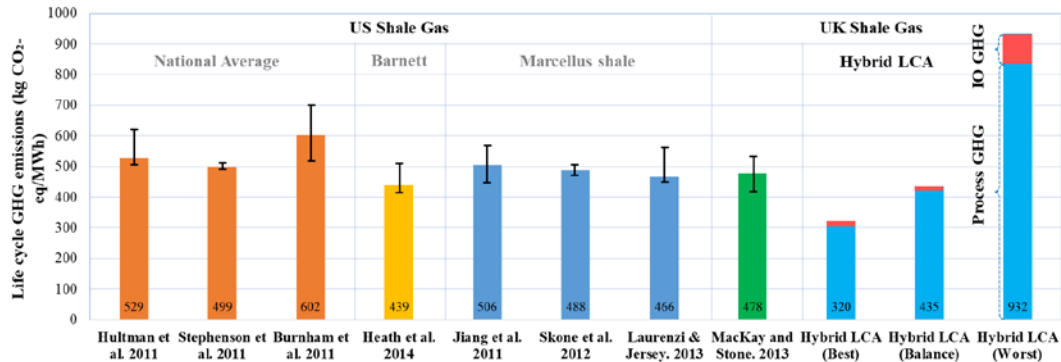


Figure 28. Result comparison of the integrated hybrid LCA with existing shale gas LCA studies [17, 79, 84, 85, 95, 118, 132, 149].

As can be seen, most LCA studies of shale gas originate in the US where shale gas extraction is much greater than other regions. The report by MacKay and Stone is the only UK-based case study evaluating the life cycle GHG emissions of shale gas [149]. All the existing shale gas LCA studies rely on process-based LCA approach except the study by Jiang et al., where tiered hybrid LCA approach is applied to estimate the total life cycle GHG emissions [118]. With the integrated hybrid LCA approach, we can quantify both the process GHG emissions as well as the IO GHG emissions, which are presented in blue and red, respectively. In the best and the balance cases, the IO GHG emissions are relatively small mainly because the downstream combustion at CCGT power plants plays a dominant role (up to 90%) in generating GHG emissions.

Meanwhile, the indirect GHG emissions are comparable to the total GHG emissions from all the upstream activities. In the worst case, due to the pessimistic estimation of LCI, the resulting life cycle GHG emissions are 932 kg CO<sub>2</sub>-eq/MWh. The process and IO GHG emissions increase correspondingly to 841 kg CO<sub>2</sub>-eq/MWh and 91 kg CO<sub>2</sub>-eq/MWh, respectively.

In this section, we also compare the life cycle GHG emissions of shale gas with other fossil fuels, namely coal, oil, and conventional natural gas, for electricity generation. Notably, all the results presented in Figure 29 are evaluated based on the integrated hybrid LCA approach [137, 150]. We use stacked columns to show the breakdowns of direct GHG emissions (blue), such as CO<sub>2</sub>, CH<sub>4</sub>, and N<sub>2</sub>O, and indirect GHG emissions (red) resulting from material inputs and process activities. As can be observed, under the three specific cases considered in this study, namely the best, balance, and worst cases adopted from existing literature [81], the life cycle GHG emissions of shale gas estimated by the integrated hybrid LCA approach are lower than those of coal and oil. However, the results may vary when different sets of data are adopted. However, the carbon footprint of shale gas is comparable to that of conventional natural gas and may vary within a wide range from region to region. For all the energy sources, although the direct GHG emissions are the dominant source, the indirect GHG emissions are significant enough to be explicitly considered.

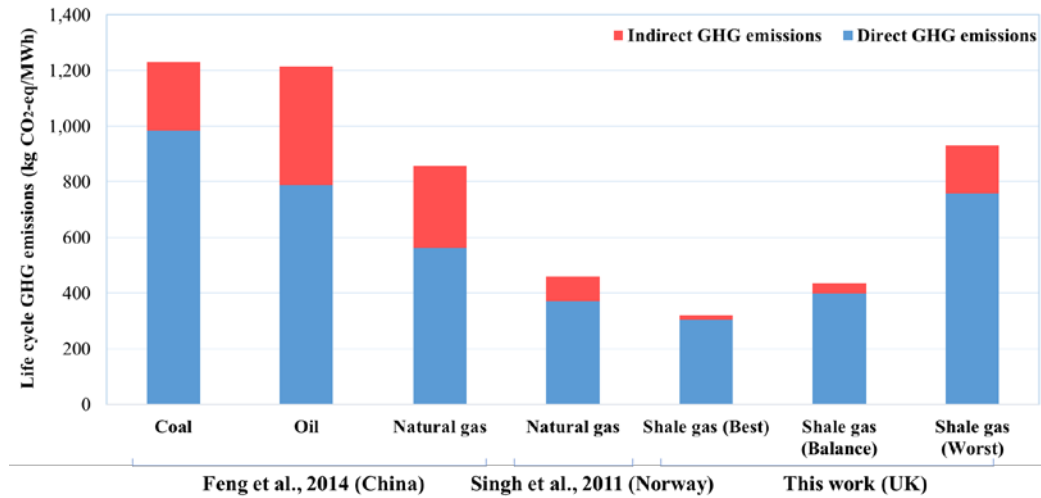


Figure 29. Comparison of life cycle GHG emissions of shale gas and other fossil fuels for electricity generation [137, 150].

### 3.3 Integrated hybrid LCO model of shale gas supply chains

In general, the application of LCA approaches is limited to the analysis phase with static LCI data. Thus, all the processes and exchanges within the investigated system are predetermined and fixed. However, a typical shale gas supply chain involves various design and operational decisions, such as exploration of shale reserves, drilling schedules of shale wells, water management strategies, gas production planning, construction of processing and transportation infrastructure, and transmission of sales gas. The combination of these decisions can lead to a huge number of scenarios that cannot be analyzed one by one [129]. Therefore, we further propose an integrated hybrid LCO model that seamlessly integrates the integrated hybrid LCA model with multiobjective optimization techniques. On the one hand, the integrated hybrid LCA of shale gas provides the necessary LCI data for the integrated hybrid LCO model that

connects the major design and operational decisions with their environmental impacts. On the other hand, the integrated hybrid LCO model includes numerous design and operational alternatives that cannot be investigated explicitly one-by-one with the integrated hybrid LCA approach. Although there are existing shale gas supply chain models considering environmental impacts in the optimization, the corresponding environmental impact estimations are all based on process-based LCIs and miss the environmental impacts associated the EIO systems [6, 7, 59]. As the first integrated hybrid LCO model of shale gas supply chains, this model captures the environmental impacts from both the process systems and the EIO systems, and it enables automatic identification of optimal design and operational alternatives in a shale gas supply chain [67].

### **3.3.1 Problem statement of hybrid LCO model**

The general problem statement of this hybrid LCO model is presented as follows. A planning horizon consisting of a set of time periods is given, so the resulting hybrid LCO problem is a multi-period optimization problem. There are a set of shale sites. Some of them already exist with drilled shale wells, and the remaining shale sites are potential ones to be developed. At each shale site, the maximum number of wells that can be drilled is known. In addition, the production profile, estimated ultimate recovery, and shale gas composition of each shale well are given. Both drilling and hydraulic fracturing activities require freshwater supply and generate wastewater simultaneously. Thus, it is necessary to make corresponding decisions regarding water management. Two wastewater treatment options are considered, including centralized wastewater

treatment (CWT) facilities and onsite wastewater treatment units. For the latter, we consider three typical wastewater treatment technologies, namely multi-stage flash (MSF), multi-effect distillation (MED), and reverse osmosis (RO) [99, 100]. The technological information regarding each water treatment option, such as the treatment capacities, energy efficiency, and recovery factors, is given.

Raw shale gas can be produced at shale sites once the corresponding shale wells are completed. The raw shale gas is first sent to processing plants, where impurities, such as water, acid gas, and nitrogen are removed, and the pipeline-quality natural gas and heavier hydrocarbons, known as natural gas liquids (NGLs), are separated. The transportation of raw shale gas from shale sites to processing plants requires the construction of gathering pipelines. There are a set of pipeline specs with given capital costs and capacities to select from. The processing plants include existing ones with fixed processing capacities and potential ones to be designed and constructed.

After the processing plants, natural gas is sent to a set of CCGT power plants for electricity generation. The distribution of natural gas from processing plants to power plants also requires the readiness of transmission pipelines. The transportation distance between each pair of locations is given. For the power plants, we are given the electricity demand in each time period as well as the electricity generation efficiency.

All the economic data, including the capital and operating costs associated with all the design and operational decisions are given. Meanwhile, the environmental data corresponding to the process systems as well as the EIO systems are given as well. In this hybrid LCO model, we consider three environmental impact indicators, namely the life cycle GHG emissions, water consumption, and energy consumption. Since life cycle

GHG emissions are commonly applied as environmental impact indicator in relevant literature, we focus on this environmental impact factor in the case study section, although other environmental impact indicators could be similarly used in LCO [6, 79, 85, 130]. In this model, the shutdowns and failures of shale wells are not considered. Instead, we use distinct estimated ultimate recoveries to address the uncertain outcomes of drilled shale wells. To avoid the over-complexity of model formulations, we choose not to model the composition of wastewater explicitly. The optimization results of extra case studies minimizing the life cycle water consumption and energy consumption are provided in Appendix B for interested readers. Additionally, we also provide a case study based on the traditional process-based LCO model for comparison. The detailed optimization results are included in Appendix C. Consistent with the “well-to-wire” system boundary, a functional unit of generating one Megawatt-hour (MWh) of electric power is employed. To simultaneously optimize the economic and environmental performances associated with production of one functional unit, we adapt the following fractional objectives, which reflect the life cycle performances of the shale gas supply chain [6, 151].

- Minimizing the levelized cost of electricity (LCOE) generated from shale gas, formulated as the total net present cost (i.e., the summation of all the discounted future costs) divided by the total amount of electricity generated from shale gas.
- Minimizing the total life cycle GHG emissions per MWh of electricity generation, formulated as the total GHG emissions generated throughout the process systems and EIO systems divided by the total electricity generation from shale gas.

- Minimizing the total water consumption per MWh of electricity generation, formulated as the total water consumption throughout the process systems and EIO systems divided by the total electricity generation from shale gas.
- Minimizing the total energy consumption per MWh of electricity generation, formulated as the total energy consumption throughout the process systems and EIO systems divided by the total electricity generation from shale gas.

These economic and environmental objectives are optimized considering the following design and operational decisions:

- Development planning of shale sites;
- Drilling schedule, production profile, and water management strategies at each shale site;
- Locations and capacities of shale gas processing plants;
- Installation and spec selection of transportation pipelines, as well as planning of corresponding transportation activities;
- Electricity generation profiles at CCGT power plants.

### 3.3.2 Model formulation and solution algorithm

A multi-objective, multi-period MINLP model (P0) is developed to address the sustainable design and operations of shale gas supply chains. For compactness, we provide the detailed model formulation in Appendix A.

$$\text{Economic Objective: } \min LCOE = \frac{TC^{cap} + \sum_{t \in T} \frac{TC^{oper}}{(1+dr)^t}}{TGE} \quad (2)$$

$$\text{Environmental Objectives: } \min UE = \frac{TE^{pro} + TE^{IO}}{TGE} \quad (3)$$

$$\min UW = \frac{TW^{pro} + TW^{IO}}{TGE} \quad (4)$$

$$\min UG = \frac{TG^{pro} + TG^{IO}}{TGE} \quad (5)$$

s.t. Economic Constraints (A3)-(A15)

Environmental Constraints (A16)-(A26)

Mass Balance Constraints (A27)-(A37)

(P0) Capacity Constraints (A38)-(A43)

Composition Constraints (A44)

Bounding Constraints (A45)-(A47)

Logic Constraints (A48)-(A53)

As stated in the problem statement section, *LCOE* indicates the levelized cost of electricity, which is formulated as the summation of total capital cost ( $TC^{cap}$ ) and the total discounted value of operating cost ( $TC^{oper}$ ) divided by the total electricity generation ( $TGE$ ). *UE* denotes the life cycle GHG emissions associated with one MWh of electricity generation, formulated as the summation of process emissions ( $TE^{pro}$ ) and IO emissions ( $TE^{IO}$ ) divided by the total electricity generation. *UW* denotes the life cycle water consumption associated with one MWh of electricity generation, formulated as the summation of process water consumption ( $TW^{pro}$ ) and IO water consumption ( $TW^{IO}$ ) divided by the total electricity generation. *UG* denotes the life cycle energy consumption associated with one MWh of electricity generation, formulated as the summation of process energy consumption ( $TG^{pro}$ ) and IO energy consumption ( $TG^{IO}$ ) divided by the total electricity generation. These objectives are optimized subject to the following constraints:

- Economic constraints calculating the capital and operating costs associated with all the design and operational decisions across the shale gas supply chain.
- Environmental constraints calculating the GHG emissions resulting from both the process systems and the EIO systems following the integrated hybrid LCA approach.
- Mass balance constraints describing the detailed input-output mass balance relationships among shale sites, processing plants, and CCGT power plants throughout the shale gas supply chain.
- Capacity constraints describing the capacity restrictions of different unit processes, including water management options, gas processing, transportation, and demand of electricity generation at power plants.
- Composition constraints describing the reuse specification of onsite treatment technologies.
- Bounding constraints linking the supply chain design decisions with corresponding operational decisions, including those associated with processing plants and transportation pipelines.
- Logic constraints describing the logic relationships among strategic decisions, including those regarding well drilling, wastewater treatment, construction of processing plant, and pipeline installment.

Both the economic and environmental objective functions are formulated as fractional terms to reflect the functional-unit-based life cycle performances. There are nonlinear terms introduced in the economic objective function to calculate the capital cost of processing plants. All the other constraints are linear with both integer and continuous

variables. Thus, the resulting problem is a nonconvex MINLP problem. Due to the combinatorial nature and pseudo-convexity of fractional objectives as well as separable concave terms for capital cost estimation, mixed-integer nonlinear fractional programming problems have been known as computationally challenging problems for general-purpose MINLP solvers [102-104, 152]. Therefore, we apply a tailored global optimization algorithm that integrates the parametric algorithm [107] with a branch-and-refine algorithm [103, 106] to tackle this computational challenge. A pseudo-code of this algorithm is given below.

---

```

1: Set  $q_0 = 0$ ,  $Iter^{out} = 1$ ,  $obj = +\infty$ 
2: while  $obj \geq Tol^{out}$ 
3:   Set  $LB = -\infty$ ,  $UB = +\infty$ ,  $Iter^{in} = 1$ ,  $gap = +\infty$ 
4:   Initialize the insertion points for piecewise approximation
5:   while  $gap \geq Tol^{in}$ 
6:     Solve piecewise approximated problem, and obtain optimal solution
7:      $x^*$  and optimal objective function value  $obj^{lo}$ 
8:     Evaluate the original objective function with  $x^*$ , and obtain  $obj^{up}$ 
9:     Reconstruct relaxed problem by adding a new partition point
10:    Set  $LB = \max\{LB, obj^{lo}\}$ ,  $UB = \min\{UB, obj^{up}\}$ ,  $gap = |1 - LB / UB|$ ,
11:     $Iter^{in} = Iter^{in} + 1$ 
12:  end while
13:  Update  $q^* = \frac{TC^*}{TGE^*}$ ,  $Iter^{out} = Iter^{out} + 1$ 
14: end while
15: output  $q^*$  and  $x^*$ 

```

---

Figure 30. Pseudo-code of the tailored global optimization algorithm.

In this tailored global optimization algorithm, an auxiliary parameter  $q$  is introduced to reformulate the fractional objective into a parametric function  $F(q)$  following the parametric algorithm. Thus, the optimal solution of the original MINLP problem is identical to the optimal solution of the reformulated parametric problem with the parameter  $q^*$  such that  $F(q^*)=0$  [107]. We apply the exact Newton's method to

iteratively update the parameter  $q$  in each iteration of the parametric algorithm. Meanwhile, we adopt a branch-and-refine algorithm based on successive piecewise linear approximations to tackle the separable concave functions for modeling the capital costs in the economic objective. The optimal solution of the resulting mixed-integer linear programming (MILP) problem provides a lower bound for the objective function ( $obj^{lo}$ ). An upper bound ( $obj^{up}$ ) can be obtained by evaluating the original nonlinear objective function based on the optimal solution  $x^*$  of this MILP. When the optimality criterion in the inner loop is satisfied, the next outer loop iteration starts with updated parameter  $q^*$ . This tailored global optimization algorithm is guaranteed to converge within finite iterations [108, 153].

### **3.3.3 Application to a shale gas supply chain**

To illustrate the applicability of the proposed integrated hybrid LCO model of shale gas supply chains and the tailored global optimization algorithm, we considered a case study of a “well-to-wire” shale gas supply chain in the UK. As shown in Figure 31, a reference map of the shale gas supply chain is provided consisting of shale sites, processing plants, and CCGT power plants [154, 155]. Specifically, there were seven existing shale sites with active shale wells, and eight potential shale sites to be developed. Each shale site allowed multiple shale wells to be drilled. A total of four processing plants were considered, among which two processing plants already existed with given capacities, and two processing plants were potential ones to be designed. The pipeline-quality sales gas obtained at processing plants was distributed to six CCGT power plants for electricity generation. Meanwhile, the NGLs were sold separately as by-products. The

average efficiency of the CCGT power plants was 50% on a lower heating value (LHV) basis [96, 120]. Both the raw shale gas and the processed sales gas were transported through pipelines. We considered three capacity levels of pipelines, which correspond to 4-inch, 8-inch, and 12-inch diameter, respectively. A 10-year planning horizon and 40 time periods with equal time intervals were considered. In this case study, we focused on the environmental impact indicator of life cycle GHG emissions following the existing literature [79, 95, 118]. The extra case studies considering other environmental categories (e.g. water consumption and energy consumption) are presented in Appendix B.



Figure 31. Reference map of the shale gas supply chain in the UK [154, 156].

The resulting MINLP problem has 414 integer variables, 11,797 continuous variables, and 15,370 constraints. All the models and solution procedures are coded in GAMS 24.7.3 [122] on a PC with an Intel® Core™ i7-6700 CPU and 32GB RAM, running the Windows 10 Enterprise, 64-bit operating system. Furthermore, the MILP subproblems are solved using CPLEX 12.7.0. The absolute optimality tolerance of CPLEX is set to be  $10^{-6}$ . The absolute optimality gap for the outer loop parametric algorithm ( $Tol^{out}$ ) is set as  $10^{-6}$ . The relative optimality gap ( $Tol^{in}$ ) for the inner loop branch-and-refine algorithm is set as  $10^{-2}$ . For all the Pareto-optimal solutions, the outer loop corresponding to the parametric algorithm converges within 4 to 6 iterations, and the

inner loop takes 2 to 6 iterations to converge. The total computational time varies from a few thousand CPU seconds to more than 10 hours depending on the number of inner and outer iterations involved. An illustrative figure on the converging process of the tailored global optimization algorithm is provided in Appendix D. Additionally, we solve the resulting MINLP problem with general-purpose global optimizers, including the SCIP 3.2 and BARON 15, for comparison [157, 158]. However, both optimizers failed to converge to the global optimum within the 20-hour computational time limit, and the optimality gaps were still positive infinite.

By solving the resulting MINLP problem, we obtain the Pareto-optimal curve consisting of 10 Pareto-optimal solutions in Figure 32. The  $x$ -axis represents the life cycle GHG emissions for generating one MWh of electricity from shale gas. The  $y$ -axis represents the LCOE across the shale gas supply chain. We select two extreme Pareto-optimal solutions, namely point A with the lowest life cycle GHG emissions and point B with the lowest LCOE, for further investigation and comparison. Additionally, the cost breakdowns as well as GHG emission breakdowns for some of the Pareto-optimal solutions are provided by pie charts and donut charts, respectively. The sizes of these charts are proportional to the absolute values of GHG emissions and total cost.

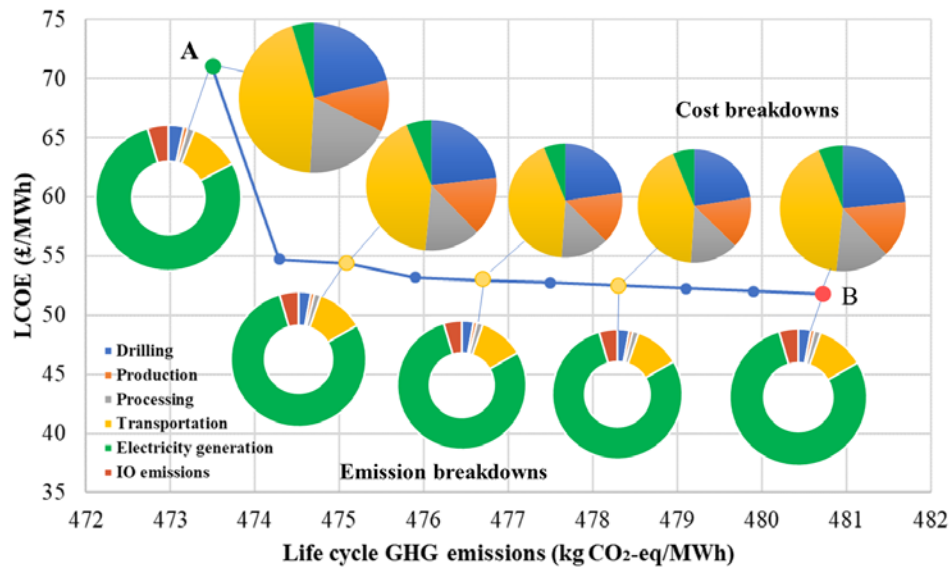


Figure 32. Pareto-optimal curve illustrating the trade-offs between LCOE and life cycle GHG emissions with breakdowns: pie charts for the LCOE breakdowns and donut charts for the breakdowns of life cycle GHG emissions.

Pareto-optimal solution point A has the lowest life cycle GHG emissions of 473.5 kg CO<sub>2</sub>-eq/MWh and the highest LCOE of £71.1/MWh. By contrast, point B has lowest LCOE of £51.8/MWh, but the corresponding life cycle GHG emissions are 480.7 kg CO<sub>2</sub>-eq/MWh. From the cost breakdowns, we can see that the upstream activities across the shale gas supply chain, including shale well drilling, gas production, processing, and transportation activities contribute the most to the total cost. However, downstream electricity generation plays a dominant role in terms of life cycle GHG emissions. Apart from electricity generation, upstream activities, including well drilling and gas transportation, as well as the EIO systems, also contribute significant amounts of GHG emissions. Both cost and GHG emission breakdowns for these Pareto-optimal solutions are similar, and the overall trend is consistent with that of the hybrid LCA results. To

further investigate the key impact factors associated with the life cycle GHG emissions, we present the following GHG emission breakdowns based on the 40 basic processes of the process systems (listed in Table 1).

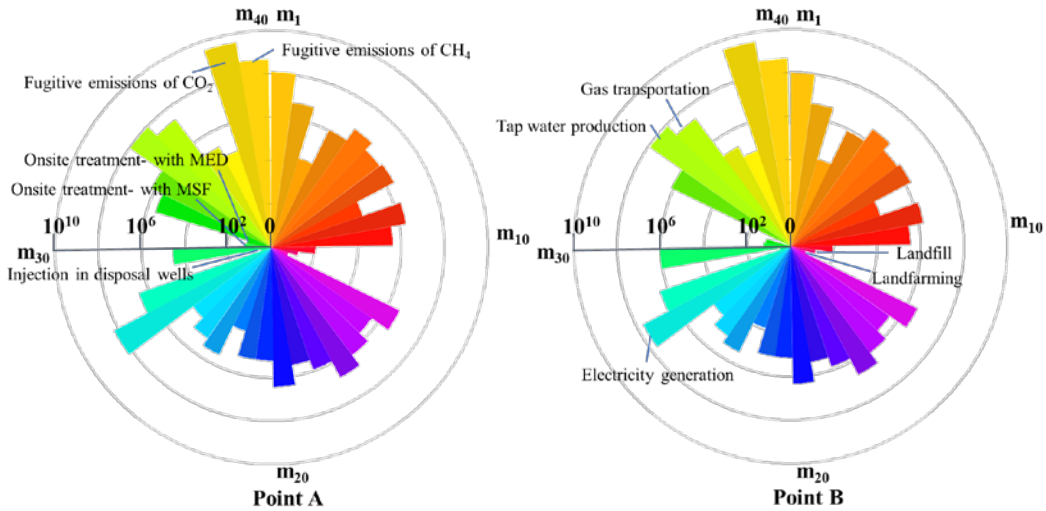


Figure 33. Life cycle GHG emission breakdowns based on the 40 basic processes (indexed by  $m$ ) of the process systems listed in Table 1.

Figure 33 presents the life cycle GHG emissions contributed by each basic process following the clockwise sequence. The detailed descriptions of these 40 processes are provided in Table 1. As a result, we can easily recognize the key processes in the process systems that lead to the most life cycle GHG emissions. Fugitive emissions of  $\text{CO}_2$  and  $\text{CH}_4$  are identified as the major impact factors, which in total contribute about 93% of the total process GHG emissions. Other processes, including electricity generation, tap water production, and gas transportation, also contribute a significant amount of GHG emissions throughout the process systems. The overall GHG emission breakdowns of both solutions are similar. However, we can see that the process of wastewater treatment by CWT facility results in less GHG emissions in point A. Meanwhile, the process of

onsite treatment with RO technology incurs a considerable amount of GHG emissions in point A, but this process contributes no GHG emissions in point B. Such a difference is due to the different optimal water management strategies obtained in these Pareto-optimal solutions.

In Figure 34, we summarize and present the optimal drilling schedules and shale gas productions profiles of solution point A (minimizing the life cycle GHG emissions) and point B (minimizing the LCOE). More shale wells are drilled in the optimal solution of point A than that of point B. Specifically, a total of 105 shale wells are drilled in the optimal solution of point A, and 82 shale wells are drilled in the optimal solution of point B. Here we highlight the development of shale site 15 in the optimal solution of point A. With these extra wells at shale site 15 drilled, the corresponding shale gas production of point A is expected to be larger than that of point B. The shale gas production profiles of both solution points are similar, where the production peak is reached around the 13th quarter, namely the beginning of the fourth year. This is the time when no more shale wells are drilled, and overall shale gas production starts to decrease afterwards due to the decreasing production profiles of existing shale wells.

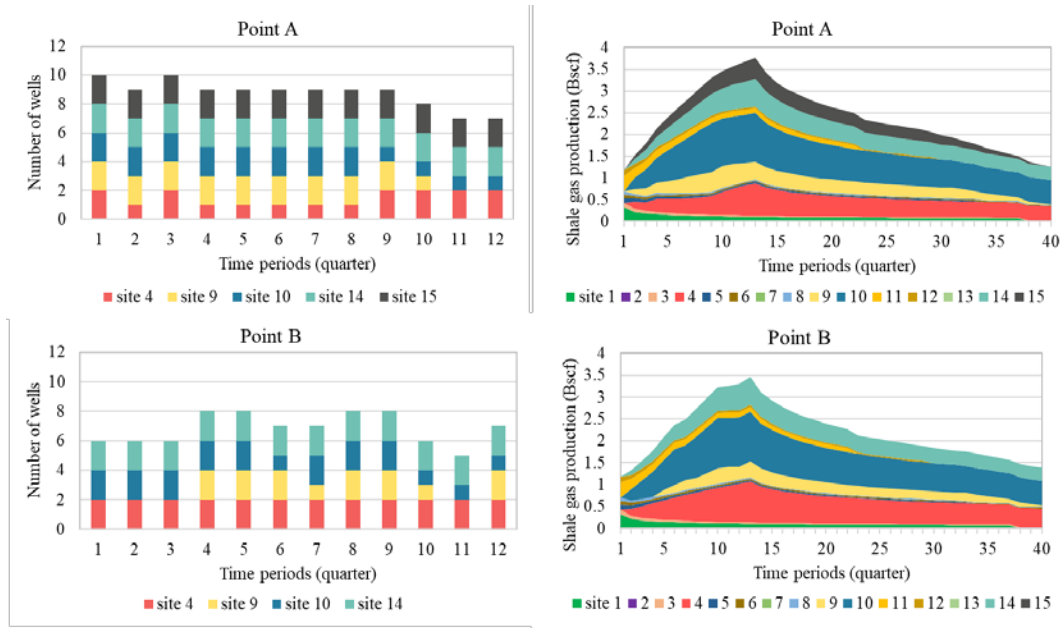


Figure 34. Drilling schedules and production profiles of solution points A and B.

The optimal shale gas supply chain designs with corresponding mass flows are summarized in Figure 35, which is given in the form of a Sankey diagram. As can be seen, although the structures of both shale gas supply chains in points A and B are similar, the overall shale gas production at each shale site, the capacities of processing plants, and the distribution planning of sales gas are different in these two solution points. As discussed above, shale site 15 is developed in the optimal solution of point A, resulting in a larger shale gas production near processing plant 4. Therefore, the working capacity of shale gas processing plant 4 is 3.50 billion standard cubic feet (Bscf) per year in the optimal solution of point A in contrast to 3.18 Bscf per year in the optimal solution of point B. For a similar reason, the capacity of processing plant 3 in the optimal solution of point A is 6.27 Bscf per year, greater than the 6.05 Bscf per year of processing plant 3 in the optimal solution of point B. The sales gas from processing plant 1 is mainly consumed by power plants 1 and 2. All the sales gas from processing

plant 2 is sent to power plants. Power plants 3 and 6 obtain all their gas feedstock from processing plant 3. The sales gas from processing plant 4 is distributed to power plants 4 and 5. The NGLs are sold to its own market for extra income.

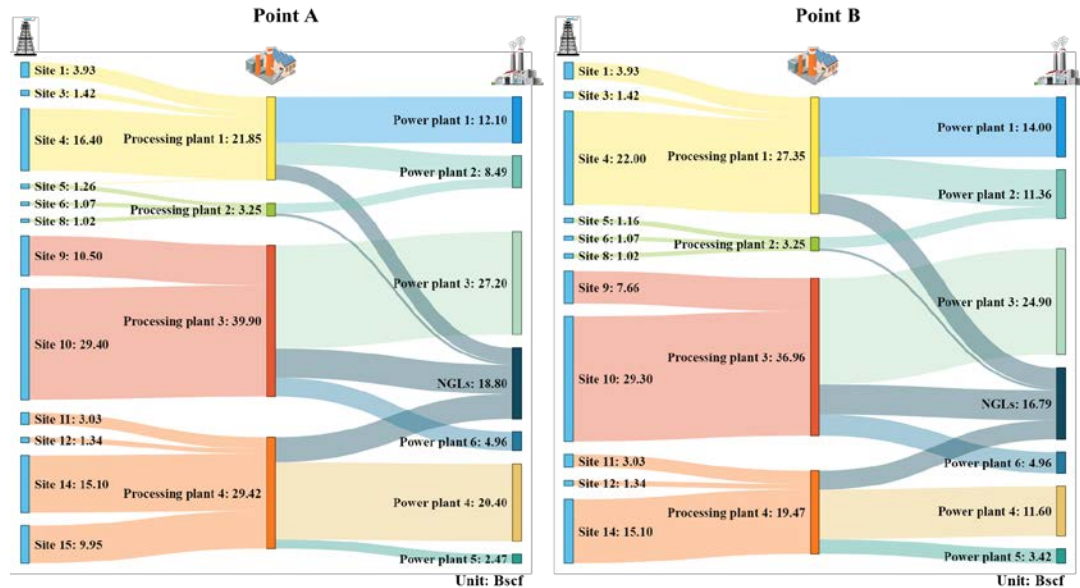


Figure 35. Summary of shale gas supply chain design and flow information for Pareto-optimal solution point A and point B.

Next, we summarize the optimal water management strategies of solution points A and B in Figure 36. As can be observed, for both solution points, the hydraulic fracturing process results in more wastewater than the drilling process. In the optimal solution of point A, the onsite treatment with RO technology is selected as the main water treatment option that handles a total of 109,409 m<sup>3</sup> wastewater. Meanwhile, 3,636 m<sup>3</sup> water is transported to the CWT facility for centralized treatment. Thanks to the application of onsite treatment technology, 71,116 m<sup>3</sup> of treated water can be recycled as inputs for drilling and hydraulic fracturing. As a result, even though more shale wells are drilled in the optimal solution of point A, the total freshwater consumption is smaller than that

of point B. By contrast, in the optimal solution of point B, a total of 106,032 m<sup>3</sup> wastewater is sent to CWT facility for treatment, which is considered more cost-effective than the onsite treatment options. The corresponding requirement of freshwater input is 512,947 m<sup>3</sup>.

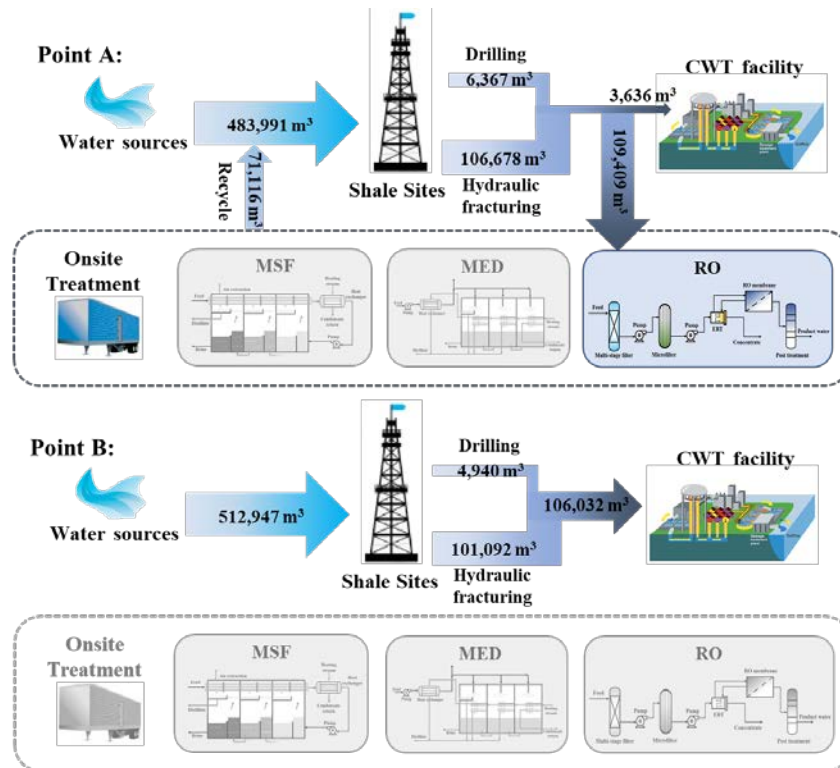


Figure 36. Optimal water management strategies of solution points A and B.

### 3.4 Summary

We analyzed the life cycle environmental impacts of shale gas using the integrated hybrid LCA approach. In contrast to the traditional process-based LCA approach that suffered system boundary truncation, this integrated hybrid LCA approach provided a way to estimate the total environmental impacts resulted from both the process systems and the EIO systems. We considered three environmental impact factors, including GHG emissions, water consumption, and energy consumption, for the integrated hybrid

LCA of shale gas. The LCA results were comprehensively compared with existing shale gas LCA studies as well as integrated hybrid LCA studies of other fossil fuels. We further developed a hybrid LCO model to automatically identify the optimal design and operational alternatives in a “well-to-wire” shale gas supply chain considering both economic and environmental criteria. A tailored global optimization algorithm integrating the parametric algorithm and a branch-and-refine algorithm was implemented to tackle the resulting MINLP problem. The applicability of the proposed hybrid LCO model and global optimization algorithm was illustrated through a case study of shale gas supply chain. In this case study, the lowest levelized cost of electricity generated from shale gas was £51.8/MWh, and the optimal life cycle GHG emissions, water consumption, and energy consumption were 473.5 kg CO<sub>2</sub>-eq/MWh, 2,263 kg/MWh, and 1,009 MJ/MWh, respectively. Based on the results, we concluded that environmental impacts induced by the EIO systems could constitute a significant part of the overall life cycle environmental impacts of shale gas, especially with pessimistic LCI estimations or certain environmental categories.

### **3.5 Appendix A: Detailed model formulation for the hybrid LCO model of shale gas supply chains**

The hybrid LCO model is a mixed-integer nonlinear program, of which the general formulation is provided in the main text. Here we present the detailed description of all the constraints as well as objective functions. All the parameters are denoted with lower-case symbols, and all the variables are denoted with upper-case symbols.

### 3.5.1 Objective functions

#### 3.5.1.1 Economic objective

The economic objective is to minimize the LCOE generated from shale gas, formulated as the total net present cost divided by the total electric power generation ( $TGE$ ). The total net present cost comprises the capital investment ( $TC^{cap}$ ) associated with shale gas processing plants and gas pipelines, and the operating cost ( $TC_i^{oper}$ ) related to water management, drilling activities, shale gas production operations, shale gas processing, transportation activities, and electric power generation. Since the GHG emissions are modeled as an individual environmental objective function, we do not consider any types of externalities in this model.

$$\min LCOE = \frac{TC^{cap} + \sum_{i \in T} \frac{TC_i^{oper}}{(1+dr)^i}}{TGE} \quad (A1)$$

#### 3.5.1.2 Life Cycle GHG Emissions Objective

The environmental objective is to minimize the life cycle GHG emissions associated with generating one MWh electricity in the “well-to-wire” shale gas supply chain network ( $UE$ ), defined as summation of process emissions ( $TE^{pro}$ ) and IO emissions ( $TE^{IO}$ ) divided by the total electricity generation ( $TGE$ ).

$$\min UE = \frac{TE^{pro} + TE^{IO}}{TGE} \quad (A2)$$

## 3.5.2 Constraints

### 3.5.2.1 Economic constraints

The total capital investment equals the summation of capital cost for constructing processing plants and capital cost for installing pipeline networks.

$$TC^{cap} = C_{proc}^{cap} + C_{pipe}^{cap} \quad (A3)$$

$C_{proc}^{cap}$  is the total capital cost associated with construction of processing plants, calculated by the following nonlinear function,

$$C_{proc}^{cap} = \sum_{p \in P_n} pri \cdot \left( \frac{PC_p}{prc} \right)^{sfp} \cdot \left( \frac{pci}{rpci} \right) \quad (A4)$$

where  $pri$  denotes the reference capital cost of constructing processing plants.  $PC_p$  denotes the capacity of processing plant  $p$ .  $prc$  denotes the reference capacity of processing plants.  $sfp$  denotes the size factor of processing plants.  $pci$  denotes the chemical engineering plant cost index for processing plants.  $rpci$  denotes the chemical engineering plant cost index for processing plant of the reference year. Notably, this is a separable concave function. In addition to the fractional objective functions, this constraint is identified as the only nonlinear term involved in the MINLP model.

$C_{pipe}^{cap}$  indicates the total capital cost of installing pipelines, including the gathering pipelines transporting raw shale gas from shale sites to processing plants and the distribution pipelines transporting processed sales gas from processing plants to CCGT power plants, calculated by,

$$C_{pipe}^{cap} = \sum_{i \in I} \sum_{p \in P} \sum_{r \in R} tpri_r \cdot XP_{i,p,r} \cdot lsp_{i,p} + \sum_{p \in P} \sum_{g \in G} \sum_{r \in R} tpri_r \cdot XPG_{p,g,r} \cdot lpg_{p,g} \quad (A5)$$

where  $tpri_r$  denotes the reference capital cost of pipelines with capacity level  $r$ .  $lsp_{i,p}$  is the distance between shale site  $i$  and processing plant  $p$ .  $lpg_{p,g}$  is the distance between processing plant  $p$  and CCGT power plant  $g$ .

The total operating cost in each time period includes the operating costs associated with water management, drilling activities, shale gas production operations, shale gas processing, transportation activities, and electric power generation.

$$TC_t^{oper} = C_{water,t}^{oper} + C_{drill,t}^{oper} + C_{prod,t}^{oper} + C_{proc,t}^{oper} + C_{trans,t}^{oper} + C_{power,t}^{oper} \quad (A6)$$

The water management cost consists of water acquisition cost ( $C_{acq,t}$ ) and wastewater treatment costs corresponding to CWT facilities ( $C_{cwt,t}$ ), and onsite treatment ( $C_{onsite,t}$ ).

$$C_{water,t}^{oper} = C_{acq,t} + C_{cwt,t} + C_{onsite,t} \quad (A7)$$

$C_{acq,t}$  indicates the acquisition cost of freshwater in time period  $t$ , which is proportional to the amount of freshwater,

$$C_{acq,t} = \sum_{i \in I} fac \cdot FW_{i,t} \quad (A8)$$

where  $fac$  denotes the unit acquisition cost of freshwater.

$C_{cwt,t}$  indicates the cost associated with CWT treatment facilities in time period  $t$ , calculated by,

$$C_{cwt,t} = \sum_{i \in I} vc \cdot WTC_{i,t} \quad (A9)$$

where  $vc$  denotes the unit wastewater treatment cost of CWT facilities.

$C_{onsite,t}$  is the total onsite treatment cost in time period  $t$ , given by,

$$C_{onsite,t} = \sum_{i \in I} \sum_{o \in O} vo_o \cdot WTO_{i,o,t} \quad (A10)$$

where  $vo_o$  denotes the unit wastewater treatment cost of onsite treatment units with technology  $o$ .

$C_{drill,t}^{oper}$  indicates the total operating cost associated with drilling activities in time period  $t$ ,

$$C_{drill,t}^{oper} = \sum_{i \in I_n} sdc_{i,t} \cdot NN_{i,t} \quad (A11)$$

where  $sdc_{i,t}$  denotes the unit cost for shale well drilling and completion at shale site  $i$  in time period  $t$ .

$C_{prod,t}^{oper}$  stands for the total operating cost associated with shale gas production activities in time period  $t$ , which is proportional to the amount of shale gas production.

$$C_{prod,t}^{oper} = \sum_{i \in I} spc_{i,t} \cdot SP_{i,t} \quad (A12)$$

where  $spc_{i,t}$  denotes the unit operating cost for shale gas production at shale site  $i$  in time period  $t$ .

$C_{proc,t}^{oper}$  indicates the total operating cost for processing plants in time period  $t$ , given as the gross cost of shale gas processing subtracted by the income from sales of NGLs.

$$C_{proc,t}^{oper} = \sum_{i \in I} \sum_{p \in P} vp_p \cdot STP_{i,p,t} - \sum_{p \in P} pl_t \cdot SPL_{p,t} \quad (A13)$$

where  $vp_p$  denotes the unit operating cost for processing plant  $p$ .  $pl_t$  denotes the average unit price of NGLs in time period  $t$ .

$C_{trans,t}^{oper}$  stands for the total operating cost associated with all the transportation activities in time period  $t$ , given by,

$$C_{trans,t}^{oper} = \sum_{i \in I} \sum_{p \in P} vtp \cdot lsp_{i,p} \cdot STP_{i,p,t} + \sum_{p \in P} \sum_{g \in G} vtp \cdot lpg_{p,g} \cdot STPG_{p,g,t} \quad (A14)$$

where  $vtp$  denotes the unit gas transportation cost via pipelines.

$C_{power,t}^{oper}$  indicates the total operating cost associated with electric power generation in time period  $t$ , calculated by,

$$C_{power,t}^{oper} = \sum_{p \in P} \sum_{g \in G} ve_g \cdot STPG_{p,g,t} \quad (A15)$$

where  $ve_g$  denotes the unit cost for electricity generation from natural gas at power plant  $g$ .

### 3.5.2.2 Environmental constraints

The process emissions indicate the GHG emissions generated during all the activities in the process systems, calculated by the following equation.

$$TE^{pro} = e_m^{pro} Q_m \quad (A16)$$

where  $e_m^{pro}$  is the environmental impact factors of basic process  $m$ .  $Q_m$  is the total net input of process  $m$  from all activities, including water management, well drilling, shale gas production, processing, transportation, and electricity generation, in the process systems.

Based on the definition of  $Q_m$ , it can be calculated by the following equation.

$$Q_m = Q_{water,m} + Q_{drill,m} + Q_{prod,m} + Q_{proc,m} + Q_{trans,m} + Q_{power,m} \quad (A17)$$

$Q_{water,m}$  is the total input of process  $m$  associated with water management activities, including wastewater treatment at CWT facilities and onsite treatment units.

$$Q_{water,m} = \sum_{i \in I} \sum_{t \in T} WTC_{i,t} \cdot inv\_cwt_{i,m} + \sum_{i \in I} \sum_{o \in O} \sum_{t \in T} WTO_{i,o,t} \cdot inv\_onsite_{o,m} \quad (A18)$$

where  $inv\_cwt_{i,m}$  is the amount of input from process  $m$  for treating unit amount of wastewater from shale site  $i$  at CWT facilities.  $inv\_onsite_{o,m}$  indicates the amount of input from process  $m$  for treating unit amount of wastewater with onsite treatment technology  $o$ .

$Q_{drill,m}$  is the total input of process  $m$  regarding drilling activities, which can be calculated by,

$$Q_{drill,m} = \sum_{i \in I_n} \sum_{t \in T} NN_{i,t} \cdot inv\_drill_{i,m} \quad (A19)$$

where  $inv\_drill_{i,m}$  indicates the amount of input from process  $m$  for drilling a shale well at potential shale site  $i$ .

$Q_{prod,m}$  represents the total input of process  $m$  associated with shale gas production activities, given by,

$$Q_{prod,m} = \sum_{i \in I} \sum_{t \in T} SP_{i,t} \cdot inv\_prod_{i,m} \quad (A20)$$

where  $inv\_prod_{i,m}$  indicates the amount of input from process  $m$  for producing unit amount of shale gas at shale site  $i$ .

$Q_{proc,m}$  represents the total input of process  $m$  associated with shale gas processing activities, calculated by,

$$Q_{proc,m} = \sum_{i \in I} \sum_{p \in P} \sum_{t \in T} STP_{i,p,t} \cdot inv\_proc_{p,m} \quad (A21)$$

where  $inv\_proc_{p,m}$  indicates the amount of input from process  $m$  for processing unit amount of raw shale gas at processing plant  $p$ .

$Q_{trans,m}$  represents the total input of process  $m$  associated with gas transportation activities, which is calculated by,

$$Q_{trans,m} = \sum_{i \in I} \sum_{p \in P} \sum_{t \in T} STP_{i,t} \cdot lsp_{i,p} \cdot inv\_trans_m + \sum_{p \in P} \sum_{g \in G} \sum_{t \in T} STPG_{i,t} \cdot lpg_{p,g} \cdot inv\_trans_m \quad (A22)$$

where  $inv\_trans_m$  indicates the amount of input from process  $m$  for transporting unit amount of shale gas for unit distance.

$Q_{power,m}$  represents the total input of process  $m$  associated with electricity generation activities, given by,

$$Q_{power,m} = \sum_{p \in P} \sum_{g \in G} \sum_{t \in T} STPG_{p,g,t} \cdot inv\_power_{g,m} \quad (A23)$$

where  $inv\_power_{g,m}$  indicates the amount of input from process  $m$  for consuming unit amount of shale gas to generate electricity at CCGT power plant  $g$ .

The IO emissions indicate the GHG emissions generated in the EIO systems, calculated by the following equation.

$$TE^{IO} = e_{ns}^{IO} P_{ns} \quad (A24)$$

where  $e_{ns}^{IO}$  is the environmental impact factors of industrial sector  $ns$ .  $P_{ns}$  is the total output of sector  $ns$  in the EIO systems.

The total output of each industrial sector  $P_{ns}$  minus the direct requirement of all sectors in the EIO systems should be no less than the upstream inputs required by the process systems, given by,

$$P_{ns} - \sum_{ns' \in NS} aio_{ns,ns'} \cdot P_{ns} \geq UP_{ns} \quad (A25)$$

where  $aio_{ns,ns'}$  is the technical coefficient connecting industrial sector  $ns$  and  $ns'$  in the EIO table.  $UP_{ns}$  indicates the upstream input from industrial sector  $ns$  to the process systems.

The upstream input from industry sector  $ns$  to the process systems  $UP_{ns}$  can be calculated by the following equation,

$$UP_{ns} = \sum_{m \in M} c_{ns,m} \cdot price_m \cdot Q_m \quad (A26)$$

where  $c_{ns,m}$  is the upstream technical coefficient linking industrial sector  $ns$  and process  $m$ .  $price_m$  indicates the unit price input from process  $m$ .

### 3.5.2.3 Mass balance constraints

The total water supply at each shale site comprises of freshwater from water sources and reused water from onsite treatment.

$$FW_{i,t} + \sum_{o \in O} lo_o \cdot WTO_{i,o,t} = FDW_{i,t}, \forall i, t \quad (A27)$$

where  $FW_{i,t}$  stands for the amount of freshwater acquired from water sources to shale site  $i$  in time period  $t$ .  $lo_o$  denotes the recovery factor for treating wastewater of onsite treatment technology  $o$ .  $WTO_{i,o,t}$  denotes the amount of wastewater treated by onsite treatment technology  $o$  at shale site  $i$  in time period  $t$ .  $FDW_{i,t}$  denotes the freshwater demand of shale site  $i$  in time period  $t$ .

The amount of freshwater required at each shale site in each time period equals the summation of water usage for drilling and hydraulic fracturing. The drilling water usage is proportional to the number of wells being drilled, and the hydraulic fracturing water usage is proportional to the amount of wastewater produced at shale site  $i$ .

$$FDW_{i,t} = \frac{WP_{i,t}}{wrf_i} + wd_i \cdot NN_{i,t}, \forall i, t \quad (A28)$$

where  $WP_{i,t}$  denotes the wastewater production rate during fracking process at shale site  $i$  in time period  $t$ .  $wrf_i$  is the recovery ratio of water for hydraulic fracturing process at shale site  $i$ .  $wd_i$  denotes the average drilling water usage at shale site  $i$ .  $NN_{i,t}$  stands for the number of wells drilled at shale site  $i$  in time period  $t$ .

The wastewater production rate during the fracking process is proportional to the total shale gas production rate at a shale site, and the coefficient is estimated based on real data.[124]

$$WP_{i,t} = cc_i \cdot SP_{i,t}, \forall i, t \quad (A29)$$

where  $cc_i$  is the correlation coefficient for shale gas production and wastewater production of a shale well at shale site  $i$ .  $SP_{i,t}$  is the shale gas production rate at shale site  $i$  in time period  $t$ .

At each shale site, the total amount of wastewater, including the wastewater from drilling, hydraulic fracturing, and completion, should equal to the total amount of water treated by different water management options, including CWT and onsite treatment.

$$WP_{i,t} + wd_i \cdot wrd_i \cdot NN_{i,t} = WTC_{i,t} + \sum_{o \in O} WTO_{i,o,t}, \quad \forall i, t \quad (\text{A30})$$

where  $wrd_i$  denotes the recovery ratio for drilling process at shale site  $i$ .  $WTC_{i,t}$  denotes the amount of wastewater transported from shale site  $i$  to CWT facilities in time period  $t$ .

The total amount of shale gas produced at any existing shale site  $i$  at any time period  $t$  can be calculated by,

$$SP_{i,t} = ne_i \cdot spp_{i,t}, \quad \forall i \in I_e, t \quad (\text{A31})$$

where  $ne_i$  denotes the number of existing shale wells drilled at shale site  $i$ .  $spp_{i,t}$  denotes the shale gas production of a shale well of age  $t$  at shale site  $i$ .

The total shale gas production rate at a shale site equals the summation of that of different wells.

$$SP_{i,t} = \sum_{t'=1}^{t-1} NN_{i,t'} \cdot spp_{i,t-t'}, \quad \forall i \in I_n, t \geq 2 \quad (\text{A32})$$

where  $spp_{i,t-t'}$  denotes the shale gas production profile of a shale well drilled at time period  $t'$  at shale site  $i$  in time period  $t$ . Thus, the age of this well would be  $t-t'$ . We use

this time-dependent parameter to describe the decreasing feature of the shale gas production profile of a certain well.

The shale gas production at each shale site is then transported to different processing plants.

$$SP_{i,t} = \sum_{p \in P} STP_{i,p,t}, \forall i, t \quad (\text{A33})$$

where  $STP_{i,p,t}$  denotes the amount of shale gas transported from shale site  $i$  to processing plant  $p$  in time period  $t$ .

The methane and NGLs are separated at processing plants, and their corresponding amounts are dependent on the processing efficiency and the composition of raw shale gas.

$$\sum_{i \in I} STP_{i,p,t} \cdot \text{pef} \cdot mc_i = SPM_{p,t}, \forall p, t \quad (\text{A34})$$

$$\sum_{i \in I} STP_{i,p,t} \cdot \text{pef} \cdot lc_i = SPL_{p,t}, \forall p, t \quad (\text{A35})$$

where  $\text{pef}$  denotes the NGL recovery efficiency at processing plants.  $mc_i$  denotes the methane composition in shale gas at shale site  $i$ .  $lc_i$  denotes the NGL composition at shale site  $i$ .  $SPM_{p,t}$  is the amount of natural gas produced at processing plant  $p$  in time period  $t$ .  $lc_i$  is the average NGLs composition in shale gas at site  $i$ .  $SPL_{p,t}$  stands for the amount of NGLs produced at processing plant  $p$  in time period  $t$ .

The total amount of natural gas separated at a processing plant equals the summation of natural gas transported from the processing plant to different power plants.

$$SPM_{p,t} = \sum_{g \in G} STPG_{p,g,t}, \forall p, t \quad (\text{A36})$$

where  $STPG_{p,g,t}$  denotes the amount of natural gas transported from processing plant  $p$  to power plant  $g$  in time period  $t$ .

The total amount of electricity generation at a power plant in each time period is proportional to the amount of natural gas transported to the power plant from processing plants.

$$GE_{g,t} = ue \cdot \sum_{p \in P} STPG_{p,g,t}, \forall g, t \quad (\text{A37})$$

where  $GE_{g,t}$  denotes the amount of electricity generated at power plant  $g$  in time period  $t$ .  $ue$  denotes the amount of electricity generated from unit natural gas input.

#### 3.5.2.4 Capacity constraints

The total amount of wastewater from different shale sites treated by each CWT facility cannot exceed its capacity, given by,

$$\sum_{i \in I} WTC_{i,t} \leq cca_t, \forall t \quad (\text{A38})$$

where  $cca_t$  denotes the capacity for wastewater treatment at CWT facility in time period  $t$ .

If a certain onsite treatment technology is applied at a shale site, the amount of wastewater treated onsite should be bounded by its capacity; otherwise, the amount of wastewater treated onsite should be zero. This relationship can be modeled by the following inequality,

$$ocl_o \cdot YO_{i,o} \leq WTO_{i,o,t} \leq ocu_o \cdot YO_{i,o}, \forall i, o, t \quad (\text{A39})$$

where  $ocl_o$  and  $ocu_o$  denote the minimum and maximum treatment capacities for onsite treatment technology  $o$ , respectively.  $YO_{i,o}$  is a binary variable that equals 1 if onsite treatment technology  $o$  is applied at shale site  $i$ .

The total amount of shale gas processed at a processing plant cannot exceed its capacity,

$$\sum_{i \in I} STP_{i,p,t} \leq PC_p, \forall p, t \quad (A40)$$

where  $PC_p$  denotes the capacity of processing plant  $p$ .

The total amount of shale gas transported from a shale site to a processing plant is constrained by the transportation capacity of corresponding gathering pipeline.

$$STP_{i,p,t} \leq \sum_{r \in R} TCP_{i,p,r}, \forall i, p, t \quad (A41)$$

where  $TCP_{i,p,r}$  denotes the capacity of pipeline from shale site  $i$  to processing plant  $p$  with capacity level  $r$ .

Similarly, the amount of natural gas transported from processing plant  $p$  to power plant  $g$  is bounded by the capacity of corresponding pipeline,

$$STPG_{p,g,t} \leq \sum_{r \in R} TCPG_{p,g,r}, \forall p, g, t \quad (A42)$$

where  $TCPG_{p,g,r}$  denotes the capacity of pipeline from processing plant  $p$  to power plant  $g$  with capacity level  $r$ .

The total electric power generation is constrained by the lower bound and upper bound of local demand.

$$dgl_{g,t} \leq GE_{g,t} \leq dgup_{g,t}, \forall g, t \quad (A43)$$

where  $dgl_{g,t}$  and  $dgup_{g,t}$  denote the minimum demand and maximum demand of electricity at power plant  $g$  in time period  $t$ , respectively.

### 3.5.2.5 Composition constraints

To satisfy the reuse specification for hydraulic fracturing, the blending ratio of freshwater to treated water from onsite treatment must be greater than a certain value, given by,

$$\sum_{o \in O} rf_o \cdot lo_o \cdot WTO_{i,o,t} \leq FW_{i,t}, \forall i, t \quad (\text{A44})$$

where  $rf_o$  denotes the ratio of freshwater to wastewater required for blending after treatment by onsite treatment technology  $o$ .

### 3.5.2.6 Bounding constraints

If a gathering pipeline is installed, its capacity equals the reference capacity corresponding to its capacity level; otherwise, its capacity should be zero.

The constraints for the capacity of pipeline transporting shale gas from shale site  $i$  to processing plant  $p$  are given by,

$$TCP_{i,p,r} = tprc_r \cdot XP_{i,p,r}, \forall i, p, r \quad (\text{A45})$$

where  $tprc_r$  denotes the reference capacity of gathering pipelines with capacity level  $r$ .  $XP_{i,p}$  is a binary variable that equals 1 if pipeline is installed to transport shale gas from shale site  $i$  to processing plant  $p$ .

Similarly, the constraints for the capacity of pipeline transporting natural gas from processing plant  $p$  to power plant  $g$  are given by,

$$TCPG_{p,g,r} = tprc_r \cdot XPG_{p,g,r}, \forall p \in p, g, r \quad (\text{A46})$$

where  $XPG_{p,g}$  is a binary variable that equals 1 if corresponding pipeline is installed between potential processing plant  $p$  and power plant  $g$ .

If a processing plant is established, its processing capacity should be bounded by the corresponding capacity range; otherwise, its capacity should be zero. This relationship can be modeled by the following inequality:

$$pcl \cdot YP_p \leq PC_p \leq pcup \cdot YP_p, \forall p \in PN \quad (A47)$$

where  $pcl$  and  $pcup$  denote the minimum and maximum capacities of potential processing plants, respectively.  $YP_p$  is a binary variable that equals 1 if processing plant  $p$  is constructed.

### 3.5.2.7 Logic constraints

For the selection of onsite treatment technologies, we note that at most one technology can be chosen. This constraint is given by,

$$\sum_{o \in O} YO_{i,o} \leq 1, \forall i \quad (A48)$$

There can only be a certain number of wells drilled at each shale site in each time period,

$$\sum_{n=0}^{mn_i} YD_{i,n,t} = 1, \forall i \in I_n, t \quad (A49)$$

where  $YD_{i,n,t}$  is a binary variable that equals 1 if  $n$  shale wells at potential shale site  $i$  are drilled in time period  $t$ .  $mn_i$  denotes the maximum number of wells that can be drilled at potential shale site  $i$  per time period.

The total number of wells drilled at potential shale site  $i$  in time period  $t$  can be calculated by,

$$NN_{i,t} = \sum_{n=0}^{mn_i} n \cdot YD_{i,n,t}, \forall i \in I_n, t \quad (A50)$$

The total number of wells that can be drilled at potential shale site  $in$  over the planning horizon is bounded, given by,

$$\sum_{t \in T} NN_{i,t} \leq tmn_{in}, \forall i \in I_n \quad (\text{A51})$$

where  $tmn_{in}$  denotes the maximum number of wells that can be drilled at potential shale site  $in$  over the planning horizon.

Only one capacity level can be selected for the gathering pipeline from shale site  $i$  to processing plant  $p$ , given by,

$$\sum_{r \in R} XP_{i,p,r} \leq 1, \forall i, p \quad (\text{A52})$$

Similarly, there can only be one capacity level for the transmission pipeline from processing plant  $p$  to power plant  $g$ , given by,

$$\sum_{r \in R} XPG_{p,g,r} \leq 1, \forall p, g \quad (\text{A53})$$

### **3.6 Appendix B: Hybrid LCO models minimizing life cycle water consumption and energy consumption**

In this section, we present the optimization results of extra case studies considering other environmental categories, namely the water consumption (P1) and energy consumption (P2), using the proposed hybrid LCO model of shale gas supply chains. Compared with the hybrid LCO model minimizing the life cycle GHG emissions, these extra hybrid LCO models adopt different environmental objectives minimizing the life cycle water consumption ( $UW$ ) and energy consumption ( $UG$ ), respectively.  $TW^{pro}$  and  $TW^{IO}$  indicate the life cycle water consumption resulting from activities in the process systems

and industrial sectors in the EIO systems, respectively. Similarly,  $TG^{pro}$  and  $TG^{IO}$  are the total energy consumption associated with the process systems and the EIO systems, respectively. All the remaining constraints are identical to those presented in Appendix A.

$$(P1) \quad \min UW = \frac{TW^{pro} + TW^{IO}}{TGE} \quad (B1)$$

s.t. Constraints (A3)-(A53)

$$(P2) \quad \min UG = \frac{TG^{pro} + TG^{IO}}{TGE} \quad (B2)$$

s.t. Constraints (A3)-(A53)

In Figure B1, we summarize the optimal life cycle economic and environmental performances of both hybrid LCO models (P1) and (P2). As can be seen, in the optimal solution of (P1), the unit water consumption is 2,263 kg/MWh, most of which is contributed by shale gas processing and electricity generation activities. The IO water consumption is even greater than that of drilling activities. The corresponding LCOE is £71.4/MWh, close to the optimal LCOE obtained in the original hybrid LCO model minimizing the life cycle GHG emissions. The detailed cost breakdown regarding different processes is consistent with that given in Figure 32, where drilling and transportation activities result in a large portion of total cost. In the optimal solution of (P2), the EIO systems are identified as the most significant impact factor in terms of energy consumption. The unit energy consumption is 1,009 MJ/MWh, and the IO energy consumption itself contributes 643 MJ/MWh energy consumption. In the process systems, well drilling, gas processing, and transportation activities are all energy-intense

processes. The corresponding LCOE is £58.2/MWh, 18% lower than that obtained in model (P1).

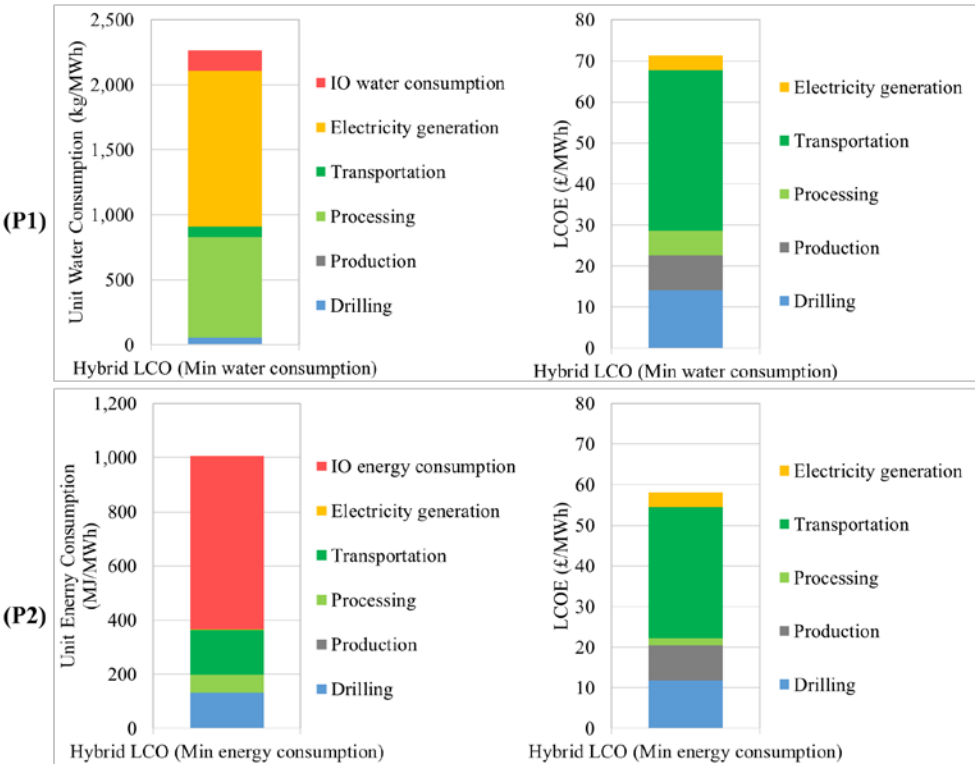


Figure B1. Optimal economic and environmental performances of hybrid LCO models: (P1) minimizing the life cycle water consumption and (P2) minimizing the life cycle energy consumption.

The distinct economic and environmental performances obtained in (P1) and (P2) are essentially caused by their corresponding optimal design and operational decisions made across the shale gas supply chain. In Figure B2, we summarize the optimal drilling schedules and shale gas production profiles obtained in models (P1) and (P2) minimizing life cycle water consumption and energy consumption, respectively. As can be seen, shale site 9 is developed in the optimal solution of (P1), resulting in a total of 83 shale wells. By contrast, only 59 shale wells are drilled in the optimal solution of

(P2), and the resulting shale gas production in each time period is smaller than that of (P1).

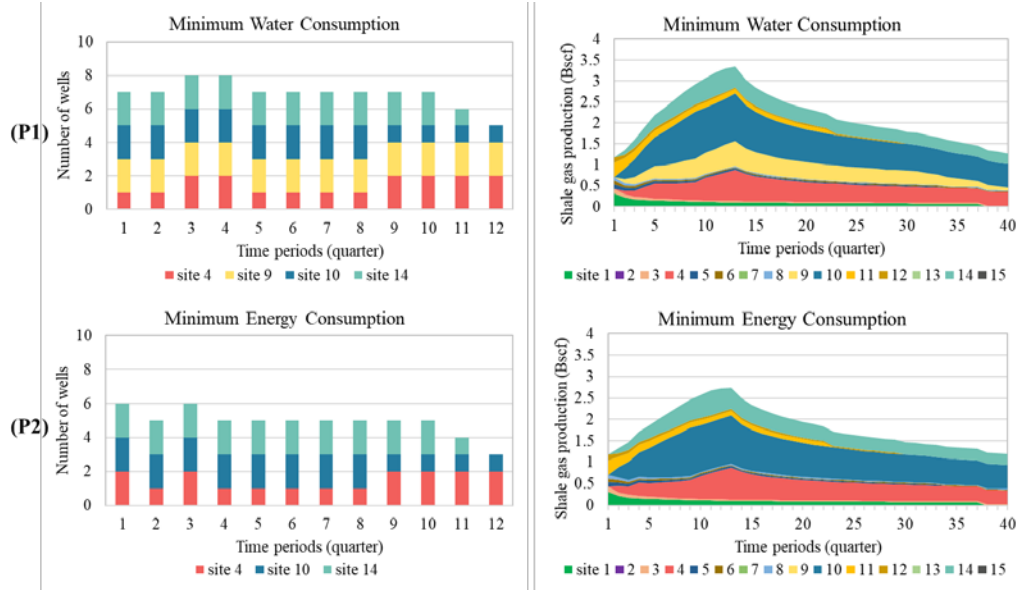


Figure B2. Comparison of drilling schedules and production profiles in the optimal solutions of models (P1) and (P2) for minimizing the life cycle water consumption and minimizing the life cycle energy consumption, respectively.

### 3.7 Appendix C: Optimization results of process-based LCO model

To demonstrate the difference between the integrated hybrid LCO model and the traditional process-based LCO model, we consider another case study that focuses on the process systems. In this process-based LCO model (P3), the objective is to minimize the life cycle process GHG emissions, as given in equation (C1). All the constraints remain the same to those provided in Appendix A.

$$(P3) \quad \min UE^P = \frac{TW^{pro}}{TGE} \quad (C1)$$

s.t. Constraints (A3)-(A53)

The optimal economic and environmental performances are summarized in Figure C1. The resulting life cycle GHG emissions are 475.2 kg CO<sub>2</sub>-eq/MWh, where the process systems contribute 450.9 kg CO<sub>2</sub>-eq/MWh GHG emissions. Although the process GHG emissions are lower than that (451.6 kg CO<sub>2</sub>-eq/MWh) obtained in the original hybrid LCO model (P0), the EIO systems result in more GHG emissions, which are 24.3 kg CO<sub>2</sub>-eq/MWh. The optimal LCOE is £66.1/MWh, which lies between the highest LCOE (£71.1/MWh) and the lowest LCOE (£51.8/MWh) of Pareto optimal solutions A and B.

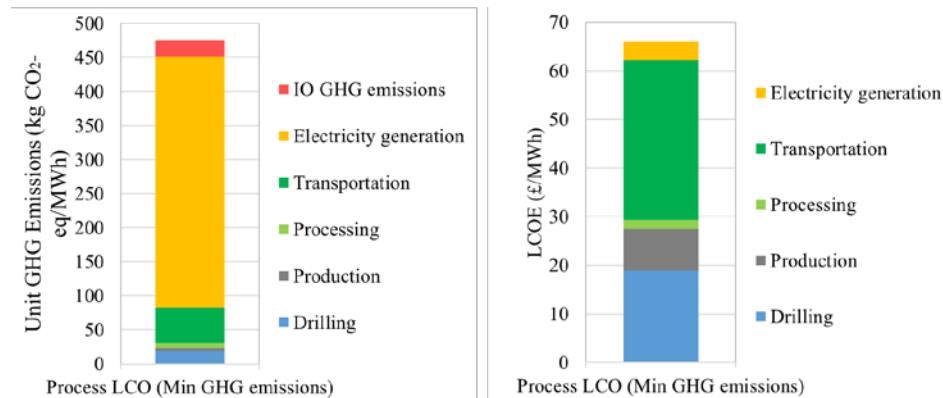


Figure C1. Optimal economic and environmental performances of process-based LCO model (P3) minimizing the life cycle process GHG emissions.

Moreover, we note that this process-based LCO model leads to a completely different production strategy in the shale gas supply chain. The detailed drilling schedule and corresponding shale gas production profile are provided in Figure C2. Up to six potential shale sites are developed in addition to the existing ones, and a total of 129 shale wells are drilled throughout the planning horizon. As a result, the quantity of shale gas flow is greater than that of point A. From this extra case study, we demonstrate the necessity of incorporating EIO systems in analyzing the life cycle environmental impacts. In the

LCO of shale gas supply chains, the integrated hybrid model can lead to a completely different optimal solution compared with the traditional process-based LCO model.

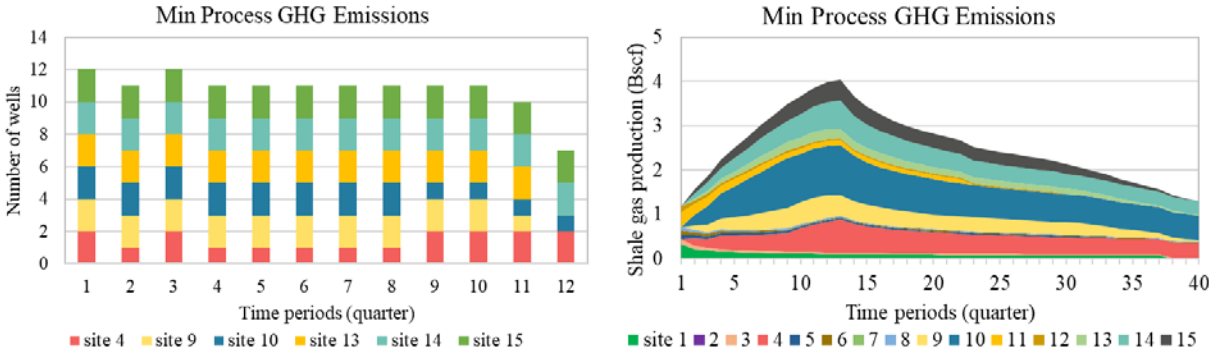


Figure C2. Optimal drilling schedule and production profile of process-based LCO model (P3).

### 3.8 Appendix D: Computational performance of the proposed tailored global optimization algorithm

In this section, we present the detailed converging process for the solution point B using the proposed tailored global optimization algorithm. As can be seen in Figure D1, the proposed tailored global optimization algorithm takes four outer loop iterations to converge. Apart from the first outer loop iteration that converges in one inner loop iteration, all the remaining outer loop iterations take two inner loop iterations to converge. In the last outer loop iteration, the reformulated linear objective function  $F(q)$  converges to 0, indicating the convergence of this tailored global optimization algorithm. The total computational time is 38,973 CPU seconds, and the computational time of each inner loop iteration ranges from 4,126 to 7,973 CPU seconds.

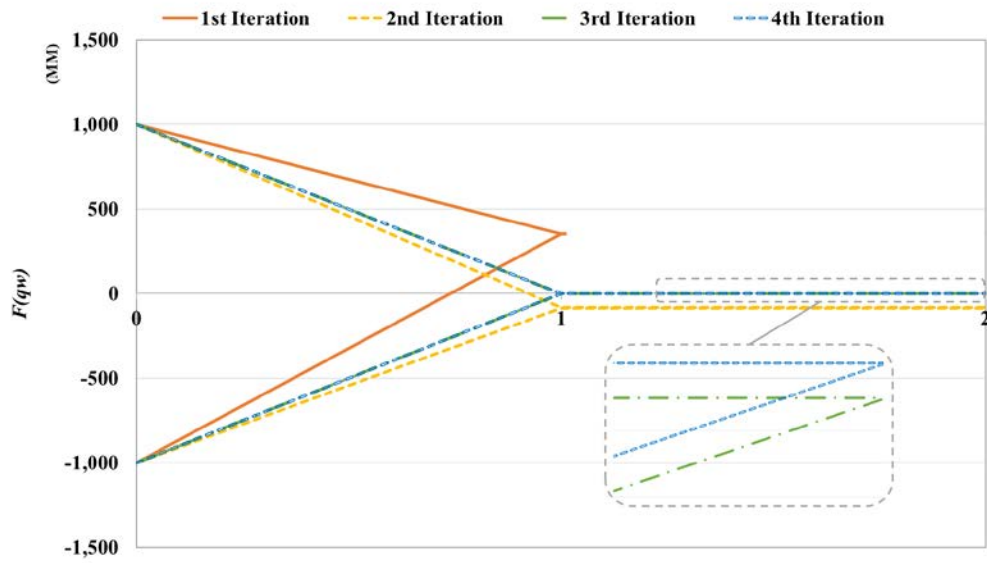


Figure D1. Converging process for the solution of point B.

### 3.9 Nomenclature

#### Sets

- $G$  Set of power plants indexed by  $g$
- $I$  Set of shale sites indexed by  $i$
- $M$  Set of processes indexed by  $m$
- $N$  Set of number of wells indexed by  $n$
- $NS$  Set of industrial sectors indexed by  $ns$
- $O$  Set of onsite treatment technologies indexed by  $o$   
( $o_1$ : MSF;  $o_2$ : MED;  $o_3$ : RO)
- $P$  Set of processing plants indexed by  $p$
- $R$  Set of capacity levels for gas pipelines indexed by  $r$
- $T$  Set of time periods indexed by  $t$

#### Subsets

$I_e(i)$	Subset of existing shale sites indexed by $i$
$I_n(i)$	Subset of potential shale sites indexed by $i$
$P_n(p)$	Subset of potential processing plants to be constructed indexed by $p$
$T'(t)$	Subset of time periods when wells are drilled indexed by $t'$

### Parameters

$aio_{ns,ns'}$	Technical coefficient connecting industrial sector $ns$ and $ns'$ in the EIO table
$c_{ns,m}$	Upstream technical coefficient linking industrial sector $ns$ and process $m$
$cc_i$	Correlation coefficient for shale gas production and wastewater production of a shale well at shale site $i$
$cca_t$	Capacity for wastewater treatment at CWT facility in time period $t$
$dgl_{g,t}$	Minimum demand of electricity at CCGT power plant $g$ in time period $t$
$dgup_{g,t}$	Maximum demand of electricity at CCGT power plant $g$ in time period $t$
$dr$	Discount rate per time period
$e_m^{pro}$	Environmental impact factors of basic process $m$
$e_{ns}^{io}$	Environmental impact factors of industrial sector $ns$
$fac$	Unit acquisition cost of freshwater
$inv\_cwt_{i,m}$	Amount of input from process $m$ for treating unit amount of wastewater from shale site $i$ at CWT facilities

$inv\_onsite_{o,m}$	Amount of input from process $m$ for treating unit amount of wastewater with onsite treatment technology $o$
$inv\_drill_{i,m}$	Amount of input from process $m$ for drilling a shale well at shale site $i$ .
$inv\_prod_{i,m}$	Amount of input from process $m$ for producing unit amount of shale gas at shale site $i$
$inv\_proc_{p,m}$	Amount of input from process $m$ for processing unit amount of raw shale gas at processing plant $p$
$inv\_trans_m$	Amount of input from process $m$ for transporting unit amount of shale gas for unit distance
$inv\_power_{g,m}$	Amount of input from process $m$ for consuming unit amount of shale gas to generate electricity at CCGT power plant $g$
$lc_i$	NGL composition in shale gas at shale site $i$
$lo_o$	Recovery factor for treating wastewater of onsite treatment technology $o$
$lpg_{p,g}$	Distance from processing plant $p$ to power plant $g$
$lsp_{i,p}$	Distance from shale site $i$ to processing plant $p$
$mc_i$	Methane composition in shale gas at shale site $i$
$mn_i$	Maximum number of wells that can be drilled at shale site $i$ per time period
$ne_i$	Number of existing shale wells drilled at shale site $i$
$ocl_o$	Minimum treatment capacity for onsite treatment technology $o$
$ocu_o$	Maximum treatment capacity for onsite treatment technology $o$
$pce_p$	Capacity of existing processing plant $p$
$pci$	Chemical engineering plant cost index for processing plant

$pcl$	Minimum capacity of processing plants
$pcup$	Maximum capacity of processing plants
$pef$	NGL recovery efficiency at processing plants
$pl_t$	Average unit price of NGLs in time period $t$
$prc$	Reference capacity of processing plant
$pri$	Reference capital investment of processing plant
$price_m$	Unit price input from process $m$
$rf_o$	Ratio of freshwater to wastewater required for blending after treatment of onsite treatment technology $o$
$rpci$	Chemical engineering plant cost index for processing plant of the reference year
$sdc_{i,t}$	Unit cost for shale well drilling and completion at shale site $i$ in time period $t$
$sfp$	Size factor of processing plants
$spc_{i,t}$	Unit cost for shale gas production at shale site $i$ in time period $t$
$spp_{i,t}$	Shale gas production of a shale well with age $t$ at shale site $i$
$tmn_i$	Maximum number of wells that can be drilled at shale site $i$ over the planning horizon
$tprc_r$	Reference capacity of gas pipeline with capacity level $r$
$tpri_r$	Reference capital investment of gas pipeline with capacity level $r$
$ue$	Amount of electricity generated per unit natural gas input
$vc$	Unit cost for wastewater treatment at CWT facility
$ve_g$	Unit cost for electricity generation from natural gas at CCGT power plant $g$

$vo_o$	Unit cost for wastewater treatment of onsite treatment technology $o$
$vp_p$	Unit processing cost at processing plant $p$
$vt_p$	Unit transportation cost of shale gas via pipelines
$wd_i$	Average drilling water usage for each well at shale site $i$
$wrd_i$	Recovery ratio of water for drilling process at shale site $i$
$wrf_i$	Recovery ratio of water for hydraulic fracturing process at shale site $i$

### **Nonnegative Continuous variables**

$FDW_{i,t}$	Freshwater demand of shale site $i$ in time period $t$
$FW_{i,t}$	Amount of freshwater acquired from water source to shale site $i$ in time period $t$
$GE_{g,t}$	Amount of electricity generated at power plant $g$ in time period $t$
$NN_{i,t}$	Number of wells drilled at shale site $i$ in time period $t$
$P_{ns}$	Total output of industrial sector $ns$ in the EIO systems
$PC_p$	Capacity of processing plant $p$
$Q_m$	Total net input of process $m$ from all activities in the process systems
$Q_{water,m}$	Total input of process $m$ associated with water management activities
$Q_{drill,m}$	Total input of process $m$ regarding drilling activities

$Q_{prod,m}$	Total input of process $m$ associated with shale gas production activities
$Q_{proc,m}$	Total input of process $m$ associated with shale gas processing activities
$Q_{trans,m}$	Total input of process $m$ associated with gas transportation activities
$Q_{power,m}$	Total input of process $m$ associated with electricity generation activities
$SP_{i,t}$	Shale gas production rate at shale site $i$ in time period $t$
$STP_{i,p,t}$	Amount of shale gas transported from shale site $i$ to processing plant $p$ in time period $t$
$STPG_{p,g,t}$	Amount of sales gas transported from processing plant $p$ to CCGT power plant $g$ in time period $t$
$SPL_{p,t}$	Amount of NGLs produced at processing plant $p$ in time period $t$
$SPM_{p,t}$	Amount of methane produced at processing plant $p$ in time period $t$
$TCP_{i,p,r}$	Capacity of gas pipeline with capacity level $r$ between shale site $i$ and processing plant $p$
$TCPG_{p,g,r}$	Capacity of gas pipeline with capacity level $r$ between processing plant $p$ and CCGT power plant $g$
$UP_{ns}$	Upstream input from industrial sector $ns$ to the process systems
$WP_{i,t}$	Wastewater production rate at shale site $i$ in time period $t$

$WTC_{i,t}$  Amount of wastewater transported from shale site  $i$  to CWT facilities in time period  $t$

$WTO_{i,o,t}$  Amount of wastewater treated by onsite treatment technology  $o$  at shale site  $i$  in time period  $t$

**Binary variables**

$XP_{i,p,r}$  0-1 variable. Equal to 1 if gathering pipeline with capacity level  $r$  is installed to transport shale gas from shale site  $i$  to processing plant  $p$

$XPG_{p,g,r}$  0-1 variable. Equal to 1 if gathering pipeline with capacity level  $r$  is installed to transport sales gas from processing plant  $p$  to CCGT power plant  $g$

$YD_{i,n,t}$  0-1 variable. Equal to 1 if  $n$  shale wells at shale site  $i$  are drilled in time period  $t$

$YO_{i,o}$  0-1 variable. Equal to 1 if onsite treatment technology  $o$  is applied at shale site  $i$

$YP_p$  0-1 variable. Equal to 1 if processing plant  $p$  is constructed

CHAPTER 4  
DYNAMIC MATERIAL FLOW ANALYSIS-BASED LIFE CYCLE  
OPTIMIZATION

## **4.1 Introduction**

Sustainability has received increasing research attention in design and operations of energy systems. Thus, tools and indicators are developed for assessing and benchmarking sustainability performance of different systems [159]. Among these tools, LCA is one of the most widely applied methods to systematically quantify the environmental impacts of a product from a life cycle perspective [138, 160]. As an analysis tool, LCA is designed to evaluate the environmental impacts based on a certain or a collection of design alternatives. However, the sustainable design and operations of energy systems generally involve substantially large number of design alternatives [161]. Using LCA approach to manually analyze each alternative system can be tedious or even infeasible. Therefore, it is imperative to develop an optimization framework that can automatically identify sustainable alternatives in energy systems design and operations.

To tackle this challenge, the LCO methodology was developed, which integrates LCA with multiobjective optimization technique into a holistic optimization model [151, 162]. In an LCO model, both the design and operational decisions are connected to their corresponding environmental consequences through mathematical constraints. By solving the resulting LCO problem, we can obtain the optimal design and operational decisions considering both economic and environmental performances [155, 163]. Despite the successful application of LCO in various energy systems, the framework

itself has its shortcomings inherited from LCA approaches [129, 161]. First, LCA is normally designed for general product systems based on simplified models, and the corresponding inventory data are estimated based on average values [17, 79-81, 84, 86, 95, 118]. This leads to the loss of precision and lack of customization in the investigation of specific systems. Additionally, it is challenging to depict the material flow relationships in systems with complex recycling flows using LCA. Consequently, the benefits of recycling for improving sustainability in certain complex energy systems may not be properly addressed with traditional LCO. More importantly, LCA might not holistically recognize resource depletion as a potential sustainability concern [164-166]. By solely evaluating the environmental impacts, the optimal design obtained in traditional LCO could not be truly sustainable, especially in terms of resource efficiency. To tackle these research challenges, it is necessary to develop a novel LCO framework that can effectively overcome the shortcomings of LCA by integrating with dynamic material flow (MFA) analysis.

In this study, we propose a dynamic MFA-based LCO framework in pursuit of sustainable design and operations of energy systems. MFA is considered as a complementary tool to LCA that can capture flows and stocks of materials with high-fidelity models and sufficient details for specific complex systems [167-170]. Moreover, dynamic MFA enables establishment of life cycle material flow profiles and investigation of detailed environmental mechanisms for more sustainable decisions [171-174]. Therefore, with the integration of dynamic MFA and LCA, we expect to overcome their shortcomings and contribute to better sustainable designs of energy systems [175-177]. Specifically, in this dynamic MFA-based LCO framework, various

input, output, and recycling material/energy flows of processes are captured with precision throughout their life time. Meanwhile, by introducing an extra dimension of resource sustainability in addition to economic and environmental performances, we aim to provide a more comprehensive evaluation of sustainable system designs. Based on the functional unit, we define three fractional objective functions, corresponding to the economic, environmental, and resource sustainability performances, respectively. The resulting optimization problem is formulated as a multiobjective mixed-integer linear fractional programming (MILFP) problem that is computationally challenging due to the fractional objective functions. Thus, we further adopt an efficient parametric algorithm to facilitate the solution [107]. To illustrate the applicability of proposed modeling framework and solution algorithm, we consider an application to a Marcellus shale gas supply chain. In this application, major design and operational decisions, including shale pad development, well drilling schedule, water treatment and recycling, pipeline network design, allocation and capacity selection of processing plants, production planning, transportation arrangement, and more, are fully addressed. The corresponding key material flows, such as concrete, steel, barite, bentonite, organic/inorganic chemical additives, proppant, water diesel, electricity, heat, steam, and more, are taken into account and incorporated into the MFA-based LCO model. Through a detailed result analysis, a Pareto optimal solution balancing economic, environmental, and resource performances can be recognized, and the corresponding optimal material flow profiles are obtained.

## 4.2 Dynamic MFA-based LCO framework

In this section, we formally introduce the dynamic MFA-based LCO framework. To facilitate the introduction, an illustrative diagram is presented in Figure 37, where four major phases are identified. The first phase is goal and scope definition, where key settings of this dynamic MFA-based LCO framework are defined, including the goal of this study, functional unit, system boundary, and key assumptions. For instance, the goal of this study is improving the sustainability of shale gas supply chains considering both design and operational decisions. The functional unit is generally defined as generating unit amount of major product or performing a certain service, such as producing unit amount of shale gas or supplying unit energy output. By defining the system boundary, we can identify the main life cycle stages and corresponding processes that need to be considered in the model. Identifying key assumptions helps us determine and describe the quantitative and logical relationships to be included in the LCO model.

Next, based on the functional unit and system boundary, we enter the second phase of conducting dynamic MFA for each unit process. After the process diagram is constructed, we can identify and summarize the basic materials involved in all the unit processes. Then, the mass balance relationship among input, stock, and output flows of each basic material in each time period is established [178]. In contrast to the static life cycle inventory analysis, the material stock and flow in a certain time period is derived from the input, output, and earlier stock, thus providing high-fidelity, time-dependent material flow profiles [174]. The second phase lays the foundation of the dynamic MFA-based LCO model.

The third phase involves linking the design and operational decisions in the investigated system with their corresponding optimization indicators. As shown in Figure 37, the proposed modeling framework allows consideration of multiple optimization criteria, including economic, environmental, and resource performances. Based on the dynamic MFA in the previous phase, we establish unit material flow matrices corresponding to different design and operational decisions. Each unit material flow matrix contains full profiles of input, output, and stock flows related to a certain design or operational decision. Therefore, by choosing appropriate environmental impact assessment and resource consumption quantification methods, we can connect design and operational decisions with their corresponding environmental impacts and resource consumption. In addition to certain midpoint indicators, such as GHG emissions, for evaluating the environmental impacts [92, 96], we can also adopt up-to-date endpoint-oriented life cycle impact assessment approaches, such as ReCiPe, to quantify the full spectrum of life cycle environmental impacts [82]. Moreover, this dynamic MFA-based LCO framework offers sufficient flexibility in evaluating resource sustainability through incorporation of customizable resource indicators.

In the last phase, a holistic dynamic MFA-based LCO model is formulated to optimize the economic, environmental, and resource sustainability criteria simultaneously subject to constraints for mass balances, capacity limitation, logic relationships, economic evaluation, environmental impact assessment, and resource consumption. Through a comprehensive analysis of the trade-offs among economic, environmental, and resource performances, we can seek a balance among these criteria and identify the corresponding optimal design and operational decisions. Moreover, with the optimal

material flow profiles, we can better understand the transition of material flow with time and gain more insights on the relationship between design and operational decisions, as well as their impacts on the sustainability performances of the investigated system [179].

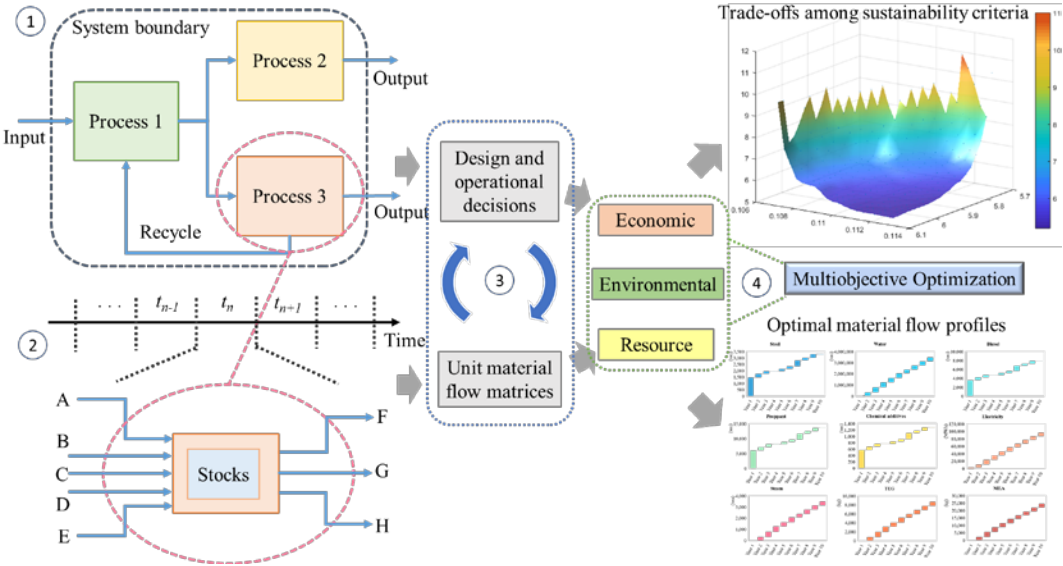


Figure 37. Illustration of the dynamic MFA-based LCO framework.

### 4.3 Problem statement

In this study, we consider an application to the sustainable design and operations of a Marcellus shale gas supply chain with the proposed dynamic MFA-based LCO framework. The life cycle system boundary is restricted to “well-to-gate”, which starts from the shale pad development at wellhead to the gate of natural gas market [56]. The functional unit is defined as generating one megajoule (MJ) net energy from shale gas. Following the dynamic MFA methodology, we keep track of the material flows associated with all the life cycle stages in this shale gas supply chain throughout the planning horizon. Specifically, a total of 36 key material flows are considered, including

concrete, steel, barite, bentonite, lignite, inorganic chemicals, organic chemicals, proppant, friction reducer, surfactant, hydrochloric acid, scale inhibitor, clay stabilizer, gelling agent, pH adjusting agent, breaker, crosslinker, iron control, biocide, corrosion inhibitor, water, diesel, electricity, heat, steam, ethanolamine (MEA), triethylene glycol (TEG), drilling wastewater, flowback water, produced water, raw shale gas, natural gas, natural gas liquids (NGL), solid waste, fugitive methane, and carbon dioxide. An illustrative MFA diagram for this shale gas energy system is presented in Figure 38.

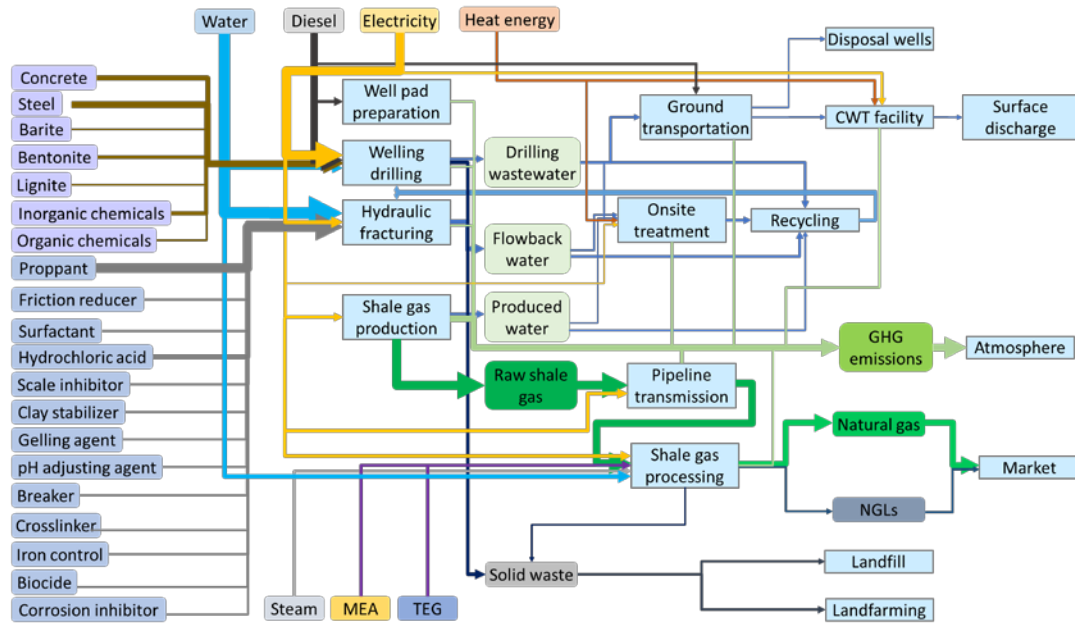


Figure 38. Illustrative MFA figure of the shale gas energy system.

In this shale gas supply chain, a set of shale sites are given, including existing ones with active shale wells and potential ones to be developed. Each potential shale site allows drilling of multiple shale wells. The maximum number of shale wells and their corresponding production profiles at each shale site are given. As shown in Figure 38, development of shale pads and drilling and fracturing of shale wells require a series of material inputs, including water, diesel, electricity, concrete, steel, bentonite, chemicals,

etc. Meanwhile, raw shale gas and wastewater is generated at shale sites. Depending on the life cycle stages of shale wells, wastewater can be further classified into drilling wastewater, flowback water, and produced water with different properties, corresponding to well drilling, hydraulic fracturing, and gas production stages, respectively. The wastewater can be handled in three ways, including the underground injection into remote Class-II disposal wells, treatment by centralized wastewater treatment (CWT) facilities, and onsite wastewater treatment and recycling through mobile water treatment units [21]. For the onsite wastewater treatment option, three types of water treatment technologies are considered, namely multi-stage flash, multi-effect distillation, and reverse osmosis [58, 180]. The wastewater injected underground is considered as consumptive water use. The treated water from CWT facilities is sent to surface discharge and considered as nonconsumptive water use. The wastewater treated onsite by mobile water treatment units can be mixed with freshwater and recycled for future drilling and fracturing activities at corresponding shale sites [19, 181].

Once the raw shale gas exits the shale wells, after the initial processing near the wellhead, it is transported to a set of potential processing plants through the gathering pipeline network. At the processing plants, raw shale gas goes through a series of processes, including gas sweetening, dehydration, NGL recovery, and  $N_2$  rejection [64]. At the processing plants, impurities including water, acid gas, and nitrogen are removed from the raw shale gas, and the pipeline-quality natural gas and heavier hydrocarbons, known as natural gas liquids (NGLs), are separated. The pipeline-quality natural gas is the main product of this shale gas supply chain that will be sold to the market for later

energy generation. The NGLs, on the other hand, are considered as byproducts and sold for extra income. The shale gas processing stage requires the following key material inputs: cooling water, electricity, steam, MEA, and TEG [74]. Throughout the life cycle of shale gas, solid waste and GHG emissions are generated. The solid waste from different life cycle stages can be sent to landfill and landfarming. The GHG emissions mainly consist of the methane leakage from the drilling and production phases, and direct/indirect CO<sub>2</sub> emissions associated with activities, materials, and energy inputs [128, 182, 183].

To comprehensively address the sustainability concern in the design and operations of shale gas supply chains, we consider three distinct objective functions in this problem. The aim is to simultaneously optimize the economic, environmental, and resource performances of this shale gas supply chain for generating one functional unit of product. Specifically, the economic performance is evaluated by the levelized cost of unit net energy output. The environmental performance is quantified with the GHG emissions (in terms of CO<sub>2</sub> equivalent based on 100-year time horizon) [97]. The water consumption is adopted as the resource indicator [19]. We note that the selection of indicators is not limited to any specific ones. In this study, we stick to the most representative indicators following the existing literature [96, 129]. Notably, these three objective functions are all formulated into fractional form with both numerators and denominators dependent on the design and operational decisions. Compared with their linear counterparts, these fractional objective functions address the optimization criteria from a functional-unit perspective. In the models with linear objective functions, the production of functional units is always pushed to the maximum/minimum level, which

may not be the most sustainable design from a functional-unit perspective. By contrast, the functional-unit-based fractional objectives can automatically identify the optimal amount of functional units to generate for the best sustainability performance. Moreover, there are extensive studies in the literature demonstrating the advantage of fractional objective functions in leading to more sustainable system designs [6, 130]. Therefore, we adopt the following fractional objectives in this study:

Minimizing the levelized cost of one MJ net energy output, formulated as the total net present cost (i.e., the summation of all discounted future costs) divided by the total amount of net energy generation from shale gas;

- Minimizing the GHG emissions associated with one MJ net energy output, formulated as the total life cycle GHG emissions throughout the shale gas supply chain divided by the total amount of net energy generation from shale gas;
- Minimizing the water consumption associated with one MJ net energy output, formulated as the total water consumption throughout the shale gas supply chain divided by the total amount of net energy generation from shale gas.

The net energy generation can be calculated by subtracting the energy consumption (in terms of fossil fuel, electricity, heat, etc.) throughout the shale gas supply chain from the direct energy output of produced shale gas. These three objectives are optimized simultaneously considering the following design and operational decisions:

- Development of potential shale sites;
- Drilling schedule of shale wells at each shale site;
- Design of gathering pipeline networks;
- Allocation and capacity selection of processing plants;

- Shale gas production profile of each shale well;
- Water management strategy at each shale site;
- Transportation planning of water and shale gas;
- Sales of natural gas and NGLs.

#### 4.4 Model formulation and solution algorithm

Following the proposed MFA-based LCO framework, the resulting problem is formulated as a multiobjective MILFP problem. The general model formulation is given below, followed by the detailed formulations of objective functions and constraints. All the variables are denoted with upper-case symbols, and all the parameters are denoted with lower-case symbols.

$$\min \frac{TC}{TENG} \quad (27)$$

$$\min \frac{TE}{TENG} \quad (38)$$

$$\min \frac{TW}{TENG} \quad (49)$$

s.t. Mass balance constraints (1)-(10)

Capacity constraints (11)-(19)

Logic constraints (20)-(26)

Economic constraints (28)-(37)

Environmental constraints (39)-(48)

Resource constraints (50)-(70)

Here  $TC$  stands for the total net present cost.  $TE$  is the total life cycle GHG emissions.  $TW$  represents the total water consumption.  $TENG$  indicates the total net energy

generation from shale gas, which equals the direct energy output of produced shale gas minus the energy consumption throughout the shale gas supply chain. These three objective functions are optimized simultaneously subject to the following constraints:

- Mass balance constraints describing the basic input-output mass balance relationships for each unit process involved in the shale gas supply chain.
- Capacity constraints addressing the capacity limitations of unit processes, including various water management options, shale gas processing at each processing plant, gas transportation through pipeline network, and demand of shale gas at corresponding market.
- Logic constraints modeling the logic relationships and basic assumptions among design decisions, including those associated with shale well drilling, pipeline installment, selection of water treatment technology, and design of processing facilities.
- Economic constraints calculating the capital investment and operating costs associated with the design and operational decisions in the shale gas supply chain, including those regarding shale well drilling, shale gas production, gas processing, transportation, and water management.
- Environmental constraints quantifying the GHG emissions resulting from different unit processes throughout the shale gas supply chain, including well pad development, well drilling, hydraulic fracturing, shale gas production, water management, gas transportation, gas processing, and solid waste handling.

- Resource constraints calculating the total water consumption crossing the shale gas supply chain and net energy output from shale gas at the gate of natural gas market.

The economic, environmental, and resource objectives are all formulated in fractional form as a ratio of two linear functions, representing the functional-unit-based economic performance, environmental impact, and resource efficiency, respectively. All the constraints are linear ones with both integer and continuous variables. Therefore, the resulting problem is a multiobjective MILFP problem. The detailed model formulation is presented in the following subsections.

#### 4.4.1 Constraints

The water supply at each shale site in each time period is satisfied by both the fresh water acquisition and recycled water from onsite wastewater treatment.

$$FW_{i,t} + \sum_{o \in O} lo_o \cdot WTO_{i,o,t} = FDW_{i,t}, \forall i, t \quad (1)$$

where  $lo_o$  denotes the recovery factor for treating wastewater of onsite wastewater treatment technology  $o$ .  $FDW_{i,t}$  denotes the freshwater demand of shale site  $i$  in time period  $t$ .

The water supplied at each shale site is used to satisfy the shale well drilling and hydraulic fracturing activities. In this model, the drilling water usage is proportional to the number of wells drilled, and the water usage for hydraulic fracturing is proportional to the amount of wastewater generated at shale sites [41].

$$FDW_{i,t} = \frac{WP_{i,t}}{wrf_i} + wd_i \cdot NN_{i,t}, \forall i, t \quad (2)$$

where  $WP_{i,t}$  denotes the amount of wastewater generated at shale site  $i$  in time period  $t$ .  $wrf_i$  is the recovery ratio of water at shale site  $i$ .  $wd_i$  denotes the average drilling water usage of a shale well at shale site  $i$ .

The amount of wastewater generated during hydraulic fracturing at each shale site is proportional to the shale gas production rate, and the coefficient is estimated based on given industrial data [124].

$$WP_{i,t} = cc_i \cdot SP_{i,t}, \forall i, t \quad (3)$$

where  $cc_i$  is the correlation coefficient between shale gas production and wastewater production.

The wastewater generated from both drilling and hydraulic fracturing activities is handled in three ways, namely treatment by CWT facilities, underground injection into Class-II disposal wells, and onsite wastewater treatment and recycling, given as follows,

$$WP_{i,t} + wd_i \cdot wrd_i \cdot NN_{i,t} = WTC_{i,t} + WTD_{i,t} + \sum_{o \in O} WTO_{i,o,t}, \forall i, t \quad (4)$$

where  $wrd_i$  is the recovery ratio of water for drilling process at shale site  $i$ .

The raw shale gas is produced from both existing shale sites and potential ones to be developed. The shale gas output from existing shale sites can be calculated by the following equation.

$$SP_{i,t} = ne_i \cdot spp_{i,t}, \forall i \in I_e, t \quad (5)$$

where  $ne_i$  denotes the number of existing shale wells at shale site  $i$ .  $spp_{i,t}$  denotes the shale gas production rate of a shale well of age  $t$  at shale site  $i$ .

The shale gas production of potential shale sites in each time period is dependent on the specific drilling schedule, specifically when and how many shale wells are drilled at each shale site in each time period.

$$SP_{i,t} = \sum_{t'=1}^{t-1} NN_{i,t'} \cdot spp_{i,t-t'}, \quad \forall i \in I_n, t \geq 2 \quad (6)$$

where  $spp_{i,t-t'}$  represents the shale gas production profile of a shale well drilled at time period  $t'$  at shale site  $i$  in time period  $t$ . Thus, the age of this well would be  $t - t'$ . This time-dependent parameter is used to describe the decreasing shale gas production profiles of shale wells.

As stated in the problem statement section, the raw shale gas produced at each shale site is transported to the midstream processing plants for further separation. This mass balance relationship is described as follows.

$$SP_{i,t} = \sum_{p \in P} STP_{i,p,t}, \quad \forall i, t \quad (7)$$

At the processing plants, raw shale gas goes through a series of processes to remove the impurities and separate two major products, the pipeline-quality sales gas and NGLs. The sales gas output and NGL output can be calculated using the following equations (8) and (9), respectively.

$$\sum_{i \in I} STP_{i,p,t} \cdot pef \cdot mec_i = STPM_{p,t}, \quad \forall p, t \quad (8)$$

$$\sum_{i \in I} STP_{i,p,t} \cdot pef \cdot lc_i = STPL_{p,t}, \quad \forall p, t \quad (9)$$

where  $pef$  denotes the processing efficiency at processing plants.  $mec_i$  and  $lc_i$  are the methane and NGL composition in shale gas at shale site  $i$ , respectively.  $STPM_{p,t}$  denotes the amount of natural gas produced at processing plant  $p$  in time period  $t$ .

The sales gas produced at processing plants is the source of energy output in this shale gas supply chain, given by,

$$STPM_{p,t} = SPM_{p,t}, \forall p, t \quad (10)$$

The amount of wastewater handled by each of the water management options cannot exceed its corresponding capacity, given by the following constraints.

$$\sum_{i \in I} WTC_{i,t} \leq cca_t, \forall t \quad (11)$$

$$\sum_{i \in I} WTD_{i,t} \leq dca_t, \forall t \quad (12)$$

$$WTO_{i,o,t} \leq ocu_o \cdot YO_{i,o}, \forall i, o, t \quad (13)$$

where  $cca_t$ ,  $dca_t$ , and  $ocu_o$  are the capacities of underground injection, the CWT facility, and onsite wastewater treatment with technology  $o$ , respectively.  $YO_{i,o}$  is a binary variable that equals 1 if onsite wastewater treatment technology  $o$  is applied at shale site  $i$ .

The wastewater treated onsite for recycling needs to be blended with a certain percentage of freshwater to satisfy the reuse specification, given by,

$$\sum_{o \in O} rf_o \cdot lo_o \cdot WTO_{i,o,t} \leq FW_{i,t}, \forall i, t \quad (14)$$

where  $rf_o$  denotes the required blending ratio of freshwater to wastewater after treatment by onsite wastewater treatment technology  $o$ .

The piecewise linear approximation approach with specially ordered set variables of type 2 (SOS2) variables is used to estimate the capital cost for processing plant construction. Accordingly, the processing capacity of a processing plant can be calculated using the following equation, given as,

$$PC_p = \sum_{pt \in PT} pcap_{p,pt} \cdot Y_{p,t}, \forall p \quad (15)$$

where  $PC_p$  is the capacity of processing plant  $p$ , and  $pcap_{p,pt}$  denotes the corresponding reference capacity of processing plant  $p$ .

The amount of raw shale gas processed at a processing plant cannot exceed its processing capacity, given as,

$$\sum_{i \in I} STP_{i,p,t} \leq PC_p, \forall p, t \quad (16)$$

There are a set of pipeline capacity levels that can be selected for the installation of gathering pipeline networks between shale sites and processing plants. The capacity of a certain gathering pipeline can be calculated by,

$$TCP_{i,p,r} = tprc_r \cdot XP_{i,p,r}, \forall i, p, r \quad (17)$$

where  $TCP_{i,p,r}$  denotes the capacity of gathering pipeline between shale site  $i$  and processing plant  $p$  with capacity level  $r$ , and  $tprc_r$  is the corresponding reference pipeline capacity.

The amount of shale gas transported from a shale site to a processing plant is constrained by the corresponding gathering pipeline capacity, given as,

$$STP_{i,p,t} \leq \sum_{r \in R} TCP_{i,p,r}, \forall i, p, t \quad (18)$$

The total amount of sales gas produced from the shale gas supply chain in each time period is bounded by the minimum demand and maximum demand of the market.

$$dml_t \leq SPM_{p,t} \leq dmup_t, \forall t \quad (19)$$

where  $dml_t$  and  $dmup_t$  are the minimum demand and maximum demand of natural gas in time period  $t$ , respectively.

In each time period, a certain number of shale wells can be drilled at each potential shale site, given as,

$$\sum_{n=0}^{mn_i} YD_{i,n,t} = 1, \forall i \in I_n, t \quad (20)$$

where  $YD_{i,n,t}$  is a binary variable that equals 1 if  $n$  wells are drilled at shale site  $i$  in time period  $t$ .

The number of shale wells drilled at each shale site in each time period is calculated by,

$$NN_{i,t} = \sum_{n=0}^{mn_i} n \cdot YD_{i,n,t}, \forall i \in I_n, t \quad (21)$$

The maximum number of shale wells that can be drilled in each shale site is given as,

$$\sum_{t \in T} NN_{i,t} \leq tmn_i, \forall i \in I_n \quad (22)$$

where  $tmn_i$  is the maximum number of wells that can be drilled at shale site  $i$ .

In this model, no extra shale wells will be drilled in the existing shale sites, given by,

$$NN_{i,t} = 0, \forall i \in I_e \quad (23)$$

In each shale site, at most one onsite wastewater treatment technology will be selected.

$$\sum_{o \in O} YO_{i,o} \leq 1, \forall i \quad (24)$$

For each transportation link between shale sites and processing plants, at most one capacity level can be selected for the corresponding gathering pipeline, given as,

$$\sum_{r \in R} XP_{i,p,r} \leq 1, \forall i, p \quad (25)$$

The SOS2 variable regarding construction of processing plants should satisfy the following constraint.

$$\sum_{pt \in PT} YP_{p,pt} = 1, \forall p \quad (26)$$

## 4.4.2 Objective functions

### 4.4.2.1 Economic objective

The economic objective is to minimize the levelized cost of one MJ net energy output, formulated as the total net present cost ( $TC$ ) divided by the total amount of net energy generation from shale gas ( $TENG$ ).

$$\min \frac{TC}{TENG} \quad (27)$$

The total net present cost  $TC$  includes the capital and operating costs associated with water management ( $C_{water}$ ), well drilling ( $C_{drilling}$ ), shale gas production ( $C_{production}$ ), processing ( $C_{processing}$ ), and transportation ( $C_{transportation}$ ), given as follows.

$$TC = C_{water} + C_{drilling} + C_{production} + C_{processing} + C_{transportation} \quad (28)$$

The water management cost can be further sorted into water acquisition cost ( $C_{acquisition}$ ), water handling cost by Class-II disposal wells ( $C_{disposal}$ ), water treatment cost by CWT facilities ( $C_{cwt}$ ), and onsite water treatment cost ( $C_{onsite}$ ).

$$C_{water} = C_{acquisition} + C_{disposal} + C_{cwt} + C_{onsite} \quad (29)$$

The water acquisition cost is proportional to the amount of freshwater acquired, calculated by,

$$C_{acquisition} = \sum_{i \in I} \sum_{t \in T} \frac{fac \cdot FW_{i,t}}{(1 + dr)^t} \quad (30)$$

where  $fac$  denotes the unit freshwater acquisition cost.  $FW_{i,t}$  represents the amount of freshwater acquired at shale site  $i$  in time period  $t$ .  $dr$  is the average discount rate for each time period.

Similarly, the wastewater treatment costs associated with different water management options can be calculated by the following equations,

$$C_{disposal} = \sum_{i \in I} \sum_{t \in T} \frac{vd \cdot WTD_{i,t}}{(1 + dr)^t} \quad (31)$$

$$C_{cwt} = \sum_{i \in I} \sum_{t \in T} \frac{vc \cdot WTC_{i,t}}{(1 + dr)^t} \quad (32)$$

$$C_{onsite} = \sum_{i \in I} \sum_{o \in O} \sum_{t \in T} \frac{vo_o \cdot WTO_{i,o,t}}{(1 + dr)^t} \quad (33)$$

where  $vd$ ,  $vc$ , and  $vo_o$  are the unit treatment costs associated with underground injection, CWT facility, and onsite wastewater treatment with technology  $o$ .  $WTD_{i,t}$ ,  $WTC_{i,t}$ , and  $WTO_{i,o,t}$  are the corresponding variables indicating the amount of wastewater handled by each of these options at shale site  $i$  in time period  $t$ .

The total shale well drilling cost is calculated by the following equation,

$$C_{drilling} = \sum_{i \in I} \sum_{t \in T} \frac{sdc_{i,t} \cdot NN_{i,t}}{(1 + dr)^t} \quad (34)$$

where  $sdc_{i,t}$  indicates the unit drilling cost at shale site  $i$  in time period  $t$ .  $NN_{i,t}$  denotes the number of wells drilled at shale site  $i$  in time period  $t$ .

The total shale gas production cost equals the total operating cost associated with shale gas production subtracted by the remaining value of shale gas to be produced at the end of planning horizon, calculated by,

$$C_{production} = \sum_{i \in I} \sum_{t \in T} \frac{spc_{i,t} \cdot SP_{i,t}}{(1+dr)^t} - \sum_{i \in I} \sum_{t \in T} \frac{psg \cdot (NN_{i,t} \cdot eur_i - SP_{i,t})}{(1+dr)^t} \quad (35)$$

where  $spc_{i,t}$  denotes the unit shale gas production cost, and  $SP_{i,t}$  is the corresponding shale gas production at shale site  $i$  in time period  $t$ .  $psg$  indicates the estimated unit value of shale gas to be produced.  $eur_i$  is the average estimated ultimate recovery of shale wells at shale site  $i$ .

The total cost associated with shale gas processing includes three parts, namely the capital investment for construction of processing plants, operating cost associated with shale gas processing, and income from sales of NGL products.

$$C_{processing} = \sum_{p \in P} \sum_{pt \in PT} pcc_{p,pt} \cdot Y_{p,pt} + \sum_{i \in I} \sum_{p \in P} \sum_{t \in T} \frac{vro_p \cdot STP_{i,p,t}}{(1+dr)^t} - \sum_{p \in P} \sum_{t \in T} \frac{pl_t \cdot STPL_{p,t}}{(1+dr)^t} \quad (36)$$

Notably, here we adopt piecewise linear approximation approach with SOS2 to estimate the capital cost for processing plant construction [184].  $pcc_{p,pt}$  denotes the capital cost of processing plant  $p$  associated with interpolated point  $pt$ , and  $Y_{p,pt}$  is an SOS2 variable for calculating the capital cost of processing plant  $p$  with interpolated point  $pt$ .  $vro_p$  is the unit processing cost at processing plant  $p$ .  $STP_{i,p,t}$  represents the amount of raw shale gas transported from shale site  $i$  to processing plant  $p$  in time period  $t$ .  $pl_t$  is the unit price of NGLs in time period  $t$ , and  $STPL_{p,t}$  denotes the amount of NGLs produced at processing plant  $p$  in time period  $t$ .

The total transportation cost is comprised of three parts, including the capital cost for installment of the gathering pipeline network between shale sites and processing plants, the operating cost for transporting raw shale gas from shale sites to processing plants,

and the operating cost for transporting processed natural gas from processing plants to the corresponding market, calculated by,

$$C_{transportation} = \sum_{i \in I} \sum_{p \in P} \sum_{r \in R} tpri_r \cdot XP_{i,p,r} \cdot lsp_{i,p} + \sum_{i \in I} \sum_{p \in P} \sum_{t \in T} \frac{vrt \cdot lsp_{i,p} \cdot STP_{i,p,t}}{(1+dr)^t} + \sum_{p \in P} \sum_{t \in T} \frac{vtp \cdot lpm_p \cdot SPM_{p,t}}{(1+dr)^t} \quad (37)$$

where  $tpri_r$  denotes the reference capital cost of gathering pipeline with capacity level  $r$ .  $XP_{i,p,r}$  is a binary variable that equals 1 if a gathering pipeline with capacity  $r$  is installed between shale site  $i$  and processing plant  $p$ .  $lsp_{i,p}$  is the distance between shale site  $i$  and processing plant  $p$ .  $vrt$  and  $vtp$  are the unit transportation cost of raw shale gas and sales gas, respectively.  $lpm_p$  denotes the distance from processing plant  $p$  to the market.  $SPM_{p,t}$  denotes the amount of sales gas sold to the market from processing plant  $p$  in time period  $t$ .

#### 4.4.2.2 Environmental objective

The environmental objective is to minimize the GHG emissions associated with one MJ net energy output, formulated as the total life cycle GHG emissions ( $TE$ ) throughout the shale gas supply chain divided by the total amount of net energy generation from shale gas ( $TENG$ ).

$$\min \frac{TE}{TENG} \quad (38)$$

The total life cycle GHG emissions ( $TE$ ) equals the sum of GHG emissions from life cycle stages including water management ( $E_{water}$ ), well drilling ( $E_{drilling}$ ), shale gas production ( $E_{production}$ ), processing ( $E_{processing}$ ), and transportation ( $E_{transportation}$ ), given as follows.

$$TE = E_{water} + E_{drilling} + E_{production} + E_{processing} + E_{transportation} \quad (39)$$

The GHG emissions generated from the water management activities are contributed by the water acquisition activities ( $E_{acquisition}$ ), underground injection into Class-II disposal wells ( $E_{disposal}$ ), water treatment by CWT facilities ( $E_{cwt}$ ), and onsite water treatment activities ( $E_{onsite}$ ).

$$E_{water} = E_{acquisition} + E_{disposal} + E_{cwt} + E_{onsite} \quad (40)$$

Specifically, the GHG emissions resulting from each of these water management activities can be calculate by the following equations, given as,

$$E_{acquisition} = \sum_{i \in I} \sum_{mm \in MM} \sum_{t \in T} fems_{mm} \cdot inv\_acquisition_{i,mm} \cdot FW_{i,t} \quad (41)$$

$$E_{disposal} = \sum_{i \in I} \sum_{mm \in MM} \sum_{t \in T} fems_{mm} \cdot inv\_disposal_{i,mm} \cdot WTD_{i,t} \quad (42)$$

$$E_{cwt} = \sum_{i \in I} \sum_{mm \in MM} \sum_{t \in T} fems_{mm} \cdot inv\_cwt_{i,mm} \cdot WTC_{i,t} \quad (43)$$

$$E_{onsite} = \sum_{i \in I} \sum_{mm \in MM} \sum_{t \in T} fems_{mm} \cdot inv\_onsite_{o,mm} \cdot WTO_{i,o,t} \quad (44)$$

where  $fems_{mm}$  denotes the GHG emission factor associated with basic material flow  $mm$ . The unit material flow matrices corresponding to different water management activities, namely freshwater acquisition at shale site  $i$ , wastewater underground injection from shale site  $i$ , wastewater treatment by CWT facility from shale site  $i$ , and onsite wastewater treatment with technology  $o$ , are given by  $inv\_acquisition_{i,mm}$ ,  $inv\_disposal_{i,mm}$ ,  $inv\_cwt_{i,mm}$ , and  $inv\_onsite_{o,mm}$ , respectively.

Similarly, the GHG emissions generated from well drilling activities can be calculated by,

$$E_{drilling} = \sum_{i \in I} \sum_{mm \in MM} \sum_{t \in T} fems_{mm} \cdot inv\_drilling_{i,mm} \cdot NN_{i,t} \quad (45)$$

where  $inv\_drilling_{i,mm}$  is the unit material flow matrix associated with shale well drilling activity representing the input of basic material  $mm$  for drilling one shale well at shale site  $i$ .

The GHG emissions resulting from shale gas production can be calculated as follows.

$$E_{production} = \sum_{i \in I} \sum_{mm \in MM} \sum_{t \in T} fems_{mm} \cdot inv\_production_{i,mm} \cdot SP_{i,t} \quad (46)$$

where  $inv\_production_{i,mm}$  is the unit material flow matrix associated with shale gas production indicating the input of material  $mm$  for producing a unit amount of raw shale gas at shale site  $i$ .

The GHG emissions contributed by shale gas processing is calculated by the following equation.

$$E_{processing} = \sum_{i \in I} \sum_{p \in P} \sum_{mm \in MM} \sum_{t \in T} fems_{mm} \cdot inv\_processing_{p,mm} \cdot STP_{i,p,t} \quad (47)$$

where  $inv\_processing_{p,mm}$  denotes the unit material flow matrix for shale gas processing activity representing the input of material  $mm$  for processing a unit amount of raw shale gas at processing plant  $p$ .

The GHG emissions from transportation activities can be calculated by the following equation.

$$E_{transportation} = \sum_{i \in I} \sum_{p \in P} \sum_{mm \in MM} \sum_{t \in T} fems_{mm} \cdot inv\_trans_{mm} \cdot lsp_{i,p} \cdot STP_{i,p,t} \\ + \sum_{p \in P} \sum_{mm \in MM} \sum_{t \in T} fems_{mm} \cdot inv\_trans_{mm} \cdot lpm_p \cdot SPM_{p,t} \quad (48)$$

where  $inv\_trans_{mm}$  is the unit material flow matrix for transportation activity indicating the input of material  $mm$  for transporting a unit amount of shale gas through pipeline for unit distance.

#### 4.4.2.3 Resource objective

The resource objective is to minimize the water consumption associated with one MJ net energy output, formulated as the total water consumption ( $TW$ ) throughout the shale gas supply chain divided by the total amount of net energy generation from shale gas ( $TENG$ ).

$$\min \frac{TW}{TENG} \quad (49)$$

The total water consumption ( $TW$ ) equals the sum of water consumed in water management ( $W_{water}$ ), well drilling ( $W_{drilling}$ ), shale gas production ( $W_{production}$ ), processing ( $W_{processing}$ ), and transportation ( $W_{transportation}$ ) activities, calculated by,

$$TW = W_{water} + W_{drilling} + W_{production} + W_{processing} + W_{transportation} \quad (50)$$

The water consumption in the water management activities consists of water consumption in water acquisition activity ( $W_{acquisition}$ ), water consumption in underground injection into Class-II disposal wells ( $W_{disposal}$ ), water consumption in water treatment by CWT facilities ( $W_{cwt}$ ), and water consumption in onsite water treatment activity ( $W_{onsite}$ ).

$$W_{water} = W_{acquisition} + W_{disposal} + W_{cwt} + W_{onsite} \quad (51)$$

The amount of water resource consumed in each of these water management activities can be calculated by the following equations.

$$W_{acquisition} = \sum_{i \in I} \sum_{mm \in MM} \sum_{t \in T} fwat_{mm} \cdot inv\_acquisition_{i,mm} \cdot FW_{i,t} \quad (52)$$

$$W_{disposal} = \sum_{i \in I} \sum_{mm \in MM} \sum_{t \in T} fwat_{mm} \cdot inv\_disposal_{i,mm} \cdot WTD_{i,t} \quad (53)$$

$$W_{cwt} = \sum_{i \in I} \sum_{mm \in MM} \sum_{t \in T} fwat_{mm} \cdot inv\_cwt_{i,mm} \cdot WTC_{i,t} \quad (54)$$

$$W_{onsite} = \sum_{i \in I} \sum_{mm \in MM} \sum_{t \in T} fwat_{mm} \cdot inv\_onsite_{o,mm} \cdot WTO_{i,o,t} \quad (55)$$

where  $fwat_{mm}$  denotes the water consumption factor of basic material  $mm$ .

Similar to the environmental constraints, the water consumption in the life cycle stage of shale well drilling can be calculated by,

$$W_{drilling} = \sum_{i \in I} \sum_{mm \in MM} \sum_{t \in T} fwat_{mm} \cdot inv\_drilling_{i,mm} \cdot NN_{i,t} \quad (56)$$

The water consumption associated with shale gas production can be calculated as follows.

$$W_{production} = \sum_{i \in I} \sum_{mm \in MM} \sum_{t \in T} fwat_{mm} \cdot inv\_production_{i,mm} \cdot SP_{i,t} \quad (57)$$

The water consumption during shale gas processing is calculated by,

$$W_{processing} = \sum_{i \in I} \sum_{p \in P} \sum_{mm \in MM} \sum_{t \in T} fwat_{mm} \cdot inv\_processing_{i,mm} \cdot STP_{i,p,t} \quad (58)$$

The water consumption resulting from transportation activities can be calculated by the following equation.

$$W_{transportation} = \sum_{i \in I} \sum_{p \in P} \sum_{mm \in MM} \sum_{t \in T} fwat_{mm} \cdot inv\_trans_{mm} \cdot lsp_{i,p} \cdot STP_{i,p,t} \\ + \sum_{p \in P} \sum_{mm \in MM} \sum_{t \in T} fwat_{mm} \cdot inv\_trans_{mm} \cdot lpm_p \cdot SPM_{p,t} \quad (59)$$

The total net energy output ( $TENG$ ) equals the total energy generation from shale gas minus the total energy consumed in the shale gas supply chain ( $TEC$ ), given by:

$$TENG = \sum_{p \in P} \sum_{t \in T} ue \cdot SPM_{p,t} - TEC \quad (60)$$

where  $ue$  denotes the unit heat content of natural gas.

The total energy consumption  $TEC$  throughout the shale gas supply chain can be calculated with the following equations.

$$TEC = EC_{water} + EC_{drilling} + EC_{production} + EC_{processing} + EC_{transportation} \quad (61)$$

where the energy consumption in the water management activities equals the sum of energy consumption in water acquisition activity ( $EC_{acquisition}$ ), underground injection into Class-II disposal wells ( $EC_{disposal}$ ), water treatment by CWT facilities ( $EC_{cwt}$ ), and onsite water treatment activity ( $EC_{onsite}$ ).

$$EC_{water} = EC_{acquisition} + EC_{disposal} + EC_{cwt} + EC_{onsite} \quad (62)$$

The energy consumption in each of these water management activities can be calculated by the following equations.

$$EC_{acquisition} = \sum_{i \in I} \sum_{mm \in MM} \sum_{t \in T} feng_{mm} \cdot inv\_acquisition_{i,mm} \cdot FW_{i,t} \quad (63)$$

$$EC_{disposal} = \sum_{i \in I} \sum_{mm \in MM} \sum_{t \in T} feng_{mm} \cdot inv\_disposal_{i,mm} \cdot WTD_{i,t} \quad (64)$$

$$EC_{cwt} = \sum_{i \in I} \sum_{mm \in MM} \sum_{t \in T} feng_{mm} \cdot inv\_cwt_{i,mm} \cdot WTC_{i,t} \quad (65)$$

$$EC_{onsite} = \sum_{i \in I} \sum_{mm \in MM} \sum_{t \in T} feng_{mm} \cdot inv\_onsite_{o,mm} \cdot WTO_{i,o,t} \quad (66)$$

where  $feng_{mm}$  represents the energy consumption factor of basic material  $mm$ .

The energy consumption in life cycle stage of shale well drilling can be calculated by,

$$EC_{drilling} = \sum_{i \in I} \sum_{mm \in MM} \sum_{t \in T} feng_{mm} \cdot inv\_drilling_{i,mm} \cdot NN_{i,t} \quad (67)$$

The energy consumption associated with shale gas production can be calculated as follows.

$$EC_{production} = \sum_{i \in I} \sum_{mm \in MM} \sum_{t \in T} feng_{mm} \cdot inv\_production_{i,mm} \cdot SP_{i,t} \quad (68)$$

The energy consumed in shale gas processing can be calculated by the following equation.

$$EC_{processing} = \sum_{i \in I} \sum_{p \in P} \sum_{mm \in MM} \sum_{t \in T} feng_{mm} \cdot inv\_processing_{i,mm} \cdot STP_{i,p,t} \quad (69)$$

The energy consumption resulting from transportation activities can be calculated by the following equation.

$$EC_{transportation} = \sum_{i \in I} \sum_{p \in P} \sum_{mm \in MM} \sum_{t \in T} feng_{mm} \cdot inv\_trans_{mm} \cdot lsp_{i,p} \cdot STP_{i,p,t} \\ + \sum_{p \in P} \sum_{mm \in MM} \sum_{t \in T} feng_{mm} \cdot inv\_trans_{mm} \cdot lpm_p \cdot SPM_{p,t} \quad (70)$$

#### 4.4.3 Solution algorithm

The resulting problem is formulated as a multiobjective MILFP problem. Both design and operational decisions, including those for drilling schedule, pipeline installment, processing plant construction, technology selection, production planning, and transportation arrangement, are described with corresponding integer and continuous variables. As a special class of MINLP, this MILFP problem features three fractional objective functions formulated as ratios of linear functions. All the constraints are linear ones, and both discrete and continuous variables are involved in the objective functions and constraints. Notably, MILFP problems can be solved with general-purpose MINLP algorithms. However, large-scale MILFP problems, due to its combinatorial nature and pseudo-convexity, can be computationally intractable for general-purpose MINLP

methods. Local MINLP solvers, such as DICOPT and SBB, are generally more computationally efficient than global optimizers. Nevertheless, they cannot guarantee the global optimality and may lead to suboptimal solutions. To overcome this challenge, we adopt the parametric algorithm based on Newton's method in this study for efficient solution of this MILFP problem [107]. The original MILFP problem is first transformed into an equivalent parametric MILP problem  $F(q)$ , which has the same constraints as the original MILFP problem and new objective functions given as the difference between the numerator and the denominator multiplied by a parameter  $q$ . The parametric function  $F(q)$  has such an important property that when  $F(q)=0$ , the reformulated MILP problem has a unique optimal solution that is identical to that of the original MILFP problem. Since  $F(q)$  does not have a closed-form analytical expression, we apply numerical root-finding methods, namely Newton's method, to find the optimal value of parameter  $q$ . By iteratively updating the parameter  $q$  based on the optimal solutions obtained from solving the corresponding MILP subproblems, we can guarantee the convergence to the global optimum within a finite number of iterations. The detailed procedures are illustrated by the Pseudo code provided in Figure 39.

---

***Parametric Algorithm***

---

1.  $\min TC/TENG \rightarrow \min F(q) = (TC - q \cdot TENG)$
2. Initialization:  $q = 0, Iter = 1$
3. **while** ( $F(q) \geq Tol$ ) **do**
  - Solve the resulting MILP subproblem
  - Denote the optimal solution as  $TC^*$  and  $TENG^*$

```

4.   |           Update  $q = TC^* / TENG^*$  ,
      |            $Iter = Iter + 1$  .
5.   | end while
6.   | Output  $q^*$ 

```

---

Figure 39. Pseudo code of the parametric algorithm for MILFP problems.

## 4.5 Results and discussion

To illustrate the applicability of the proposed dynamic MFA-based LCO framework, we consider a case study of a “well-to-gate” shale gas supply chain based on Marcellus shale. In this shale gas supply chain, a total of 12 shale sites are considered, where six shale sites are existing ones with active shale wells and six shale sites are potential ones to be developed. Each shale site allows for drilling of up to five shale wells. Three potential locations are considered for the construction of midstream shale gas processing plants. A 10-year planning horizon is considered, which is further divided into 10 equal time periods. A 10% discount rate is adopted for each year. The material flow profiles of 36 key materials are tracked throughout the given planning horizon. The resulting problem has 627 integer variables, 7,553 continuous variables, and 7,718 constraints. All the models and solution procedures are coded in GAMS 24.8.5. on a PC with an Intel® Core™ i7-6700 CPU and 32GB RAM, running the Windows 10 Enterprise, 64-bit operating system. The reformulated MILP subproblems are solved using CPLEX 12.7.1.0. The optimality tolerance is set to 0.1%. For all the Pareto-optimal solution points, the parametric algorithm converges in 3 to 5 iterations.

The total computational time varies from a few CPU seconds to a few hundred seconds depending on the number of iterations.

#### **4.5.1 Pareto optimal surface**

In this case study, we choose the economic objective function as the primary objective function and transform the remaining environmental and resource objective functions into  $\varepsilon$ -constraints. By first optimizing the economic, environmental, and resource objectives individually, we obtain the lower bounds and upper bounds of the  $\varepsilon$ -constraints associated with environmental and resource performances. Based on the bounding information, we choose 20 points for the environmental  $\varepsilon$ -parameter and 20 points for the resource  $\varepsilon$ -parameter with identical intervals. Thus, by varying the combination of these two types of  $\varepsilon$ -parameters, a total of 400 Pareto-optimal solutions are obtained. A 3D-Pareto optimal surface is plotted using these solutions, as shown in Figure 40.

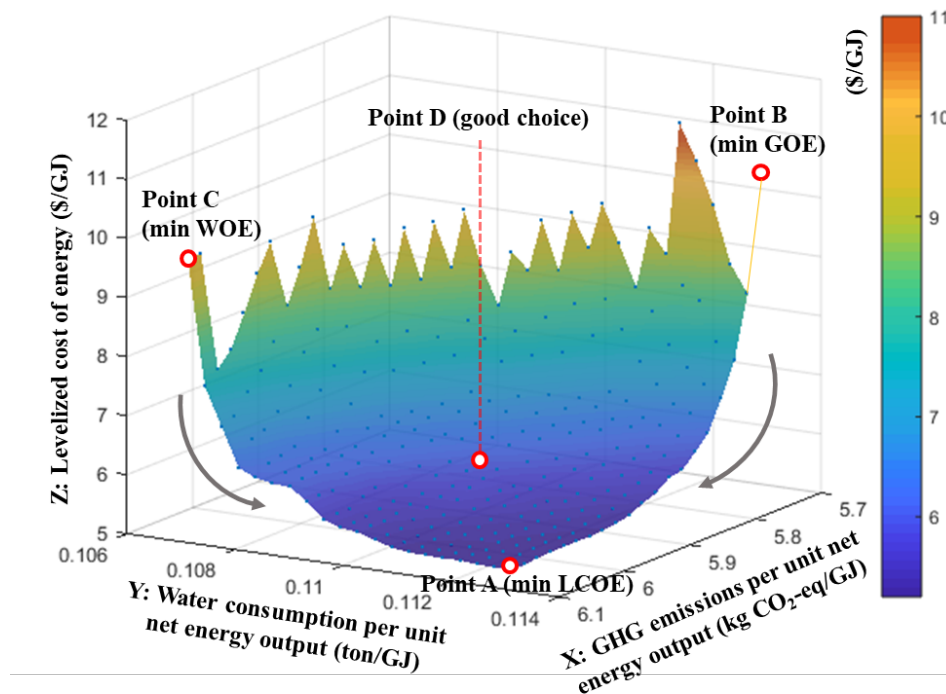


Figure 40. 3D-Pareto optimal surface illustrating the trade-offs between economic, environmental, and resource performances.

In Figure 40, the  $x$ -axis represents the life cycle GHG emissions corresponding to unit net energy output, given in kg CO<sub>2</sub>-eq/GJ. The  $y$ -axis represents the water consumption associated with unit net energy output, given in ton/GJ. The  $z$ -axis represents the levelized cost of unit net energy output, given in \$/GJ. On the Pareto optimal surface, we choose four representative Pareto-optimal solution points for further demonstration. Point A is the extreme solution with the best economic performance, namely the lowest levelized cost per unit net energy output of \$5.22/GJ. Point B is the extreme solution with the least environmental impacts, namely the lowest GHG emissions per unit net energy output of 5.70 kg CO<sub>2</sub>-eq/GJ. Point C is the extreme solution with the best resource performance, namely the lowest water consumption per

unit net energy output, which is 0.107 ton/GJ. In addition to these three extreme solution points, we pick a “good choice” solution point that maintains a good balance among the three optimization criteria. Specifically, the levelized cost of unit net energy output of point D is \$6.05/GJ, 15.9% higher than that of extreme solution point A (\$5.22/GJ), but 37.5% lower than that of point B (\$9.68/GJ) and 41.0% lower than that of point C (\$10.26/GJ). However, the GHG emissions and water consumption per unit net energy output of point D are only 5.91 kg CO<sub>2</sub>-eq/GJ and 0.110 ton/GJ, respectively. To provide a better illustration of the Pareto optimal surface, we present the contour plot of the 3D-Pareto optimal surface projected on the X-Y surface in Figure 41.

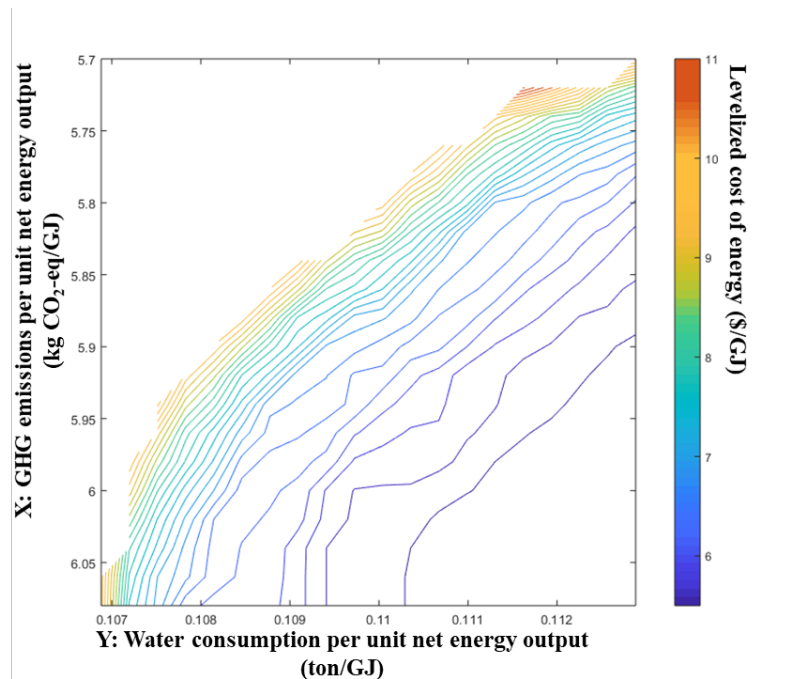


Figure 41. Contour plot of the Pareto optimal surface on the X-Y surface.

The Pareto optimal surface is not a smooth surface, as can be seen from the contour lines. The trade-off between economic performance and environmental performance is similar to that between the economic performance and resource performance. To

mitigate the life cycle GHG emissions and water consumption associated with unit net energy output, some sacrifice in economic performance is necessary, reflected by a higher levelized cost of energy. Moreover, when the GHG emissions per unit net energy output is greater than 5.90 kg CO<sub>2</sub>-eq/GJ, and the water consumption per unit net energy output is greater than 0.110 ton/GJ, the corresponding Pareto optimal surface area is relatively flat, indicating insignificant trade-offs among these criteria in this region. However, once crossing the aforementioned boundaries, the trade-offs between economic and the other criteria become increasingly significant. This trend can be observed from the increasing density of contour lines toward the top left corner in Figure 41. Notably, we select the “good choice” solution point D based on this observation, which lies near the turning point of this 3D-Pareto optimal surface.

#### **4.5.2 Comparison among Pareto optimal solutions**

In Figure 42, we present the detailed breakdowns of the economic, environmental, and resource performances regarding five key life cycle stages in the shale gas supply chain, namely water management, shale well drilling, shale gas production, shale gas processing, and transportation. We summarize the results of Pareto optimal solutions points A to D for better comparison and analysis. As can be seen, solution point A leads to the lowest levelized cost for generating unit amount of net energy, followed by point D. In descending order, the activities that contribute most to the total cost are shale gas processing, transportation, shale gas production, and well drilling activities. Pareto optimal solution points B and C result in much higher levelized cost of unit net energy output mainly due to extraordinarily higher transportation costs. By checking their

corresponding supply chain design decisions, we note that the high transportation cost of points B and C results from their radical design strategy of gathering pipeline network with extensive transportation links and large pipeline capacities. For instance, the capital investment associated with gathering pipelines of points B and C are \$221.3 MM and \$212.3 MM, respectively. Meanwhile, the pipeline network design of point D only leads to \$78.5 MM capital cost. In terms of GHG emissions per unit net energy output, point B outperform other solution points by a small margin. All the four solution points share similar GHG emission breakdowns, where the transportation life cycle stage contributes the most GHG emissions due to the direct methane leakage and indirect emissions from energy consumption in compressing and pumping the gas. Other life cycle stages, including shale well drilling, shale gas production, and processing, contribute significant amount of GHG emissions as well. By contrast, the GHG emissions incurred during the water management activities, namely water acquisition and different wastewater handling options, are relatively negligible. The water consumption breakdowns in terms of different life cycle stages are quite different from the others. Point C results in the least water consumption for unit net energy output, although all four points have similar water consumption breakdowns. While drilling and fracturing even a single shale wells requires significant amount of freshwater, the water consumption for generating unit amount of energy in a shale gas supply chain in this study is significantly mitigated by onsite wastewater treatment and recycling operations. However, the shale gas processing stage, where a large amount of cooling water is consumed, is a relatively water-intensive process, contributing the most to water consumption from a functional-unit perspective.

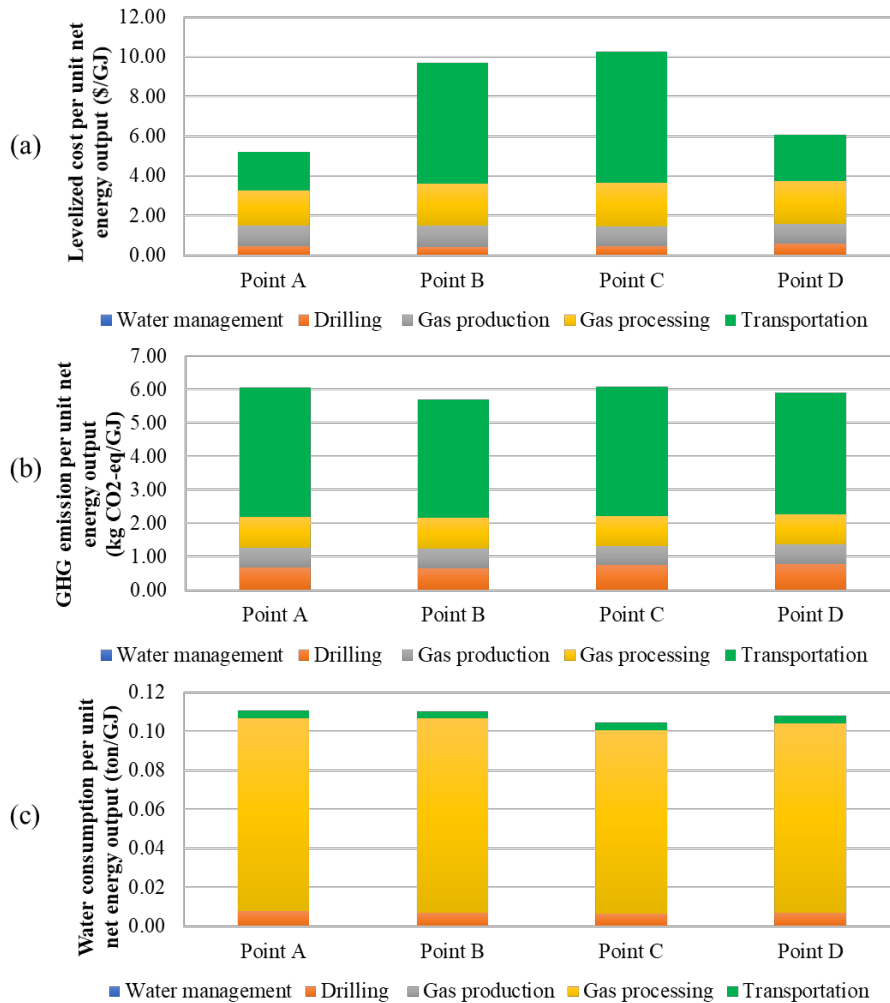


Figure 42. Breakdowns of (a) levelized cost of unit net energy output, (b) GHG emissions per unit net energy output, and (c) water consumption per unit net energy output.

As mentioned in the introduction section, one advantage of the dynamic MFA-based LCO framework is that it enables tracking of the environmental impacts and resource consumption throughout the planning horizon. In Figure 43, we summarize the life cycle profiles regarding total GHG emissions and water consumption of the Pareto optimal solution points A to D. As can be observed, all the Pareto-optimal solution points confront a peak of GHG emissions and water consumption in the third year, and slowly

return to a stable level afterwards. By comparing the four Pareto-optimal solution points, we note that point A maintains high GHG emissions and water consumption throughout the 10-year planning horizon in exchange for the best economic performance. Points B and C sacrifice part of the economic performance to achieve relatively stable GHG emissions and water consumption, respectively. It is worth pointing out that point C not only features the lowest water consumption per unit net energy output, but also results in the least total GHG emissions and water consumption throughout the planning horizon. Meanwhile, although the total GHG emissions and water consumption of point B is the second highest, it outperforms other solution points in terms of GHG emissions per unit net energy output. From this comparison, we conclude that the solution with the lowest total GHG emissions/water consumption is not necessarily the most sustainable one from a functional-unit perspective. Point D in general maintains the most stable GHG emission and water consumption profiles, which lie between those of point A and points B and C.

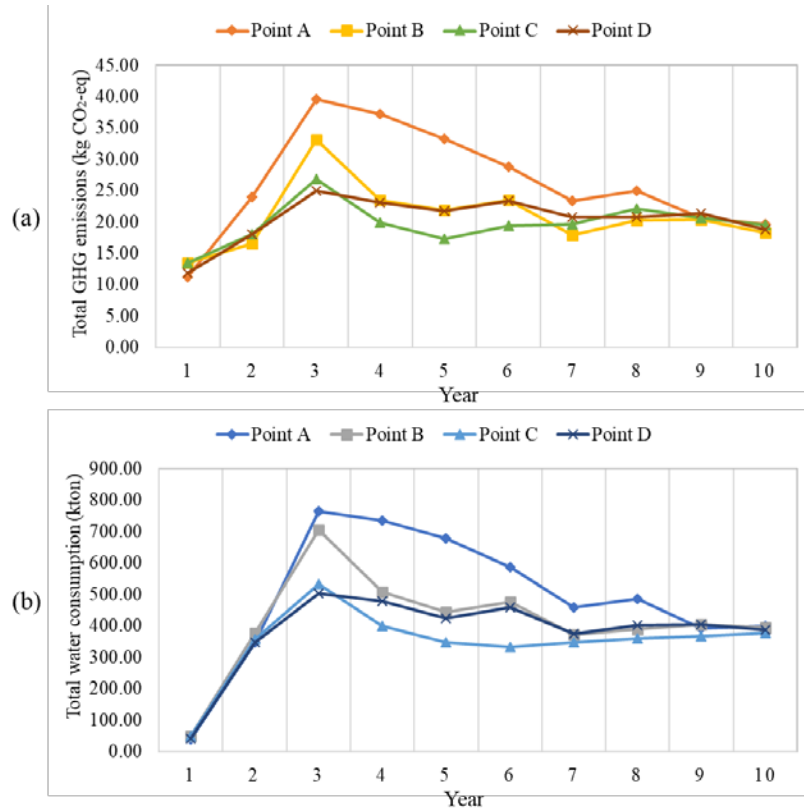


Figure 43. Life cycle profiles of (a) total GHG emissions and (b) total water consumption of Pareto optimal solution points A, B, C, and D.

To further investigate the design decisions associated with different solution points that lead to distinct economic, environmental, and resource performances, we present the optimal drilling schedules and corresponding shale gas production profiles associated with points A through D in Figure 44. The drilling schedules are presented with stacked columns, and the total shale gas production profiles for different solution points are illustrated by scatter plots with lines. We note the total shale gas production includes both the existing shale wells and the newly drilled shale wells. Overall, all four solution points have similar trends in terms of drilling activities. Most new shale wells are drilled in the beginning of the planning horizon. As the drilled shale wells age, the

corresponding productivity decreases rapidly. Thus, extra shale wells are drilled to maintain a relatively stable raw shale gas output. The total number of shale wells drilled in point A, point B, point C, and point D are 16 shale wells, 13 shale wells, 13 shale wells, and 14 shale wells, respectively, in addition to the existing 10 shale wells. Notably, the profiles of shale gas production have similar shapes as those of total GHG emissions and water consumption. This implies that the total carbon footprint and water resource consumption are directly related to the amount of shale gas produced.

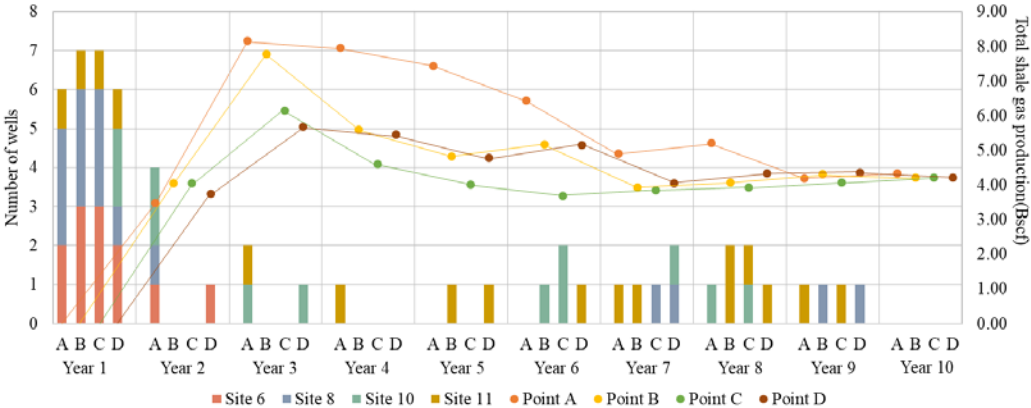


Figure 44. Optimal drilling schedules (axis on the left) and shale gas production profiles (axis on the right) of Pareto optimal solution points A, B, C, and D throughout the planning horizon.

### 4.5.3 Optimal material flow profiles of the “good choice” Pareto optimal solution

Next, we investigate the detailed design decisions of “good choice” solution point D for more insights into the sustainable design of shale gas supply chains. A comprehensive MFA of point D is presented in Figure 45. The width of each flow shape is proportional

to the quantity of corresponding material flow. Based on the optimal drilling schedule of point D, a total of 14 shale wells are drilled, where shale site 6, shale site 8, shale site 10, and shale site 11 have 3 wells, 3 wells, 4 wells, and 4 wells drilled, respectively. To support the drilling and fracturing activities, key materials, namely steel, proppant, chemicals, electricity, diesel, and water are sent to these shale sites. The chemicals here denote all the chemical additives (such as those listed in Figure 38) used during the drilling and hydraulic fracturing processes. In addition to the newly developed shale sites, existing shale sites, namely shale site 4, shale site 5, shale site 7, and shale site 9, are producing shale gas as well. Meanwhile, wastewater is generated at each shale site. Up to 99.7% of the wastewater will be treated onsite with reverse osmosis technology and blended with freshwater for recycling. The remaining 0.3% of the generated wastewater will be transported to Class-II disposal wells for underground injection. By examining the specific water management operations, we find that the disposal wells function as a supplemental option to onsite treatment for wastewater handling, especially in years when intense drilling activities are observed. In the midstream, two shale gas processing plants at location 2 and location 3 are constructed, where processing plant 2 is designed with a processing capacity of 12.43 billion standard cubic feet (Bscf) raw shale gas per year, and processing plant 3 is capable of processing 10.00 Bscf raw shale gas per year. Although processing plant 2 is designed with larger processing capacity to handle peak shale gas output in certain years, most raw shale gas is eventually sent to processing plant 3 for impurity removal and further separation. From the specific flow results, we note that processing plant 3 processes 87.2% of the total raw shale gas, and processing plant 2 receives 12.8% of the raw shale gas. Due to

the varying composition of raw shale gas from different shale sites, processing plant 3 consequently produces 85.3% of the natural gas and 84.7% of the NGL. The remaining natural gas and NGL output is contributed by processing plant 2. The life cycle stage of shale gas processing requires the inputs of water, steam, MEA, and TEG. The processed pipeline-quality natural gas and NGL are sold to the market afterwards. Across the shale gas supply chain, a significant amount of methane will be leaked, and both direct and indirect CO<sub>2</sub> emissions will be generated, resulting in the key sources of GHG emissions. Although the quantity of methane leakage is comparable to that of CO<sub>2</sub> emissions, methane leakage results in more significant GHG emissions due to the high global warming potential of methane. From this MFA, we identify transportation activities as the main source of methane leakage. By contrast, the CO<sub>2</sub> emissions are mainly contributed by the drilling and production activities at shale sites as well as shale gas processing activities at processing plants. The solid waste produced during shale site development is sent to landfill and landfarming, which handle 40.0% and 60.0% of the solid waste, respectively.

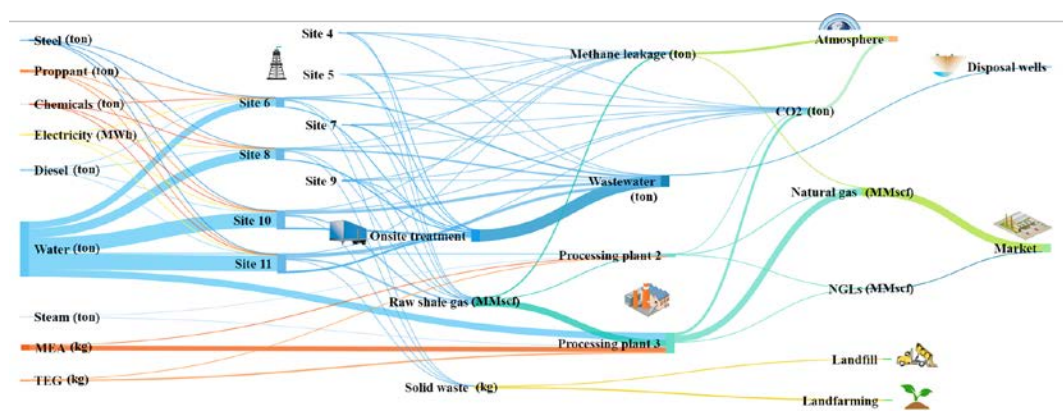


Figure 45. MFA of Pareto optimal solution point D.

In Figure 46, we summarize the profiles of nine key material flows, including steel, water, diesel, proppant, chemical additives, electricity, steam, TEG, and MEA, associated with Pareto optimal solution point D. As can be seen, among the nine materials, material flows of steel, diesel, proppant, and chemical additives share similar profiles, where nearly half of the total material flows occur in the first year, and a small peak is observed near year 7. These profiles are consistent with the optimal drilling schedule of point D, indicating that these four materials flows are mainly consumed in the shale site development and well drilling phases. The other material flows, namely water, electricity, steam, TEG, and MEA, have relatively stable profiles, which match the constant shale gas output associated with point D. This observation indicates that these five materials are mainly consumed in shale gas production, processing, and transportation activities.

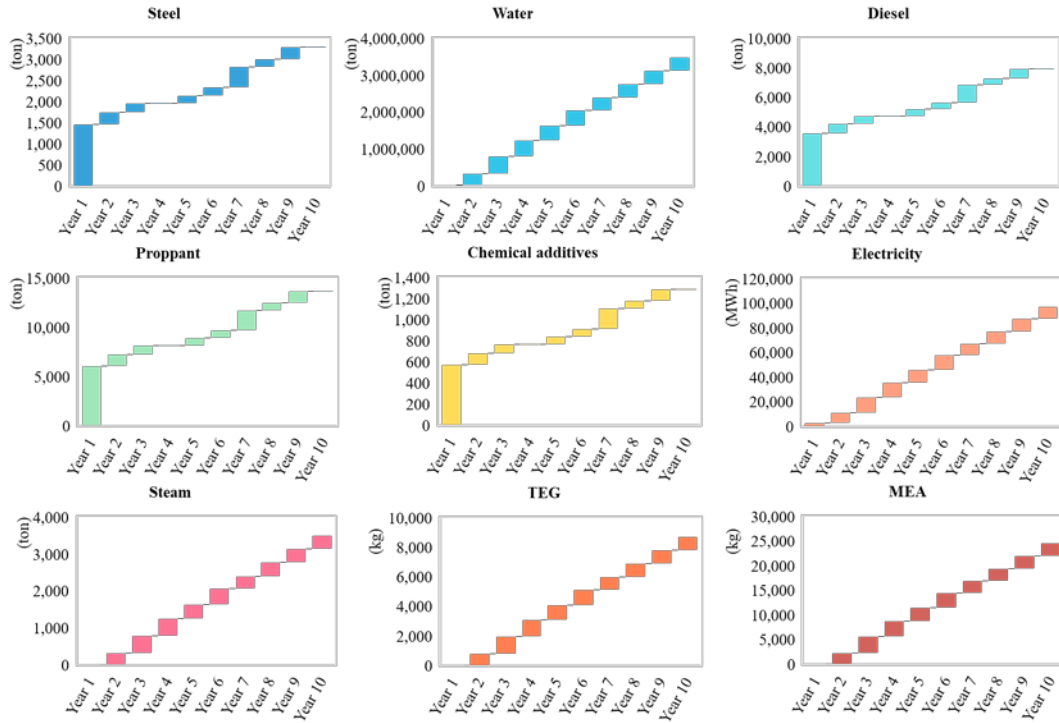


Figure 46. Key material flow profiles associated with Pareto optimal solution point D.

## 4.6 Summary

We developed a dynamic MFA-based LCO framework to investigate the sustainable design of energy systems. In contrast to the traditional LCO framework, the integration of dynamic MFA approach enabled high-fidelity modeling of the various input, output, and recycling material flows within the complex energy systems. Moreover, both the environmental impacts and resource efficiency were incorporated in a holistic optimization model, which provides comprehensive evaluation of a system's sustainability performance. The resulting problem was formulated as a multiobjective MILFP problem that simultaneously optimized the economic, environmental, and resource performances associated with one functional unit of major product. An efficient parametric algorithm was implemented to tackle the resulting MILFP problem.

To illustrate the applicability of the proposed modeling framework, we presented a case study on the sustainable design and operations of a Marcellus shale gas supply chain. The results and analysis lead to the following conclusions: (1) there are clear trade-offs among economic, environmental, and resource performances in the shale gas energy system, and the proposed MFA-based LCO framework offers an effective way to find an optimal solution with well-balanced sustainability performance; (2) the investigation of optimal material flow profiles provides more insights in the mechanisms of environmental impacts and resource consumption; (3) the application of recycling technology, such as onsite wastewater treatment in shale gas supply chains, can substantially improve the sustainability of an energy system.

## 4.7 Nomenclature

### Sets

$I$	Set of shale sites indexed by $i$
$MM$	Set of basic materials indexed by $mm$
$N$	Set of number of wells indexed by $n$
$O$	Set of onsite wastewater treatment technologies indexed by $o$ ( $o_1$ : MSF; $o_2$ : MED; $o_3$ : RO)
$P$	Set of processing plants indexed by $p$
$PT$	Set of interpolated points indexed by $pt$
$R$	Set of capacity levels for gas pipelines indexed by $r$
$T$	Set of time periods indexed by $t$

### Subsets

$I_e(i)$	Subset of existing shale sites indexed by $i$
$I_n(i)$	Subset of potential shale sites indexed by $i$
$T'(t)$	Subset of time periods when wells are drilled indexed by $t'$

## Parameters

$cc_i$	Correlation coefficient for shale gas production and wastewater production of a shale well at shale site $i$
$cca_t$	Capacity for wastewater treatment at CWT facility in time period $t$
$dca_t$	Capacity for underground injection in Class-II disposal wells in time period $t$
$dml_t$	Minimum demand of natural gas at local market in time period $t$
$dmup_t$	Maximum demand of natural gas at local market in time period $t$
$dr$	Discount rate per time period
$eur_i$	Estimated ultimate recovery of shale gas at shale site $i$
$fac$	Unit acquisition cost of freshwater
$fems_{mm}$	GHG emission factor associated with basic material $mm$
$fwat_{mm}$	Water consumption factor associated with basic material $mm$
$feng_{mm}$	Energy consumption factor associated with basic material $mm$
$inv\_acquisition_{i,mm}$	Unit material flow matrices corresponding to freshwater acquisition at shale site $i$ and basic material $mm$
$inv\_disposal_{i,mm}$	Unit material flow matrices corresponding to wastewater underground injection from shale site $i$ and basic material $mm$

$inv\_cwt_{i,mm}$	Unit material flow matrices corresponding to wastewater treatment by CWT facility from shale site $i$ and basic material $mm$
$inv\_onsite_{o,mm}$	Unit material flow matrices corresponding to onsite wastewater treatment with technology $o$ and basic material $mm$
$inv\_drilling_{i,mm}$	Unit material flow matrices corresponding to shale well drilling at shale site $i$ and basic material $mm$
$inv\_production_{i,mm}$	Unit material flow matrices corresponding to shale gas production at shale site $i$ and basic material $mm$
$inv\_processing_{p,mm}$	Unit material flow matrices corresponding to shale gas processing at processing plant $p$ and basic material $mm$
$inv\_trans_{mm}$	Unit material flow matrices corresponding to transportation and basic material $mm$
$lc_i$	NGL composition in shale gas at shale site $i$
$lo_o$	Recovery factor for onsite wastewater treatment technology $o$
$lpm_p$	Distance from processing plant $p$ to local market
$lsp_{i,p}$	Distance from shale site $i$ to processing plant $p$
$mec_i$	Methane composition in shale gas at shale site $i$
$mn_i$	Maximum number of wells that can be drilled at shale site $i$ per time period
$ne_i$	Number of existing shale wells drilled at shale site $i$
$ocl_o$	Minimum capacity for onsite wastewater treatment technology $o$
$ocu_o$	Maximum capacity for onsite wastewater treatment technology $o$

$pcap_{p,pt}$	Reference capacity of processing plant $p$ with interpolated point $pt$
$pcc_{p,pt}$	Capital cost of processing plant $p$ associated with interpolated point $pt$
$pef$	NGL recovery efficiency at processing plants
$pl_t$	Average unit price of NGLs in time period $t$
$psg$	Estimated average unit profit of shale gas remains to be produced in shale wells
$rf_o$	Ratio of freshwater to wastewater required for blending after treatment of onsite wastewater treatment technology $o$
$sd_{i,t}$	Unit cost for shale well drilling and completion at shale site $i$ in time period $t$
$spc_{i,t}$	Unit cost for shale gas production at shale site $i$ in time period $t$
$spp_{i,t}$	Shale gas production of a shale well with age $t$ at shale site $i$
$tmn_i$	Maximum number of wells that can be drilled at shale site $i$ over the planning horizon
$tprc_r$	Reference capacity of gas pipeline with capacity level $r$
$tpri_r$	Reference capital investment of gas pipeline with capacity level $r$
$ue$	Unit heat content in unit amount of natural gas
$vc$	Unit cost for wastewater treatment at CWT facility
$vd$	Unit cost for underground injection of wastewater into disposal wells
$vo_o$	Unit cost for wastewater treatment of onsite wastewater treatment technology $o$
$vro_p$	Unit processing cost at processing plant $p$

$vrt$	Unit transportation cost of shale gas from shale sites to processing plant
$vt_p$	Unit transportation cost for transportation natural gas from processing plants to local market
$wd_i$	Average drilling water usage for each well at shale site $i$
$wrd_i$	Recovery ratio of water for drilling process at shale site $i$
$wrf_i$	Recovery ratio of water for hydraulic fracturing process at shale site $i$

### **Nonnegative Continuous variables**

$FDW_{i,t}$	Freshwater demand of shale site $i$ in time period $t$
$FW_{i,t}$	Amount of freshwater acquired from water source to shale site $i$ in time period $t$
$NN_{i,t}$	Number of wells drilled at shale site $i$ in time period $t$
$PC_p$	Capacity of processing plant $p$
$SP_{i,t}$	Shale gas production rate at shale site $i$ in time period $t$
$STP_{i,p,t}$	Amount of shale gas transported from shale site $i$ to processing plant $p$ in time period $t$
$STPM_{p,t}$	Amount of natural gas produced at processing plant $p$ in time period $t$
$STPL_{p,t}$	Amount of NGLs produced at processing plant $p$ in time period $t$
$SPM_{p,t}$	Amount of natural gas sold to market from processing plant $p$ in time period $t$

$TCP_{i,p,r}$	Capacity of gas pipeline with capacity level $r$ between shale site $i$ and processing plant $p$
$WP_{i,t}$	Wastewater production rate at shale site $i$ in time period $t$
$WTC_{i,t}$	Amount of wastewater transported from shale site $i$ to CWT facilities in time period $t$
$WTD_{i,t}$	Amount of wastewater transported from shale site $i$ to Class-II disposal wells in time period $t$
$WTO_{i,o,t}$	Amount of wastewater treated by onsite wastewater treatment technology $o$ at shale site $i$ in time period $t$

#### **Binary variables**

$XP_{i,p,r}$	0-1 variable. Equal to 1 if gathering pipeline with capacity level $r$ is installed to transport shale gas from shale site $i$ to processing plant $p$
$YD_{i,n,t}$	0-1 variable. Equal to 1 if $n$ shale wells at shale site $i$ are drilled in time period $t$
$YO_{i,o}$	0-1 variable. Equal to 1 if onsite wastewater treatment technology $o$ is applied at shale site $i$

#### **SOS2 variables**

$Y_{p,pt}$	SOS2 variable for calculating the capital cost of processing plant $p$ with interpolated point $pt$ .
------------	---

CHAPTER 5  
DECIPHERING AND HANDLING UNCERTAINTY WITH TWO-STAGE  
STOCHASTIC PROGRAMMING

## **5.1 Introduction**

In recent years, the widespread application of horizontal drilling and hydraulic fracturing has led to a “shale revolution”, which further results in the U.S. transitioning from an importer to a net exporter of natural gas [1]. Despite the optimistic forecast of shale gas production given by the EIA, a recent report by Post Carbon Institute unveils the fact that the actual future of shale gas may not be as bright as the EIA suggests [12]. From a well-by-well based calculation of shale gas production throughout the U.S., they conclude that the actual profitability of a shale well can be significantly affected by the uncertainty in the estimated ultimate recovery (EUR) and astounding decline rates of production ranging from 60% to 90% in the first three years. Considering the significant influence of the shale gas industry on the overall U.S. energy sector, it is essential to design and operate emerging shale gas supply chains with explicit consideration of EUR uncertainty and actual shale gas production profiles.

Supply chain design and optimization under uncertainty has long been known as a challenging problem that is vital to the success of industrial concerns [185, 186]. Currently, there are publications regarding design and operations of shale gas supply chains [38, 79, 187, 188], and some works present a general analysis of the uncertainty in shale gas supply chains [189-192], while only a few of them provide a quantitative solution using mathematical programming tools. Yang and Grossmann [57] presented a mixed-integer linear programming (MILP) model optimizing water use life cycle for

shale wells. Cafaro and Grossmann [116] proposed a mixed-integer nonlinear programming (MINLP) model to determine the optimal design of a shale gas supply chain. However, operational decisions are not addressed, and the actual lifetime of shale wells are not properly addressed. Gao and You [58] proposed a mixed-integer linear fractional programming (MILFP) model to address the optimal design and operations of a shale water supply chain. Yang and Grossmann [125] presented a new MILP model for optimizing capital investment decisions for water use for shale gas production through a State-Task Network. Recently, Gao and You [6] conducted a life cycle optimization of the shale gas supply chain addressing both design and operational decisions to reveal the trade-off between economic performance and GHG emissions. By reviewing the existing works, we have identified the absence of a comprehensive shale gas supply chain model that considers design and planning decisions under uncertainty. Meanwhile, recently published papers on the life cycle assessment of shale gas highlights the large influence of EUR uncertainty, identified as the most critical source of uncertainty that can significantly influence both the economic and environmental performances of shale gas supply chains [79, 80, 96, 97]. Therefore, we consider it necessary and important to develop a shale gas supply chain model that not only considers both design and planning decisions, but also properly addresses EUR uncertainty.

To achieve this goal, the following challenges need to be addressed. First, it is necessary to select the correct data and approach to decipher EUR uncertainty. The second challenge is to develop a novel and comprehensive model based on the EUR distribution that can optimize the economic performance regarding both design and planning

decisions under uncertainty. Finally, we need to be able to solve the resulting large-scale optimization problem in a reasonable amount of time. In this work, we derive the EUR distribution based on real data reported in existing literature [1, 113]. There are two methods commonly applied to handle uncertainty in optimization problems [193]. The first one involves Robust Optimization (RO) methods [194, 195]. Although RO is known for its superior computational tractability, it is designed to address optimization problems with uncertain data that are only known to belong to some uncertainty set. Moreover, because RO considers the worst case, it may suffer from its conservativeness and fail to give an economically attractive optimal solution. By reviewing the reported EUR data, we identify a wide distribution of EUR with distinct “long tails”, which is not suitable for applying RO approach. Therefore, we adopt the scenario-based stochastic programming approach to explicitly account for the EUR uncertainty. Stochastic programming has been widely used to quantitatively account for uncertainty in design, planning and scheduling problems [196, 197]. A two-stage stochastic mixed-integer linear fractional programming (SMILFP) model is hereby proposed to minimize the levelized cost of energy in a shale gas supply chain. The objective is to find a solution with the best expected performance under all scenarios. Due to the dependence of stochastic programming on the scenarios, the resulting problem size may increase exponentially as the number of scenarios increases. To tackle this challenge, we adopt a sample average approximation (SAA) approach to generate scenarios based on the real-world EUR distribution data [196, 198]. This is combined with statistical methods to determine the required number of scenarios to achieve the desired accuracy [199, 200]. The required number of scenarios is significantly reduced with guaranteed

solution quality due to the SAA method. In order to further boost the solution process of the resulting two-stage SMILFP problem, a novel algorithm integrating the parametric approach and the L-shaped method is developed to solve large-scale problems efficiently. Finally, a case study based on the Marcellus shale play is presented to illustrate the application of the proposed modeling framework and solution approaches.

### 5.2 Problem statement

In this section, we formally state the problem of optimal design and operations of a shale gas supply chain under uncertainty. A superstructure of the shale gas supply chain network taken as a reference in this study is depicted in Figure 47.

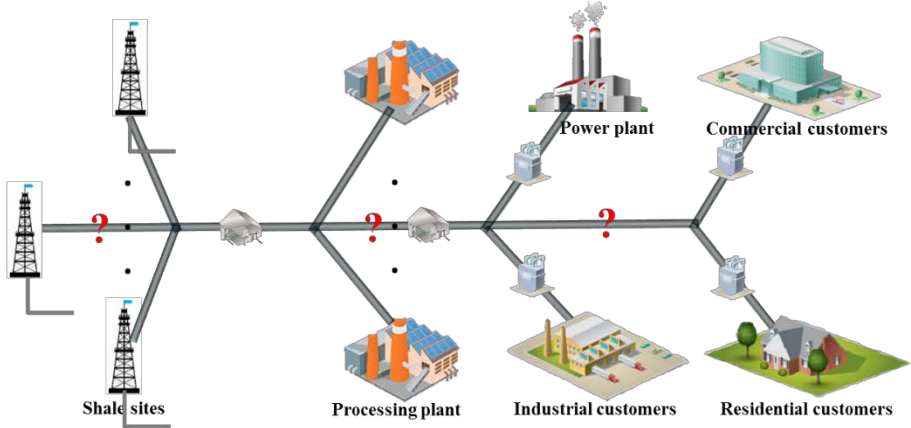


Figure 47. Superstructure of shale gas supply chain network.

As can be seen, such a network includes a set of shale sites with potential wells that can be drilled, a set of processing plants where sales gas and NGLs are separated, and a set of end customers, namely power plants, industrial customers, commercial customers, and residential customers, where natural gas is consumed to provide energy. Following existing literature, the storage option is neglected in this shale gas supply chain to

simplify the complex network [116], although the proposed modeling framework and solution algorithm are general enough to be easily adapted to consider this issue. Shale gas is transported through pipelines that need to be designed with appropriate capacity.

In this problem, we are given the following parameters:

- Reference capital investment data regarding well drilling, construction of processing plants, and installation of gas pipelines;
- Operating costs with respect to hydraulic fracturing, shale gas production, shale gas processing, and transportation;
- Reference capacity data related to potential processing plants and pipelines;
- Problem specific data, including the reference production profile of shale gas, EUR sampling data of shale well, maximum number of wells that can be drilled for each shale site, composition of shale gas, processing efficiency at processing plants, sale price of NGL, minimum demand of natural gas and average energy generation efficiency for different end customers.

Corresponding to the two-stage stochastic programming method, major decision variables comprise two stages. The first-stage decisions correspond to all the design decisions, which are made “here-and-now” prior to the realization of EUR uncertainty. The second-stage decisions are all the operational decisions that are postponed to a “wait-and-see” mode after EUR uncertainty and the shale gas production profile is revealed. Details of these decisions variables are given as the following:

#### **Stage I: Design Decisions**

- Number of wells to be drilled in each shale site;
- Constructions of processing plants and corresponding capacities;

- Installation and corresponding capacities of pipelines between shale sites, processing plants, and end customers.

### **Stage II: Operational Decisions**

- Amount of shale gas produced at each shale site in each time period;
- Amount of shale gas processed at each processing plant in each time period;
- Amount of gas being sent to each end customer in each time period;
- Amount of energy generated corresponding to different end use.

In this work, we make the following assumptions:

- Maximum number of wells that can be drilled at each shale site is known beforehand;
- Shale wells within the same shale site is lumped together in the supply chain;
- The total operational cost regarding all the activities related to shale gas production, such as hydraulic fracturing, pumping, water management, etc., is proportional to the amount of shale gas produced;
- NGL is known to have higher unit economic value than methane. Yet, NGL is considered as by-product of shale gas and sold at processing plants, because we focus on shale gas supply chain in this work;
- Minimum demand of natural gas for different end customer is estimated based on the overall scale of shale gas supply chain considered in this work.

The objective of this two-stage stochastic programming problem is to optimize the expected Levelized Cost of Energy (*LCOE*) generated from Shale gas, which is formulated as minimizing the total expected cost of shale gas supply chain divided by the total energy generation [115]. The *LCOE* can be regarded as the cost at which energy

must be generated in order to break-even over the lifetime of the project [201]. Therefore, it is considered as an ideal economic indicator in a shale gas supply chain [6]. As a result, the goal of this model is to seek the best average economic performance of shale gas for energy generation under uncertainties of EUR of shale sites. It is also worth noting that currently the non-cooperative supply chain optimization problem is still very challenging to tackle. In this work, we assume a cooperative model in this work following the pattern of most existing supply chain optimization work.

### 5.3 Model formulation

According to the general problem statement in the previous section, we present the model formulation for the optimal design and operations of shale gas supply chain networks. A list of indices, sets, parameters and variables is given in the Nomenclature, where all of the parameters are denoted with lower-case symbols, and all of the variables are denoted with upper-case symbols. A general description of the mathematical model is given as follows:

$$\text{Objective: } \min E(LCOE) = \frac{TC}{TEG} = \frac{TC_{1st} + \sum_{js \in JS} TC_{2nd, js} \cdot p_{js}}{\sum_{js \in JS} TEG_{2nd, js} \cdot p_{js}}$$

s.t. Mass balance constraints (11)-(15)

Capacity constraints (16)-(20)

Bounding constraints (21)-(23)

Logic constraints (24)-(28)

### 5.3.1 Objective function

The objective of this stochastic programming model is to optimize the expected  $LCOE$ , which is formulated as total expected net present cost ( $TC$ ) divided by total expected energy generation ( $TEG$ ). The numerator  $TC$  equals the sum of the first-stage cost ( $TC_{1st}$ ) and the expected second-stage cost.  $TC_{1st}$  accounts for the total capital investment, including the capital cost of shale well drilling and completion, installation of pipelines, and construction of processing plants. The expected second-stage cost is the summation of the products of the scenario probability  $p_{js}$  and the associated scenario cost  $TC_{2nd,js}$ . Since we consider NGLs as by-products of sales gas, there are negative terms accounting for the extra income from selling NGLs. Positive terms include costs related to shale gas production operations, shale gas processing, and gas transportation. The denominator is the product of the scenario probability  $p_{js}$  and the associated scenario energy generation  $TEG_{2nd,js}$ .

The first-stage cost refers to total capital investment at the beginning of the planning horizon, calculated by:

$$TC_{1st} = C_{1st}^{drilling} + C_{1st}^{processing} + C_{1st}^{pipeline} \quad (1)$$

where  $C_{1st}^{drilling}$  is the capital investment of shale well drilling and completion.  $C_{1st}^{processing}$  is the capital investment for construction of processing plants, and  $C_{1st}^{pipeline}$  is the capital investment of pipeline networks that connect shale sites, processing plants, and end customers of natural gas. The first term is calculated by:

$$C_{1st}^{drilling} = \sum_{i \in I} sdc_i \cdot NN_i \quad (2)$$

where  $NN_i$  is an integer variable that denotes the number of wells to be drilled at shale site  $i$ ;  $sdc_i$  denotes the capital cost for shale well drilling and completion at shale site  $i$ ;

The second term is given by:

$$C_{1st}^{processing} = \sum_{p \in P} \sum_{r \in R} \left( pri_{r-1} \cdot YP_{p,r} + (PC_{p,r} - prc_{r-1} \cdot YP_{p,r}) \cdot \left( \frac{pri_r - pri_{r-1}}{prc_r - prc_{r-1}} \right) \right) \quad (3)$$

where  $PC_{p,r}$  denotes the processing capacity for range  $r$  processing plant  $p$ ;  $YP_p$  is binary variable that equals 1 if processing plant  $p$  is constructed;  $pri_r$  is the reference capital investment for processing plant with capacity range  $r$ ; and  $prc_r$  is the corresponding reference capacity for processing plant with capacity range  $r$ .

The last term is modelled as follows:

$$C_{1st}^{pipeline} = \sum_{i \in I} \sum_{p \in P} \sum_{r \in R} \left( tpri_{r-1} \cdot XP_{i,p,r} + (TPC_{i,p,r} - tprc_{r-1} \cdot XP_{i,p,r}) \cdot \left( \frac{tpri_r - tpri_{r-1}}{tprc_r - tprc_{r-1}} \right) \right) \\ + \sum_{p \in P} \sum_{m \in M} \sum_{r \in R} \left( tpri_{r-1} \cdot XPM_{p,m,r} + (TPMC_{p,m,r} - tprc_{r-1} \cdot XPM_{p,m,r}) \cdot \left( \frac{tpri_r - tpri_{r-1}}{tprc_r - tprc_{r-1}} \right) \right) \quad (4)$$

where  $TPC_{i,p,r}$  denotes the transportation capacity of a range  $r$  pipeline from shale site  $i$  to processing plant  $p$ ;  $TPMC_{p,m,r}$  denotes the transportation capacity of a range  $r$  pipeline from processing plant  $p$  to end customer  $m$ ;  $XP_{i,p,r}$  is a binary variable that equals 1 if a pipeline is installed to transport shale gas from shale site  $i$  to processing plant  $p$ ;  $XPM_{p,m,r}$  is a similar binary variable indicating the construction of a pipeline transporting natural gas from processing plant  $p$  to end customer  $m$ ;  $tpri_r$  is the reference capital investment of a pipeline within capacity range  $r$  for transporting gases; and  $tprc_r$  is the corresponding reference capacity of a pipeline within capacity range  $r$ .

The second-stage cost equals the summation of expected costs for shale gas production, shale gas processing, and gas transportation, subtracted by the expected income from sales of NGLs, given as:

$$TC_{2nd,js} = C_{2nd,js}^{production} + C_{2nd,js}^{processing} + C_{2nd,js}^{transportation} - I_{2nd,js}^{NGLs} \quad (5)$$

$C_{2nd,js}^{production}$  refers to the operating costs in shale gas production that is proportional to the amount of shale gas produced, calculated by:

$$C_{2nd,js}^{production} = \sum_{i \in I} \sum_{t \in T} \frac{spc_{i,t} \cdot SP_{i,t,js}}{(1+dr)^t} \quad (6)$$

where  $SP_{i,t,js}$  is the shale gas production rate at shale site  $i$  in time period  $t$  in scenario  $js$ ;  $spc_{i,t}$  is the unit cost for shale gas production at shale site  $i$  in time period  $t$ ;  $dr$  is the discount rate per time period.

$C_{2nd,js}^{processing}$  refers to the operating costs in processing plants that is proportional to the amount of shale gas processed, given by:

$$C_{2nd,js}^{processing} = \sum_{i \in I} \sum_{p \in P} \sum_{t \in T} \frac{vp \cdot STP_{i,p,t,js}}{(1+dr)^t} \quad (7)$$

where  $STP_{i,p,t,js}$  denotes amount of shale gas transported from shale site  $i$  to processing plant  $p$  in time period  $t$  in scenario  $js$ ;  $vp$  is the unit processing cost for shale gas.

$C_{2nd,js}^{transportation}$  indicates the total transportation cost, including the transportation of shale gas from shale sites to processing plants and transportation of sales gas between processing plants and different end customers.

$$C_{2nd,js}^{transportation} = \sum_{i \in I} \sum_{p \in P} \sum_{t \in T} \frac{vtcs \cdot lsp_{i,p} \cdot STP_{i,p,t,js}}{(1+dr)^t} + \sum_{p \in P} \sum_{m \in M} \sum_{t \in T} \frac{vtcm \cdot lpm_{p,m} \cdot STPM_{p,m,t,js}}{(1+dr)^t} \quad (8)$$

where  $STPM_{p,m,t,js}$  denotes the amount of natural gas transported from processing plant  $p$  to end customer  $m$  in time period  $t$  in scenario  $js$ ;  $vtcs$  and  $vcm$  indicate unit variable transportation costs for pipeline transportation of shale gas and sales gas, respectively;  $lsp_{i,p}$  and  $lpm_{p,m}$  indicate the distance from shale site  $i$  to processing plant  $p$  and the distance from processing plant  $p$  to end customers  $m$ , respectively.

$I_{2nd,js}^{NGLs}$  denotes the income of selling NGL at processing plants, calculated by,

$$I_{2nd,js}^{NGLs} = \sum_{p \in P} \sum_{t \in T} \frac{pl_t \cdot PLS_{p,t,js}}{(1 + dr)^t} \quad (9)$$

where  $PLS_{p,t,js}$  denotes the amount of NGL sold at processing plant  $p$  in time period  $t$  in scenario  $js$ ;  $pl_t$  denotes the average unit price of NGL in time period  $t$ .

The total energy generation  $TEG_{2nd,js}$  corresponding to scenario  $js$  equals the summation of energy generated from different end customers, including the electric power consumption, industrial consumption, commercial consumption, and residential consumption, calculated by:

$$TEG_{2nd,js} = \sum_{m \in M} \sum_{t \in T} \sum_{js \in JS} ue_m \cdot ect \cdot \sum_{p \in P} STPM_{p,m,t,js} \quad (10)$$

where  $ue_m$  denotes the average energy utilizing efficiency at end customer  $m$ ;  $ect$  is the energy content of natural gas.

## 5.3.2 Constraints

### 5.3.2.1 Mass balance constraints

The total shale gas production rate at a shale site equals the sum of the individual production rates of the different wells. Therefore, the total shale gas production at each shale site in each time period can be calculated by:

$$SP_{i,t,js} = NN_i \cdot spp_{i,t} \cdot eur_{i,js}, \forall i, t, js \quad (11)$$

where  $spp_{i,t}$  denotes the shale gas production profile of a shale well at shale site  $i$  in time period  $t$ ; we use this time-dependent parameter to account for the decreasing feature of the shale gas production profile of a certain well [6, 116].  $eur_{i,js}$  is the parameter accounting for different EURs of the shale well at shale site  $i$  in scenario  $js$ .

The total amount of shale gas production at each shale site is equal to the total amount of shale gas transported to different processing plants,

$$SP_{i,t,js} = \sum_{p \in P} STP_{i,p,t,js}, \forall i, t, js \quad (12)$$

The total methane produced at a processing plant is equal to the methane composition of the total shale gas transported from different shale sites taking into account processing efficiency. The amount of NGLs produced at a processing plant is determined by similar equations.

$$\sum_{i \in I} STP_{i,p,t,js} \cdot pef \cdot mc_i = SPM_{p,t,js}, \forall p, t, js \quad (13)$$

$$\sum_{i \in I} STP_{i,p,t,js} \cdot pef \cdot lc_i = SPL_{p,t,js}, \forall p, t, js \quad (14)$$

where  $SPM_{p,t,js}$  is the amount of natural gas produced at processing plant  $p$  in time period  $t$  in scenario  $js$ ;  $pef$  is the processing efficiency in terms of raw shale gas;  $mc_i$  denotes the average methane composition in shale gas at shale site  $i$ ;  $SPL_{p,t,js}$  stands for the amount of NGLs produced at processing plant  $p$  in time period  $t$  in scenario  $js$ ;  $lc_i$  is the average NGL composition in shale gas at site  $i$ .

The total amount of natural gas produced at a processing plant is equal to the sum of natural gas transported from the processing plant to different end customers.

$$SPM_{p,t,js} = \sum_{m \in M} STPM_{p,m,t,js}, \forall p, t, js \quad (15)$$

### 5.3.2.2 Capacity constraints

The amount of shale gas transported by pipeline from shale site  $i$  to processing plant  $p$  is bounded by the capacity of pipelines, given by:

$$STP_{i,p,t,js} \leq \sum_{r \in R} TPC_{i,p,r}, \quad \forall i, p, t, js \quad (16)$$

The amount of natural gas transported by pipeline from processing plant  $p$  to end customer  $m$  is bounded by the capacity of pipelines, given by the following constraints:

$$STPM_{p,m,t,js} \leq \sum_{r \in R} TPMC_{p,m,r}, \quad \forall p, m, t, js \quad (17)$$

The total amount of shale gas from all the shale sites processed by each processing plant should not exceed its processing capacity,

$$\sum_{i \in I} STP_{i,p,t,js} \leq \sum_{r \in R} PC_{p,r}, \quad \forall p, t, js \quad (18)$$

The total amount of natural gas transported from all the processing plants to each end customer should meet their minimum demands,

$$dm_{m,t} \leq \sum_{p \in P} STPM_{p,m,t,js}, \quad \forall m, t, js \quad (19)$$

where  $dm_{m,t}$  denotes the minimum demand of natural gas at demand node  $m$  in time period  $t$ .

Similarly, the total amount of NGLs sold at all the processing plants is also bounded below by its minimum demand, given as:

$$dl_t \leq \sum_{p \in P} PLS_{p,t,js}, \quad \forall t, js \quad (20)$$

where  $dl_t$  denotes the minimum demand for NGLs in time period  $t$ .

### 5.3.2.3 Bounding constraints

The constraints for the capacity of pipeline transporting shale gas from shale site  $i$  to processing plant  $p$  are given by:

$$tprc_{r-1} \cdot XP_{i,p,r} \leq TPC_{i,p,r} \leq tprc_r \cdot XP_{i,p,r}, \forall i, p, r \geq 2 \quad (21)$$

Similarly, the constraints for the capacity of pipelines transporting natural gas are given by:

$$tprc_{r-1} \cdot XPM_{p,m,r} \leq TPMC_{p,m,r} \leq tprc_r \cdot XPM_{p,m,r}, \forall p, m, r \geq 2 \quad (22)$$

If a processing plant is established, its processing capacity should be bounded by the corresponding capacity range; otherwise, its capacity should be zero. This relationship can be modeled by the following inequality:

$$prc_{r-1} \cdot YP_{p,r} \leq PC_{p,r} \leq prc_r \cdot YP_{p,r}, \forall p, r \geq 2 \quad (23)$$

#### 5.3.2.4 Logic constraints

For the drilling issue of the shale well, we have the following logic constraints.

The total number of wells drilled all shale sites should satisfy the following constraint:

$$\sum_{i \in I} NN_i \geq tln, \forall i \quad (24)$$

where  $tln$  denotes the minimum total number of wells that are planned to be drilled in this project.

The total number of wells that can be drilled at shale site  $i$  over the planning horizon is bounded by:

$$NN_i \leq tmn_i, \forall i \quad (25)$$

where  $tmn_i$  denotes the maximum number of wells that can be drilled at shale site  $i$ .

For all the pipelines in this supply chain, we assume only one capacity range  $r$  can be chosen,

$$\sum_{r \in R} XP_{i,p,r} \leq 1, \forall i, p \quad (26)$$

$$\sum_{r \in R} XPM_{p,m,r} \leq 1, \forall p, m \quad (27)$$

Similarly, only one capacity range  $r$  can be selected for all processing plants.

$$\sum_{r \in R} YP_{p,r} \leq 1, \forall p \quad (28)$$

## 5.4 Solution approaches

Scenario-based stochastic programming models are often computationally demanding, because their model size will increase exponentially as the number of scenarios increases [202]. In this shale gas supply chain model, if we only consider 3 shale sites in total and 100 independent EUR scenarios for each of them, then there will be  $100^3 = 1,000,000$  scenarios in total. Moreover, the resulting problem is a large-scale two-stage SMILFP problem, which is known to be computationally challenging due to its combinatorial nature and pseudo-convexity [107]. Considering the complexity of this shale gas supply chain model, it is necessary to develop solution strategies to circumvent these computational challenges and improve solution efficiency.

### 5.4.1 Sample average approximation method

In this work, we consider a Sample Average Approximation (SAA) approach for the 2-stage stochastic programming problem [198]. As a common approach to reduce a scenario set to a manageable size, the basic idea of this approach is to generate a sample of the uncertain parameter (normally the parameters are assumed to be independent identically distributed) to approximate the original expected objective value by calculating the sample average. We use Monte Carlo methods to generate scenarios based on existing EUR data of 2,600 shale wells as reported in the Marcellus shale play [113, 200]. Oracle Crystal Ball [203] software is applied as the sample generator.

In the SAA approach, the number of scenarios is determined by the desired level of solution accuracy, which can be measured by the confidence interval of the optimal

solution. A well-controlled choice of the sample can significantly reduce the computational time and improve the accuracy of optimal solutions. In this work, we determine the proper sample size following the framework given in Figure 48 [196].

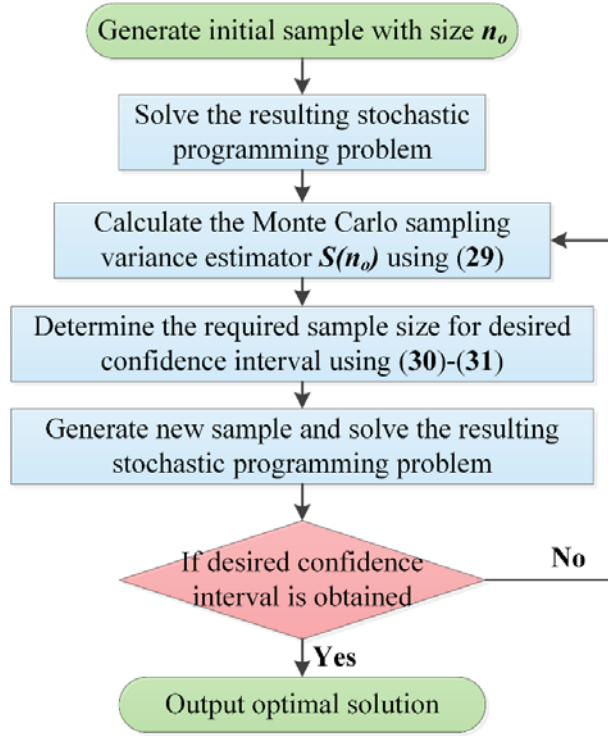


Figure 48. Flowchart on determining the sample size.

As can be seen in Figure 48, to determine the “optimal” number of scenarios  $N^*$ , we first solve the stochastic programming problem with a small initial sample size  $n_0$  (e.g. 10-100). Based on the optimal solutions obtained, we can then calculate the Monte Carlo sampling variance estimator  $S(n_0)$  using the following equation:

$$S(n_0) = \sqrt{\frac{\sum_{s=1}^{n_0} (E(LCOE) - LCOE_s)^2}{n_0 - 1}} \quad (29)$$

where  $LCOE$ , as mentioned before, is the levelized cost of energy generated from shale gas, i.e. our objective value, and  $LCOE_s$  corresponds to scenario  $s$ . Based on this

sampling variance estimator, we are able to calculate the confidence interval of  $1-\alpha$ , given as:

$$\left[ E(LCOE) - \frac{z_{\alpha/2} S(n_0)}{\sqrt{n_0}}, E(LCOE) + \frac{z_{\alpha/2} S(n_0)}{\sqrt{n_0}} \right] \quad (30)$$

where  $z_{\alpha/2}$  is the standard normal deviation such that  $1-\alpha/2$  satisfies a standard normal distributed variable  $z \sim N(0,1)$ ,  $Pr(z \leq z_{\alpha/2}) = 1-\alpha/2$ . For example, if we consider a 98% confidence interval ( $1-\alpha = 98\%$ ), then  $z_{\alpha/2} = 2.06$ .

Given the sampling variance estimator  $S(n_0)$  and the desired confidence interval  $H$ , we can calculate the minimum number of required scenarios by the following equation:

$$N^* = \left[ \frac{z_{\alpha/2} S(n_0)}{H} \right]^2 \quad (31)$$

Based on the minimum number of scenarios obtained above, we update the sample size and then solve the new stochastic programming problem again following the same strategy. A verifying step is added to make sure the required confidence interval is achieved after solving the updated stochastic programming problem. If this stopping criterion is satisfied, the corresponding optimal solution is taken as a good approximation of the exact optimal solution of the original stochastic programming problem [196, 199].

In this work, by setting an initial sample size of 100 scenarios and considering a 98% confidence interval, we finalize the required number of scenarios as 300. In Figure 49, a comparison between the exact EUR distribution data derived from literature [113] and that from sample approximation is presented.

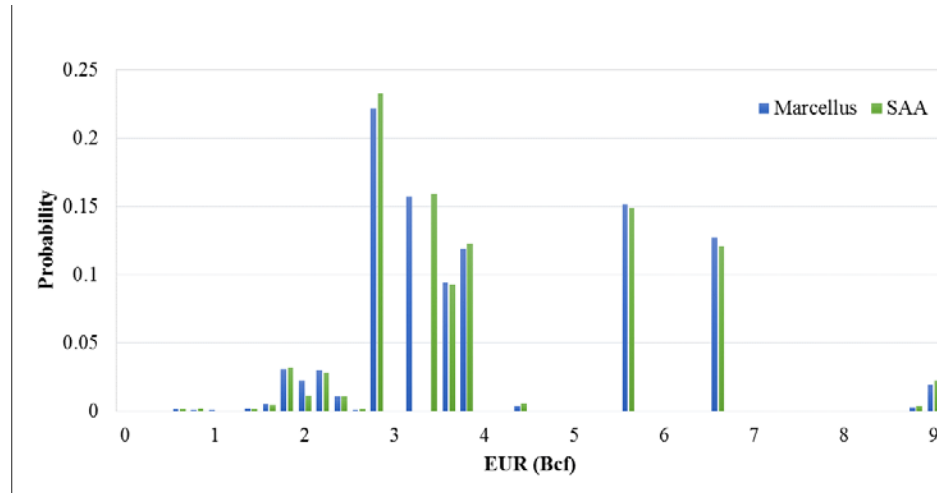


Figure 49. Comparison of EUR distribution between exact data for Marcellus derived from literature and data from sample average approximation.

As can be seen, the SAA approach provides an excellent approximation of the original EUR distribution. In addition, suppose we consider 100 discrete EUR scenarios for each of the 10 shale sites, the total number of scenarios would be  $100^{10}$  ( $\sim 10^{20}$ ). By applying the SAA technique, a sample size of around 300 is enough to find the optimal solution with 98% possibility. However, we note that the resulting stochastic program is still a large-scale two-stage SMILFP problem that can be challenging to solve. In the following section, we introduce a novel algorithm taking advantage of the special structure of the problem to tackle the resulting SMILFP problem.

#### 5.4.2 A novel optimization algorithm

SMILFP is a specially class of MINLP that includes both fractional objective resulting from MILFP and L-shaped constraints due to the stochastic programming formulation. The large-scale two-stage stochastic programming problem is difficult to solve [202, 204]. Moreover, it is known that global optimization of MILFP problems can be

computationally intractable because of their combinatorial nature and pseudo-convexity [6, 151, 205]. Consequently, as a combination of these two types of challenging optimization problems, the resulting two-stage SMILFP problem is not expected to be solved efficiently by any off-the-shelf solvers. By exploiting the problem structure, we propose a novel and efficient optimization algorithm that combines the parametric approach as well as the L-shaped method as an effective way to tackle this difficult problem. In this work, we first apply the parametric algorithm based on the exact Newton's method to circumvent the computational challenge resulting from the fractional objective function [107]. As a result, a parameter  $uc$  is introduced to replace the fractional objective function with a linear parametric function, and the original SMILFP problem is transformed to a set of stochastic mixed-integer linear programming (SMILP) subproblems targeting on finding the optimal value of  $uc$ . In order to further improve the computational efficiency, the resulting two-stage SMILP subproblem is solved using the L-shaped method [196, 206, 207]. To provide a comprehensive idea of this algorithm, a flowchart of this novel solution algorithm is given at first. Afterwards we present the general-form model formulation and solution strategies. At last, a pseudo-code of this novel solution algorithm is provided. The detailed model formulations of dual-subproblems and the corresponding cutting planes are included in Appendix B.

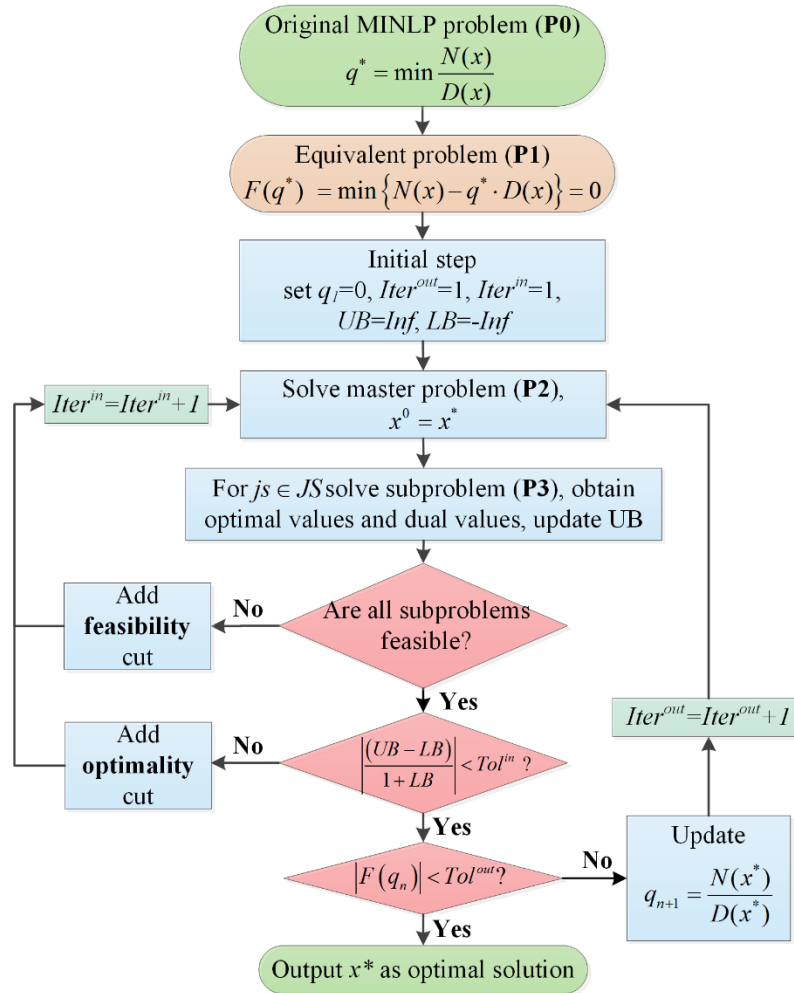


Figure 50. Flowchart of the solution algorithm integrating parametric approach and L-shaped method.

The whole solution algorithm is summarized in Figure 50. As can be seen, this solution algorithm integrates the parametric algorithm and the L-shaped method through the inner and outer loops. In the outer loop, we apply the parametric algorithm to transform the original SMILFP problem to an equivalent parametric SMILP problem. In the inner loop, L-shaped method is used to tackle the two-stage SMILP problem. Based on the solution of each subproblem corresponding to different scenarios considered, we are able to updates either optimality cuts or feasibility cuts to the master problem, thus

updating the  $LB$  and  $UB$  in the inner loop. Once the inner loop converges, the parameter  $uc$  can be updated, which leads to the next outer iteration.

Next, we consider a general form of the SMILFP model formulation **(P0)** to illustrate this solution approach in detail.

$$\text{(P0)} \quad \min_{x, y_s} \frac{c^T x + \sum_{s \in S} p_s q_s^T y_s}{\sum_{s \in S} p_s r_s^T y_s} \quad (32)$$

$$\text{s.t.} \quad Ax = b, \quad x \geq 0 \quad (33)$$

$$Wy_s = h_s - T_s x, \quad y_s \geq 0, \quad s \in S \quad (34)$$

First, by applying parametric algorithm, **(P0)** can be transformed into the following parametric form **(P1)**:

$$\text{(P1)} \quad \min_{x, y_s} F(uc) = c^T x + \sum_{s \in S} p_s q_s^T y_s - uc \cdot \sum_{s \in S} p_s r_s^T y_s \quad (35)$$

$$\text{s.t.} \quad Ax = b, \quad x \geq 0 \quad (36)$$

$$Wy_s = h_s - T_s x, \quad y_s \geq 0, \quad s \in S \quad (37)$$

then the target is to find a parameter  $uc$  such that  $F(uc) = 0$  [107]. Since  $F(uc)$  does not have a closed-form analytical expression, we can apply a numerical root finding method, namely the exact Newton's method, to solve the subproblem and update the parameter  $uc$ .

Because **(P1)** is an SMILP problem, we can apply the well-known L-shaped method and solve the resulting two-stage SMILP [208, 209]. The corresponding master problem and subproblem are given as follows:

**Master Problem:**

$$(P2) \quad \min_{x, y_s} c^T x + \theta \quad (38)$$

$$\text{s.t.} \quad Ax = b, \quad x \geq 0 \quad (39)$$

$$\theta \geq e_o x + d_o, \quad o = 1 \dots N \quad (40)$$

$$e_f x + d_f \leq 0, \quad o = 1 \dots N' \quad (41)$$

**Subproblem:**

$$(P3) \quad \min_{x, y_s} F(uc) = \sum_{s \in S} p_s q_s^T y_s - uc \cdot \sum_{s \in S} p_s r_s^T y_s \quad (42)$$

$$\text{s.t.} \quad Wy_s = h_s - T_s x, \quad y_s \geq 0, \quad s \in S \quad (43)$$

where the inequalities (40) and (41) in **(P2)** are “optimality cuts” and “feasibility cuts”, respectively that link the master problem and the subproblem;  $e_o$ ,  $d_o$ ,  $e_f$  and  $d_f$  are coefficients for the Benders cut, which can be calculated based on the solution to the corresponding subproblems. In each inner iteration of the L-shaped method, we first solve the master problem to obtain the initial first-stage decisions. These design decisions are then fixed in the solution of subproblems. Corresponding optimality cuts and feasibility cuts are generated following the above formulations. Depending on the solution of all the subproblems, we update the cut planes in the master problem and go to the next iteration. Detailed formulation of these equations are provided in Appendix B. To better illustrate the proposed solution algorithm, a pseudo-code is given in the following Figure 51.

---

**Global Optimization Algorithm**

---

```
1:  $uc \leftarrow 0, Iter^{out} \leftarrow 1,$   
2: while ( $F(uc) \geq Tol^{out}$ ) do  
3:    $Iter^{out} \leftarrow Iter^{out} + 1$   
4:    $LB \leftarrow -\infty, UB \leftarrow +\infty, Iter^{in} \leftarrow 1, Gap \leftarrow +\infty$   
5:   Solve (P2) to obtain initial first-stage decisions  
6:   while ( $Gap \geq Tol^{in}$ ) do  
7:      $Iter^{in} \leftarrow Iter^{in} + 1$   
8:     while ( $terminate = false$ ) do  
9:       Scenario  $s \leftarrow s+1$   
10:      Solve (P3) with given first-stage decisions  
      if ((P3) of scenario  $s$  is feasible) then  
        Generate optimality cut:  $\theta \geq e_o x + d_o$   
11:      else  
        Generate feasibility cut:  $e_f x + d_f \leq 0$   
      end if  
      if  $count(s) \geq |S|$  then  
12:         $terminate \leftarrow true$   
      end if  
13:    end while  
    if (all the (P3) are feasible) then  
      Add  $\theta \geq e_o x + d_o$  to (P2), update  $UB$   
14:    else  
      Add  $e_f x + d_f \leq 0$  to (P2)  
    end if  
15:    Solve (P2) with updated cuts  
16:    Update  $LB$   
17:  end while  
18:  Update parameter  $uc$   
19: end while  
20: Output  $uc^*$  as global optimal value
```

---

Figure 51. Pseudo-code of the global optimization algorithm.

## 5.5 Results and discussion

In order to illustrate the applicability of the proposed model and solution strategy, one specific case study based on the Marcellus shale play is considered in this work. A detailed description of this problem is given below. It is worth noting that the proposed modeling framework and optimization algorithm are general enough, so their application is not limited to any specific case study region. Moreover, to illustrate the practicality of the proposed SMILFP model, we consider a traditional SMILP model that minimizes the total cost for comparison. The corresponding results are summarized in Appendix D.

In this case study, a total of 10 potential shale sites are considered, and each of them can drill up to 4 to 8 shale wells at maximum [112]. All the drilling decisions are made at the beginning of the planning horizon. An exponentially decreasing approximation of the shale gas production profile is considered, which is a function of time and given in Appendix A [116]. There are 3 potential shale gas processing plants. Four types of end customers of shale gas are considered, including power plants, industrial customers, commercial customers, and residential customers. The capital investment of processing plants and pipelines are evaluated using a piecewise approximation approach, and 4 capacity ranges are considered with respect to corresponding design decisions. The total planning horizon is 10 years, which is close to the real lifetime of shale wells, and it is divided into 10 time periods (one year per time period) [116, 210]. In this work, we adopt a 10% discount rate for each year [121]. All the detailed input data are based on existing literature and given in Appendix A. The resulting problem has 174,375

continuous variables (Stage I: 180; Stage II: 174,195), 190 discrete variables (Stage I: 190; Stage II: 0), and 249,421 (Stage I: 433; Stage II: 248,988) constraints. All of the models and solution procedures are coded in GAMS 24.4.1 [122] on a PC with an Intel® Core™ i5-2400 CPU @ 3.10GHz and 8.00 GB RAM, running Window 8, 64-bit operating system. Furthermore, the MILP problems are solved using CPLEX 12.6. The absolute optimality tolerance for all solvers is set to  $10^{-6}$ . The optimality tolerance for the inner loop in the proposed global optimization method is set to  $10^{-2}$ , and the optimality tolerance for the outer loop is set to  $10^{-3}$ .

### 5.5.1 Computational results

As discussed in the solution approach section, we propose a novel global optimization algorithm to tackle this two-stage SMILFP problem, which integrates the parametric algorithm as well as the L-shaped method. By applying the parametric algorithm, we are able to circumvent the fractional-form objective and solve an MILP problem instead. In each iteration of the outer loop, the introduced parameter  $uc$  is updated. Meanwhile, the inner loop of this algorithm consists of the L-shaped method. Through a set of iterations between the master problem and subproblem, the lower bound and upper bound keep updating until the final stopping criterion is satisfied. In this work, we choose CPLEX as the MILP solver, and the initial value of  $uc$  is set to 0. We note that general-purpose global MINLP solvers, namely BARON and SBB, cannot return any feasible solution to this problem within 10 hours, so we only present the computational results of the proposed solution algorithm. In Figure 52, we explicitly present the converging process of this algorithm as it solves the case study.

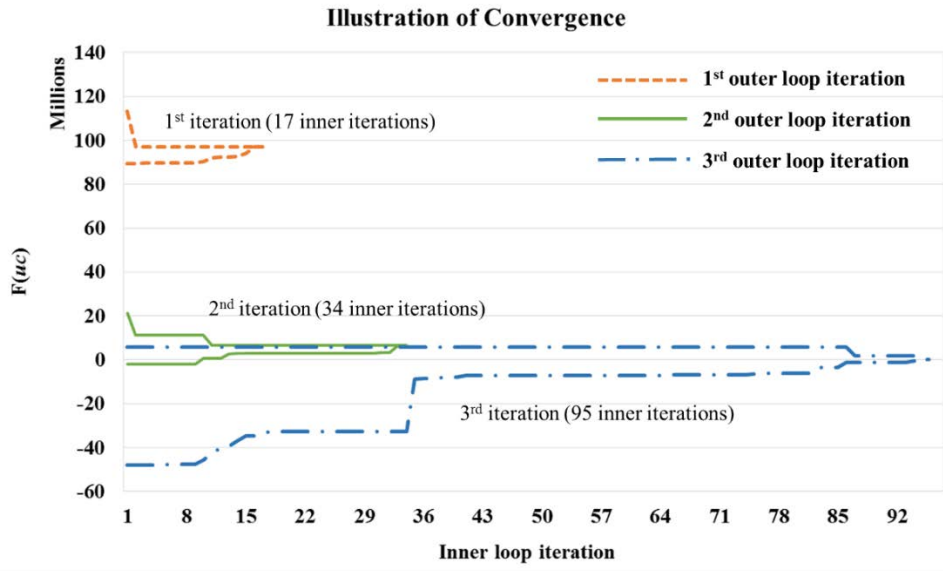


Figure 52. Converging process of the proposed algorithm.

The total computational time is 1,590 CPU seconds, and there are a total of three outer loop iterations corresponding to the parametric algorithm. In the first outer loop iteration, the L-shaped method takes 17 inner iterations to converge. In the second outer loop iteration, where the parameter  $uc$  is updated, the L-shaped method takes 34 inner iterations to converge. In the third outer loop iteration, 95 inner iterations are required for the L-shaped method to converge to the optimal value of parameter  $uc^*$ , such that  $F(uc^*)$  is smaller than the optimality tolerance. It is worth noting that as the value of the parametric objective function approaches the optimal value, more inner iterations are required to converge to the specified tolerance.

## 5.5.2 Optimization results

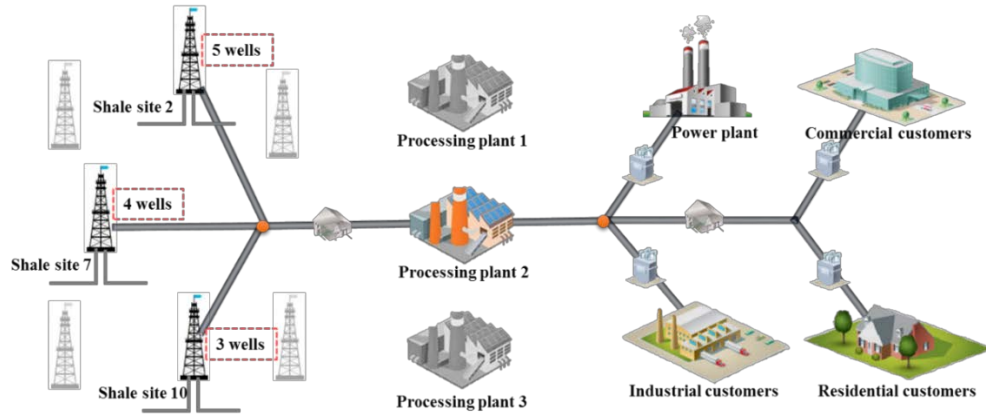


Figure 53. Optimal design of shale gas supply chain network under EUR uncertainty. As can be seen in Figure 53, we present the optimal design of the shale gas supply chain under EUR uncertainty. The overall trend is to build a centralized supply chain network. Instead of drilling evenly in more shale sites with less shale wells for each site, only 3 shale sites, namely shale site 2, shale site 7, and shale site 10, are selected among the 10 potential shale sites as the optimal shale gas producers. A total of 12 shale wells are drilled, of which 5 wells are assigned to shale site 2, 4 wells are assigned to shale site 7, and 3 wells are assigned to shale site 10. By exploring the possible reasons, we find that: firstly, the chosen shale sites 2, 7 and 10 have relatively higher average EUR considering the given sample data. In addition, the distances between the aforementioned shale sites and processing plant 2, which is planned to be constructed, are relatively shorter. Therefore, we conclude that the final selection of these shale sites is a decision based on simultaneous considerations of both EUR and transportation factors. As a result, more shale gas is expected to be produced under a fixed drilling, fracturing, and completion cost. Moreover, the corresponding transportation investment as well as operating cost can be reduced to some extent. Similar to the drilling decisions, only one

of the three potential shale gas processing plants is constructed with a large processing capacity, given as 22.8 Billion Standard Cubic Feet per year (Bscf/year). Although it might be possible to reduce the overall transportation cost by building more processing plants with smaller sizes considering the relative position of shale sites and processing plants, the overall capital investment of processing plants is expected to be greater due to the economies of scale, and more importantly, uncertain shale gas production for each shale site. To summarize, we conclude that a single, large size processing plant is a more reliable and economical choice under EUR uncertainty.

In order to illustrate the value of our stochastic programming model, we present the results of the Expected Value of Perfect Information (EVPI) and the Value of the Stochastic Solution (VSS) [208]. The EVPI measures the maximum price a decision maker would be ready to pay in return for complete and accurate information about the future (i.e. the exact EUR data in this work). To calculate the EVPI, we solve each scenario in isolation and then compute the average of the individual optimal solutions. This value is known as the average performance in case of perfect information. The EVPI is defined as the difference between the average performance with perfect information and the optimal stochastic solution. On the other hand, The VSS shows the superiority of the optimal stochastic solution over that of a single deterministic model with all uncertainties replaced by their expected values. To obtain the VSS, we solve the deterministic model where all EUR parameters are replaced by their expectations, and then we evaluate that solution (fixing all design decisions) against all the scenarios, and compute its average performance. The VSS is defined as the difference between the

optimal stochastic solution and the average performance of the deterministic solution. The results are given in Figure 54.

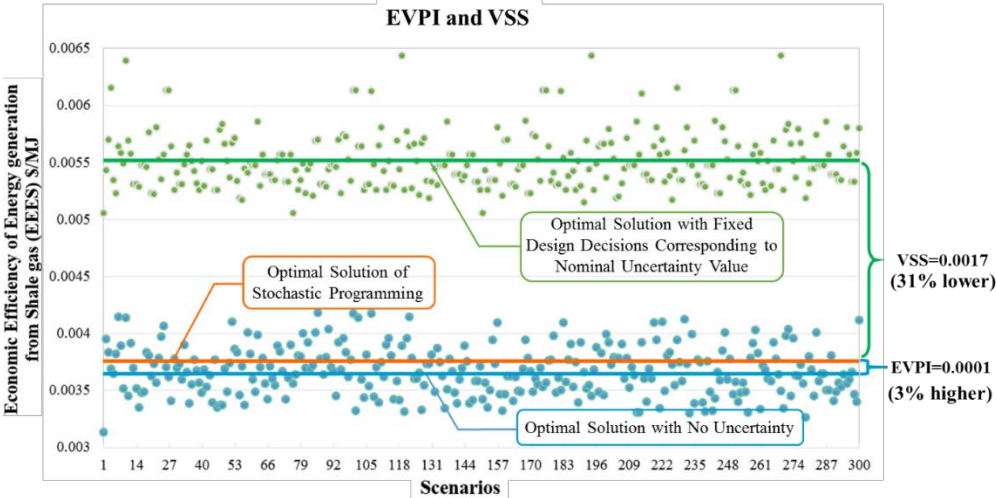
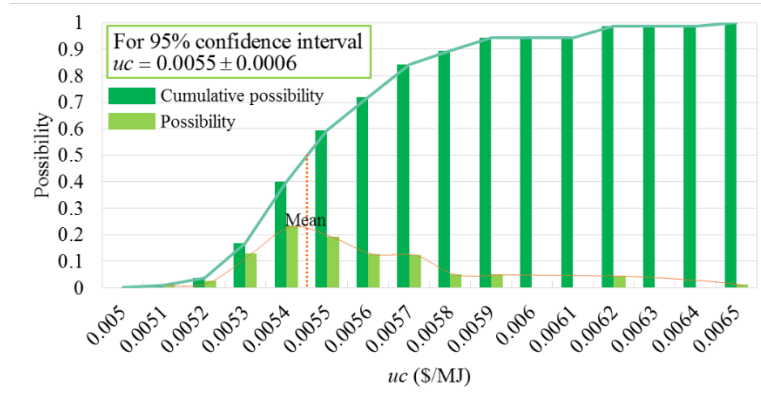


Figure 54. Results of EVPI and VSS with 300 scenarios considered.

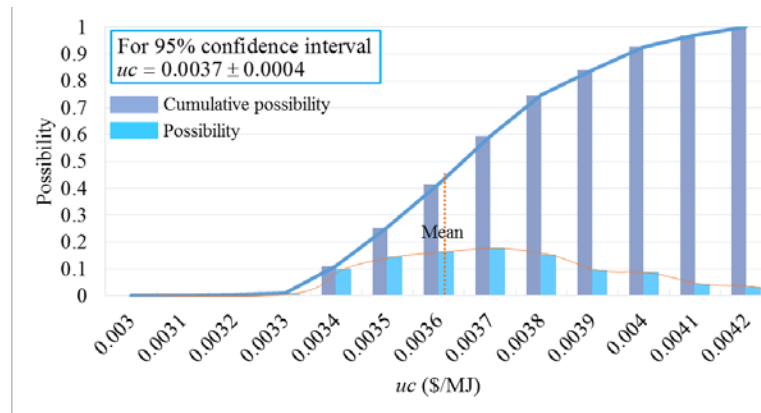
As shown in Figure 54, the orange line is the objective value obtained by solving the SMILFP problem, which is \$0.0038/MJ. The green dots indicate the exact objective values obtained with fixed design decisions from the deterministic model. Depending on the exact scenarios, the deviation can be significant, leading to the conclusion that EUR uncertainty does pose great impacts on the final economic efficiency of a shale gas supply chain. The green line crossing these green dots shows the average performance of the deterministic model, which is \$0.0055/MJ. Similarly, the blue dots are the objective values obtained with perfect information (no uncertainty) on EUR for all scenarios, and the corresponding blue line shows the average performance in case of perfect information, which is \$0.0037/MJ. We notice a smaller spread of the blue dots compared with that of the green dots, which indicates that improper design decisions from deterministic models will exaggerate the impacts of uncertain EUR on economic performance. Based on these values, we calculate the EVPI and VSS as \$0.0001/MJ and

\$0.0017/MJ, respectively. The stochastic programming model certainly shows great potential to improve the overall economic performance of shale gas supply chain over a deterministic one: the *LCOE* is improved by over 30%. Additionally, the stochastic programming model performs quite well even compared with the perfect information model, of which the *LCOE* is only 3% less.

In Figure 55, we rearrange the results of the green and blue dots to present the corresponding possibility distributions to better present the solutions from both the deterministic model and the model with perfect information. In addition, we present the drilling schedule and the supply chain design corresponding to the deterministic model for a better comparison, included in Appendix C.



(a) Possibility distribution of solution with fixed design corresponding to deterministic model



(b) Possibility distribution of solution with perfect information

Figure 55. Possibility distribution of solutions from (a) deterministic model with nominal uncertainty value and (b) model with perfect information.

From the comparison, we conclude that when EUR uncertainty are taken into account, the deterministic model based on nominal values will result in significant variance of economic performance depending on the exact realization of uncertainty, and the average economic performance is much worse than that of stochastic model (30% higher *LCOE*). Moreover, it is impressive to see that the stochastic model can provides an optimal solution whose average performance is very close to the ideal one with perfect

information (3% lower *LCOE*). Therefore, it is proven to be of great importance to account for the EUR uncertainty when conducting shale gas supply chain optimization. In the rest of this section, we focus on analyzing the optimal solutions obtained from the stochastic programming problem. One important concern is about the shale gas flow through the shale gas supply chain network. In Figure 56, we use a Sankey diagram to visualize the flow of shale gas within this shale gas supply chain network. As can be seen, with different shale wells drilled, shale sites 2, 7, and 10 produce different amounts of shale gas. Approximately 19.9 Bscf of shale gas is expected to be produced at shale site 2, 15.0 Bscf of shale gas is expected to be produced at shale site 7, and 11.7 Bscf at shale site 10. A total of 46.6 Bscf of shale gas is transported to processing plant 2 via pipeline. After being processed and separated, the sales gas is transported to different end customers, while NGLs are sold to nearby market. According to the optimal results, 3.2% of the natural gas is sent directly to power plants for electricity generation; 4.2% of the natural gas is transported to industrial customers; 70.4% of the natural gas is transported commercial customers, and 22.1% of the natural gas is sent to residential customers. The decision on the final distribution of natural gas involves comprehensive consideration of product transportation as well as the average energy generation efficiency corresponding to different end customers.

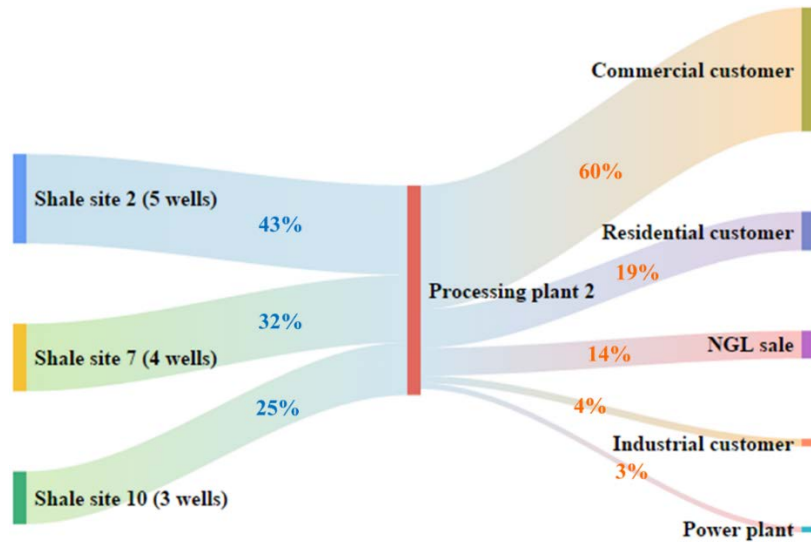


Figure 56. Sankey diagram of shale gas flow in the supply chain network.

The overall cost distribution is summarized in Figure 57, in which the total expected cost is classified into two categories, namely capital investment and operating cost, and further analyzed corresponding to different processes within this shale gas supply chain. A total cost of \$275.1 million is expected over this planning horizon, of which 61.0% is the operating cost, including \$2.9 million spent on transportation, \$121.1 million on shale gas processing, and \$43.8 million on the shale gas production. The remaining 39% of the total cost is capital investment, of which \$18.9 million is spent on pipeline installation, \$55.0 million is contributed to construction of processing plants, and \$33.4 million is for well drilling activities. The detailed cost breakdowns are given in the pie-charts as shown below. From this cost breakdown, we conclude that shale gas production and processing account for the major operating costs, and decisions on construction of processing plants and drilling activities lead to the greatest capital investment. Correspondingly, the variables related to these activities are expected to be the key drivers for operating cost and capital invest.

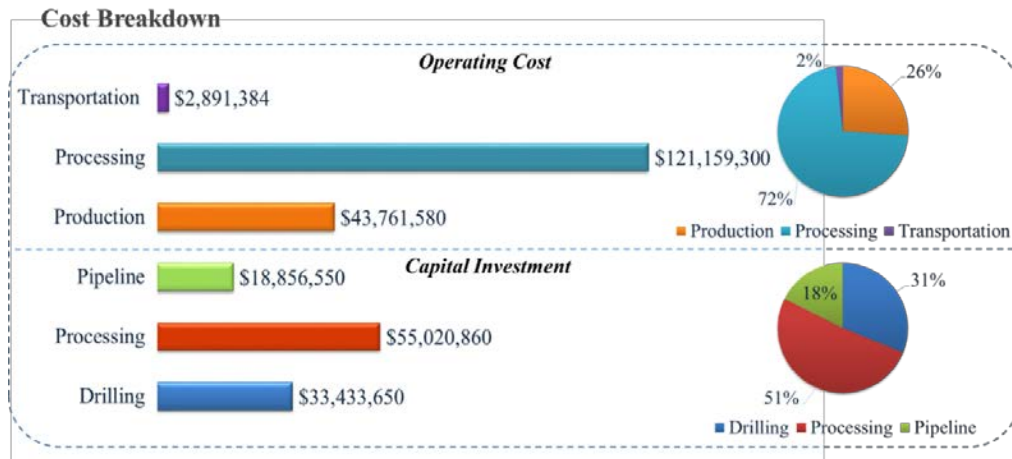


Figure 57. Cost breakdown regarding capital investment and operating cost.

## 5.6 Summary

To the best of our knowledge, this is the first work that systematically addresses the optimal design and operations of shale gas supply chains under uncertainty. A scenario-based two-stage stochastic programming model was developed as a large-scale SMILFP problem. The objective was to optimize the levelized cost of energy generated from shale gas. All of the design decisions are made in the master problem, including drilling schedule, decisions on construction of processing plants, and corresponding pipeline designs. Meanwhile, recourse operating decisions are made in subproblems corresponding to different EUR sampling data, including the shale gas production, planning on shale gas processing, and distribution to end customers. To solve this computationally challenging problem efficiently, we applied the sample average approximation method and proposed a novel algorithm integrating the parametric algorithm and the L-shaped method to take advantage of the model structure. One case study based on the Marcellus shale play was presented to illustrate the applicability of

the proposed modeling framework and solution algorithm. The results indicated that the stochastic programming model was a superior choice for determining the optimal economic performance of a shale gas supply chain under EUR uncertainty. The shale gas production and processing activities account for the major operating costs, and decisions on construction of processing plants and drilling activities lead to the greatest capital investment. It is worth noting that the proposed model and solution approaches could be easily extended to consider other uncertainties, such as prices, demands, and property parameters.

## 5.7 Appendix A

In this section, we provide the input data of the Case Studies Section.

Table A1. Input Data for the Case Studies.

Parameter	Indices	Value	Reference
$dl_t$ (Mscf/year)	-	2,000-3,000	[211]
$dm_{m,t}$ (Mscf/year)	$m1$	87,934-107,474	[211]
	$m2$	50,011-61,125	
	$m3$	34,258-41,871	
	$m4$	55,699-68,076	
$ect$ (MJ/Mscf)	-	1,105	[212]
$eur_{i,js}$	-	2.46-49.79	[1, 113]
$lc_i$	-	0.05-0.15	[116]
$lpm_{p,m}$ (mile)	-	5-30	[116]
$lsp_{i,p}$ (mile)	-	5-30	[116]

$mc_i$	-	0.85-0.95	[116]
$pef$	-	0.97	[116]
$pl_t$ (\$/Mscf gas)	-	20-40	[213]
$prc_r$ (Mscf/year)	$r1$	12,000,000	
	$r2$	120,000,000	[49]
	$r3$	1,200,000,000	
$pri_r$ (\$)	$r1$	40,326,500	
	$r2$	160,542,690	[49]
	$r3$	639,131,600	
$sdci$ (\$/well)	-	270,000-292,000	[19]
$spc_{i,t}$ (\$/Mscf)	-	1.2-1.4	[19]
$spp_{i,\tau}$ (Mscf/year)	-	$spp_{i,\tau} = a \cdot t^b$ ; $a: 16,000-18,000$ ; $b:-$	[116]
		0.37	
$tl_n$	-	12	[112, 211]
$tmn_i$	-	4-8	[112]
$tprc_r$ (Mscf/year)	$r1$	64,094	
	$r2$	402,213	
	$r3$	2,600,166	[116]
	$r4$	16,809,161	
$tpri_r$ (Mscf/year)	$r1$	45,954	
	$r2$	138,327	[116]
	$r3$	423,871	

	<i>r4</i>	1,297,056	
	<i>m1</i>	0.50	
<i>ue<sub>m</sub></i>	<i>m2</i>	0.64	[214-216]
	<i>m3</i>	0.80	
	<i>m4</i>	0.76	
<i>vp</i> (\$/Mscf)	-	3.6	[49]
<i>vtcm</i> (\$/Mscf)	-	0.003	[19, 116]
<i>vtcs</i> (\$/Mscf)	-	0.003	[19, 116]

## 5.8 Appendix B

In this work, we propose a novel solution algorithm integrating parametric approach and L-shaped method to tackle the two-stage SMILFP problem. In the inner loop of this novel algorithm, a classical L-shaped method is implemented. By solving the dual-problem of the original subproblem in the inner iteration, we are able to obtain the corresponding Benders cut and update solution to the master problem. In this section, we present the detailed model formulation of both the dual-subproblem and Benders cuts:

$$\begin{aligned}
\max f_{sub} = & \sum_{i \in I} \sum_{t \in T} NN_{i,t}^{fix} \cdot eur_{i,j_s} \cdot spp_{i,t} \cdot umb1_{i,t} \\
& - \sum_{i \in I} \sum_{p \in P} \sum_{t \in T} \sum_{r \in R} TPC_{i,p,r}^{fix} \cdot vcp1_{i,p,t} \\
& - \sum_{p \in P} \sum_{m \in M} \sum_{t \in T} \sum_{r \in R} TPMC_{p,m,r}^{fix} \cdot vcp2_{p,m,t} \\
& - \sum_{p \in P} \sum_{t \in T} \sum_{r \in R} PC_{p,r}^{fix} \cdot vcp3_{p,t} \\
& + \sum_{m \in M} \sum_{t \in T} dm_{m,t} \cdot vcp4_{m,t} \\
& + \sum_{t \in T} dl_t \cdot vcp5_t
\end{aligned} \tag{44}$$

$$\text{s.t. } umb1_{i,t} + umb2_{i,t} \leq \frac{spc_{i,t}}{(1+dr)^t} \quad (45)$$

$$-umb4_{p,t} + vcp5_t \leq -\frac{pl_t}{(1+dr)^t} \quad (46)$$

$$-umb3_{p,t} + umb5_{p,t} \leq 0 \quad (47)$$

$$-umb2_{i,t} + pef \cdot mc_i \cdot umb3_{p,t} + pef \cdot lc_i \cdot umb4_{p,t} - vcp1_{i,p,t} - vcp3_{p,t} \leq \frac{vp + vtcs \cdot lsp_{i,p}}{(1+dr)^t} \quad (48)$$

$$umb6 \leq -uc \quad (49)$$

Where  $umb1_{i,t}$ ,  $umb2_{i,t}$ ,  $umb3_{p,t}$ ,  $umb4_{p,t}$ ,  $umb5_{p,t}$ ,  $umb6$  are dual variables corresponding to original mass balance constraints (11), (12), (13), (14), (15), and (10), respectively. Similarly,  $vcp1_{i,p,t}$ ,  $vcp2_{p,m,t}$ ,  $vcp3_{p,t}$ ,  $vcp4_{m,t}$ ,  $vcp5_t$  are dual variables corresponding to original capacity constraints (16), (17), (18), (19), and (20), respectively. After solving the subproblem, the corresponding optimality cut and feasibility cut can be calculated by the following equations:

*Optimality Cut:*

$$\begin{aligned} \theta \geq & \sum_{m \in M} \sum_{t \in T} dm_{m,t} \cdot vcp4_{m,t}^{fix} + \sum_{m \in M} \sum_{t \in T} dl_t \cdot vcp5_t^{fix} + eur_{i,j_s} \cdot spp_{i,t} \cdot umb1_{i,t}^{fix} \cdot NN_i \\ & - vcp1_{i,p,t}^{fix} \cdot TPC_{i,p,r} - vcp2_{p,m,t}^{fix} \cdot TPMC_{p,m,r} - vcp3_{p,t}^{fix} \cdot PC_{p,r} \end{aligned} \quad (50)$$

*Feasibility Cut:*

$$\begin{aligned} & \sum_{m \in M} \sum_{t \in T} dm_{m,t} \cdot vcp4_{m,t}^{fix} + \sum_{m \in M} \sum_{t \in T} dl_t \cdot vcp5_t^{fix} + eur_{i,j_s} \cdot spp_{i,t} \cdot umb1_{i,t}^{fix} \cdot NN_i \\ & - vcp1_{i,p,t}^{fix} \cdot TPC_{i,p,r} - vcp2_{p,m,t}^{fix} \cdot TPMC_{p,m,r} - vcp3_{p,t}^{fix} \cdot PC_{p,r} \leq 0 \end{aligned} \quad (51)$$

By adding these newly generated cuts to the master problem, we can solve the updated master problem to obtain an updated solution, which further leads to the updates of lower and upper bounds for this two-stage SMILFP problem.

## 5.9 Appendix C

In this section, we present the detailed design decisions obtained by solving the deterministic model, which is given by the following Figure C1.

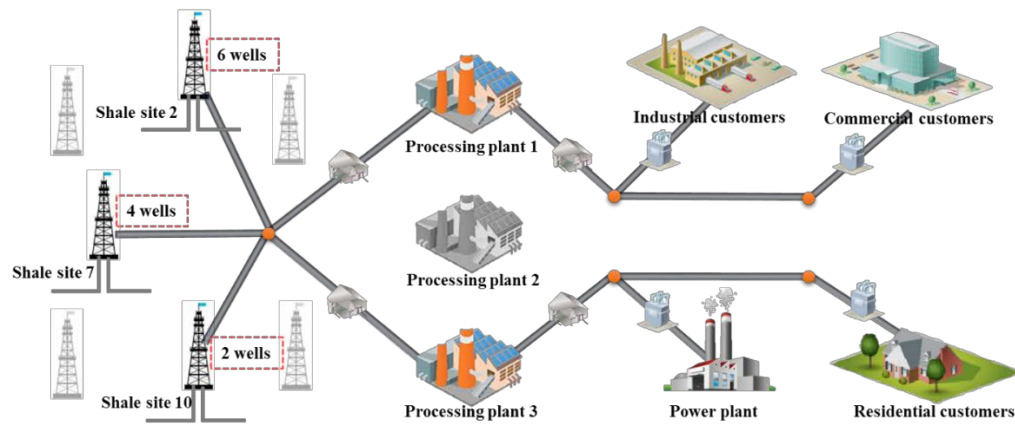


Figure C1. Optimal design of shale gas supply chain network for deterministic model.

As can be seen in Figure C1, though the same shale sites are chosen, the number of wells being drilled in each shale site is different. The main difference regarding the design decisions is on the construction of the processing plants. In the two-stage SMILFP model, only processing plant 2 is constructed, while in the deterministic model, both processing plant 1 and processing plant 3 are constructed with 5.0 Bscf/year and 5.2 Bscf/year processing capacity, respectively. As a result, the downstream distribution of natural gas is different. Natural gas from processing plant 1 will be transported to industrial and commercial customers for end use. Meanwhile, processing plant 3 targets on satisfying the demand of power plants and residential customers. The different design

decisions of deterministic model result in the sacrifice of economic efficiency when the EUR uncertainty is taken into account, causing a 31% higher unit cost of energy in the deterministic model than the stochastic programming one.

### 5.10 Appendix D

In this section, we summarize the difference between solutions from the proposed SMILFP model and that from a SMILP model. The objectives of them are minimizing the *LCOE* generated from shale gas and minimizing the total cost, respectively. A similar optimal shale gas supply chain network can be obtained from this SMILP model, as shown in Figure D1.

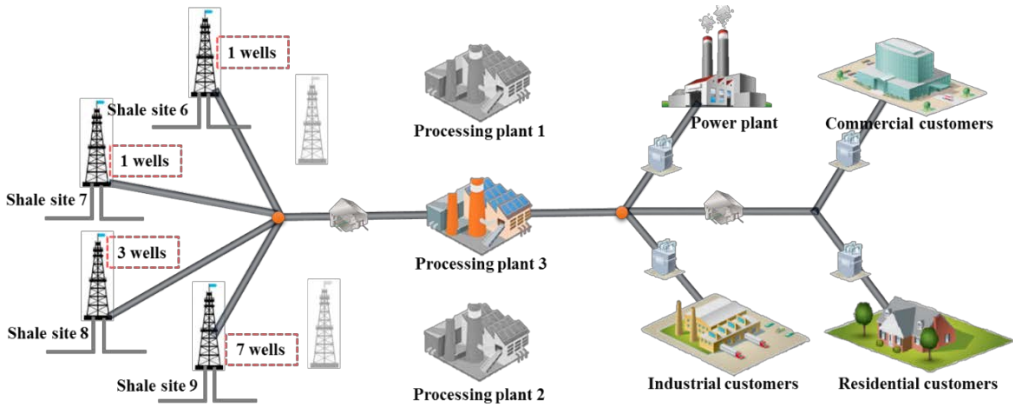


Figure D1. Optimal design of shale gas supply chain network under EUR uncertainty for SMILP model.

As can be seen, the major difference is about the drilling schedule. Shale sites 6, 7, 8 and 9 are chosen for shale gas production, and up to 7 wells are drilled in shale site 9. In the SMILFP model, the processing plant 3 is constructed with identical capacity to processing plant 2 as in the SMILFP model. Although the total cost of the SMILP model

is 2.2% lower due to a 9.6% reduction in shale gas production, the corresponding *LCOE* is \$0.0041/MJ, 11% higher than \$0.0037/MJ obtained from SMILFP model.

The expected shale gas flow is presented in a similar Sankey diagram as shown in Figure D2. As can be seen, since in the SMILP model, the only objective is minimizing the total cost without considering economic efficiency. Thus, almost all of the natural gas is transported to the nearest customer, known as industrial customer in this specific case study, to save corresponding transportation cost and investment. Obviously, a more balanced end-use distribution of natural gas can be obtained by solving the SMILFP model against the SMILP one.

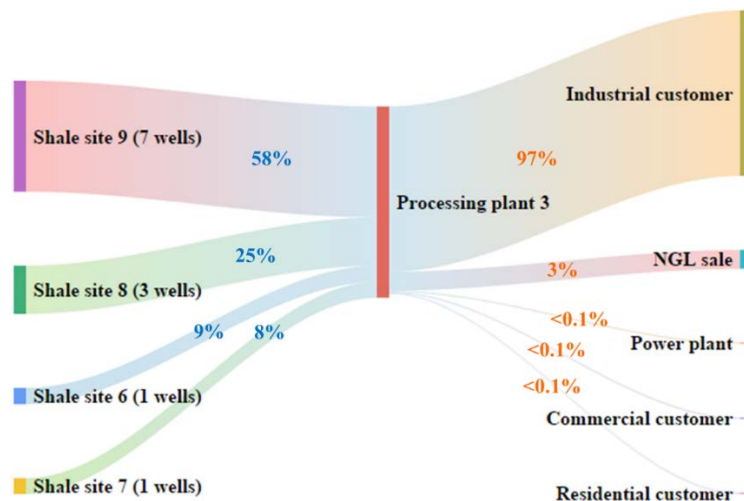


Figure D2. Sankey diagram of shale gas flow in the supply chain network for SMILP model.

At last, we present the cost breakdown of the solution to this SMILP model in Figure D3. As can be observed, though the exact costs for different process in this shale gas supply chain are different, the overall cost breakdowns for both operating cost as well as capital investment remain the same.

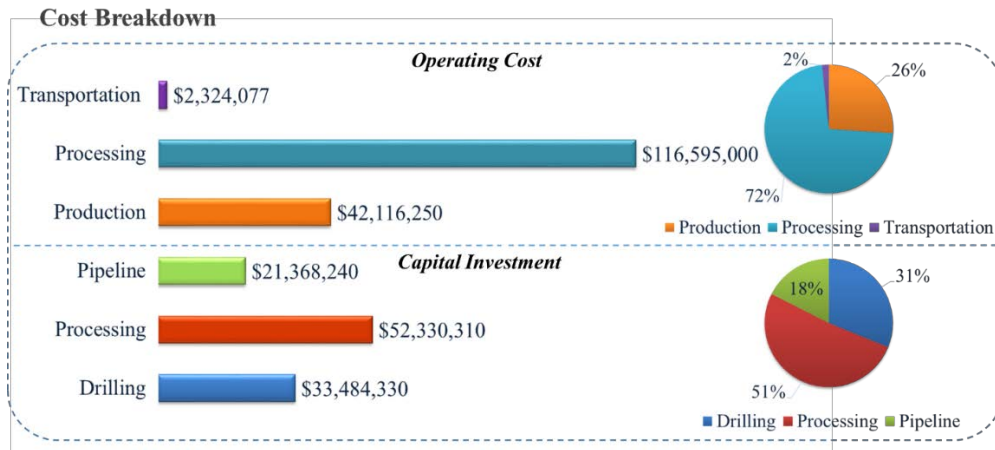


Figure D3. Cost breakdown regarding capital investment and operating cost for SMILP model.

To conclude, first of all the SMILP model verifies some of the results obtained from the proposed SMILFP model, namely the supply chain design and cost breakdown. Meanwhile, the advantage of SMILFP model over the SMILP model in obtaining more meaningful solutions is demonstrated through the analysis of shale gas flow and *LCOE*.

## 5.11 Nomenclature

### Sets

- $I$  Set of shale sites indexed by  $i$
- $M$  Set of end customers indexed by  $m$
- $P$  Set of processing plants indexed by  $p$
- $T$  Set of time periods indexed by  $t$
- $R$  Set of capacity levels indexed by  $r$
- $JS$  Set of scenarios indexed by  $js$

### Parameters

$dl_t$	Minimum demand for NGL in time period $t$
$dm_{m,t}$	Minimum demand of natural gas at end customer $m$ in time period $t$
$dr$	Discount rate per time period
$ect$	Energy content of natural gas
$eur_{i,js}$	Parameter accounting for different EUR at shale site $i$ in scenario $js$
$lc_i$	NGL composition in shale gas at shale site $i$
$lpm_{p,m}$	Distance from processing plant $p$ to end customer $m$
$lsp_{i,p}$	Distance from shale site $i$ to processing plant $p$
$mc_i$	Methane composition in shale gas at shale site $i$
$pef$	Processing efficiency of shale gas
$pl_t$	Average unit price of NGL in time period $t$
$prc_r$	Reference capacity for processing plant with capacity range $r$
$pri_r$	Reference capital investment for processing plant with capacity range $r$
$sdci$	Unit cost for shale well drilling and completion at shale site $i$ in time period $t$
$spc_{i,t}$	Unit cost for shale gas production at shale site $i$ in time period $t$
$spp_{i,\tau}$	Shale gas production of a shale well of age $\tau$ at shale site $i$
$tn$	Minimum total number of wells to be drilled in this project

$tmn_i$	Maximum number of wells that can be drilled at shale site $i$ over the planning horizon
$tprc_r$	Reference capacity of pipeline with capacity range $r$ transporting gases
$tpri_r$	Reference capital investment of pipeline with capacity range $r$ transporting gases
$ue$	Average energy utilizing efficiency at end customer $m$
$vp$	Unit processing cost for shale gas
$vtcm$	Unit variable transportation cost for pipeline transporting natural gas
$vtcs$	Unit variable transportation cost for pipeline transporting shale gas

### Continuous Variables

$PC_{p,r}$	Processing capacity for range $r$ processing plant $p$
$PLS_{p,t,js}$	Amount of NGL sold at processing plant $p$ in time period $t$ in scenario $js$
$SP_{i,t,js}$	Shale gas production rate at shale site $i$ in time period $t$ in scenario $js$
$SPL_{p,t,js}$	Amount of NGL produced at processing plant $p$ in time period $t$ in scenario $js$
$SPM_{p,t,js}$	Amount of natural gas produced at processing plant $p$ in time period $t$ in scenario $js$
$STP_{i,p,t,js}$	Amount of shale gas transported from shale site $i$ to processing plant $p$ in time period $t$ in scenario $js$

$STPM_{p,m,t,js}$	Amount of natural gas transported from processing plant $p$ to end customer $m$ in time period $t$ in scenario $js$
$TPC_{i,p,r}$	Transportation capacity of range $r$ pipeline from shale site $i$ to processing plant $p$
$TPMC_{p,m,r}$	Transportation capacity of range $r$ pipeline from processing plant $p$ to end customer $m$

### Binary Variables

$XP_{i,p}$	0-1 variable. Equal to 1 if pipeline is installed to transport shale gas from shale site $i$ to processing plant $p$
$XPM_{p,m}$	0-1 variable. Equal to 1 if pipeline is installed to transport natural gas from processing plant $p$ to end customer $m$
$YP_p$	0-1 variable. Equal to 1 if processing plant $p$ is constructed

### Integer Variables

$NN_i$	Number of wells to be drilled at shale site $i$
--------	---

## CHAPTER 6

### A STOCHASTIC GAME THEORETIC FRAMEWORK FOR DECENTRALIZED OPTIMIZATION OF MULTI-STAKEHOLDER SUPPLY CHAINS UNDER UNCERTAINTY

#### **6.1 Introduction**

The management of supply chains normally involves multiple stakeholders, each of which controls part of the supply chain. These stakeholders may pursue different objectives, thus leading to compromised solutions [217]. Nevertheless, most existing studies on optimal design and operations of supply chains rely on centralized optimization models, where a single decision maker is assumed to optimize the design and operations decisions under a universal objective function for the whole supply chain [161, 185, 218-220]. Consequently, the optimal solutions of centralized models can be suboptimal or even infeasible in a decentralized, multi-stakeholder supply chain, because the actual interest of each stakeholder is not properly captured in such centralized optimization models. To address this research challenge, multiple game theoretic models are developed to explicitly account for the performance of multi-stakeholder systems. Examples include optimization models for cooperative multi-enterprise supply chains based on the generalized Nash bargaining solution approach [221-224]. On the other hand, optimization models integrating Stackelberg game and Nash-equilibrium are proposed for noncooperative supply chain optimization [77, 130, 225-227]. However, these models assume perfect information sharing among different stakeholders. In other words, the resulting optimal decisions are based on deterministic information. In practice, various types of uncertainties, such as price and productivity

fluctuation, exist concerning the decision-making processes of stakeholders. These uncertainties may significantly influence the rational behaviors of stakeholders. There are a couple of studies aiming to analyze the influences of uncertainty on the optimization of decentralized supply chains [228, 229]. However, they use a post-optimization Monte-Carlo sampling approach to study the influences of uncertainty, instead of directly accounting for uncertainty in the stakeholders' decision-making process. Therefore, it remains a research challenge to simultaneously consider decentralized features of multi-stakeholder supply chains and incorporate uncertainty in the noncooperative stakeholders' optimal decision-making process for supply chain design and operations. To fill this knowledge gap, it is necessary to develop a holistic game theoretic model of multi-stakeholder decentralized supply chains that captures the influences of uncertainty on stakeholders' optimal decisions in a systematical way.

In this work, we propose a novel modeling framework to investigate the influences of uncertainty in decentralized optimization of supply chains. This modeling framework integrates the Stackelberg game with stochastic programming approach into a holistic two-stage stochastic game theoretic model. Specifically, this modeling framework allows consideration of one leader and multiple followers. Following the sequence of decision making process, decision variables for both the leader and the followers are classified into design decisions that must be made "here-and-now" and operational decisions that are postponed to a "wait-and-see" mode after the realization of uncertainties. As a result, both types of stakeholders interact with each other to determine their optimal design strategies at the first stage. After uncertainties from both the leader and the followers are realized, all stakeholders then determine their

operational strategies as “recourse” decisions of the uncertainty information based on their previous design decisions. Following the stochastic programming approach, uncertainties are depicted with discrete scenarios with known probabilities. The objectives of the leader and the followers are to maximize their own expected net present value (NPV). The resulting problem is formulated as a two-stage stochastic mixed-integer bilevel programming (MIBP) problem. The upper-level problem corresponding to the leader’s optimization problem is formulated as a mixed-integer nonlinear programming (MINLP) problem with bilinear terms, each of which is a product of a continuous variable and a binary variable. The lower-level problems corresponding to the planning optimization problems of the followers are formulated as linear programming (LP) problems with continuous variables only. The applicability of the proposed modeling framework is demonstrated with an illustrative example on flight booking under uncertain flight delays and a large-scale application to Marcellus shale gas supply chains.

## **6.2 General problem statement and model formulation**

In this section, we formally state the general modeling framework for decentralized optimization of multi-stakeholder supply chains under uncertainty. The general model formulation is provided as well.

### **6.2.1 General problem statement**

In this work, we consider a multi-stakeholder decentralized supply chain with one (aggregated) leader and a set of followers. Stackelberg games with multiple leaders are

beyond the scope of this paper [230]. An illustrative figure is presented in Figure 58. Following the Stackelberg game, two types of stakeholders are identified, namely the leader and the followers [230]. The leader enjoys priority in the decision-making process to optimize its own objective, whereas each follower is considered as an individual stakeholder driven by its own interest. After the observation of the leader's decisions, the followers react rationally to pursue their own objectives [226]. The optimality of such a noncooperative supply chain optimization problem is defined by the generalized Nash equilibrium [231]. In the proposed modeling framework, we adopt the two-stage stochastic programming approach to tackle uncertainty [202, 208]. In this way, all possible outcomes of uncertainties are captured with discrete scenarios, and all stakeholders seek to optimize their expected performance under all the scenarios. Additionally, based on the sequence of decision making, each stakeholder's decisions can be classified into first-stage decisions and second-stage decisions. In general, the first-stage decisions are mainly design decisions, such as those associated with infrastructure development, technology selection, and price setting, which must be made "here-and-now" before the realization of uncertainties. In such a multi-stakeholder supply chain, there are various types of uncertainties related to both the leader and the followers. Consequently, both the leader and the followers need to account for uncertainties before making their design decisions. The second-stage decisions are related to detailed operations that can be postponed to "wait-and-see" mode after the uncertainty realization. For instance, the planning of production, transportation, and inventory of each stakeholder are generally considered as operational decisions, which are made based on the actual performance of other stakeholders. Therefore, in the first

stage, the leader and followers interact with each other to determine their design decisions based on their expectations of the uncertain performances of other stakeholders. After the uncertainties are realized, the leader and followers enter the second stage to make corrective actions and determine their operational decisions based on the given uncertainty realization as well as their predetermined design decisions.

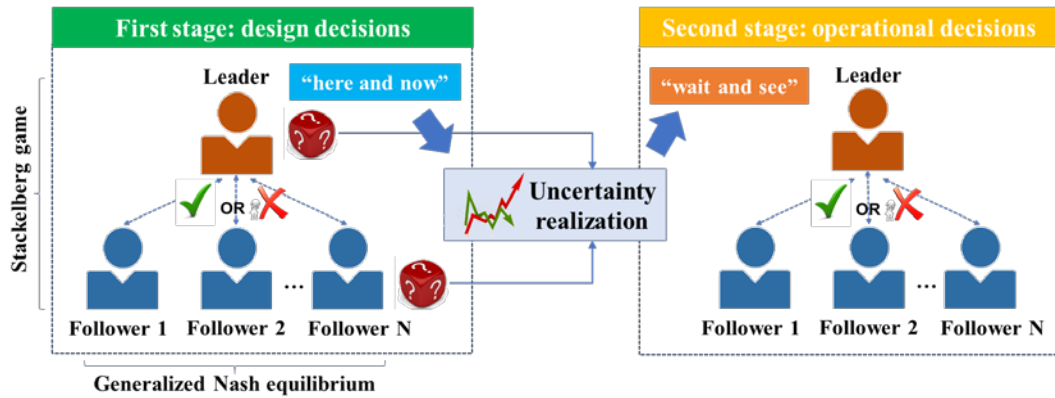


Figure 58. Illustration of the modeling framework for optimization of decentralized multi-stakeholder supply chains under uncertainty.

### 6.2.2 General model formulation

According to the general problem statement, we develop a two-stage stochastic MIBP model to tackle the optimization problem of decentralized supply chains with multiple stakeholders under uncertainty. The general mathematical model formulation (P0) is presented as follows.

$$\begin{aligned}
 \min \quad & EC^{leader} = F(y^u, y^l) + \mathbb{E}_{\mathbb{P}} \left[ G(x_{\xi}^u, x_{\xi}^l) \right] \\
 \text{(P0)} \quad & \text{s.t. } H(x_{\xi}^u, y^u, x_{\xi}^l, y^l) \leq r_{\xi},
 \end{aligned}$$

$$x_{\xi}^u \in \mathbb{R}_+, y^u \in \mathbb{Z}_+$$

$$(x_{\xi}^l, y^l) \in \operatorname{argmax} \left\{ \begin{array}{l} EP^{follower,l} = f(y^l) + \mathbb{E}_{\mathbb{P}} \left[ g(x_{\xi}^l) \right]: \\ h(x_{\xi}^u, y^u, x_{\xi}^l, y^l) \leq s_{\xi} \\ x_{\xi}^l \in \mathbb{R}_+, y^l \in \mathbb{R}_+ \end{array} \right\} \quad \forall l \in L$$

In this general model formulation, the upper-level problem and the lower-level problems correspond to the leader's and the followers' optimization problems, respectively. All the optimization problems need to be optimized simultaneously to reach an optimum defined by generalized Nash equilibrium. The leader's objective function is to minimize its total expected cost, denoted by  $EC^{leader}$ . We note that  $EC^{leader}$  equals the sum of capital investment associated with the first-stage design decisions (calculated by function  $F(y^u, y^l)$ ) and the expected operating cost dependent on the second-stage operational decisions (calculated by function  $G(x_{\xi}^u, x_{\xi}^l)$ ). Specifically, the leader's design decisions and operational decisions are denoted by  $y^u$  and  $x_{\xi}^u$ , respectively. The subscript  $\xi$  indicates that the variables are dependent on the uncertain parameters. Meanwhile, the objective function of the  $l$ th follower is to maximize its own total expected profit  $EP^{follower,l}$ , which equals the sum of the negative follower's capital investment (calculated by  $f(y^l)$ ) and the follower's expected profit (calculated by  $g(x_{\xi}^l)$ ). The follower's design decisions and operational decisions are denoted by  $y^l$  and  $x_{\xi}^l$ , respectively. Notably, the choice of objective functions of the leader and the followers in this modeling framework is flexible, and the minimizing/maximizing forms

are interchangeable. The constraints for the optimization problems of the leader and the followers can be classified into four groups:

- Mass balance constraints that describe the input-output balance relationships of material flows at each node.
- Economic constraints calculating the economic performance associated with design and operational decisions for different stakeholders.
- Capacity constraints describing the capacity limits of different activities, including supply availability, production capacity, transportation, inventory level, market demand, etc.
- Logic constraints addressing the basic assumptions and logical relationships of major decisions, especially those regarding infrastructure construction, technology selection, and price setting.

The resulting problem is a two-stage stochastic MIBP problem, where the upper-level problem is an MINLP problem with bilinear terms formulated as products of a continuous variable and a binary variable, and a set of lower-level LP problems are involved in the constraints. Such bilevel optimization problems cannot be directly handled using any off-the-shelf mathematical programming solvers. Thus, we reformulate this MIBP problem into a single-level MINLP problem by replacing the lower-level problems with their equivalent Karush-Kuhn-Tucker (KKT) conditions [232]. The KKT conditions are sufficient and necessary conditions for optimality, because all the lower-level problems are LPs [226]. To make this MINLP problem more tractable, we apply the Glover's linearization approach to tackle the bilinear terms in

the upper-level problem. Meanwhile, the bilinear terms introduced in the complementary slackness constraints are handled using the big-M approach [232]. Therefore, the single-level MINLP problem can be eventually reformulated into an equivalent mixed-integer linear programming (MILP) problem by introducing auxiliary variables and constraints [233]. We note that the extended mathematical programming (EMP) tools embedded in GAMS suit the same purpose through reformulation based on KKT conditions and solution with nonlinear subsolvers. In this paper, we aim to provide a more general approach to tackle this two-stage stochastic MIBP problem with only MILP solvers.

### **6.3 Application to multi-stakeholder shale gas supply chain optimization**

To further demonstrate the applicability of the proposed optimization framework for decentralized supply chains with multiple stakeholders under uncertainty, we consider an application to a shale gas supply chain in this section. There are several existing shale gas supply chain models [4-7, 58-60, 125], including those addressing optimization under uncertainty [56, 76] and those considering noncooperative shale gas supply chains [77, 130]. However, none of these studies tackle the uncertainties of multiple stakeholders with a holistic optimization framework [129]. In this work, we consider a shale gas supply chain based on the Marcellus shale following existing literature [77, 79]. The specific problem statement and model formulation are presented in the following subsections.

### **6.3.1 Specific problem statement of the shale gas supply chain application**

Following the proposed general modeling framework, the upstream shale gas producer is regarded as the leader in this shale gas supply chain, and the midstream shale gas processors are identified as the followers. As the leader in this Stackelberg game, the shale gas producer seeks to optimize its design and operational decisions to maximize its expected NPV. The leader's major decisions include:

First-stage design decisions:

- Exploration of candidate shale sites;
- Scheduling of drilling activities at each shale site;
- Design of gathering pipeline network;
- Selection of processing contracts offered by processors.

Second-stage operational decisions:

- Amount of freshwater acquired for drilling and hydraulic fracturing in each time period;
- Amount of wastewater handled by different types of water management options in each time period;
- Amount of raw shale gas produced at each shale well in each time period;
- Amount of raw shale gas transported from shale sites to processing plants in each time period;
- Amount of raw shale gas sold to markets directly in each time period.

The leader makes decisions based on the following given information:

- Potential shale sites to be developed and corresponding shale wells to be drilled;

- Actual shale well productivity of each shale site in each scenario;
- Estimated ultimate recovery of each shale well;
- Shale gas composition at each shale site;
- Candidate water management options for wastewater handling;
- Cost data on capital investment and operating cost associated with different design and operational decisions;
- Actual performance ratio of processing plants in each time period;
- Demand and price of natural gas and natural gas liquids at the market;
- Planning horizon of this project.

Once observing the leader's decisions, the followers react rationally to maximize their own NPVs. In this study, we consider the fee-based processing contracts between the shale gas producer and the processors [14, 43]. In other words, the processing plants will offer a fixed fee for unit processing capacity to the shale gas producer in each time period. Depending on the raw shale gas output, the producer may choose to sign processing contracts of varying processing capacities with the processors [5]. The followers' major decisions include:

*First-stage design decisions:*

- Unit processing fee for their processing contracts.

*Second-stage operational decisions:*

- Amount of shale gas processed in each time period;
- Amount of natural gas and natural gas liquid sold to the market.

These decisions are made according to the following information:

- Actual shale well productivity of each shale site in each scenario;
- Composition of raw shale gas from each shale site;
- Cost data on capital investment and operating cost associated with different design and operational decisions;
- Actual performance ratio of processing plants in each time period;
- Demand and price of natural gas and natural gas liquids at the market;
- Planning horizon of this project.

In this problem, we consider the following assumptions:

- All the design decisions are considered as the first-stage decisions to be made at the beginning of project;
- The probability distributions of uncertainties are known;
- Time delays regarding water treatment, well development, and transportation activities can be neglected compared with the long-term planning horizon.

The resulting problem is a multi-period decentralized supply chain optimization problem under uncertainty. There are uncertainties associated with both the leader and the followers, namely the uncertain shale well productivity in each time period and the uncertain performance ratio of processing plants in each time period. The uncertainty associated with shale well productivity accounts for the production fluctuations of active shale wells, and the uncertainty of performance ratio describes the uncertain processing performance of existing processing facilities. Therefore, both types of stakeholders need to take into account the uncertain performances of other stakeholders before making their design and operational decisions.

### 6.3.2 Specific model formulation of the shale gas supply chain application

The specific model formulation for this shale gas supply chain application is presented in this section. The economic objective function in the leader's problem is given by equation (1) maximizing the expected NPV of the shale gas producer. The objective in the follower's problem is given by equation (29) maximizing the expected NPV of each shale gas processor. Four types of constraints are included in this model, including economic constraints, mass balance constraints, capacity constraints, and logic constraints. Specifically, constraints (2)-(13) are the economic constraints for the leader's problem; constraints (14)-(19) refer to the mass balance relationship in the leader's problem; constraints (20)-(23) describe the capacity constraints in the leader's problem; and constraints (24)-(28) correspond to the logic constraints in the leader's problem. Meanwhile, constraints (30)-(31) calculate the economic performance in the follower's problem, and constraint (32) determines the capacity constraints in the follower's problem. All the parameters are denoted with lower-case symbols, and all the variables are denoted with upper-case symbols.

#### 6.3.2.1 Leader's objective function

As stated above, the upstream shale gas producer is considered as the leader, whose objective is to maximize its own expected NPV, given by,

$$\max TP^{producer} = -TC_{1st}^{producer} + \sum_{s \in S} TP_{2nd,s}^{producer} \cdot pr_s \quad (1)$$

where  $TC_{1st}^{producer}$  is the leader's first-stage cost accounting for various "here-and-now" capital investments.  $TP_{2nd,s}^{producer}$  is the leader's second-stage NPV of scenario  $s$ . The parameter  $pr_s$  is the probability of scenario  $s$ .

Specifically,  $TC_{1st}^{producer}$  covers the first-stage capital investment on shale well drilling and completion ( $TC_{1st}^{drill}$ ), gathering pipeline installation ( $TC_{1st}^{pipeline}$ ), and processing contracts ( $TC_{1st}^{contract}$ ), calculated by,

$$TC_{1st}^{producer} = TC_{1st}^{drill} + TC_{1st}^{pipeline} + TC_{1st}^{contract} \quad (2)$$

The first-stage cost on shale well drilling and completion can be calculated by,

$$TC_{1st}^{drill} = \sum_{i \in I} \sum_{t \in T} \frac{sdci \cdot NN_{i,t}}{(1 + dr)^t} \quad (3)$$

where  $sdci$  is the capital cost for drilling and completion of a single shale well at shale site  $i$ .  $NN_{i,t}$  is an integer variable indicating the number of wells to be drilled at shale site  $i$  in time period  $t$ . The parameter  $dr$  is the discount rate per time period.

The first-stage cost on installation of gathering pipelines is calculated by,

$$TC_{1st}^{pipeline} = \sum_{i \in I} \sum_{p \in P} \sum_{r \in R} \left( tpri_{r-1} \cdot XP_{i,r} \cdot lsp_{i,p} + (TCP_{i,r} - tprc_{r-1} \cdot XP_{i,r}) \cdot \left( \frac{tpri_r - tpri_{r-1}}{tprc_r - tprc_{r-1}} \right) \cdot lsp_{i,p} \right) \quad (4)$$

where  $TCP_{i,r}$  denotes the transportation capacity of a range  $r$  gathering pipeline associated with shale site  $i$  and processing plants.  $XP_{i,r}$  is a binary variable that equals 1 if the gathering pipeline within capacity range  $r$  associated with shale site  $i$  and processing plants is installed. The parameter  $tpri_r$  is the reference capital investment of

a pipeline within capacity range  $r$  for transporting gases; and  $tprc_r$  is the corresponding reference capacity of a pipeline within capacity range  $r$ . The parameter  $lsp_{i,p}$  denotes the distance between shale site  $i$  and processing plant  $p$ .

The first-stage cost on processing contracts are calculated by,

$$TC_{1st}^{contract} = \sum_{c \in C} \sum_{p \in P} \sum_{t \in T} \frac{pc_{c,p} \cdot VP_{c,p,t} \cdot XSC_{c,p,t}}{(1+dr)^t} \quad (5)$$

where  $pc_{c,p}$  is the reference processing capacity of processing contract  $c$  at processing plant  $p$ .  $VP_{c,p,t}$  is the unit processing fee of processing contract  $c$  offered by processing plant  $p$  in time period  $t$ .  $XSC_{c,p,t}$  is a binary variable that equals 1 if processing contract  $c$  offered by processing plant  $p$  is selected by the producer in time period  $t$ . We highlight the bilinear term as a product of lower-level continuous variable  $VP_{c,p,t}$  and upper-level binary variable  $XSC_{c,p,t}$ .

The leader's second-stage profit is scenario-dependent, which equals the difference between the second-stage income and cost. The second-stage income consists of revenue from sales of natural gas and natural gas liquids (NGL) ( $TR_{2nd,s}^{sales}$ ), the salvage value of shale wells at the end of planning horizon ( $TR_{2nd,s}^{salvage}$ ), and income from sales of raw shale gas ( $TR_{2nd,s}^{raw}$ ). The second-stage cost includes the costs involved in shale gas production activities ( $TC_{2nd,s}^{production}$ ), water management activities ( $TC_{2nd,s}^{water}$ ), transportation activities ( $TC_{2nd,s}^{transportation}$ ), and royalty payment ( $TC_{2nd,s}^{royalty}$ ).

$$TP_{2nd,s}^{producer} = TR_{2nd,s}^{sales} + TR_{2nd,s}^{salvage} + TR_{2nd,s}^{raw} - TC_{2nd,s}^{production} - TC_{2nd,s}^{water} - TC_{2nd,s}^{transportation} - TC_{2nd,s}^{royalty} \quad (6)$$

$TR_{2nd,s}^{sales}$  indicates the total income from sales of separated natural gas and NGL, calculated by,

$$TR_{2nd,s}^{sales} = \sum_{t \in T} \frac{png_t \cdot TNG_{t,s}}{(1+dr)^t} + \sum_{t \in T} \frac{pnl_t \cdot TNL_{t,s}}{(1+dr)^t} \quad (7)$$

where  $png_t$  is the unit price of natural gas in time period  $t$ .  $TNG_{t,s}$  is the amount of natural gas extracted at processing plants in time period  $t$  of scenario  $s$ . Similarly,  $pnl_t$  is the unit price of NGL in time period  $t$ .  $TNL_{t,s}$  is the amount of NGL extracted at processing plants in time period  $t$  of scenario  $s$ .

$TR_{2nd,s}^{salvage}$  denotes the total salvage value of shale wells at the end of the planning horizon, calculated by,

$$TR_{2nd,s}^{salvage} = \sum_{i \in I} \sum_{t \in T} psgd \cdot (NN_{i,t} \cdot eur_i - SP_{i,t,s}) \quad (8)$$

where  $psgd$  is the average estimated unit profit of shale gas remained to be produced in shale wells. The parameter  $eur_i$  is the estimated ultimate recovery of wells at shale site  $i$ .  $SP_{i,t,s}$  is the amount of raw shale gas produced at shale site  $i$  in time period  $t$  of scenario  $s$ .

The shale gas producer has the option to sell raw shale gas to local markets directly when the midstream processing capacity is insufficient for the raw shale gas output. The corresponding income is denoted as  $TR_{2nd,s}^{raw}$  and calculated by,

$$TR_{2nd,s}^{raw} = \sum_{i \in I} \sum_{t \in T} \frac{pse_{i,t} \cdot STPX_{i,t,s}}{(1+dr)^t} \quad (9)$$

where  $pse_{i,t}$  denotes the average unit profit gained from shale gas from shale site  $i$  sold directly in time period  $t$ .  $STPX_{i,t,s}$  is the amount of raw shale gas sold directly at shale site  $i$  in time period  $t$  of scenario  $s$ .

The second-stage shale gas production cost  $TC_{2nd,s}^{production}$  can be calculated by,

$$TC_{2nd,s}^{production} = \sum_{i \in I} \sum_{t \in T} \frac{spc_i \cdot SP_{i,t,s}}{(1+dr)^t} \quad (10)$$

where  $spc_i$  denotes the unit production cost of raw shale gas at shale site  $i$ .

The second-stage water management cost  $TC_{2nd,s}^{water}$  includes freshwater acquisition cost and wastewater handling cost, and it is calculated by,

$$TC_{2nd,s}^{water} = \sum_{i \in I} \sum_{t \in T} \frac{fwc \cdot FW_{i,t,s}}{(1+dr)^t} + \sum_{i \in I} \sum_{w \in W} \sum_{t \in T} \frac{wtc_w \cdot WW_{i,w,t,s}}{(1+dr)^t} \quad (11)$$

where  $fwc$  is the unit freshwater acquisition cost,  $FW_{i,t,s}$  represents the amount of freshwater acquired at shale site  $i$  in time period  $t$  of scenario  $s$ . The parameter  $wtc_w$  denotes the unit wastewater handling cost with water management option  $w$ .  $WW_{i,w,t,s}$  is the amount of wastewater handled at shale site  $i$  by water management option  $w$  in time period  $t$  of scenario  $s$ .

The second-stage transportation cost includes the cost of transporting shale gas from shale sites to processing plants, the cost of transporting natural gas from processing plants to markets, and the cost of transporting NGL to markets. This cost item is given by,

$$TC_{2nd,s}^{transportation} = \sum_{i \in I} \sum_{p \in P} \sum_{t \in T} \frac{vtcs \cdot lsp_{i,p} \cdot STP_{i,p,t,s}}{(1+dr)^t} + \sum_{t \in T} \frac{vtcm \cdot lpd \cdot TNG_{t,s}}{(1+dr)^t} + \sum_{t \in T} \frac{vtcl \cdot lpm \cdot TNL_{t,s}}{(1+dr)^t} \quad (12)$$

where  $vtcs$  is the unit transportation cost for pipeline transporting shale gas,  $STP_{i,p,t,s}$  indicates the amount of shale gas transported from shale site  $i$  to processing plant  $p$  in time period  $t$  of scenario  $s$ . The parameters  $vtcm$  and  $vtcl$  are the unit transportation costs for natural gas and NGL, respectively. The parameters  $lpd$  and  $lpm$  are the distance from processing plants to natural gas market and the distance from processing plants to NGL market, respectively.

The second-stage cost regarding royalty payment is calculated as follows,

$$TC_{2nd,s}^{royalty} = \sum_{i \in I} \sum_{t \in T} \frac{\gamma_i \cdot psg_{i,t} \cdot SP_{i,t,s}}{(1+dr)^t} \quad (13)$$

where  $\gamma_i$  indicates the percentage of the value of extracted shale gas paid for royalty at shale site  $i$ . The parameter  $psg_{i,t}$  is the average unit price of raw shale gas produced at wellhead  $i$  in time period  $t$ .

### 6.3.2.2 Leader's constraints

The leader's objective function is optimized subject to the following constraints:

The total shale gas production rate at a shale site equals the sum of that of different wells, which can be calculated by:

$$SP_{i,t,s} = \sum_{t'=1}^{t-1} ufp_{i,t,s} \cdot spp_{i,t-t'} \cdot NN_{i,t'}, \quad \forall i, t \geq 2, s \quad (14)$$

where  $ufp_{i,t,s}$  is the uncertainty factor accounting for the actual shale gas production at shale site  $i$  in time period  $t$  of scenario  $s$ . The parameter  $spp_{i,t}$  indicates the shale gas production of a shale well with age  $t$  at shale site  $i$ . The subscript  $t'$  denotes the time

period that a certain shale well is drilled. Therefore,  $t-t'$  is the age of a shale well drilled at  $t'$  in time period  $t$ .

The shale gas produced at each shale site can be either transported to different processing plants or sold directly to local markets. This mass balance relationship is modeled by,

$$SP_{i,t,s} = \sum_{p \in P} STP_{i,p,t,s} + STPX_{i,t,s}, \quad \forall i, t, s \quad (15)$$

The total amount of freshwater required for shale site  $i$  is dependent on the shale gas production rate as well as the number of wells drilled,

$$FW_{i,t,s} = wf_i \cdot SP_{i,t,s} + wd_i \cdot NN_{i,t}, \quad \forall i, t, s \quad (16)$$

where  $wf_i$  is the unit water usage for hydraulic fracturing and production at shale site  $i$ , and  $wd_i$  denotes the average drilling water usage for each well at shale site  $i$ .

The total amount of wastewater is approximately proportional to the shale gas production rate [58, 124].

$$\sum_{w \in W} WW_{i,w,t} = wt_i \cdot SP_{i,t,s}, \quad \forall i, t, s \quad (17)$$

where  $wt_i$  indicates the produced water generation rate associated with unit shale gas production at shale site  $i$ .

The total amount of methane separated from processing plants is determined by the methane composition of the shale gas transported from different shale sites as well as processing efficiency. The amount of NGLs produced at a processing plant is calculated by a similar equation, given by,

$$TNG_{t,s} = \sum_{i \in I} \sum_{p \in P} STP_{i,p,t,s} \cdot pef \cdot mc_i, \forall t, s \quad (18)$$

$$TNL_{t,s} = \sum_{i \in I} \sum_{p \in P} STP_{i,p,t,s} \cdot pefl \cdot lc_i, \forall t, s \quad (19)$$

where  $pef$  is the processing factor accounting for processing efficiency of natural gas. The parameter  $pefl$  denotes the processing factor accounting for NGL processing efficiency. The parameters  $mc_i$  and  $lc_i$  are the composition factors for methane and NGLs, respectively.

The total amount of shale gas transported from shale site  $i$  in time period  $t$  of scenario  $s$  should not exceed the capacity of corresponding gathering pipelines,

$$\sum_{p \in P} STP_{i,p,t,s} \leq \sum_{r \in R} TCP_{i,r}, \forall i, t, s \quad (20)$$

The total amount of shale gas from all the shale sites processed by each processing plant should not exceed its available processing capacity determined by both the processing contract and the performance ratio,

$$\sum_{i \in I} STP_{i,p,t,s} \leq \sum_{c \in C} ufc_{p,t,s} \cdot pc_{c,p} \cdot XSC_{c,p,t}, \forall p, t, s \quad (21)$$

where  $ufc_{p,t,s}$  is the uncertainty factor accounting for the actual processing capacity of processing plant  $p$  available in time period  $t$  of scenario  $s$ .

The producer's total processing cost cannot exceed its budget for shale gas processing services, given by,

$$\sum_{c \in C} \sum_{p \in P} \sum_{t \in T} \frac{pc_{c,p} \cdot VP_{c,p,t} \cdot XSC_{c,p,t}}{(1+dr)^t} \leq bgt \quad (22)$$

where  $bgt$  is the producer's total budget for the processing service of processing plants.

The total amount of natural gas produced is bounded by the minimum and maximum demands of the local market in each time period, given by,

$$dmlp_t \leq TNG_{t,s} \leq dmup_t, \forall t, s \quad (23)$$

where  $dmlp_t$  is the minimum demand of natural gas in time period  $t$ , and  $dmup_t$  is the maximum demand of natural gas in time period  $t$ .

The number of wells that can be drilled in each time period is constrained by the number of available drilling rigs. This relationship is given by,

$$\sum_{i \in I} NN_{i,t} \leq mn, \forall t \quad (24)$$

where  $mn$  indicates the maximum number of wells that can be drilled for all shale sites in each time period.

At each shale site, there is normally a maximum number of wells that can be drilled. In other words, the total number of wells that can be drilled at shale site  $i$  over the planning horizon is bounded. This relationship is given by,

$$\sum_{t \in T} NN_{i,t} \leq tmn_i, \forall i \quad (25)$$

where  $tmn_i$  denotes the maximum number of wells that can be drilled at shale site  $i$  over the planning horizon.

If a gathering pipeline is installed, its transportation capacity should be bounded by the corresponding capacity range; otherwise, its capacity should be zero. This relationship can be modeled by the following inequality:

$$tprc_{r-1} \cdot XP_{i,r} \leq TCP_{i,r} \leq tprc_r \cdot XP_{i,r}, \forall i, r \quad (26)$$

At most one capacity range of gathering pipeline can be chosen for a shale site. This constraint is modeled by,

$$\sum_{r \in R} XP_{i,r} \leq 1, \forall i \quad (27)$$

At most one processing contract can be selected for each processing plant in each time period  $t$ , given by,

$$\sum_{c \in C} XSC_{c,p,t} \leq 1, \forall p, t \quad (28)$$

### 6.3.2.3 Followers' objective function

Each shale gas processor seeks to maximize its own expected NPV, given as the difference between income from processing contracts and the expected operating cost.

$$\max TP_p^{processor} = TP_{1st,p}^{processor} - \sum_{s \in S} TC_{2nd,p,s}^{processor} \cdot pr_s, \forall p \quad (29)$$

The first-stage income of shale gas processor  $p$  is denoted by  $TP_{1st,p}^{processor}$ , calculated by,

$$TP_{1st,p}^{processor} = \sum_{c \in C} \sum_{p \in P} \sum_{t \in T} \frac{pc_{c,p} \cdot VP_{c,p,t} \cdot XSC_{c,p,t}}{(1+dr)^t} \quad (30)$$

Notably, the upper-level binary variables  $XSC_{c,p,t}$  are considered as fixed values in the lower-level optimization problems.

The second-stage operating cost of processing plant  $p$  of scenario  $s$  is denoted by  $TC_{2nd,p,s}^{processor}$ , which is calculated by,

$$TC_{2nd,p,s}^{processor} = \sum_{i \in I} \sum_{t \in T} \frac{vpc_p \cdot STP_{i,p,t,s}}{(1+dr)^t} \quad (31)$$

where  $vpc_p$  is the unit operating cost at processing plant  $p$ .

#### 6.3.2.4 Followers' constraints

Each follower's objective function is optimized subject to the following constraints:

The unit processing fee of processing contract  $c$  offered by processing plant  $p$  in time period  $t$  cannot exceed its corresponding lower and upper bounds, as given by,

$$vplp \leq VP_{c,p,t} \leq vpup, \forall c, p, t \quad (32)$$

where  $vplp$  and  $vpup$  are the minimum unit processing fee and maximum unit processing fee, respectively. The corresponding data are obtained from the financial data reported by midstream processing companies [44].

Similar to the illustrative example of flight booking problem, the resulting problem is a two-stage stochastic MIBP problem with MINLP upper-level problem and LP lower-level problems. Thus, by simultaneously applying the KKT conditions and Glover's linearization approach, we can reformulate it into a more tractable single-level MILP problem.

### 6.3.3 Results and discussion

In this application, we consider a case study of a Marcellus shale gas supply chain [77]. A total of five candidate shale sites are considered, and each shale site allows drilling of up to four to eight horizontal shale wells [234]. The composition of raw shale gas from different shale sites ranges from 1% to 20% [235]. Each shale well features a distinct shale gas production profile that decreases with time [4]. The estimated ultimate recovery of each shale site is taken from literature data [113]. The wastewater generated during drilling and fracturing stages at shale sites can be handled by five water management options, including the underground injection into Class-II disposal wells

[37], centralized treatment by commercial facilities [21], and onsite treatment with multi-stage flash, multi-effect distillation, and reverse osmosis technologies [99]. Three shale gas processing plants are considered, representing three autonomous followers. Each processing plant offers three types of fee-based processing contracts to the shale gas producer, corresponding to 50%, 75%, and 100% of their total processing capacities, respectively. Four capacity levels are considered for the design of gathering pipelines. The total planning horizon is 10 years, which is divided into 10 time periods (one year per time period) [4, 188]. Two types of uncertainties are considered, namely the uncertain shale well productivity in each time period and the uncertain performance ratio of processing plants in each time period. We consider normal distributions for these uncertainties following existing studies [76]. In addition, a sample average approximation approach is adopted to discretize the continuous probability distribution functions and to generate scenarios [198]. Specifically, by setting an initial sample size of 100 scenarios and considering a 98% confidence interval, we finalize the required number of scenarios as 200 [236]. The resulting problem is a two-stage stochastic MIBP problem, where the upper-level MINLP problem has 160 integer variables, 114,221 continuous variables, and 64,292 constraints; and the lower-level LP problem has 90 continuous variables, and 184 constraints. After applying the KKT conditions and Glover's linearization approach, the reformulated single-level MILP problem has 341 integer variables, 115,016 continuous variables, and 65,557 constraints. The MILP problems are solved using CPLEX 12.7.1. The absolute optimality tolerance is set to  $10^{-6}$ . The resulting single-level MILP can be globally optimized within 6,761 CPU seconds.

By solving this optimization problem, we find that the expected NPV for the leader is \$68.9 MM. The three followers corresponding to three processing plants are expected to achieve \$2.57 MM, \$3.39 MM, and \$1.21 MM NPVs, respectively. To evaluate the value of the obtained stochastic solution, in Figure 59, we summarize the leader's and the followers' NPVs in 200 scenarios generated using Monte-Carlo simulation to demonstrate the impact of uncertainties on the overall economic performance of different stakeholders. Each point in this figure indicates a specific solution point associated with a scenario. All the solution points share the same first-stage design decisions obtained from the two-stage stochastic MIBP model. The straight line indicates the expected NPV throughout the 200 scenarios considered in this case study. For the leader, the lowest NPV is \$55.2 MM, while the highest NPV is up to \$77.4 MM. Meanwhile, the lowest NPVs of followers 1, 2 and 3 are \$1.61 MM, \$2.15 MM, and \$0.72 MM, respectively. The highest NPVs of followers 1, 2, and 3 are \$3.71 MM, \$4.72 MM, and \$2.04 MM, respectively.

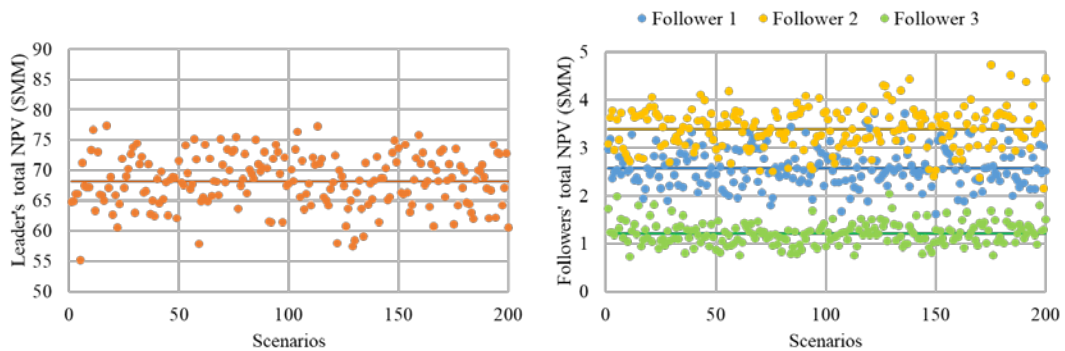


Figure 59. Optimal NPVs of leader and followers in 200 scenarios based on the optimal strategy obtained in the two-stage stochastic MIBP model.

To demonstrate the advantage of this two-stage stochastic MIBP model, we further compare the optimal results obtained in the proposed two-stage stochastic game theoretic model with those of the deterministic game theoretic models. Notably, in the deterministic game theoretic model, each stakeholder makes decisions based on its deterministic expectation of other stakeholders instead of considering all the possibilities. Consequently, when the leader and the followers have different perspectives on the others' performances, there may be a significant discrepancy in the resulting optimal strategies obtained in the deterministic game theoretic models. In this case study, we use distinct cases to address this issue. To be more specific, the leader may hold optimistic, neutral, or pessimistic expectations toward the followers' actual performance, and vice versa. The optimistic expectation corresponds to 150% expectation. The neutral corresponds to 100% expectation. The pessimistic corresponds to 50% expectation. Thus, a total of nine cases are considered for the deterministic model, including the pessimistic-pessimistic, neutral-neutral, optimistic-optimistic, optimistic-pessimistic, pessimistic-optimistic, optimistic-neutral, pessimistic-neutral, neutral-pessimistic, and neutral-optimistic cases. For instance, the optimistic-pessimistic case indicates that the leader expects the followers to deliver 150% of their promised performance, and the followers expect the leader to produce only 50% of shale gas estimated in advance. The optimal expected NPVs of the leader and the followers associated with these nine cases are summarized in Figure 60.



Figure 60. Optimal expected NPVs of the leader and followers in the two-stage stochastic MIBP model and deterministic game theoretic models.

As can be observed in Figure 60, the optimistic-optimistic case returns the highest expected NPV of \$79.4 MM for this decentralized shale gas supply chain, where the leader gets a total of \$71.6 MM NPV, and the followers' NPVs are \$3.17 MM, \$1.51 MM, and \$3.10 MM, respectively. This result is followed by the neutral-neutral case with the second highest expected NPV of \$78.5 MM. The optimal solution of the proposed two-stage stochastic game theoretic model, with \$76.1 MM expected NPV, has economic performance that is close to these two deterministic cases. From this comparison, we conclude that when the leader and the followers hold a relatively positive expectation toward others, they are more likely to achieve an optimal solution with better overall performance. By contrast, when stakeholders hold a negative expectation toward other supply chain participants, they may reach a compromised strategy and lose potential profits. Such a phenomenon can be observed in the neutral-pessimistic, pessimistic-neutral, and pessimistic-pessimistic cases. However, the worst economic performance is observed in cases where the leader and the followers have

opposite expectations to each other. For example, the expected NPVs in the pessimistic-optimistic case and in the optimistic-pessimistic case are as low as \$51.9 MM and \$58.2 MM, respectively. Additionally, by comparing the optimistic-optimistic, optimistic-neutral, and optimistic-pessimistic cases, we conjecture that when the follower is pessimistic about the leader's performances, follower 1 with a smaller processing capacity is more likely to seize this opportunity and gain more profit; otherwise, follower 2 and follower 3 with relatively larger processing capacities hold more advantage. Moreover, the followers may leverage the pessimistic expectation from the leader to make more profit, as can be observed in the pessimistic-pessimistic, pessimistic-neutral, and pessimistic-optimistic cases. The expected NPVs of followers in these cases are \$10.6 MM, \$12.9 MM, and \$14.9 MM, respectively, which are significantly higher than in other cases.

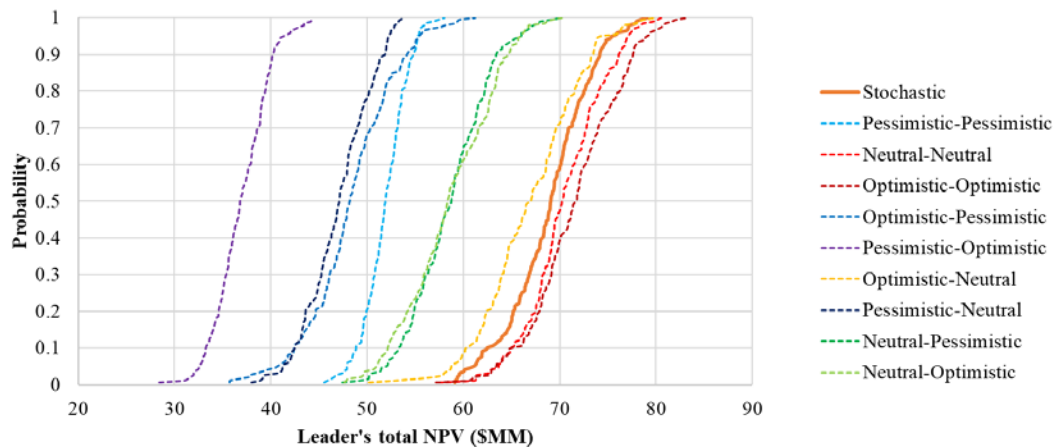


Figure 61. Cumulative probability distribution of the leader's NPV based on 200 scenarios in the two-stage stochastic MIBP model (solid line) and deterministic game theoretic models (dash lines).

In Figure 61, we further present the cumulative probability distribution of the leader's NPV based on 200 scenarios associated with the proposed stochastic game theoretic model and its deterministic counterparts. The cumulative probability distribution of the proposed two-stage stochastic MIBP model is presented in solid line, and deterministic ones are denoted by dash lines. Consistent with the previous results, positive expectations from both the leader and the followers lead to better overall economic performance, as given by the optimistic-optimistic, neutral-neutral, and optimistic-neutral cases. By contrast, negative expectations can result in compromised strategies, and the worst scenario happens when the leader and the followers hold opposite expectations toward each other. The two-stage stochastic game theoretic model provides competitive solutions by considering uncertain performances of stakeholders. Moreover, by comparing the probability distribution of the leader's NPV in different models, we notice that the proposed two-stage stochastic game theoretic model results in a "short tail" at the bottom left side of the probability distribution curve. Such a feature indicates that the stochastic game theoretic model works well in hedging against extreme cases when there is significant discrepancy between performances of the leader and the followers. For instance, the lowest leader's NPV in the stochastic game theoretic model is \$59.1 MM, which is higher than the lowest leader's NPVs in the optimistic-optimistic and neutral-neutral cases, given as \$57.2 MM and \$57.4 MM, respectively.

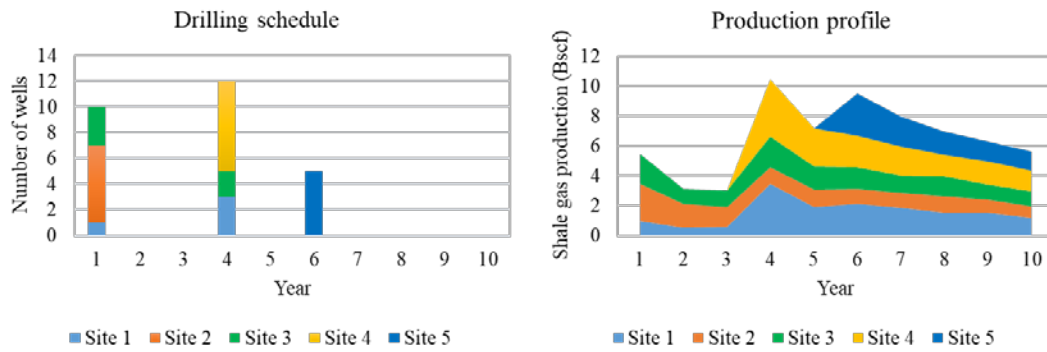


Figure 62. Optimal drilling schedule and shale gas production profile of the leader.

In Figure 62, we present the optimal drilling schedule and corresponding average shale gas production profile based on 200 scenarios. As can be seen, a total of 27 shale wells are drilled within the 10-year planning horizon. Specifically, 10 shale wells are drilled in the beginning at shale sites 1, 2 and 3 to satisfy the initial natural gas demand. Later, based on the forecasted price of natural gas, there is a price increase in the fourth year. As a result, the leader drills 12 extra shale wells at shale sites 1, 3, and 4 in year 4 to maximize the profit. Since shale wells generally feature an exponentially decreasing production profile, five more shale wells are drilled in the sixth year to compensate for the production decrease. Despite the uncertainty of productivity at each shale well, this optimal drilling schedule generally determines the overall shale gas production profile. After the initial shale gas production, two extra production peaks appear in the fourth year and the sixth year.

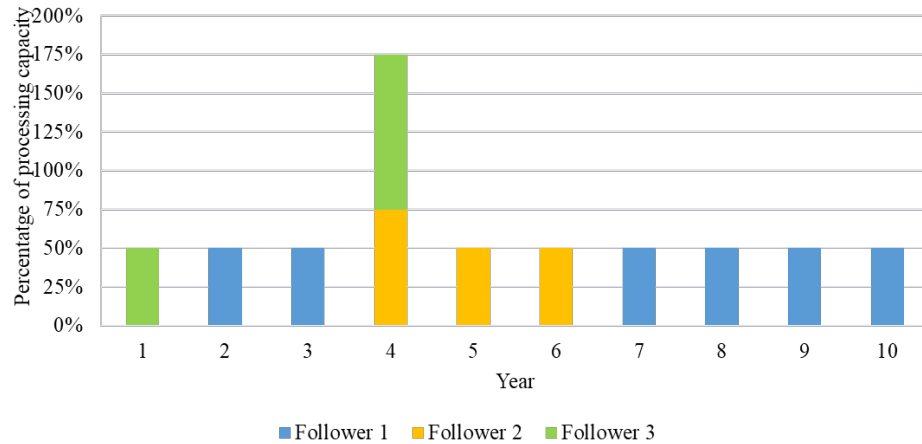


Figure 63. Leader’s optimal strategy regarding selection of processing contracts from followers.

The leader adjusts its optimal strategy on the selection of processing contracts according to the shale gas production profile. As shown in Figure 63, the leader acts conservatively to sign a processing contract with only one processing plant in most years, and 50% of the total processing capacity is generally considered enough for the total raw shale gas output. Since different processing plants have distinct processing capabilities, the leader may turn to other processing plants in response to production fluctuation. In the fourth year, with 12 extra shale wells drilled, additional processing capacity is required. Thus, the leader signs processing contracts with both processing plants 2 and 3 for 75% and 100% of their processing capacities, respectively. Similarly, after the sixth year, the leader switches to processing plant 1 with smaller processing capacity to handle the decreasing shale gas output. Notably, the leader’s strategy is also affected by the followers’ price setting decisions. In Figure 64, we summarize the unit processing fees of different processing contracts provided by the followers. By investigating the detailed price setting strategies, we can obtain the following insights: (a) processing plants tend

to offer a lower unit processing fee for smaller processing capacity contracts, which result in a lower financial risk considering the uncertain performances of other stakeholders; (b) processing plants have higher chances to be selected by the producer when their unit processing fees are lower than other competitors.

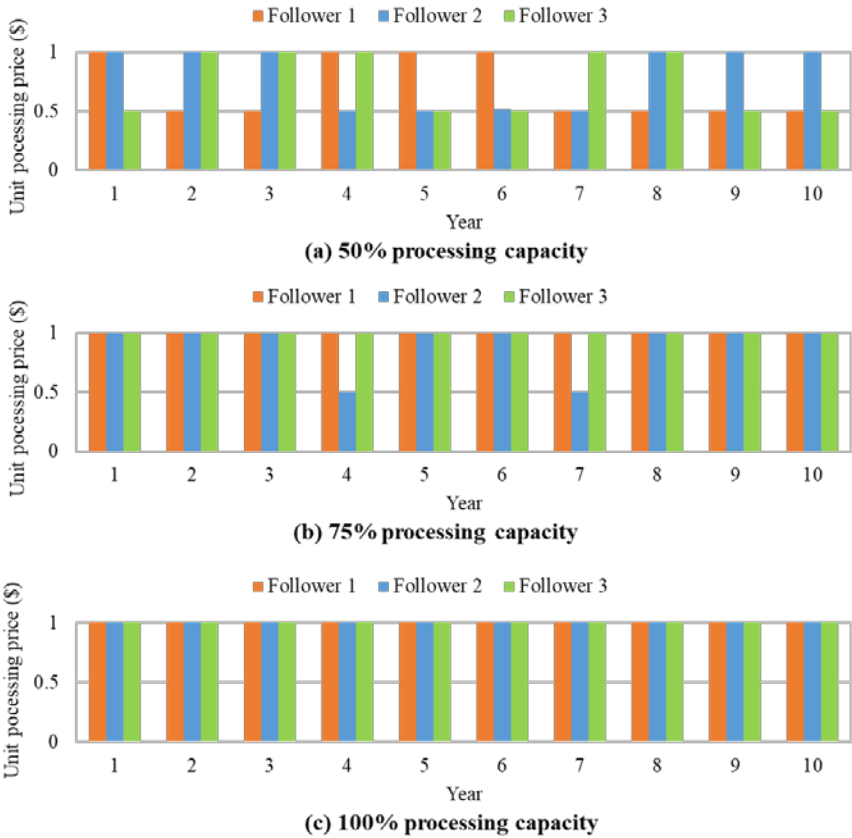


Figure 64. Optimal processing fees provided by the followers for different processing contracts.

### 6.4 Summary

A novel optimization framework was proposed that integrated the leader-follower Stackelberg game with two-stage stochastic programming approach into a holistic two-stage stochastic game theoretic model. This modeling framework enabled us to

investigate the optimal design and operations of decentralized supply chains involving multiple stakeholders under uncertainty. The resulting problem was formulated into a two-stage stochastic MIBP problem. To facilitate the solution of the resulting problem, we applied KKT conditions and Glover’s linearization approach simultaneously to reformulate this two-stage stochastic MIBP problem into a single-level MILP problem. To illustrate the application, we considered an illustrative example of a flight booking problem under uncertain flight delays. An application to a multi-stakeholder decentralized Marcellus shale gas supply chain optimization was further presented. Based on the optimization results, we concluded that stakeholders tended to choose more conservative strategies when considering uncertainties in the optimization of decentralized supply chains. Although the conservatism might affect the overall performance of stakeholders, it effectively hedged against the risk of extreme cases when stakeholders wrongly anticipated others’ performances.

## 6.5 Nomenclature

### Sets

$C$	Set of processing contracts indexed by $c$ ( $c1$ : 50% processing capacity; $c2$ : 75% processing capacity; $c3$ : 100% processing capacity)
$I$	Set of shale sites indexed by $i$
$P$	Set of candidate processing plant indexed by $p$
$R$	Set of capacity levels indexed by $r$
$S$	Set of scenarios indexed by $s$
$T$	Set of time periods indexed by $t$

$W$  Set of water treatment options indexed by  $w$  ( $w1$ : disposal well;  $w2$ : CWT;  $w3$ : onsite treatment with MSF;  $w4$ : onsite treatment with MED;  $w5$ : onsite treatment with RO)

### Parameters

$bgt$  Producer's budget for purchasing processing capacity

$dmlp_t$  Minimum demand of natural gas at delivery node in time period  $t$

$dmup_t$  Maximum demand of natural gas at delivery node in time period  $t$

$dr$  Discount rate per time period

$eur_i$  Average EUR of shale site  $i$

$fwc$  Unit cost for freshwater acquisition

$lc_i$  NGL composition factor in shale gas at shale site  $i$

$lpd$  Distance from processing plant to natural gas delivery node

$lpm$  Distance from processing plant to NGL market

$lsp_{i,p}$  Distance from shale site  $i$  to delivery node of processing plant  $p$

$mc_i$  Methane composition factor in shale gas at shale site  $i$

$mn$  Maximum total number of wells that can be drilled for in each time period

$pc_{c,p}$  Reference processing capacity of processing contract  $c$  at processing plant  $p$

$pef$  Processing factor accounting for processing efficiency of natural gas

$pefl$  Processing factor accounting for NGL processing efficiency

$png_t$  Average unit price of natural gas in time period  $t$

$pnl_t$  Average unit price of NGL in time period  $t$

$pse_{i,t}$  Average unit profit gained from shale gas at shale site  $i$  in time period  $t$

$psg_{i,t}$	Average unit price of raw shale gas produced at wellhead $i$ in time period $t$
$psgd$	Average estimated unit profit of shale gas remains to be produced
$sdc_i$	Unit cost for shale well drilling and completion at shale site $i$
$spc_i$	Unit cost for shale gas production at shale site $i$
$spp_{i,t}$	Shale gas production of a shale well of age $t$ at shale site $i$
$tmn_i$	Maximum number of wells that can be drilled at site $i$ over the planning horizon
$tpc_p$	Maximum processing capacity of processing plant $p$
$tprc_r$	Reference capacity of pipeline transporting gas with capacity range $r$
$tpri_r$	Reference capital investment of pipeline transporting gas with capacity range $r$
$ufc_{p,t,s}$	Uncertainty factors accounting for the performance ratio of processing plant $p$ in time period $t$ of scenario $s$
$ufp_{i,t,s}$	Uncertainty factors accounting for the actual shale well productivity at shale site $i$ in time period $t$ of scenario $s$
$vpc_p$	Unit operating cost at processing plant $p$
$vplp$	Minimum processing price at processing plants
$vpup$	Maximum processing price at processing plants
$vtcl$	Unit variable transportation cost for transporting NGL
$vtcm$	Unit variable transportation cost for transporting natural gas
$vtcs$	Unit variable transportation cost for transporting shale gas
$wd_i$	Average drilling water usage for each well at shale site $i$
$wf_i$	Unit water usage for hydraulic fracturing and production at shale site $i$

$w t_i$	Wastewater generation rate associated with unit gas production at shale site $i$
$w t c_w$	Unit wastewater treatment cost for treatment option $w$
$\gamma_i$	Percentage of the value of extracted shale gas paid for royalty at shale site $i$

**Nonnegative continuous variables**

$FW_{i,t,s}$	Amount of freshwater required at shale site $i$ in time period $t$ of scenario $s$
$SP_{i,t,s}$	Amount of shale gas produced at shale site $i$ in time period $t$ of scenario $s$
$STP_{i,p,t,s}$	Amount of shale gas transported from shale site $i$ to processing plant $p$ in time period $t$ of scenario $s$
$STPX_{i,t,s}$	Amount of shale gas sold directly at shale site $i$ in time period $t$ of scenario $s$
$TCP_{i,r}$	Capacity of pipeline from shale site $i$ to delivery node with capacity range $r$
$TNG_{t,s}$	Amount of natural gas extracted at processing plants in time period $t$ of scenario $s$
$TNL_{t,s}$	Amount of NGL extracted at processing plants in time period $t$ of scenario $s$
$VP_{c,p,t}$	Unit processing fee for processing contract $c$ offered by processing plant $p$ in time period $t$
$WW_{i,w,t,s}$	Amount of wastewater generated at shale site $i$ and treated by option $w$ in time period $t$ of scenario $s$

**Integer variables**

$NN_{i,t}$	Number of wells drilled at shale site $i$ in time period $t$
------------	--

**Binary variables**

- $XP_{i,r}$  0-1 variable. Equal to 1 if pipeline is installed to transport shale gas from shale site  $i$  to delivery node with capacity range  $r$
- $XSC_{c,p,t}$  0-1 variable. Equal to 1 if processing contract  $c$  offered by processing plant  $p$  is chosen by producer in time period  $t$

## CONCLUSIONS

### **6.6 Summary of the contributions**

The sustainable design and optimization of shale gas energy systems has been addressed with emphasis on three different aspects, namely the modeling of sustainability, handling of uncertainty, and decentralized optimization, in this thesis. A series of novel modeling frameworks are proposed with efficient solution algorithms to provide better strategies and insights in applications. We believe that the research presented in this dissertation lays a foundation for designing sustainable shale gas energy systems. Moreover, the proposed modeling frameworks and solution algorithms can be readily employed in the sustainable design and operations of other energy systems. The summary of the dissertation are provided in the following.

We propose a novel mixed-integer nonlinear fractional programming model to investigate the economic and environmental implications of incorporating modular manufacturing into well-to-wire shale gas supply chains. Both design and operational decisions regarding modular manufacturing are considered, including modular plant allocation, capacity selection, installment planning, moving scheduling, and salvage operation, as well as other decisions for shale gas supply chain design and operations, such as drilling schedule, water management, and pipeline network construction. To systematically evaluate the full spectrum of environmental impacts, an endpoint-oriented life cycle optimization framework is applied that accounts for up to 18 midpoint impact categories and three endpoint impact categories. Total environmental impact scores are obtained to evaluate the comprehensive life cycle environmental impacts of

shale gas supply chains. A tailored global optimization algorithm is also presented to efficiently solve the resulting computationally challenging problem. The applicability of proposed modeling framework is illustrated through a case study of a well-to-wire shale gas supply chain based on Marcellus Shale. The results show that modular manufacturing succeeds in improving the economic performance of a shale gas supply chain, but it is less attractive in terms of mitigating the comprehensive environmental impacts.

We analyze the life cycle environmental impacts of shale gas by using an integrated hybrid LCA and optimization approach. Unlike the process-based LCA that suffers system truncation, the integrated hybrid LCA supplements the truncated system with a comprehensive economic input-output system. Compared with the economic input-output-based LCA that loses accuracy from process aggregation, the integrated hybrid LCA retains the precision in modeling major unit processes within the well-to-wire system boundary. Three environmental categories, namely the life cycle greenhouse gas emissions, water consumption, and energy consumption, are considered. Based on this integrated hybrid LCA framework, we further developed an integrated hybrid life cycle optimization model, which enables automatic identification of sustainable alternatives in the design and operations of shale gas supply chains. We applied the model to a well-to-wire shale gas supply chain in the UK to illustrate the applicability. According to the optimization results, the lowest levelized cost of electricity generated from shale gas is £51.8/MWh, and the optimal life cycle GHG emissions, water consumption, and energy consumption are 473.5 kg CO<sub>2</sub>-eq/MWh, 2,263 kg/MWh, and 1,009 MJ/MWh, respectively.

We propose a novel modeling framework integrating the dynamic MFA approach with LCO methodology for sustainable design of energy systems. This dynamic MFA-based LCO framework provides high-fidelity modeling of complex material flow networks with recycling options, and it enables detailed accounting of time-dependent life cycle material flow profiles. The decisions regarding input, output, and stock of materials are seamlessly linked to their environmental impacts for rigorous quantification of environmental consequences. Moreover, by incorporating an additional dimension of resource sustainability, the proposed modeling framework facilitates the sustainable energy systems design and operations with a more comprehensive perspective. The resulting optimization problem is formulated as a mixed-integer linear fractional program and solved by an efficient parametric algorithm. To illustrate the applicability of the proposed modeling framework and solution algorithm, a case study of an energy supply chain is presented.

We address the optimal design and operations of shale gas supply chains under uncertainty of estimated ultimate recovery (EUR). A two-stage stochastic mixed-integer linear fractional programming (SMILFP) model is developed in order to optimize the levelized cost of energy generated from shale gas. In this model, both design and planning decisions are considered with respect to shale well drilling, shale gas production, processing, multiple end-uses, and transportation. In order to reduce the model size and number of scenarios, we apply a sample average approximation method to generate scenarios based on the real-world EUR data. In addition, a novel solution algorithm integrating the parametric approach and the L-shaped method is proposed for solving the resulting SMILFP problem within a reasonable computational time. The

proposed model and algorithm are illustrated through a case study based on the Marcellus shale play, and a deterministic model is considered for comparison.

We investigate the influences of uncertainty in multi-stakeholder non-cooperative supply chains, and the corresponding optimal strategies based on game theory to hedge against uncertainty in design and operations of such decentralized supply chains. We propose a novel game-theory-based stochastic model that integrates two-stage stochastic programming with a single-leader-multiple-follower Stackelberg game scheme for optimizing decentralized supply chains under uncertainty. Both the leader's and the followers' uncertainties are considered, which directly affect their design and operational decisions regarding infrastructure development, contracts selection, price setting, production profile, transportation planning, and inventory management. The resulting model is formulated as a two-stage stochastic mixed-integer bilevel nonlinear program, which can be further reformulated into a tractable single-level stochastic mixed-integer linear program by applying KKT conditions and Glover's linearization method. A large-scale application to shale gas supply chains is presented to demonstrate the applicability of the proposed framework.

## **6.7 Future work**

In this thesis, we proposed a series of life cycle optimization frameworks for more sustainable design and operations of shale gas energy systems. Despite their advantages compared with traditional approaches, there are still some knowledges gaps remaining to be addressed. First, the popularity of sustainable design has motivated the development of more and more comprehensive environmental impact indicators, such

as the ReCiPe approach adopted in the endpoint-oriented LCO framework. However, most of them still pertain a relatively restrictive perspective that is limited to the environmental dimension. Although the social dimension has long been recognized as one of the three pillars regarding sustainability, there is still no effective approach proposed to quantify the social impacts associated with design and operations of energy systems both precisely and comprehensively. The hybrid LCO framework is definitely a big step forward from the traditional LCO framework. Nevertheless, one obvious drawback of the hybrid LCO framework is its reliance on the up-to-date economic input output data, which can be hardly available in most cases. The Dynamic MFA-based LCO framework provides an effective way to overcome the inherited shortcomings from LCA approach. Yet, this framework is still immature and can be improved in many ways. For instance, although the resource consumption is incorporated as an additional sustainable optimization criterion, the current framework only allows consideration of one specific material as the optimization indicator. It is expected to develop more comprehensive resource quantification approaches for more representative results.

To hedge against uncertainty in shale gas energy systems, we proposed a two-stage stochastic MILFP model considering the EUR uncertainty. The advantage of stochastic programming relies on the assumption that the probability distribution of uncertainty is known. However, in most cases the precise probability distribution information of uncertainty is difficult to get, and only a set of historical data are available. Thus, if we continue to rely on the traditional two-stage stochastic programming approach, the optimal solutions obtained based on the estimated distribution can be biased and suboptimal for the true problem. Such a research challenge can be addressed by a data-

driven stochastic optimization approach by leveraging the power of big data analytics and machine learning for stochastic programming. Instead of assuming a known probability distribution of each uncertain parameter, a confidence set can be constructed to ensure that the true distribution of uncertainty lies within this set with a certain confidence interval based on statistical inference. In this way, the objective of this data-driven stochastic optimization problem is to optimize the expected performance under the worst-case distribution in the given confidence set. The data-driven stochastic optimization approach is a promising choice for hedging against uncertainty in shale gas energy systems: On one hand, the data-driven stochastic optimization approach provides a suitable path to taking advantage of the data information. On the other hand, by optimizing the expected performance under the worst-case distribution, the data-driven stochastic optimization approach adds extra robustness to the optimal solution. Finally, the proposed stochastic game theoretic modeling framework is first of its kind to account for the uncertain behaviors of multiple stakeholders in a decentralized system. It can certainly be extended to account for more general problems. For example, the current modeling framework only considers a one-leader-multiple-follower scenario; the lower-level optimization problem is limited to the linear programming case with no integer decision variables; the tractable problem size is still relatively small due to its complex model structure. Overcoming these challenges requires more advanced modeling techniques and development of efficient solution algorithms.

## REFERENCES

- [1] EIA, "Review of emerging resources: U.S. shale gas and shale oil plays," U. S. Energy Information Administration, Washington, DC 20585, 2011.
- [2] EIA, "Annual Energy Outlook 2015 with projections to 2040," U.S. Energy Information Administration, Washington, DC 20585, 2015.
- [3] EIA, "Technically Recoverable Shale Oil and Shale Gas Resources: An Assessment of 137 Shale Formations in 41 Countries Outside the United States," U. S. Energy Information Administration, 2015.
- [4] D. C. Cafaro and I. E. Grossmann, "Strategic planning, design, and development of the shale gas supply chain network," *AIChE J*, vol. 60, pp. 2122-2142, 2014.
- [5] M. G. Drouven and I. E. Grossmann, "Multi-period planning, design, and strategic models for long-term, quality-sensitive shale gas development," *AIChE J*, vol. 62, pp. 2296-2323, 2016.
- [6] J. Gao and F. You, "Shale gas supply chain design and operations toward better economic and life cycle environmental performance: MINLP model and global optimization algorithm," *ACS Sustain Chem Eng*, vol. 3, pp. 1282-1291, 2015.
- [7] T. V. Bartholomew and M. S. Mauter, "Multiobjective optimization model for minimizing cost and environmental impact in shale gas water and wastewater management," *ACS Sustain Chem Eng*, vol. 4, pp. 3728-3735, 2016.
- [8] M. J. Small, P. C. Stern, E. Bomberg, S. M. Christopherson, B. D. Goldstein, A. L. Israel, *et al.*, "Risks and Risk Governance in Unconventional Shale Gas Development," *Environ Sci Technol*, vol. 48, pp. 8289-8297, 2014.
- [9] A. Vengosh, R. B. Jackson, N. Warner, T. H. Darrah, and A. Kondash, "A Critical Review of the Risks to Water Resources from Unconventional Shale Gas Development and Hydraulic Fracturing in the United States," *Environ Sci Technol*, vol. 48, pp. 8334-8348, 2014.
- [10] J. D. Hughes, "Energy: A reality check on the shale revolution," *Nature*, vol. 494, pp. 307-308, 2013.
- [11] EIA, "Annual Energy Outlook 2012 with Projections to 2035," U.S. Energy Information Administration, 2012.
- [12] J. D. Hughes, "Drilling Deeper: A Reality check on U.S. Government Forecasts for A Lasting Tight Oil & Shale Gas Boom," Post Carbon Institute, California, Santa Rosa 95404, 2014.
- [13] NETL, "Modern Shale Gas Development in the United States: An Update," NATIONAL ENERGY TECHNOLOGY LABORATORY, 2013.
- [14] EIA, "Natural gas processing: The crucial link between natural gas production and its transportation to market," Energy Information Administration, Washington, DC, 2006.
- [15] R. W. Howarth, R. Santoro, and A. Ingraffea, "Methane and the greenhouse-gas footprint of natural gas from shale formations," *Climatic Change*, vol. 106, pp. 679-690, 2011.
- [16] DOE/NETL, "Role of alternative energy sources: natural gas power technology assessment," DOE/NETL, 2012.

- [17] A. Burnham, J. Han, C. E. Clark, M. Wang, J. B. Dunn, and I. Palou-Rivera, "Life-cycle greenhouse gas emissions of shale gas, natural gas, coal, and petroleum," *Environ Sci Technol*, vol. 46, pp. 619-627, 2011.
- [18] C. E. Clark, R. M. Horner, and C. B. Harto, "Life Cycle Water Consumption for Shale Gas and Conventional Natural Gas," *Environ Sci Technol*, vol. 47, pp. 11829-11836, 2013.
- [19] M. Jiang, C. T. Hendrickson, and J. M. VanBriesen, "Life Cycle Water Consumption and Wastewater Generation Impacts of a Marcellus Shale Gas Well," *Environ Sci Technol*, vol. 48, pp. 1911-1920, 2014.
- [20] B. G. Rahm and S. J. Riha, "Toward strategic management of shale gas development: Regional, collective impacts on water resources," *Environmental Science & Policy*, vol. 17, pp. 12-23, 2012.
- [21] J. A. Veil, "Final Report Water Management Technologies Used by Marcellus Shale Gas Producers," U.S. Department of Energy, Argonne, IL, 2010.
- [22] J. M. Wilson and J. M. VanBriesen, "Oil and Gas Produced Water Management and Surface Drinking Water Sources in Pennsylvania," *Environmental Practice*, vol. 14, pp. 288-300, 2012.
- [23] D. Zavala-Araiza, D. T. Allen, M. Harrison, F. C. George, and G. R. Jersey, "Allocating methane emissions to natural gas and oil production from shale formations," *ACS Sustain Chem Eng*, vol. 3, pp. 492-498, 2015.
- [24] K. A. Bulba and P. E. Krouskop, "Composition variety complicates processing plans for US shale gas," *Oil & Gas Journal*, vol. 107, pp. 50-55, 2009.
- [25] EIA. (2014, 9/21). *High value of liquids drives U.S. producers to target wet natural gas resources*. Available: <http://www.eia.gov/todayinenergy/detail.cfm?id=16191#>
- [26] J. F. Goellner, "Expanding the shale gas infrastructure," *Chemical Engineering Progress*, vol. 2, 2012.
- [27] J. J. Siirola, "The impact of shale gas in the chemical industry," *AIChE J*, vol. 60, pp. 810-819, 2014.
- [28] "Modern Shale Gas Development in the United States: A Primer," Ground Water Protection Council, Washington, DC 20585, 2009.
- [29] W. E. Hefley, S. M. Seydor, M. K. Bencho, I. Chappel, M. Dizard, J. Hallman, *et al.*, "The Economic Impact of the Value Chain of a Marcellus Shale Well," University of Pittsburgh, 2011.
- [30] J. G. Speight, "Chapter 3 - Production Technology," in *Shale Gas Production Processes* vol. <http://dx.doi.org/10.1016/B978-0-12-404571-2.00003-0>, J. G. Speight, Ed., ed Boston: Gulf Professional Publishing, 2013, pp. 69-100.
- [31] S. A. Holditch, "Getting the Gas out of the Ground," *Chemical Engineering Progress*, vol. 108, pp. 41-48, 2012.
- [32] E. Brzycki, T. Wilson, E. Wiley, S. Nelson, L. Miller, S. Vashaw, *et al.* (2016, 9/21). *Explore Shale*. Available: <http://exploreshale.org/#>
- [33] M. S. Mauter, P. J. J. Alvarez, A. Burton, D. C. Cafaro, W. Chen, K. B. Gregory, *et al.*, "Regional Variation in Water-Related Impacts of Shale Gas Development and Implications for Emerging International Plays," *Environ Sci Technol*, vol. 48, pp. 8298-8306, 2014.

- [34] M. Mauter and V. Palmer, "Expert Elicitation of Trends in Marcellus Oil and Gas Wastewater Management," *Journal of Environmental Engineering*, vol. 140, p. B4014004, 2014.
- [35] M. O. Gay, S. Fletcher, N. Meyer, and S. Gross, "Water Management in Shale Gas Plays," IHS, 2012.
- [36] J. A. Slutz, J. A. Anderson, R. Broderick, and P. H. Horner, "Key Shale Gas Water Management Strategies: An Economic Assessment," in *International Conference on Health Safety and Environment in Oil and Gas Exploration and Production*, Perth, Australia, 2012.
- [37] M. G. Puder and J. A. Veil, "Offsite Commercial Disposal of Oil and Gas Exploration and Production Waste: Availability, Options, and Costs," Argonne National Laboratory for the U.S. Department of Energy, Office of Fossil Energy, National Energy Technology Laboratory ANL/EVS/R-06/5, 2006.
- [38] S. M. Seydor, E. Clements, S. Pantelemonitis, and V. Deshpande, "Understanding the Marcellus Shale Supply Chain," Pittsburgh, PA 15260, 2012.
- [39] EPA, "Plan to Study the Potential Impacts of Hydraulic Fracturing on Drinking Water Resources," Office of Research and Development U.S. EPA, Washington, D.C., 2011.
- [40] R. D. Vidic, S. L. Brantley, J. M. Vandenbossche, D. Yoxtheimer, and J. D. Abad, "Impact of shale gas development on regional water quality," *Science*, vol. 340, p. 1235009, 2013.
- [41] H. R. Acharya, C. Henderson, H. Matis, H. Kommepalli, and H. Wang, "Cost effective recovery of low TDS frac flowback water for re-use," Department of Energy, Niskayuna, NY 12309-1027 DE-FE0000784, 2011.
- [42] EPA. (2014, August). *The Process of Hydraulic Fracturing*. Available: <http://www2.epa.gov/hydraulicfracturing/process-hydraulic-fracturing>
- [43] I. Pan. (2013, 9/21). *Natural gas processing contracts and how they affect profits and valuation*. Available: <http://marketrealist.com/2013/01/natural-gas-processing-contracts-and-how-they-affect-profits-and-valuation/>
- [44] DCP. (2016, 09/21). *Margin by Contract Type*. Available: <http://www.dcpmidstream.com/investors/margin-by-contract-type>
- [45] S. Mokhatab, W. A. Poe, and J. G. Speight, "Chapter 7 - Acid gas treating," in *Handbook of Natural Gas Transmission and Processing* vol. <http://dx.doi.org/10.1016/B978-075067776-9/50012-9>, ed Burlington: Gulf Professional Publishing, 2006, pp. 261-294.
- [46] L. E. Parks, D. Perry, and R. Fedich, "FLEXSORB ®SE A Proven Reliable Acid Gas Enrichment Solvent A2 - Benyahia, Farid," in *Proceedings of the 2nd Annual Gas Processing Symposium*. vol. 2, F. T. Eljack, Ed., ed Amsterdam: Elsevier, 2010, pp. 229-235.
- [47] S. Mokhatab, W. A. Poe, and J. G. Speight, "Chapter 9 - Natural gas dehydration," in *Handbook of Natural Gas Transmission and Processing* vol. <http://dx.doi.org/10.1016/B978-075067776-9/50014-2>, ed Burlington: Gulf Professional Publishing, 2006, pp. 323-364.
- [48] S. Mokhatab, W. A. Poe, and J. G. Speight, "Chapter 10 - Natural gas liquids recovery," in *Handbook of Natural Gas Transmission and Processing* vol.

- <http://dx.doi.org/10.1016/B978-075067776-9/50015-4>, ed Burlington: Gulf Professional Publishing, 2006, pp. 365-400.
- [49] C. He and F. You, "Shale Gas Processing Integrated with Ethylene Production: Novel Process Designs, Exergy Analysis, and Techno-Economic Analysis," *Ind Eng Chem Res*, vol. 53, pp. 11442-11459, 2014.
- [50] M. Getu, S. Mahadzir, N. V. D. Long, and M. Lee, "Techno-economic analysis of potential natural gas liquid (NGL) recovery processes under variations of feed compositions," *Chem Eng Res Des*, vol. 91, pp. 1272-1283, 2013.
- [51] EIA. (9/29). *Underground Natural Gas Storage*. Available: [http://www.eia.gov/pub/oil\\_gas/natural\\_gas/analysis\\_publications/ngpipeline/undergrnd\\_storage.html](http://www.eia.gov/pub/oil_gas/natural_gas/analysis_publications/ngpipeline/undergrnd_storage.html)
- [52] EIA. (2016, May 2016). *Natural Gas Prices*. Available: [https://www.eia.gov/dnav/ng/ng\\_pri\\_sum\\_dc\\_u\\_nus\\_m.htm](https://www.eia.gov/dnav/ng/ng_pri_sum_dc_u_nus_m.htm)
- [53] NaturalGas.org. (2013, 9/21). *Marketing*. Available: <http://naturalgas.org/naturalgas/marketing/>
- [54] M. Martín and I. E. Grossmann, "Optimal use of hybrid feedstock, switchgrass and shale gas for the simultaneous production of hydrogen and liquid fuels," *Energy*, vol. 55, pp. 378-391, 2013.
- [55] V. M. Ehlinger, K. J. Gabriel, M. M. B. Noureldin, and M. M. El-Hawagi, "Process Design and Integration of Shale Gas to Methanol," *ACS Sustain Chem Eng*, vol. 2, pp. 30-37, 2014.
- [56] J. Gao and F. You, "Deciphering and handling uncertainty in shale gas supply chain design and optimization: Novel modeling framework and computationally efficient solution algorithm," *AIChE J*, vol. 61, pp. 3739-3755, 2015.
- [57] L. Yang, I. E. Grossmann, and J. Manno, "Optimization models for shale gas water management," *AIChE J*, vol. 60, pp. 3490-3501, 2014.
- [58] J. Gao and F. You, "Optimal design and operations of supply chain networks for water management in shale gas production: MILFP model and algorithms for the water-energy nexus," *AIChE Journal*, vol. 61, pp. 1184-1208, 2015.
- [59] L. F. Lira-Barragan, J. M. Ponce-Ortega, M. Serna-Gonzalez, and M. M. El-Halwagi, "Optimal reuse of flowback wastewater in hydraulic fracturing including seasonal and environmental constraints," *AIChE J*, vol. 62, pp. 1634-1645, 2016.
- [60] O. J. Guerra, A. J. Calderón, L. G. Papageorgiou, J. J. Siirola, and G. V. Reklaitis, "An optimization framework for the integration of water management and shale gas supply chain design," *Comput Chem Eng.*, vol. 92, pp. 230-255, 2016.
- [61] M. M. B. Noureldin, N. O. Elbashir, and M. M. El-Halwagi, "Optimization and Selection of Reforming Approaches for Syngas Generation from Natural/Shale Gas," *Ind Eng Chem Res*, vol. 53, pp. 1841-1855, 2014.
- [62] L. M. Julián-Durán, A. P. Ortiz-Espinoza, M. M. El-Halwagi, and A. Jiménez-Gutiérrez, "Techno-Economic Assessment and Environmental Impact of Shale Gas Alternatives to Methanol," *ACS Sustain Chem Eng*, vol. 2, pp. 2338-2344, 2014.
- [63] C. He and F. You, "Toward more cost-effective and greener chemicals production from shale gas by integrating with bioethanol dehydration: Novel

- process design and simulation-based optimization," *AIChE J*, vol. 61, pp. 1209-1232, 2015.
- [64] C. He and F. You, "Deciphering the true life cycle environmental impacts and costs of the mega-scale shale gas-to-olefins projects in the United States," *Energy & Environmental Science*, vol. 9, pp. 820-840, 2016.
- [65] M. Wang, J. Zhang, and Q. Xu, "A novel conceptual design by integrating NGL recovery and LNG regasification processes for maximum energy savings," *AIChE J*, vol. 59, pp. 4673-4685, 2013.
- [66] J. Martinez-Gomez, F. Nápoles-Rivera, J. M. Ponce-Ortega, and M. M. El-Halwagi, "Optimization of the production of syngas from shale gas with economic and safety considerations," *Applied Thermal Engineering*, vol. 110, pp. 678-685, 2017.
- [67] D. Yue, S. Pandya, and F. You, "Integrating Hybrid Life Cycle Assessment with Multiobjective Optimization: A Modeling Framework," *Environ Sci Technol*, vol. 50, pp. 1501-1509, 2016.
- [68] S. Suh, "Functions, commodities and environmental impacts in an ecological-economic model," *Ecological Economics*, vol. 48, pp. 451-467, 2004.
- [69] J. Gong and F. You, "Sustainable design and synthesis of energy systems," *Curr Opin Chem Eng*, vol. 10, pp. 77-86, 2015.
- [70] Kevin Petak, Ananth Chikkatur, Julio Manik, Srirama Palagummi, and K. Greene, "North American Midstream Infrastructure Through 2035: Leaning into the Headwinds," The INGAA Foundation, Inc., 20 F Street, NW, Suite 450, Washington, DC 20001, 2016.
- [71] J. Gao and F. You, "Design and optimization of shale gas energy systems: Overview, research challenges, and future directions," *Comput Chem Eng.*, vol. DOI: <http://dx.doi.org/10.1016/j.compchemeng.2017.01.032>, 2017.
- [72] S. H. Tan and P. I. Barton, "Optimal dynamic allocation of mobile plants to monetize associated or stranded natural gas, part I: Bakken shale play case study," *Energy*, vol. 93, Part 2, pp. 1581-1594, 2015.
- [73] M. Stewart, "LNG on the Go: GE's Modular Liquefied Natural Gas Facility Offers Field Flexibility," GE, 2015.
- [74] J. Gong, M. Yang, and F. You, "A systematic simulation-based process intensification method for shale gas processing and NGLs recovery process systems under uncertain feedstock compositions," *Comput Chem Eng.*, vol. 105, pp. 259-275, 2017.
- [75] M. Yang and F. You, "Comparative Techno-Economic and Environmental Analysis of Ethylene and Propylene Manufacturing from Wet Shale Gas and Naphtha," *Ind Eng Chem Res*, vol. 56, pp. 4038-4051, 2017.
- [76] L. F. Lira-Barragán, J. M. Ponce-Ortega, G. Guillén-Gosálbez, and M. M. El-Halwagi, "Optimal water management under uncertainty for shale gas production," *Ind Eng Chem Res*, vol. 55, pp. 1322-1335, 2016.
- [77] J. Gao and F. You, "Game theory approach to optimal design of shale gas supply chains with consideration of economics and life cycle greenhouse gas emissions," *AIChE J*, vol. 63, pp. 2671-2693, 2017.

- [78] J. Gao and F. You, "A leader-follower game-based life cycle optimization framework and application," in *Comput Aided Chem Eng.* vol. 38, K. Zdravko and B. Miloš, Eds., ed: Elsevier, 2016, pp. 541-546.
- [79] I. J. Laurenzi and G. R. Jersey, "Life cycle greenhouse gas emissions and freshwater consumption of Marcellus shale gas," *Environ Sci Technol*, vol. 47, pp. 4896-4903, 2013.
- [80] A. T. Dale, V. Khanna, R. D. Vidic, and M. M. Bilec, "Process based life-cycle assessment of natural gas from the Marcellus shale," *Environ Sci Technol*, vol. 47, pp. 5459-5466, 2013.
- [81] L. Stamford and A. Azapagic, "Life cycle environmental impacts of UK shale gas," *Applied Energy*, vol. 134, pp. 506-518, 2014.
- [82] M. Goedkoop, R. Heijungs, M. Huijbregts, A. De Schryver, J. Struijs, and R. van Zelm, "ReCiPe 2008-A life cycle impact assessment method which comprises harmonised category indicators at the midpoint and the endpoint level," 2009.
- [83] J. Guinée, *Handbook on Life Cycle Assessment: Operational Guide to the ISO Standards* vol. 7: Springer Science & Business Media, 2002.
- [84] T. Stephenson, J. E. Valle, and X. Riera-Palou, "Modeling the relative GHG emissions of conventional and shale gas production," *Environ Sci Technol*, vol. 45, pp. 10757-10764, 2011.
- [85] G. A. Heath, J. Meldrum, N. Fisher, D. Arent, and M. Bazilian, "Life cycle greenhouse gas emissions from Barnett Shale gas used to generate electricity," *Journal of Unconventional Oil and Gas Resources*, vol. 8, pp. 46-55, 2014.
- [86] P. R. O'Donoghue, G. A. Heath, S. L. Dolan, and M. Vorum, "Life cycle greenhouse gas emissions of electricity generated from conventionally produced natural gas," *Journal of Industrial Ecology*, vol. 18, pp. 125-144, 2014.
- [87] J. Tobin, P. Shambaugh, and E. Mastrangelo, "Natural Gas Processing: The Crucial Link Between Natural Gas Production and Its Transportation to Market," EIA, 2006.
- [88] DOE. (2005, September 2017). *Liquefied Natural Gas: Understanding the Basic Facts*. Available: [https://energy.gov/sites/prod/files/2013/04/f0/LNG\\_primerupd.pdf](https://energy.gov/sites/prod/files/2013/04/f0/LNG_primerupd.pdf)
- [89] M. Stewart. (2015, September 2017). *LNG on the Go: GE's Modular Liquefied Natural Gas Facility Offers Field Flexibility*. Available: <https://gereports.ca/lng-go-ges-modular-liquefied-natural-gas-facility-offers-field-flexibility/#>
- [90] K. Punnonen. (2013, September 2017). *Small and Medium size LNG for Power Production*. Available: <https://www.wartsila.com/docs/default-source/oil-gas-documents/white-paper-o-ogi-2013-lng-power-production.pdf>
- [91] B. Price, M. Mahaley, and W. Shimer. (2014, September 2017). *Optimize small-scale LNG production with modular SMR technology*. Available: <http://www.gasprocessingnews.com/features/201404/optimize-small-scale-lng-production-with-modular-smr-technology.aspx>
- [92] DOE/NETL, "Life cycle greenhouse gas inventory of natural gas extraction, delivery and electricity production," 2011.

- [93] (2017, May 2017). *Ecoinvent database v3.3*. Available: <http://www.ecoinvent.org>
- [94] M. Goedkoop and R. Spriensma, "The Eco-indicator 99-A damage oriented method for Life Cycle Impact Assessment—Methodology Report, PRÉ Consultants. Amersfoort, Netherlands," ed, 1999.
- [95] N. Hultman, D. Rebois, M. Scholten, and C. Ramig, "The greenhouse impact of unconventional gas for electricity generation," *Environmental Research Letters*, vol. 6, p. 044008, 2011.
- [96] C. L. Weber and C. Clavin, "Life cycle carbon footprint of shale gas: Review of evidence and implications," *Environ Sci Technol*, vol. 46, pp. 5688-5695, 2012.
- [97] G. A. Heath, P. O'Donoghue, D. J. Arent, and M. Bazilian, "Harmonization of initial estimates of shale gas life cycle greenhouse gas emissions for electric power generation," *Proc Natl Acad Sci*, vol. 111, pp. E3167-E3176, 2014.
- [98] P. Horner, B. Halldorson, and J. A. Slutz, "Shale Gas Water Treatment Value Chain-A Review of Technologies including Case Studies," in *SPE Annual Technical Conference and Exhibition*, 2011.
- [99] M. T. Al-Nory, A. Brodsky, B. Bozkaya, and S. C. Graves, "Desalination supply chain decision analysis and optimization," *Desalination*, vol. 347, pp. 144-157, 2014.
- [100] G. Raluy, L. Serra, and J. Uche, "Life cycle assessment of MSF, MED and RO desalination technologies," *Energy*, vol. 31, pp. 2361-2372, 2006.
- [101] F. You, P. M. Castro, and I. E. Grossmann, "Dinkelbach's algorithm as an efficient method to solve a class of MINLP models for large-scale cyclic scheduling problems," *Computers and Chemical Engineering*, vol. 33, pp. 1879-1889, 2009.
- [102] W. Dinkelbach, "On Nonlinear Fractional Programming," *Management Science*, vol. 13, pp. 492-498, 1967.
- [103] F. You and I. E. Grossmann, "Stochastic inventory management for tactical process planning under uncertainties: MINLP models and algorithms," *AIChE J*, vol. 57, pp. 1250-1277, 2011.
- [104] D. Yue and F. You, "Planning and scheduling of flexible process networks under uncertainty with stochastic inventory: MINLP models and algorithm," *AIChE J*, vol. 59, pp. 1511-1532, 2013.
- [105] Z. X. Zhong and F. Q. You, "Globally convergent exact and inexact parametric algorithms for solving large-scale mixed-integer fractional programs and applications in process systems engineering," *Comput Chem Eng*, vol. 61, pp. 90-101, 2014.
- [106] F. You, J. M. Pinto, I. E. Grossmann, and L. Megan, "Optimal Distribution-Inventory Planning of Industrial Gases. II. MINLP Models and Algorithms for Stochastic Cases," *Ind Eng Chem Res*, vol. 50, pp. 2928-2945, 2011.
- [107] Z. Zhong and F. You, "Globally convergent exact and inexact parametric algorithms for solving large-scale mixed-integer fractional programs and applications in process systems engineering," *Comput Chem Eng.*, vol. 61, pp. 90-101, 2014.

- [108] J. Gong and F. You, "Global Optimization for Sustainable Design and Synthesis of Algae Processing Network for CO<sub>2</sub> Mitigation and Biofuel Production Using Life Cycle Optimization," *AIChE J*, vol. 60, pp. 3195-3210, 2014.
- [109] (2017, May 2017). *Information Related to Pennsylvania Deep Gas Well Activity*. Available: <https://www.marcellusgas.org/index.php>
- [110] (2017, May 2017). *MarkWest Energy Partners*. Available: <http://www.markwest.com/operations/marcellus/>
- [111] EIA. (2016, May 2017). *Form EIA-860 detailed data*. Available: <https://www.eia.gov/electricity/data/eia860/>
- [112] J. Ladlee and J. Jacquet, "The implications of multi-well pads in the Marcellus Shale," *Community and Regional Development Institute at Cornell (CaRDI) Research and Policy Brief Series*, vol. 43, 2011.
- [113] G. S. Swindell, "Marcellus Shale in Pennsylvania: A 2,600 Well Study of Estimated Ultimate Recovery," presented at the SPE Annual Meeting, Dallas, TX, 2014.
- [114] GE, "Helping you harness the energy of opportunity," GE Oil & Gas, 4425 Westway Park Blvd. Houston, TX 77041, 2014.
- [115] EIA, "Levelized Cost and Levelized Avoided Cost of New Generation Resources in the Annual Energy Outlook 2015," U.S. Energy Information Administration, 2015.
- [116] D. C. Cafaro and I. E. Grossmann, "Strategic planning, design, and development of the shale gas supply chain network," *AIChE Journal*, vol. 60, p. 21, 2014.
- [117] A. J. Calderón, O. J. Guerra, L. G. Papageorgiou, J. J. Siirola, and G. V. Reklaitis, "Preliminary Evaluation of Shale Gas Reservoirs: Appraisal of Different Well-Pad Designs via Performance Metrics," *Ind Eng Chem Res*, vol. 54, pp. 10334-10349, 2015.
- [118] M. Jiang, G. W. Michael, H. Chris, J. Paulina, V. Jeanne, and V. Aranya, "Life cycle greenhouse gas emissions of Marcellus shale gas," *Environmental Research Letters*, vol. 6, p. 034014, 2011.
- [119] R. Jayakumar and R. Rai, "Impact of Uncertainty in Estimation of Shale-Gas-Reservoir and Completion Properties on EUR Forecast and Optimal Development Planning: A Marcellus Case Study," vol. 10.2118/162821-PA, 2014.
- [120] EIA, "Levelized cost and levelized avoided cost of new generation resources in the annual energy outlook 2016," U.S. Energy Information Administration, Washington, DC 20585, 2016.
- [121] L. T. Biegler, I. E. Grossmann, and A. W. Westerberg, *Systematic Methods of Chemical Process Design*: Prentice Hall PTR, 1997.
- [122] A. Brooke, D. A. Kendrick, A. Meeraus, and R. E. Rosenthal, *GAMS: A User's Guide*: Course Technology, 1988.
- [123] U. Kumar, "Accelerating adoption of LNG fuelling infrastructure," GE Oil & Gas, 2013.
- [124] C. Karapataki, "Techno-economic analysis of water management options for unconventional natural gas developments in the Marcellus Shale," Master thesis,

- Engineering Systems Division, Technology and Policy Program, Massachusetts Institute of Technology, Cambridge, MA 02139-4307, 2012.
- [125] L. Yang, I. E. Grossmann, M. S. Mauter, and R. M. Dillmore, "Investment optimization model for freshwater acquisition and wastewater handling in shale gas production," *AIChE J*, vol. 61, pp. 1770-1782, 2015.
- [126] R. W. Howarth, "A bridge to nowhere: methane emissions and the greenhouse gas footprint of natural gas," *Energy Science & Engineering*, vol. 2, pp. 47-60, 2014.
- [127] D. T. Allen, "Atmospheric Emissions and Air Quality Impacts from Natural Gas Production and Use," *Annual Review of Chemical and Biomolecular Engineering*, vol. 5, pp. 55-75, 2014.
- [128] D. T. Allen, "Methane emissions from natural gas production and use: reconciling bottom-up and top-down measurements," *Curr Opin Chem Eng*, vol. 5, pp. 78-83, 2014.
- [129] J. Gao and F. You, "Design and optimization of shale gas energy systems: Overview, research challenges, and future directions," *Comput Chem Eng.*, vol. 106, pp. 699-718, 2017.
- [130] J. Gao and F. You, "Economic and Environmental Life Cycle Optimization of Noncooperative Supply Chains and Product Systems: Modeling Framework, Mixed-Integer Bilevel Fractional Programming Algorithm, and Shale Gas Application," *ACS Sustain Chem Eng*, vol. 5, pp. 3362-3381, 2017.
- [131] J. Gong and F. You, "A new superstructure optimization paradigm for process synthesis with product distribution optimization: Application to an integrated shale gas processing and chemical manufacturing process," *AIChE J*, vol. 10.1002/aic.15882.
- [132] T. Skone, J. Littlefield, and J. Marriott, "Life cycle greenhouse gas inventory of natural gas extraction, delivery and electricity production," DOE/NETL-2011/1522.: US Department of Energy, National Energy Technology Laboratory, Pittsburgh, PA, USA., 2011.
- [133] S. Suh and G. Huppes, "Methods for Life Cycle Inventory of a product," *J Clean Prod*, vol. 13, pp. 687-697, 2005.
- [134] M. Bilec, R. Ries, H. S. Matthews, and A. L. Sharrard, "Example of a Hybrid Life-Cycle Assessment of Construction Processes," *Journal of Infrastructure Systems*, vol. 12, pp. 207-215, 2006.
- [135] T. O. Wiedmann, S. Suh, K. Feng, M. Lenzen, A. Acquaye, K. Scott, *et al.*, "Application of Hybrid Life Cycle Approaches to Emerging Energy Technologies – The Case of Wind Power in the UK," *Environ Sci Technol*, vol. 45, pp. 5900-5907, 2011.
- [136] R. Bush, D. A. Jacques, K. Scott, and J. Barrett, "The carbon payback of micro-generation: An integrated hybrid input–output approach," *Applied Energy*, vol. 119, pp. 85-98, 2014.
- [137] K. Feng, K. Hubacek, Y. L. Siu, and X. Li, "The energy and water nexus in Chinese electricity production: A hybrid life cycle analysis," *Renewable and Sustainable Energy Reviews*, vol. 39, pp. 342-355, 2014.

- [138] G. Finnveden, M. Z. Hauschild, T. Ekvall, J. Guinée, R. Heijungs, S. Hellweg, *et al.*, "Recent developments in Life Cycle Assessment," *Journal of Environmental Management*, vol. 91, pp. 1-21, 2009.
- [139] Y. Moriguchi, Y. Kondo, and H. Shimizu, "Analysing the life cycle impacts of cars: the case of CO<sub>2</sub>," *Industry and Environment*, vol. 16, 1993.
- [140] G. J. Treloar, P. E. D. Love, O. O. Faniran, and U. Iyer-Raniga, "A hybrid life cycle assessment method for construction," *Construction Management and Economics*, vol. 18, pp. 5-9, 2000.
- [141] S. Suh and G. Huppes, "Missing inventory estimation tool using extended input-output analysis," *Int J Life Cycle Assess*, vol. 7, pp. 134-140, 2002.
- [142] S. Joshi, "Product environmental life - cycle assessment using input - output techniques," *Journal of industrial ecology*, vol. 3, pp. 95-120, 1999.
- [143] G. P. Peters and E. G. Hertwich, "A comment on "Functions, commodities and environmental impacts in an ecological-economic model"," *Ecological Economics*, vol. 59, pp. 1-6, 2006.
- [144] R. Heijungs and S. Suh, *The computational structure of life cycle assessment* vol. 11: Springer Science & Business Media, 2013.
- [145] Y. Kondo and S. Nakamura, "Evaluating alternative life-cycle strategies for electrical appliances by the waste input-output model," *Int J Life Cycle Assess*, vol. 9, p. 236, 2004.
- [146] BEA. (2017, August 2017). *Input-Output Accounts Data*. Available: [https://www.bea.gov/industry/io\\_annual.htm](https://www.bea.gov/industry/io_annual.htm)
- [147] "The Energy and Climate Change Committee, 2011. Shale gas: fifth report of session 2010–12.," London: The Stationery Office, 2011.
- [148] T. Stocker, *Climate change 2013: the physical science basis: Working Group I contribution to the Fifth assessment report of the Intergovernmental Panel on Climate Change*: Cambridge University Press, 2014.
- [149] D. J. MacKay and T. J. Stone, "Potential Greenhouse Gas Emissions Associated with Shale Gas Extraction and Use," 2013.
- [150] B. Singh, A. H. Strømman, and E. Hertwich, "Life cycle assessment of natural gas combined cycle power plant with post-combustion carbon capture, transport and storage," *International Journal of Greenhouse Gas Control*, vol. 5, pp. 457-466, 2011.
- [151] D. Yue, M. A. Kim, and F. You, "Design of Sustainable Product Systems and Supply Chains with Life Cycle Optimization Based on Functional Unit: General Modeling Framework, Mixed-Integer Nonlinear Programming Algorithms and Case Study on Hydrocarbon Biofuels," *ACS Sustain Chem Eng*, vol. 1, pp. 1003-1014, 2013.
- [152] F. You, P. M. Castro, and I. E. Grossmann, "Dinkelbach's algorithm as an efficient method to solve a class of MINLP models for large-scale cyclic scheduling problems," *Comput Chem Eng.*, vol. 33, pp. 1879-1889, 2009.
- [153] D. Garcia and F. You, "Network-Based Life Cycle Optimization of the Net Atmospheric CO<sub>2</sub>-eq Ratio (NACR) of Fuels and Chemicals Production from Biomass," *ACS Sustain Chem Eng*, vol. 3, pp. 1732-1744, 2015.

- [154] (2017, August 2017). *Frack off-extreme energy action network*. Available: <http://frack-off.org.uk/>
- [155] J. Gong and F. You, "Consequential Life Cycle Optimization: General Conceptual Framework and Application to Algal Renewable Diesel Production," *ACS Sustain Chem Eng*, vol. 5, pp. 5887-5911, 2017.
- [156] (2017, August 2017). *Mapped: How the UK generates its electricity*. Available: <https://www.carbonbrief.org/mapped-how-the-uk-generates-its-electricity>
- [157] T. Achterberg, "SCIP: solving constraint integer programs," *Mathematical Programming Computation*, vol. 1, pp. 1-41, 2009.
- [158] M. Tawarmalani and N. V. Sahinidis, "A polyhedral branch-and-cut approach to global optimization," *Math. Program.*, vol. 103, pp. 225-249, 2005.
- [159] G. Finnveden and Å. Moberg, "Environmental systems analysis tools – an overview," *J Clean Prod*, vol. 13, pp. 1165-1173, 2005.
- [160] J. B. Guinée, R. Heijungs, G. Huppes, A. Zamagni, P. Masoni, R. Buonamici, *et al.*, "Life Cycle Assessment: Past, Present, and Future," *Environ Sci Technol*, vol. 45, pp. 90-96, 2011.
- [161] D. Garcia and F. You, "Supply chain design and optimization: Challenges and opportunities," *Comput Chem Eng.*, vol. 81, pp. 153-170, 2015.
- [162] F. You and B. Wang, "Life Cycle Optimization of Biomass-to-Liquid Supply Chains with Distributed–Centralized Processing Networks," *Ind Eng Chem Res*, vol. 50, pp. 10102-10127, 2011.
- [163] D. Yue and F. You, "Functional-Unit-Based Life Cycle Optimization for Design of Sustainable Product Systems with Application on Biofuel Supply Chains," *Comput Aided Chem Eng*, vol. 33, pp. 1063-1068, 2014.
- [164] C.-L. Huang, J. Vause, H.-W. Ma, and C.-P. Yu, "Using material/substance flow analysis to support sustainable development assessment: A literature review and outlook," *Resources, Conservation and Recycling*, vol. 68, pp. 104-116, 2012.
- [165] E. Cimren, J. Fiksel, M. E. Posner, and K. Sikdar, "Material Flow Optimization in By-product Synergy Networks," *Journal of Industrial Ecology*, vol. 15, pp. 315-332, 2011.
- [166] M. Ruhrberg, "Assessing the recycling efficiency of copper from end-of-life products in Western Europe," *Resources, Conservation and Recycling*, vol. 48, pp. 141-165, 2006.
- [167] D. Laner and H. Rechberger, "Material Flow Analysis," in *Special Types of Life Cycle Assessment* vol. 10.1007/978-94-017-7610-3\_7, M. Finkbeiner, Ed., ed Dordrecht: Springer Netherlands, 2016, pp. 293-332.
- [168] D. B. Müller, "Stock dynamics for forecasting material flows—Case study for housing in The Netherlands," *Ecological Economics*, vol. 59, pp. 142-156, 2006.
- [169] M. D. Gerst and T. E. Graedel, "In-Use Stocks of Metals: Status and Implications," *Environ Sci Technol*, vol. 42, pp. 7038-7045, 2008.
- [170] I. Daigo, Y. Igarashi, Y. Matsuno, and Y. Adachi, "Accounting for Steel Stock in Japan," *ISIJ International*, vol. 47, pp. 1065-1069, 2007.
- [171] H. Bergsdal, H. Brattebø, R. A. Bohne, and D. B. Müller, "Dynamic material flow analysis for Norway's dwelling stock," *Building Research & Information*, vol. 35, pp. 557-570, 2007.

- [172] S. Glöser, M. Soulier, and L. A. Tercero Espinoza, "Dynamic Analysis of Global Copper Flows. Global Stocks, Postconsumer Material Flows, Recycling Indicators, and Uncertainty Evaluation," *Environ Sci Technol*, vol. 47, pp. 6564-6572, 2013.
- [173] E. Müller, L. M. Hilty, R. Widmer, M. Schluep, and M. Faulstich, "Modeling Metal Stocks and Flows: A Review of Dynamic Material Flow Analysis Methods," *Environ Sci Technol*, vol. 48, pp. 2102-2113, 2014.
- [174] H. Bergsdal, H. Brattebø, and D. B. Müller, "Dynamic material flow analysis for PCBs in the Norwegian building stock," *Building Research & Information*, vol. 42, pp. 359-370, 2014.
- [175] T. Hawkins, C. Hendrickson, C. Higgins, H. S. Matthews, and S. Suh, "A Mixed-Unit Input-Output Model for Environmental Life-Cycle Assessment and Material Flow Analysis," *Environ Sci Technol*, vol. 41, pp. 1024-1031, 2007.
- [176] L. Rincón, A. Castell, G. Pérez, C. Solé, D. Boer, and L. F. Cabeza, "Evaluation of the environmental impact of experimental buildings with different constructive systems using Material Flow Analysis and Life Cycle Assessment," *Applied Energy*, vol. 109, pp. 544-552, 2013.
- [177] C. Vadenbo, S. Hellweg, and G. Guillén-Gosálbez, "Multi-objective optimization of waste and resource management in industrial networks – Part I: Model description," *Resources, Conservation and Recycling*, vol. 89, pp. 52-63, 2014.
- [178] P. Brunner and H. Rechberger, "Practical handbook of material flow analysis. 2004," *New York: Lewis*, vol. 317.
- [179] H. Hatayama, I. Daigo, Y. Matsuno, and Y. Adachi, "Outlook of the World Steel Cycle Based on the Stock and Flow Dynamics," *Environ Sci Technol*, vol. 44, pp. 6457-6463, 2010.
- [180] V. C. Onishi, A. Carrero-Parreño, J. A. Reyes-Labarta, E. S. Fraga, and J. A. Caballero, "Desalination of shale gas produced water: A rigorous design approach for zero-liquid discharge evaporation systems," *J Clean Prod*, vol. 140, pp. 1399-1414, 2017.
- [181] V. C. Onishi, R. Ruiz-Femenia, R. Salcedo-Díaz, A. Carrero-Parreño, J. A. Reyes-Labarta, E. S. Fraga, *et al.*, "Process optimization for zero-liquid discharge desalination of shale gas flowback water under uncertainty," *J Clean Prod*, vol. 164, pp. 1219-1238, 2017.
- [182] D. Liu, R. Agarwal, and Y. Li, "Numerical simulation and optimization of CO<sub>2</sub> enhanced shale gas recovery using a genetic algorithm," *J Clean Prod*, vol. 164, pp. 1093-1104, 2017.
- [183] P. Balcombe, N. P. Brandon, and A. D. Hawkes, "Characterising the distribution of methane and carbon dioxide emissions from the natural gas supply chain," *J Clean Prod*, vol. 172, pp. 2019-2032, 2018.
- [184] B. A. McCarl, "McCarl GAMS User Guide," GAMS Development Corporation, 2014.
- [185] L. G. Papageorgiou, "Supply chain optimisation for the process industries: Advances and opportunities," *Comput Chem Eng*, vol. 33, pp. 1931-1938, 2009.

- [186] D. J. Garcia and F. You, "Supply chain design and optimization: Challenges and opportunities," *Comput Chem Eng*, vol. <http://dx.doi.org/10.1016/j.compchemeng.2015.03.015>, DOI:10.1016/j.compchemeng.2015.03.015, 2015, p.
- [187] R. Weijermars, "Value chain analysis of the natural gas industry: Lessons from the US regulatory success and opportunities for Europe," *Journal of Natural Gas Science and Engineering*, vol. 2, pp. 86-104, 2010.
- [188] A. J. Calderón, O. J. Guerra, L. G. Papageorgiou, J. J. Siirola, and G. V. Reklaitis, "Financial considerations in shale gas supply chain development," in *Comput Aided Chem Eng*. vol. 37, J. K. H. Krist V. Gernaey and G. Rafiqul, Eds., ed: Elsevier, 2015, pp. 2333-2338.
- [189] F. Gracceva and P. Zeniewski, "Exploring the uncertainty around potential shale gas development – A global energy system analysis based on TIAM (TIMES Integrated Assessment Model)," *Energy*, vol. 57, pp. 443-457, 2013.
- [190] R. Jayakumar and R. R. Rai, "Impact of Uncertainty in Estimation of Shale Gas Reservoir and Completion Properties on EUR Forecast and Optimal Development Planning: A Marcellus Case Study," 2012.
- [191] M. M. Chaudhri, "Numerical Modeling of Multifracture Horizontal Well for Uncertainty Analysis and History Matching: Case Studies From Oklahoma and Texas Shale Gas Wells," 2012.
- [192] N. R. Harding, "Application of Stochastic Prospect Analysis for Shale Gas Reservoirs," 2008.
- [193] N. V. Sahinidis, "Optimization under uncertainty: state-of-the-art and opportunities," *Comput Chem Eng*, vol. 28, pp. 971-983, 2004.
- [194] D. Bertsimas, D. B. Brown, and C. Caramanis, "Theory and Applications of Robust Optimization," *SIAM Review*, vol. 53, pp. 464-501, 2011.
- [195] A. Ben-Tal and A. Nemirovski, "Robust optimization – methodology and applications," *Math. Program.*, vol. 92, pp. 453-480, 2002.
- [196] F. You, J. M. Wassick, and I. E. Grossmann, "Risk management for a global supply chain planning under uncertainty: Models and algorithms," *AIChE Journal*, vol. 55, pp. 931-946, 2009.
- [197] B. H. Gebreslassie, Y. Yao, and F. You, "Design under Uncertainty of Hydrocarbon Biorefinery Supply Chains: Multiobjective Stochastic Programming Models, Decomposition Algorithm, and A Comparison between CVaR and Downside Risk," *AIChE J*, vol. 58, pp. 2155-2179, 2012.
- [198] A. Shapiro and T. Homem-de-Mello, "A Simulation-Based Approach to Two-Stage Stochastic Programming with Recourse," *Math. Program.*, vol. 81, pp. 301-325, 1998.
- [199] A. J. Kleywegt, A. Shapiro, and T. Homem-de-Mello, "The Sample Average Approximation Method for Stochastic Discrete Optimization," *SIAM Journal on Optimization*, vol. 12, pp. 479-502, 2002.
- [200] A. Shapiro, "Monte Carlo Sampling Methods," in *Handbooks in Operations Research and Management Science*. vol. Volume 10, A. Ruszczyński and A. Shapiro, Eds., ed: Elsevier, 2003, pp. 353-425.

- [201] N. R. C. National Academy of Engineering, Committee on America's Energy Future, Division on Engineering and Physical Sciences, *America's Energy Future: Technology and Transformation*: National Academies Press, 2009.
- [202] J. R. Birge, "State-of-the-Art-Survey—Stochastic Programming: Computation and Applications," *INFORMS Journal on Computing*, vol. 9, pp. 111-133, 1997.
- [203] Oracle. (6/19). *Oracle Crystal Ball*. Available: <http://www.oracle.com/appserver/business-intelligence/crystalball/index.html>
- [204] G. Laporte and F. V. Louveaux, "The Integer L-Shaped Method for Stochastic Integer Programs with Complete Recourse," *Operations Research Letters*, vol. 13, pp. 133-142, 1993.
- [205] S. Liu, A. S. Simaria, S. S. Farid, and L. G. Papageorgiou, "Optimising Chromatography Strategies of Antibody Purification Processes by Mixed Integer Fractional Programming Techniques," *Comput Chem Eng.*, vol. 68, pp. 151-164, 2014.
- [206] J. R. Birge and F. V. Louveaux, "A Multicut Algorithm for Two-Stage Stochastic Linear Programs," *Eur J Oper Res*, vol. 34, pp. 384-392, 1988.
- [207] R. M. V. Slyke and R. Wets, "L-Shaped Linear Programs with Applications to Optimal Control and Stochastic Programming," *SIAM Journal on Applied Mathematics*, vol. 17, pp. 638-663, 1969.
- [208] J. R. Birge and F. Louveaux, *Introduction to Stochastic Programming*: Springer, 2011.
- [209] P. Kali and S. W. Wallace, *Stochastic programming*: Wiley Press, Chichester, 1994.
- [210] Marcellus-Shale.us. (2013, 8/29). *Real Marcellus Gas Production*. Available: <http://www.marcellus-shale.us/>
- [211] EIA. (6/16). *Natural Gas Consumption by End Use*. Available: [http://www.eia.gov/dnav/ng/ng\\_cons\\_sum\\_dcua\\_a.htm](http://www.eia.gov/dnav/ng/ng_cons_sum_dcua_a.htm)
- [212] EIA. (6/16). *Heat Content of Natural Gas Consumed*. Available: [http://www.eia.gov/dnav/ng/ng\\_cons\\_heat\\_dcua\\_nus\\_a.htm](http://www.eia.gov/dnav/ng/ng_cons_heat_dcua_nus_a.htm)
- [213] EIA. (2014, 5/20). *High value of liquids drives U.S. producers to target wet natural gas resources*. Available: <http://www.eia.gov/todayinenergy/detail.cfm?id=16191#>
- [214] DOE. (6/16). *Energy Efficiency & Renewable Energy*. Available: <http://www.regulations.doe.gov/certification-data/CCMS-81578122497.html>
- [215] EIA. (6/16). *Gas furnace efficiency has large implications for residential natural gas use*. Available: <http://www.eia.gov/todayinenergy/detail.cfm?id=14051>
- [216] L. Steven and A. Thekdi, "Industrial Natural Gas Energy Efficiency Calculator Tools," Sempra Energy – Southern California Gas Company CEC - 500 - 2014 - 066, 2013.
- [217] G. Cachon and S. Netessine, "Game Theory in Supply Chain Analysis," in *Handbook of Quantitative Supply Chain Analysis*. vol. 74, D. Simchi-Levi, S. D. Wu, and Z.-J. Shen, Eds., ed: Springer US, 2004, pp. 13-65.

- [218] I. E. Grossmann, "Challenges in the new millennium: product discovery and design, enterprise and supply chain optimization, global life cycle assessment," *Comput Chem Eng.*, vol. 29, pp. 29-39, 2004.
- [219] D. Yue, F. You, and S. W. Snyder, "Biomass-to-bioenergy and biofuel supply chain optimization: Overview, key issues and challenges," *Comput Chem Eng.*, vol. 66, pp. 36-56, 2014.
- [220] C. Lima, S. Relvas, and A. P. F. D. Barbosa-Póvoa, "Downstream oil supply chain management: A critical review and future directions," *Comput Chem Eng.*, vol. 92, pp. 78-92, 2016.
- [221] J. Gjerdrum, N. Shah, and L. G. Papageorgiou, "Transfer Prices for Multienterprise Supply Chain Optimization," *Ind Eng Chem Res*, vol. 40, pp. 1650-1660, 2001.
- [222] J. Gjerdrum, N. Shah, and L. G. Papageorgiou, "Fair transfer price and inventory holding policies in two-enterprise supply chains," *Eur J Oper Res*, vol. 143, pp. 582-599, 2002.
- [223] D. Zhang, N. J. Samsatli, A. D. Hawkes, D. J. L. Brett, N. Shah, and L. G. Papageorgiou, "Fair electricity transfer price and unit capacity selection for microgrids," *Energ Econ*, vol. 36, pp. 581-593, 2013.
- [224] D. Yue and F. You, "Fair profit allocation in supply chain optimization with transfer price and revenue sharing: MINLP model and algorithm for cellulosic biofuel supply chains," *AIChE J*, vol. 60, pp. 3211-3229, 2014.
- [225] M. A. Zamarripa, A. M. Aguirre, C. A. Méndez, and A. Espuña, "Improving supply chain planning in a competitive environment," *Comput Chem Eng.*, vol. 42, pp. 178-188, 2012.
- [226] D. Yue and F. You, "Game-theoretic modeling and optimization of multi-echelon supply chain design and operation under Stackelberg game and market equilibrium," *Comput Chem Eng.*, vol. 71, pp. 347-361, 2014.
- [227] D. Yue and F. You, "Stackelberg-game-based modeling and optimization for supply chain design and operations: A mixed integer bilevel programming framework," *Comput Chem Eng.*, vol. 102, pp. 81-95, 2017.
- [228] K. Hjaila, J. M. Laínez-Aguirre, L. Puigjaner, and A. Espuña, "Scenario-based dynamic negotiation for the coordination of multi-enterprise supply chains under uncertainty," *Comput Chem Eng.*, vol. 91, pp. 445-470, 2016.
- [229] K. Hjaila, L. Puigjaner, J. M. Laínez, and A. Espuña, "Integrated game-theory modelling for multi enterprise-wide coordination and collaboration under uncertain competitive environment," *Comput Chem Eng.*, vol. 98, pp. 209-235, 2017.
- [230] H. Von Stackelberg, *Market structure and equilibrium*: Springer Science & Business Media, 2010.
- [231] J. Nash, "Non-Cooperative Games," *Annals of Mathematics*, vol. 54, pp. 286-295, 1951.
- [232] J. F. Bard, *Practical Bilevel Optimization: Algorithm and Applications*. Dordrecht: Kluwer Academic Publishers, 1998.
- [233] F. Glover, "Improved Linear Integer Programming Formulations of Nonlinear Integer Problems," *Management Science*, vol. 22, pp. 455-460, 1975.

- [234] J. Ladlee and J. Jacquet, "The implications of multi-well pads in the Marcellus Shale," *Research & Policy Brief Series*, vol. 43, 2011.
- [235] D. T. Allen, V. M. Torres, J. Thomas, D. W. Sullivan, M. Harrison, A. Hendler, *et al.*, "Measurements of methane emissions at natural gas production sites in the United States," *Proc Natl Acad Sci*, vol. 110, pp. 17768-17773, 2013.
- [236] F. Q. You, J. M. Wassick, and I. E. Grossmann, "Risk Management for a Global Supply Chain Planning Under Uncertainty: Models and Algorithms," *AIChE J*, vol. 55, pp. 931-946, 2009.